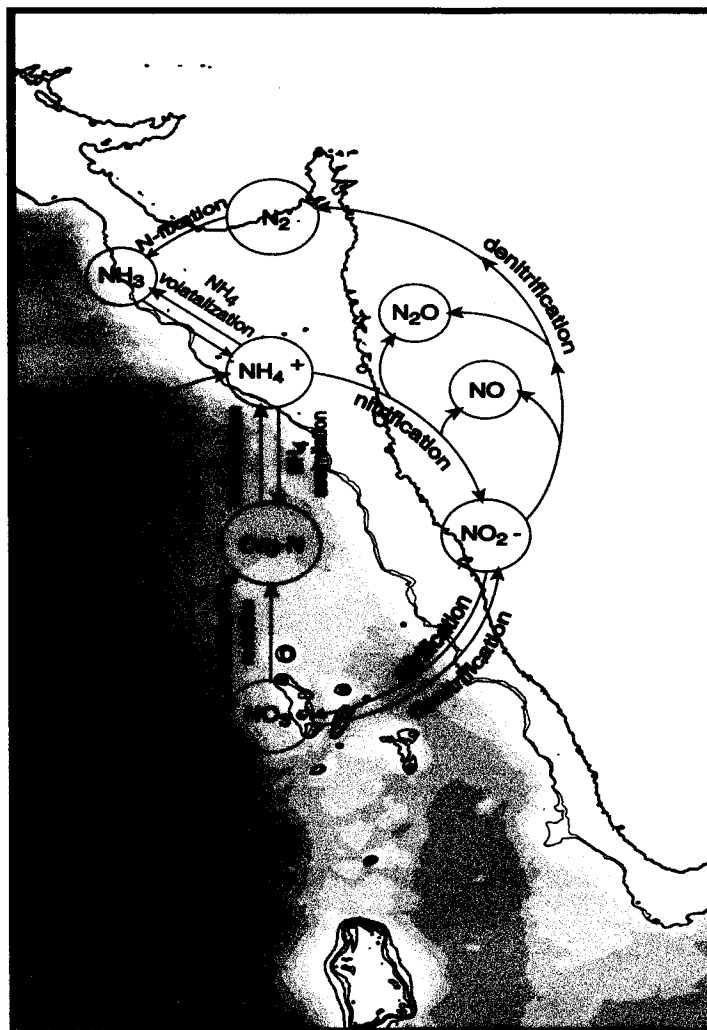# Benthic nitrogen cycling with special reference to nitrous oxide in the coastal and continental shelf environments of the eastern Arabian Sea

THESIS SUBMITTED TO
GOA UNIVERSITY

FOR THE DEGREE OF
DOCTOR OF PHILOSOPHY
IN
MARINE SCIENCES
BY
HEMA S. NAIK, M.Sc.

National Institute of Oceanography
Council of Scientific & Industrial Research
Dona Paula, Goa-403 004, INDIA.
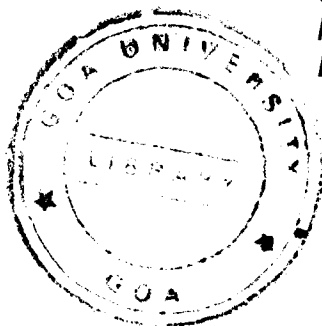
JULY 2003

574.92
————————
NAI / Ben

T - 280

CERTIFICATE

This is to certify that the thesis entitled **"Benthic nitrogen cycling with special reference to nitrous oxide in the coastal and continental shelf environments of the eastern Arabian Sea"** submitted by **Ms. Hema S. Naik** for the award of the degree of **Doctor of Philosophy in Marine Sciences** is based on her original studies carried out by her under my supervision. The thesis or any part thereof has not been previously submitted for any other degree or diploma in any university or institution.
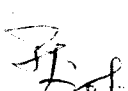
Place: Dona Paula
Date: 21 July 2003

Dr. M. Dileep Kumar
Research Guide
Scientist E-II
Chemical Oceanography Division
National Institute of Oceanography
Dona Paula-403 004, Goa

This is to certify that the suggestions made by the examiners are incorporated in the Thesis.

Prof. Jacob Chacko
Department of Chemical Oceanography
Cochin University of Science and Technology
KOCHI 682 016

STATEMENT

As required under the University ordinance 0.19.8 (vi), I state that the present thesis entitled **"Benthic nitrogen cycling with special reference to nitrous oxide in the coastal and continental shelf environments of the eastern Arabian Sea "** is my original contribution and the same has not been submitted on any previous occasion. To the best of my knowledge the present study is the first comprehensive work of its kind from the area mentioned.

The literature related to the problem investigated has been cited. Due acknowledgements have been made wherever facilities and suggestions have been availed of.

(Hema Naik)

Table of Contents

Acknowledgements

In my continuing research career, there are many people whose help and support I received so far, either volunteered or solicited. I have a great pleasure in acknowledging some of these people by name but many others in my touchy thoughts.

I am deeply indebted to Dr. S. W. A. Naqvi who has been instrumental in the conception, guidance and help in the execution of this work. It is his sustained encouragement throughout that helped me complete this work. He has been a source of inspiration and has moulded me into what I am now. I take this opportunity to express how grateful I am and owe respects to him.

I am also indebted to Dr. M. Dileep Kumar, my research guide for sustained interest, encouragement and valued guidance in my work.

I thank Dr. Ehrlich Desa, Director, National Institute of Oceanography, Goa, for his kind support, encouragement and for making necessary infrastructure facilities available for this work.

My special thanks to Dr. P.V. Narvekar for his constant encouragement and help at various stages of this work. I also thank Dr. Amal Jayakumar for familiarizing me with various analytical equipments on board ships and in the Institute. Without the much needed and timely help from Drs. Narvekar and Jayakumar, it could not have been possible for me to complete the work and meet the time targets.

I thank Prof. Karl Banse (University of Washington, Seattle), one of the pioneers in the area of study, for extensive discussions and valuable suggestions on my work.

**dedicated
to my Parents**

CHAPTER 1

Introduction

Chapter 1

Introduction

1.1 Introduction

Being an ingredient of proteins, nitrogen is an essential nutrient for all forms of life. Its speciation and chemical transformations in biogeochemical processes have played a key role in evolution of life on our planet. During the early part of the Earth's history, in the Archean atmosphere, its speciation was different from what we see today. Although dinitrogen (N_2) was, as it is today, the most stable and abundant form of nitrogen (Warneck, 1988; Kasting, 1990), the atmosphere was devoid of oxygen. Ammonification and ammonium assimilation were the two major pathways of nitrogen cycling. The anaerobic environment at that time favored the reduction of N_2 to NH_3 by N-fixing bacteria equipped with the enzyme nitrogenase. This process was of fundamental importance for supporting primitive life forms (Falkowski, 1997). Subsequently, with the evolution of organisms capable of oxygenic photosynthesis, molecular oxygen was produced and the hydrosphere and atmosphere became aerobic. The evolution of molecular oxygen gave rise to the bacterially-mediated oxidation of ammonia to nitrate (NO_3^-). This process, known as nitrification, is a crucial component of the continuing N-cycle. It consists of several reactions producing a number of intermediates of which nitrite (NO_2^-) is the most important.

1

Since the evolution of oxic conditions in the Earth's surface environment most of the combined or fixed nitrogen has been existing in the form of NO_3^-. However, the atmosphere continues to retain N_2 as its major component as well as the most abundant N species. This is because of two reasons. First, N_2 is chemically not very reactive; and secondly, nature has also provided a mechanism for the conversion of the NO_3^- to N_2, but for which all N_2 would have been fully converted to NO_3^- over geological time scales. This process, called denitrification is again mediated by bacteria that operate under anaerobic or near-anaerobic conditions. Of all the major processes involved in the nitrogen cycle, denitrification was the last to evolve (Falkowski, 1997). Denitrification and N-fixation therefore have opposing functions: one serves as a source and the other a sink of fixed nitrogen. Nevertheless, the two processes are coupled, and their balance determines the size of fixed nitrogen pool (predominantly comprising NO_3^-) in the oceanic as well as terrestrial systems, which in turn modulates photosynthetic production limited largely by the availability of fixed nitrogen.

An important chemical property of nitrogen is that it is a polyvalent element that occurs in oxidation states ranging from –3 to +5 (Table 1.1). In the organic matter nitrogen is found in the most reduced form (-3) as amino acids and their polymers, proteins. However, as pointed above, in the Earth's surface environment (soil and seawater) it is mostly present in the most oxidized form (as NO_3^-). Photosynthetic organisms must therefore reduce NO_3^- during its uptake. As the organic matter is degraded, nitrogen is first released as NH_4^+, but it is soon converted to NO_3^- by nitrifying bacteria. Of the intermediate forms N_2 (oxidation state 0) is, of course, the most stable (Fig.

Table 1.1 Nitrogen speciation and oxidation states.

Molecular formula	Oxidation number
NO_3^-	+5
N_2O_4	+4
NO_2^-	+3
NO	+2
N_2O	+1
N_2	0
NH_2OH	-1
N_2H_4	-2
NH_3	-3
NH_4^+	-3
RNH_2	-3

1.1) because of the high energy required to break the N≡N bond. Nitrous oxide (N_2O, N oxidation state +1) comes next while others [nitrite (NO_2^-, N oxidation state +3), nitric oxide (NO, N oxidation state +2) and hydroxylamine (NH_2OH, N oxidation state −1)] are largely transient species (Table 1.1).

The inability of most autotrophs to utilize the abundant N_2 owes to the fact that the responsible enzyme nitrogenase cannot function in aerobic environments. This is one handicap the N-fixing organisms have not been able to overcome in the last few billion years. Only a few organisms, mostly bacteria, have the capability to fix N_2. Some well known examples are non-symbiotic *Azotobacter* and symbiotic *Rhizobium* found in soil plants and the filamentous oceanic bacterium *Trichodesmium*.

Next to N_2, N_2O is the second most abundant species of nitrogen in the atmosphere. It is an important trace gas that plays significant roles in global warming and stratospheric ozone depletion. Aside from its reaction with ozone in the stratosphere, N_2O is quite inert in the atmosphere and also in the surface layer of the ocean. However, as it is an intermediate of the redox chemistry of the nitrogen system it is involved in chemical transformations where rapid changes in nitrogen oxidation state take place (e.g. in soils and subsurface waters).

The global nitrogen budget has been impacted over the last one-and-a-half centuries to a very large extent as a result of anthropogenic activities. The two major drivers of this change are food and energy demands. As most plants depend on fixed nitrogen for their growth, soils need to be enriched with nitrogenous nutrients. Hence, in order to boost agriculture production man has resorted to use of synthetic fertilizers. For instance, in India the
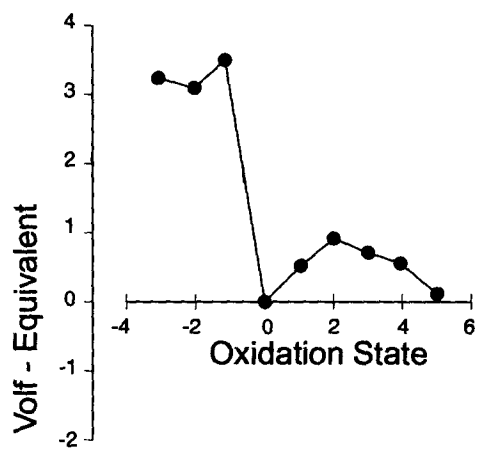
Fig. 1.1. Stability of nitrogen species in seawater
(Obtained from Wong, 1980).

consumption of nitrogenous fertilizers has increased from just about 0.05 million metric tonnes in 1951-52 to 12 million metric tonnes in 2000-2001 (Fig. 1.2). Although the enhanced production of food grains so achieved has made the country self-reliant, the excessive application of fertilizers seems to be affecting the environment and ecosystem not only on land but also in the sea. Globally, anthropogenic N-fixation is estimated to be equal to, if not more than, the natural fixation (140Tg N y^{-1}). Accordingly, the riverine fluxes of dissolved inorganic nitrogen to the ocean have gone up by a factor of 2-3 in recent times (Rabalais and Nixon, 2002). The other major perturbation is through the combustion of fossil fuel, which leads to emissions of NO_x to the atmosphere. The acidic nature of these emissions not only affects the atmospheric chemistry, but their long range transport and deposition, both wet and dry, can affect biogeochemical processes even at locations farther from their releases.

1.2 Oceanic Nitrogen Cycle

A simplified presentation of the oceanic nitrogen cycle is made in Fig. 1.3 (adopted from Codispoti et al., 2001). Nitrogen is taken up by phytoplankton in the euphotic zone mostly as NO_3^-. It is reduced to NH_4^+ through NO_2^-, a process known as the assimilatory nitrate reduction, before incorporation into the cell body. Upon death the organic material undergoes degradation during which nitrogen is first regenerated as NH_4^+. The step is referred to as ammonification. However, in the presence of O_2, NH_4^+ gets oxidized to NO_3^-, with NO_2^- as an intermediate and N_2O as a byproduct. Nitrification is mediated by microbes like *Nitrosomonas* and *Nitrobacter*. On

4
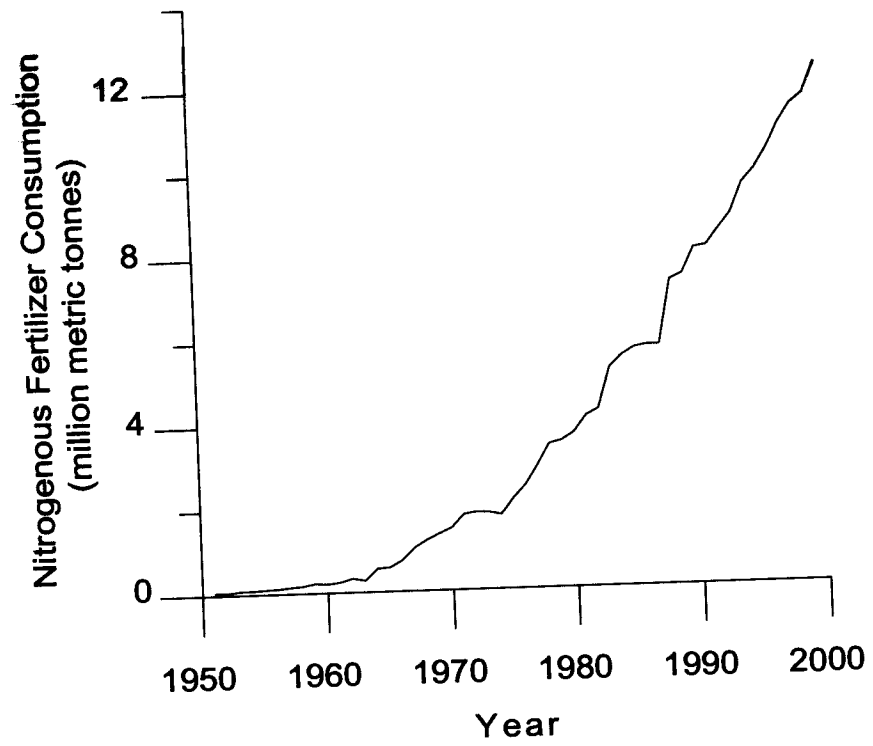
Fig. 1.2. Nitrogenous fertiliser consumption in India
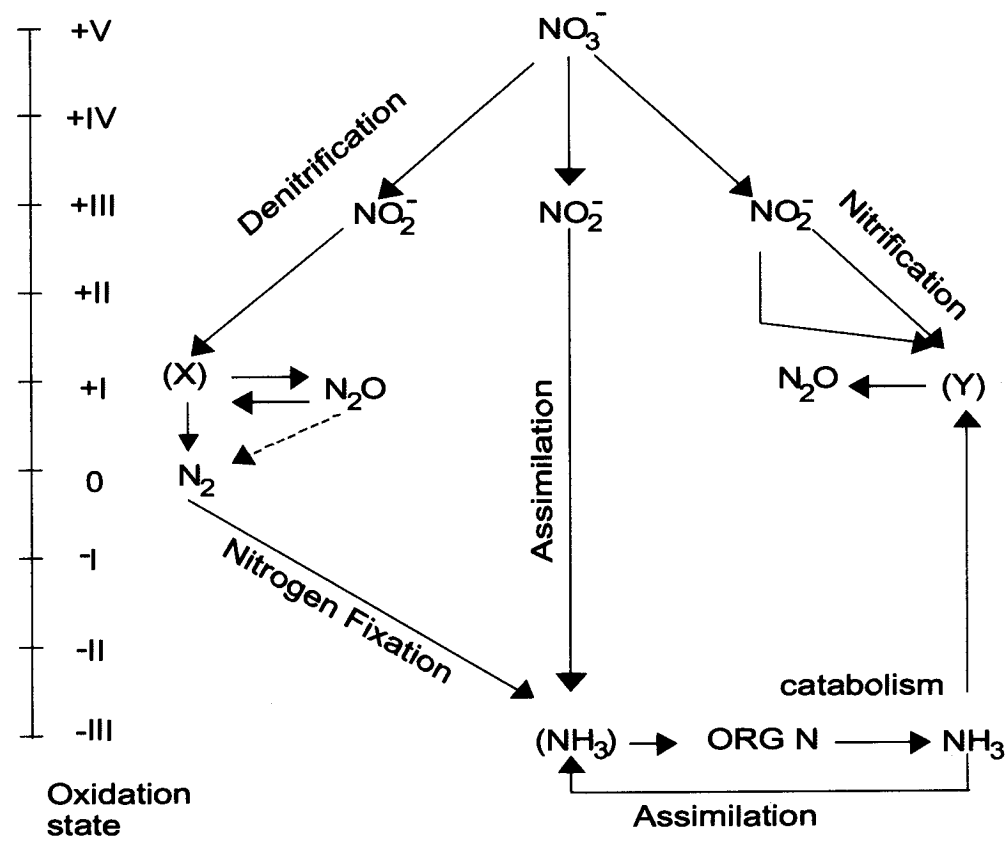
Fig. 1.3. A view of oceanic nitrogen cycle (adopted from Codispoti et al., 2001)
(X) and (Y) represent intra-cellular intermediates that do not appear to accumulate in seawater. The diagram has been modified to suggest N_2O production as well as consumption during denitrification in the sea.

the other hand, the absence of adequate oxygen supply and/or its excessive consumption arising from high organic loading may lead to the development of reducing conditions under which the facultative bacteria utilize NO_3^- as the terminal electron acceptor for the oxidation of organic matter. This process (denitrification) terminates with the production of gaseous nitrogen compounds (mostly N_2 and, to a lesser extent, N_2O), again with NO_2^- as an intermediate. Like nitrification, the denitrification is also central to global and marine nitrogen cycles. Nitrate required for this process is supplied either from the overlying water or oxic sediment surface where NH_4^+ is oxidized to NO_3^- by the process of nitrification. As an alternative process of denitrification, certain bacteria – mostly fermentative ones belonging to genera *Aeromonas, Vibrio, Clostridium* and *Desulfovibrio* – reduce NO_3^- to NH_4^+, a process known as nitrate ammonification. The significance of this process owes to the fact that unlike denitrification (which results in a loss of fixed nitrogen from the sea with important implications for oceanic productivity and atmospheric CO_2 - McElroy, 1983; Altabet et al., 1995; Ganeshram et al., 1995), nitrate ammonification enables the retention of nitrogen in the bioassimilable form. The importance of nitrate ammonification vis-à-vis denitrification in coastal marine systems has not been fully evaluated.

Nitrogen utilized by plants in the ocean belongs to one of two categories: (1) "regenerated" nitrogen that is biologically recycled within the surface layer and is available as NH_4^+ or in the dissolved organic form such as urea and also in the form of NO_3^-, and (2) "new" nitrogen added from outside the surface layer, mostly as NO_3^-, through upwelling and vertical mixing, river runoff, atmospheric deposition and nitrogen fixation (Dugdale and Goering,

1967). As stated above deposition of nitrogen from the atmosphere is also a significant source of new nitrogen to the ocean especially in offshore areas (Bange et al., 2000). For example in highly stratified oligotrophic waters the nitrogen input through rainwater (~ 10 μM) may be a significant source for primary production (Wada and Hattori, 1991). In the open ocean, the regenerated fraction accounts for the bulk of total production in the surface waters, whereas the "new" production becomes increasingly more important towards the coast. In coastal waters, nutrient exchanges with sediments must also be taken into consideration, particularly where the mixed layer touches the sea floor.

Table 1.2 reproduces the budget of fixed nitrogen in the ocean prepared by Codispoti et al., 2001. While the magnitudes of various source and sink terms of the budget are still being debated, it is almost certain that the budget is severely out of balance with the net losses from the ocean exceeding net inputs. To what extent human activities discussed above have contributed to this imbalance is not clear, but there is a good reason to believe that even prior to human interference the ocean was losing more nitrogen than received. This situation can only arise from a high denitrification rate in the oceans during the Holocene, and there is sedimentary evidence suggesting that such was also the case during most warm (interglacial) stages in the last few hundred thousand years for which sedimentary records are documented (Altabet et al., 1995, 2002). Conversely, the cold (glacial) stages have been postulated to experience an opposite imbalance (fixed nitrogen inputs to the ocean exceeding losses from it). These oscillations in the nitrogen balance of the ocean are expected to have altered the oceanic fixed

6

Table 1.2. Marine combined nitrogen budget (from Codispoti et al., 2001)

Process	Gruber and Sarmiento (1997) 10^{12}g N yr^{-1}	Codispoti et al. (2001) 10^{12}g N yr^{-1}
Sources		
Pelagic N_2 fixation	110 ± 40	110
Benthic N_2 fixation	15 ± 10	15
River Input (DN)	34 ± 10	34
River input (PON)	42 ± 10	42
Atmospheric deposition (Net)	30 ± 10	30
Atmospheric deposition (DON)		56
Total Sources	231 ± 44	287
Sinks		
Organic N export		1
Benthic denitrification	95 ± 20	300
Water column denitrification	80 ± 20	150
Sedimentation	25 ± 10	25
N_2O loss	4 ± 2	6
Total Sinks	204 ± 30	482

nitrogen inventory, oceanic productivity and consequently the atmospheric CO_2 content (Codispoti et al., 2001). Sequestration of CO_2 from the atmosphere should be lower when losses of combined nitrogen through denitrification exceed inputs from land and atmosphere (as happens today). Conversely, during periods of weak pelagic denitrification, combined nitrogen should accumulate in the ocean, stimulating new production and consequently draw-down of atmospheric CO_2; such a condition probably prevailed during glacial times. Thus nitrogen cycling in the ocean, particularly in the Arabian Sea, could well modulate global climatic changes (Altabet et al., 2002).

1.3 Significance of Nitrogen Biogeochemical Cycling in the Arabian Sea

The Arabian Sea is a small ocean basin but houses several diverse biogeochemical provinces such as eutrophic, oligotrophic and low oxygen areas. The presence of such diverse regimes within a small basin makes it an ideal natural laboratory for biogeochemical investigations.

One of the distinguishing features of the Arabian Sea oceanography is the strong seasonality in physical, chemical and biological variables due to the unique physical forcing it experiences in the form of the Southwest (SWM) and Northeast (NEM) monsoons. The mixing processes associated with these monsoons fertilizes the surface waters with essential nutrients. For example, summer upwelling can raise surface NO_3^- concentrations to 16-22 μM off Somalia, India and Oman, while winter convection can result in an enrichment of 4-6 μM NO_3^- in surface waters of the northern Arabian Sea (Naqvi et al., 2003). This greatly stimulates the growth of phytoplankton, leading to the formation of blooms. It is estimated that the annual averaged primary

production (PP) in the Arabian Sea is as high as in the North Atlantic during the spring blooms (Barber et al., 2001). The ensuing downward export of particulate organic carbon (POC) and its decomposition contribute to the maintenance of high nutrient concentrations in subsurface waters. However, as the decomposition process requires O_2, its consumption rate is high in subsurface waters of the region, and this in conjunction with limited O_2 supply (arising from the blocking of the northern Indian Ocean by the Asian land mass at low latitudes, ~25°N) leads to the formation of the thickest and the most intense oxygen minimum zone (OMZ) found in any oceanic basin. The OMZ, located in the depth range ~150-1000 m, has $O_2 < 0.1$ ml l^{-1} (~4 μM). The most O_2-deficient waters are found north of ~12°N the approximate position of the zero wind stress curl (Warren, 1994).

The subsurface O_2 deficiency makes a tremendous impact on nitrogen cycle. Due to the near total absence of O_2, denitrification sets in a layer of 150-600 m. Denitrification occurs round the year within this layer over a well defined geographical area in the central and northeastern Arabian Sea (Naqvi, 1991). Such environments that experience denitrification but not sulphate reduction are generally termed as 'suboxic'. There are two other major sites in the ocean that also experience the mid-depth suboxia of the magnitude and intensity observed in the Arabian Sea: the eastern tropical North Pacific (ETNP – off Mexico-Panama) (Cline and Richards, 1972; Codispoti and Richards, 1976) and the eastern tropical South Pacific (ETSP - off Chile-Peru) (Codispoti and Packard, 1980; Codispoti and Christensen, 1985). What makes the Arabian Sea different from these two regions, however, is that the zone of most intense denitrification is geographically

8

separated from the zones of intense upwelling and high primary productivity in the western Arabian Sea (Naqvi 1991). This is because for denitrification to occur, as identified from the accumulation of secondary NO_2^-, O_2 concentration must fall below an abruptly-defined threshold value of ~ 1 μM (~0.02 ml l^{-1}; Morrison et al., 1999; Naqvi et al., 2003). Outflows from the Red Sea and the Persian Gulf and advection of waters from the south in the western Arabian Sea generally keep minimum O_2 levels marginally above this threshold (Naqvi et al., 2003). A seasonal undercurrent bringing relatively oxygenated waters from the south during the SWM similarly suppresses denitrification just off the Indian continental margin (Naqvi et al., 1990).

Unlike the more intense upwelling zones of the western Arabian Sea suboxic conditions develop seasonally (during late summer and autumn) associated with modest upwelling in the eastern Arabian Sea. But these conditions are confined to the inner and mid-shelf region and cannot be considered analogous to the suboxic zone off Peru that extends offshore from the coastal waters (Codispoti and Packard, 1980). In fact, in the Arabian Sea the coastal and offshore suboxic systems are always separated. Although short lived, denitrification over the Indian shelf is far more intense and often leads to complete NO_3^- utilization and the onset of sulphate reduction. The present study focuses largely on this shallow system.

1.4 Previous Work

The Arabian Sea was first observed to experience intense oxygen depletion in subsurface waters during the John Murray Expedition (1933-34); that is also found to affect nitrogen cycling (Gilson, 1937). This was the first

observation of its kind anywhere in the oceans. It is surprising that the follow up studies to investigate these effects in detail were not undertaken until the 1970s. Wyrtki (1971) provided detailed maps of the distributions of nutrients (including nitrate but not nitrite) along various horizontal and vertical sections based on extensive data collected during the International Indian Ocean Expedition (IIOE). These led to the realization of the extent and intensity of the oxygen minimum and also showed that NO_3^- concentrations in intermediate layers are much lower in the Arabian Sea than in the Bay of Bengal (see, for example, NO_3^- distribution at 300 m). Even prior to that, in his classical treatment of anoxic basin and fjords, Richards (1965) had made a mention of the Arabian Sea as an open ocean denitrification site. However, it was left to Sen Gupta and coworkers (Sen Gupta et al., 1976 a, b) to initiate the first major investigation and show evidence on pelagic denitrification in the region.

Following the approach of Cline and Richards (1972) in the ETNP that is based on the Redfield-Ketchum-Richards (RKR) model (Redfield et al., 1963), Sen Gupta et al. (1976 a, b) provided the first estimates of NO_3^- losses resulting from denitrification. They calculated deficits amounting to ~25 μM and the process to extend to ~4°N. These results have been questioned by Deuser et al. (1978) who computed NO_3^- losses from NO_3^--salinity relationship. The deficits computed by these authors were lower by a factor of 3 and limited the southern boundary to ~14°N. Deuser et al. (1978) are the first to quantify the denitrification rate. This estimate (range between 0.1 and 1 Tg N y^{-1}; 1 Tg = 10^{12} g) has been arrived at first by calculating the inventory of NO_3^- deficits and then dividing it by the renewal time. Results of Deuser et al.

(1978) are, in turn, countered by Naqvi et al. (1982) who argued that the NO_3^--salinity relationship led to an underestimation of NO_3^- deficits. The deficits computed by Naqvi et al. (1982) are intermediate to the earlier two estimates. The process has been found to extend to 12°N in the south with the overall rate of 3.2 Tg N y^{-1}.

Naqvi and Sen Gupta (1985) introduced the use of the nitrate tracer NO (defined as $O_2+8.65^*NO_3^-$ following Broecker, 1974) to compute NO_3^- losses from potential temperature, nitrate and O_2 values and obtained both NO_3^- deficits and rate (5 Tg N y^{-1}) which agreed with those of Naqvi et al. (1982). This procedure has also been followed by Naqvi (1987), but he combined the estimated deficits with dynamic computations and diffusion coefficients (cf. Codispoti and Richards, 1976) and estimated a much higher denitrification rate (~30 Tg N y^{-1}). Except for the estimate by Mantoura et al. (1993), who estimated the denitrification rate to be 12 Tg N y^{-1}, most of the subsequent estimates are consistent with that of Naqvi (1987): Naqvi and Shailaja (1993) estimated denitrification rate to be 24-33 Tg N y^{-1} from the activity of respiratory electron transport system (ETS; cf. Codispoti and Packard, 1980); Howell et al. (1997) combined his estimates of NO_3^- deficit with the chorofluorocarbon (CFC)-derived ages to arrive at 21 Tg N y^{-1}; and a one-dimensional model employed by Yukashev and Neretin (1997) led to a rate of 34 Tg N y^{-1}. Most recently, Bange et al. (2000) have reviewed all data and based on a new set of measurements proposed a rate of 33 Tg N y^{-1}.

Naqvi et al. (1990) investigated the temporal variability of denitrification and found substantial seasonal oscillations in denitrification along the Indian continental margin. This was attributed to the presence of an undercurrent

11

that supplies oxygen to intermediate layers in this region; the supply of which is associated with the SWM circulation. Understandably lower deficits were found during this season. Otherwise, geographical boundaries of the denitrifying zone, demarcated by Naqvi (1991) based on the occurrence of NO_2^-, appear to be fairly stable. It was pointed out by Naqvi (1987) that the most intense denitrification occurs in the open Arabian Sea outside the continental shelf. This represents a departure from the pattern seen in the other two major denitrifying sites of the Pacific Ocean where denitrification begins from the continental shelf. Naqvi (1991) estimated the area of the denitrification zone to be 1.37×10^6 km^2.

Naqvi et al. (1993) found an intermediate nepheloid layer (INL) associated with denitrification in the Arabian Sea. As in case of the Pacific denitrifying sites (Garfield et al., 1983; Spinrad et al., 1989) the INL in the Arabian Sea also contained a particle protein maximum and a bacterial biomass maximum. Like the secondary nitrite maximum (SNM), the INL was also found to intensify offshore. It was concluded that the INL was not formed through the lateral advection of the bottom nepheloid layer from the continental margin. Instead, it was proposed that the INL was formed due to proliferation of denitrifying bacteria that presumably used the dissolved organic carbon as a carbon source.

That N_2 is the end product of denitrification has also been demonstrated by results of measurements of the N_2/Ar ratio in seawater. This ratio shows a prominent maximum coinciding with the SNM indicating the presence of excess N_2 arising from nitrate reduction (Codispoti et al., 2001). In fact the quantity of excess N_2 estimated from the ratio appears to be

substantially higher than the maximal NO_3^- deficit. This led Codispoti et al. (2001) to suggest that the deficits-based approaches might underestimate the extent of denitrification, which could be as much as 60 Tg y^{-1}.

Measurements of stable isotope abundance ($\delta^{15}N$, a measure of $^{15}N/^{14}N$ ratio) in NO_3^- and N_2 provide additional evidence for the reduction of NO_3^- to N_2 (Brandes et al., 1998). This approach is based on the observation that various biologically mediated processes involve mass-dependent fractionation of isotopes as a result of which the lighter isotopes are generally consumed preferentially and the residual reactants are enriched with heavier isotopes. For the two natural isotopes of nitrogen (^{14}N and ^{15}N), NO_3^- containing ^{14}N is lost more easily than that containing ^{15}N during denitrification. Consequently N_2, the end product of denitrification, gets depleted with ^{15}N while an enrichment of this isotope takes place in the residual NO_3^-. Such has been found to be the case: within the core of the SNM the $\delta^{15}N$ of NO_3^- has been found to reach up to 15‰ while the $\delta^{15}N$ of N_2 concomitantly decreased to 0.2 ‰ (Brandes et al., 1998). Using these data Brandes et al. (1998) computed the fractionation coefficient to be 25-28‰.

As stated earlier, suboxic conditions also develop seasonally in shallow subsurface waters over the western continental shelf of India. The O_2-deficiency is most severe in late summer when the entire shelf is covered by waters with $O_2 < 0.5$ ml l^{-1} (22 μM). The factors responsible for the occurrence of O_2-deficient conditions are primarily of natural origin and have been recognized for quite some time (Banse, 1959; Carruthers et al., 1959). However, these conditions have intensified in recent years as shown by Naqvi

et al. (2000). The complete nitrate consumption and accumulation of hydrogen sulphide provides strong evidence for the intensification of reducing conditions, which had not been reported previously from the Arabian Sea. It is likely that fertilizer inputs from land have further enhanced the naturally high PP rates in coastal waters bringing about an ecosystem shift in recent years, but subtle changes in hydrography cannot be excluded as an additional or alternative cause.

1.5 Nitrous Oxide cycling

N_2O is an important intermediate of denitrification and a byproduct of nitrification. In the stratosphere N_2O reacts with O_3 and forms 'NO' radical thereby depleting stratospheric ozone (Andrea and Crutzen, 1997; Nevison and Holland, 1997). It also affects the atmospheric radiation balance because it has a global warming potential about ~ 200 times greater than CO_2 on a molecular basis. The atmospheric concentration of N_2O is currently rising at a rate of 0.2-0.3% per year. These observations have led to several studies to better quantify sources and sinks of atmospheric N_2O. The oceans play an important role in this regard accounting for one-third of the natural inputs to the atmosphere (Nevison et al., 1995). However, N_2O flux to the atmosphere is not uniformly distributed over the oceanic surface and the tropical upwelling zones containing O_2-deficient waters make a disproportionately large contribution (Codispoti and Christensen, 1985; Suntharalingam and Sarmiento, 2000). This is because the low O_2 conditions favour greater production of N_2O, through both nitrification and denitrification (Codispoti and Christensen, 1985; Suntharalingam and Sarmiento, 2000). The intense

14

reducing conditions within the SNM of the open ocean suboxic zone force N_2O to serve as an electron acceptor for respiration of organic matter resulting in low N_2O concentrations (<10 nM). However, the peripheries of the SNM are always characterized by N_2O accumulation, which supports a high rate of N_2O supply to the surface layer. This pattern, characteristic of all oceanic suboxic zones (Cohen and Gordon, 1978), was first reported from the Arabian Sea by Law and Owens (1990) and Naqvi and Noronha (1991). It has been confirmed by several subsequent studies undertaken in the region (Bange et al., 1996, 2001; de Wilde and Helder, 1997; Lal and Patra, 1998; Patra et al., 1999; Upstill-Goddard et al., 1999). These studies have established that the Arabian Sea is an important area for emissions of N_2O to the atmosphere. However, estimates of total N_2O-flux from the region stretch over a wide range (0.16-1.5 Tg N_2O y^{-1}; Law and Owens, 1990; Naqvi and Noronha, 1991; Bange et al., 1996, 2000; Lal and Patra, 1998; Upstill-Goddard et al., 1999). Recently, the range has been narrowed down to 0.33-0.70 Tg N_2O y^{-1} by Bange et al. (2001) who have synthesized all data available from the region. This work revealed that the fluxes are dominantly contributed by coastal regions during the SWM. However, this study did not take into consideration recent measurements from the west coast of India that have revealed the highest concentrations recorded anywhere in the ocean.

1.6 Geographical Setting

The Arabian Sea forms the northwestern arm of the Indian Ocean. It is bounded by the African and Asian landmass in the west and by Asia in the north and east. Unlike these natural boundaries, the southern boundary

15

separating the Arabian Sea from the greater Indian Ocean is arbitrarily defined. For the oceanographic purpose it is generally taken to run from Goa (India) along the western side of the Laccadive and Maldive Islands to the equator and then slightly to the south to Mombassa (Kenya) (Schott, 1935). The region so demarcated occupies an area of 6.225×10^6 km^2. It does not include the Gulfs of Aden and Oman, through which the Arabian Sea is connected to two Mediterranean-type marginal seas – Red Sea and Persian Gulf, respectively. Also excluded by the above demarcation is the Laccadive Sea, a smaller water body (area 0.23×10^6 km^2) that lies to the east of the Laccadive islands. However, oceanographers often do not make a distinction between the Arabian Sea and the Laccadive Sea, especially while dealing with the processes along and off the continuous west coast of India. Such a distinction will not be made in this study either.

The most prominent bathymetric feature of the Arabian Sea is the northwest-southeast trending Carlsberg Ridge that divides the Arabian Sea into two major and deep (>4000 m) basins - the Arabian Basin in the northeast and the Somali Basin in the southwest. A deep passage in the Owen Fracture Zone connects the two basins. While almost the entire Arabian Basin is located within the Arabian Sea, a large portion of the Somali Basin falls outside. The latter is, in turn, serially connected to the Mascarene, Madagascar and Crozet Basins. A less pronounced feature is the Murray Ridge that extends southwest from the Makran margin to join the Carlsberg Ridge thereby separating the Arabian Basin from the relatively narrow and shallow (<2000 m) Oman Basin. The continental shelf is generally wide (often exceeding 100 km west of Karachi) along the Pakistani coast and all along the

16

Indian west coast with the maximal width (350 km) occurring off the Gulf of Cambay. Elsewhere the shelf width rarely exceeds 40 km (Fig. 1.4).

1.7 Climate

The climate of the North Indian Ocean region is strongly influenced by its proximity to landmasses. The Indian Ocean is the only ocean that is terminated at low latitudes (~25°N) due to presence of land in the north. This gives rise to the unique phenomenon of periodic reversal of winds, which is usually referred to as monsoon system. The excessive heating of land as compared to the sea during summer causes the development of low pressure zone over land, driving strong southwesterly winds. Opposite conditions prevail during winter when northeasterly winds blow from the continent to the sea. Of the two monsoons, the SWM is far more energetic. It starts in the month of June and lasts till September. During this period wind speeds frequently exceed 30 knots, especially along a strongly sheared low-level atmospheric jet (the Somali Jet that is often referred to as Findlater jet – Findlater, 1971), the axis of which extends toward the northeast from the Somali coast. The NEM begins in November and continues through March. The winds are lighter during this season. The periods intervening the two monsoons – March to May and October to November – are referred to as Spring Inter-monsoon (SI) and Fall Inter-monsoon (FI), respectively. These transition months are characterized by weak, slowly-reversing winds.

Almost all of the rainfall over the Arabian Sea occurs during the SWM that may exceed ~300 cm y^{-1} along its eastern shores. The amount of precipitation decreases towards the northwest, and so the balance between

17
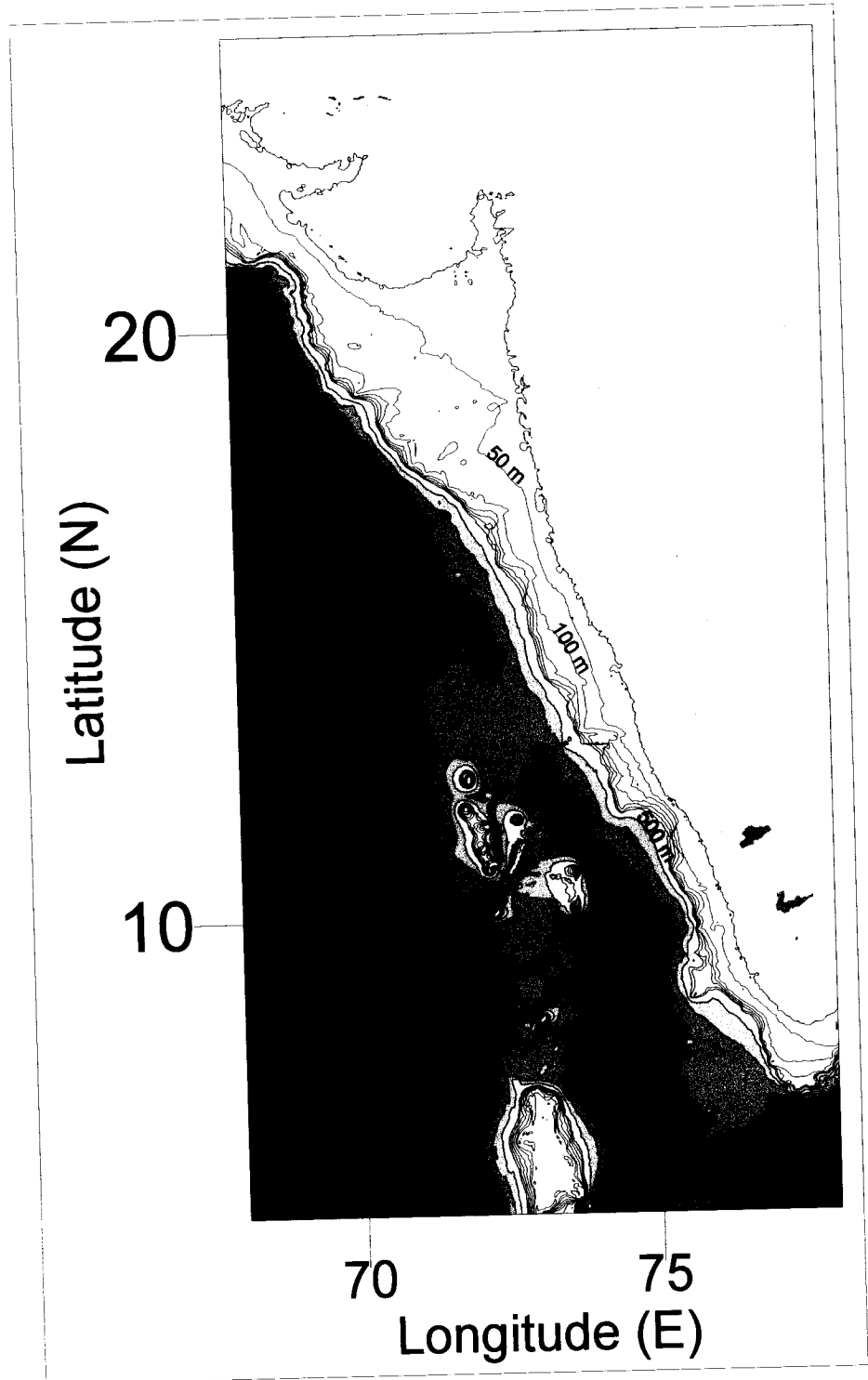
Fig. 1.4 Bathymetry of eastern Arabian Sea

evaporation and precipitation (E-P) is at its maximum off the Arabian coast and its minimum along the Indian west coast. The Arabian Sea does not receive much river runoff, the combined discharges by the main rivers (the Indus, the Narmada and the Tapti), all draining in the northeastern Arabian Sea; probably do not exceed 200 $km^3 y^{-1}$. However, there are scores of other small rivers originating in the Western Ghats (a mountain range separating the narrow western coastal plain from the Deccan Plateau and interior areas), which together may transport about 150 km^3 of freshwater annually (most of it during the SWM period; Dr. S.R. Shetye, personal communication). The large rainfall and land runoff combine to result in a positive water balance (excess of precipitation and runoff over evaporation) over a few hundred kilometer wide belt along the Indian coast. The net water balance is negative elsewhere making it a climatic feature of the Arabian Sea as a whole. Consequently, the surface waters are the least saline in the southeast and the most saline in the northwest (Wyrtki, 1971).

1.8 Importance, Objectives and Scope of the Study

While nitrogen cycling in the offshore suboxic zone has been studied in great detail over the past 25 years, as described above, very little information is available from the suboxic system over the shelf. Aside from its seasonal occurrence, the coastal system is expected to function differently from the deeper O_2-deficient zone for a variety of reasons. For instance, due to the high biological productivity and shallow depths the POC settled on the seafloor remains available for decomposition and denitrification is not limited by the supply of organic carbon. This along with the higher ambient

temperatures should result in higher denitrification rates as compared to the open ocean. Secondly, due to the proximity of land, the impact of anthropogenic activities mentioned above will be much greater in the coastal environment. The enhanced nutrient inputs through both eolian and fluvial pathways are expected to lead to coastal eutrophication. Whereas such eutrophication is occurring globally, its impact on the coastal environment of the eastern Arabian Sea is expected to be a lot more severe due to the already existing naturally-caused O_2 depletion. Finally, as the suboxic waters are directly in contact with the sediments the exchanges of material across the sediment water interface are extremely important. The settling and burial of copious amounts of organic matter are expected to result in high rates of respiration including denitrification and sulphate reduction in the continental margin sediments. This issue is important because benthic denitrification can counter to some extent the effect of coastal eutrophication. However, practically nothing is known about the role of coastal sediments in biogeochemical cycling in the Arabian Sea. In fact, there are no published measurements on the rate of sedimentary denitrification not only from the Arabian Sea but also from the Indian Ocean as a whole. The present study was therefore aimed to collect the much-needed data and gain insights into nitrogen biogeochemical cycling in this unique environment.

The main objectives of the study are:

i)   To understand the physical and biological processes leading to the development of O_2-deficient conditions in near-bottom waters over

the western continental shelf of India and to investigate their variability in space and time,

ii) To assess the impact of O_2-deficiency on benthic nitrogen cycling especially N_2O production and consumption,

iii) To quantify the rates of denitrification in water column and shelf sediments and evaluate the impact of coastal eutrophication, and

iv) To improve understanding of pathways of nitrogen transformations in the shallow O_2-depleted environments.

In order to fulfill these objectives extensive measurements were carried out and the results are presented here. The organization of the thesis is as follows:

Chapter 2 provides details about the field work, techniques used for the collection and handling of samples and their analyses on board research vessels and in the shore laboratory.

Chapter 3 gives the salient feature of the hydrography and circulation in the Arabian Sea highlighting the seasonal changes that affect the biogeochemical cycling over the western continental margin of India.

Chapter 4 presents the results of observations made during various seasons along a number of cross-shelf sections off the west coast of India, as well as along a more-frequently-visited shallow (depth < 30 m) section off Candolim (Goa). The latter are used to construct the first-ever complete picture of seasonality of oceanographic variables, including the evolution of the O_2-deficiency in shallow waters, in response to the monsoonal forcing. An

assessment of inter-annual changes in the suboxic conditions is also made. Also presented for the first time are data on primary productivity based on in-situ measurements of ^{14}C uptake. An estimate of the denitrification rate in the water column is made and the flux of N_2O to the atmosphere is quantified.

Chapter 5 examines the relationships between biogeochemical variables in order to gain insights into pathways of nitrogen transformations. The first ever data on the isotopic composition of NO_3^- from the shallow suboxic zone are also used and compared with those from the open ocean.

Chapter 6 deals with sedimentary nitrogen cycling. Experimental details of incubation of sediment cores for measurements of denitrification rates and of benthic flux measurements are also given. Results of sedimentary denitrification rate determined with the acetylene block technique are presented. Porewater profiles of NO_3^-, NO_2^- and NH_4^+ are also included as are the N_2O profiles to assess whether the sediments serve as a net source or sink of N_2O for the overlying water column. Porewater profiles of NO_3^- are used in a one-dimensional model, and the first ever data on benthic fluxes obtained with an indigenous benthic chamber are presented and discussed.

Chapter 7 summarizes the major findings of the study and makes recommendations for future research.

CHAPTER 2

Material and Methods

Chapter 2

Material and Methods

2.1 Introduction

In the present study the strategies adopted were to a) cover study area extensively in time and space b) to conduct experiments in field and laboratory and c) to sample diverse sedimentary environments for benthic rate estimations. The field data collection and experiments were undertaken during the period from 1997 to 2002. The data for the period 1987 to 1996 were the archived sets available with our group. The detailed descriptions of sampling and material and methods are given below:

2.2 Field Observations

2.2.1 Oceanic Expeditions

Twenty four cruises on the board research vessels ORV Sagar Kanya, FORV Sagar Sampada, CRV Sagar Sukti and AA Sidorenko were organized over the five year period (Table 2.1). With the exception of one cruise (SK148), in which some observations were also made in the Bay of Bengal, all cruises focused on the western Indian continental margin. Attempts were made to collect data in all seasons with a particular emphasis to cover the period when the O_2-deficient conditions are most severe along the west coast of India. Data from a total of 294 stations were utilized. The locations of the stations occupied were shown in Fig. 2.1.

Table 2.1. List of cruises undertaken to collect data used in the present study.

Sr. No.	Vessel	Cruise No.	Period	Season
1.	ORV Sagar Kanya	34	6.7-8.8.1987	SWM
2.	ORV Sagar Kanya	38	7.1-6.2.1988	NEM
3.	FORV Sagar Sampada	98	9-27.2.1992	NEM
4.	FORV Sagar Sampada	118	3-23.3.1994	SI
5.	FORV Sagar Sampada	128	19-29.1.1995	NEM
6.	ORV Sagar Kanya	103	26.6-15.7.1995	SWM
7.	FORV Sagar Sampada	136	10-19.9.1995	SWM
8.	FORV Sagar Sampada	141	24.4-14.5.1996	SI
9.	FORV Sagar Sampada	158	24.8-2.9.1997	SWM
10.	FORV Sagar Sampada	161	29.12-21.1.1998	NEM
11.	ORV Sagar Kanya	137	20.7-7.8.1998	SWM
12.	ORV Sagar Kanya	138	1.9-4.10.1998	FI
13.	ORV Sagar Kanya	140	1-28.12.1998	NEM
14.	ORV Sagar Kanya	148	13.9-10.10.1999	FI
15.	ORV Sagar Kanya	149	2-8.12.1999	NEM
16.	CRV Sagar Sukti	PI 1	12-14.9.2001	SWM
17.	CRV Sagar Sukti	PI 2	17-23.9.2001	SWM
18.	CRV Sagar Sukti	1	5-10.10.2001	FI
19.	CRV Sagar Sukti	6	26-26.10.2001	FI
20.	CRV Sagar Sukti	12	19-21.12.2001	NEM
21.	CRV Sagar Sukti	22	13-15.5.2002	SI
22.	AA Sidorenko	42	14.2-6.3.2002	NEM
23.	ORV Sagar Kanya	180	19.8-3.9.2002	SWM
24.	CRV Sagar Sukti	24	18-21.9.2002	SWM
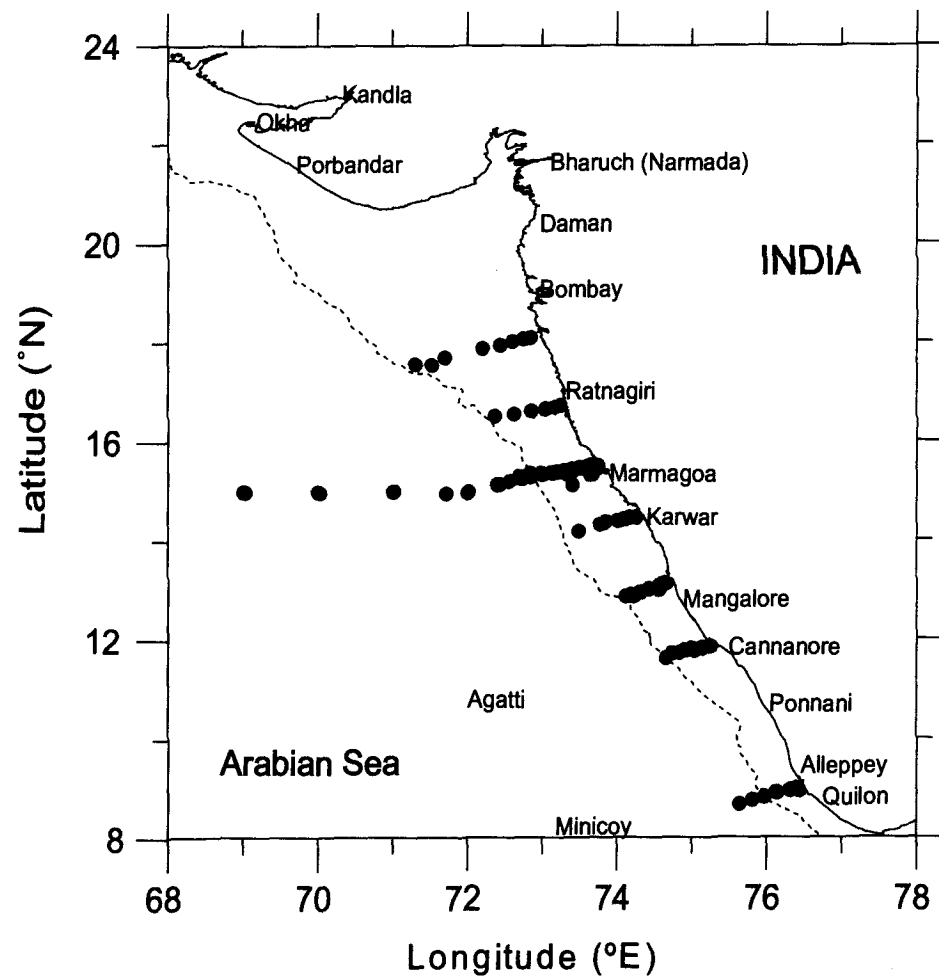
Fig. 2.1. Station locations

2.2.2 Coastal Expeditions Off Goa

Frequent trips were made along a shallow section of 5 stations (depth 6-30 m) off Candolim (Goa) using mechanized trawlers. The transect (Fig. 2.2) was sampled on 29 occasions from 1997 to 2002. The observations were not periodic, as the sampling could not be made during the early SW monsoon following a ban on boat traffic by The Captain of Ports, Government of Goa because of heavy weather. Nevertheless, the period of most intense O_2-deficient conditions (August-November) was covered – generally once but at times twice or thrice in a month - during the five-year study period. The details of the coastal cruises were shown in Table 2.2. The deepest station of the Candolim section was repeated in most of the open ocean expeditions so as to study the quasi-time series variability in oceanographic parameters.

2.2.3 Field (Benthic chamber) experiment

The benthic chamber experiment was carried out twice in estuarine waters of Goa. Experimental details are given in Chapter 6.

2.3 Laboratory (Incubation) Experiments

Sedimentary denitrification rates were determined through deck incubations aboard ORV Sagar Kanya on two occasions. The locations of the cores collected during the cruises are shown in Fig. 2.3, details listed in Table 2.3 and in Chapter 6.

23

Table 2.2. List of Coastal cruises undertaken off Candolim (Goa).

Field trip ID	Sampling Date
Candolim 1	4.9.1997
Candolim 2	18.9.1997
Candolim 3	3.10.1997
Candolim 4	21.4.1998
Candolim 5	19.5.1998
Candolim 8	17.9.1998
Candolim 9	21.9.1998
Candolim 10	26.9.1998
Candolim 11	14.10.1998
Candolim 12	5.11.1998
Candolim 13	11.11.1998
Candolim 14	2.2.1999
Candolim 15	15.4.1999
Candolim 16	17.8.1999
Candolim 17	26.8.1999
Candolim 18	22.9.1999
Candolim 19	11.11.1999
Candolim 20	23.12.1999
Candolim 21	30.3.2000
Candolim 22	12.9.2000
Candolim 23	29.9.2000
Candolim 24	28.3.2001
Candolim 25	2.5.2001
Candolim 26	18.5.2001
Candolim 27	27.11.2001
Candolim 28	5.9.2002
Candolim 29	20.11.2002
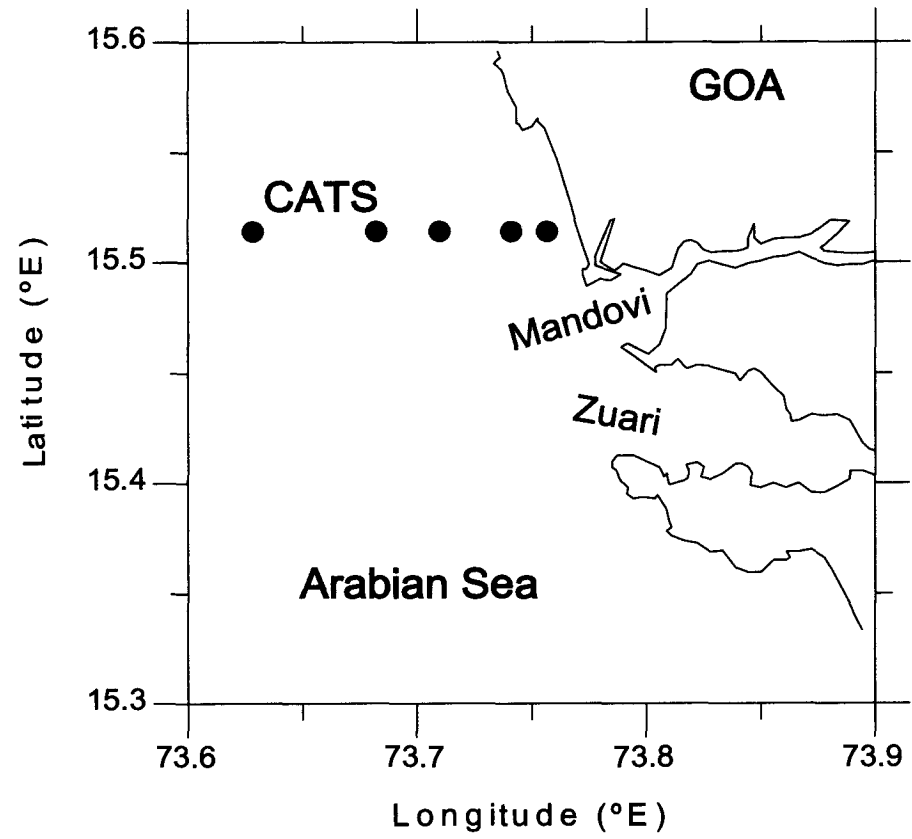
Fig. 2.2. Time series transect off Candolim (CATS, Goa)

Table 2.3. List of sediment cores and their locations.

Sr. No.	Cruise No.	Date	Core No.	Latitude (°N)	Longitude (°E)	Water Depth (m)
1	SK – 148	4.9.99	1b	13.016	80.616	150
2	SK – 148	20.9.99	15b	14.890	72.970	300
3	SK – 148	22.9.99	19b	15.400	73.197	76
4	SK – 148	22.9.99	20b	15.516	73.649	23
5	SK – 149d	3.12.99	2	15.512	73.598	29
6	SK – 149d	6.12.99	16	17.558	71.217	27
7	SK – 149d	7.12.99	19	17.949	72.428	39
8	SK – 149d	8.12.99	22	17.090	72.937	43
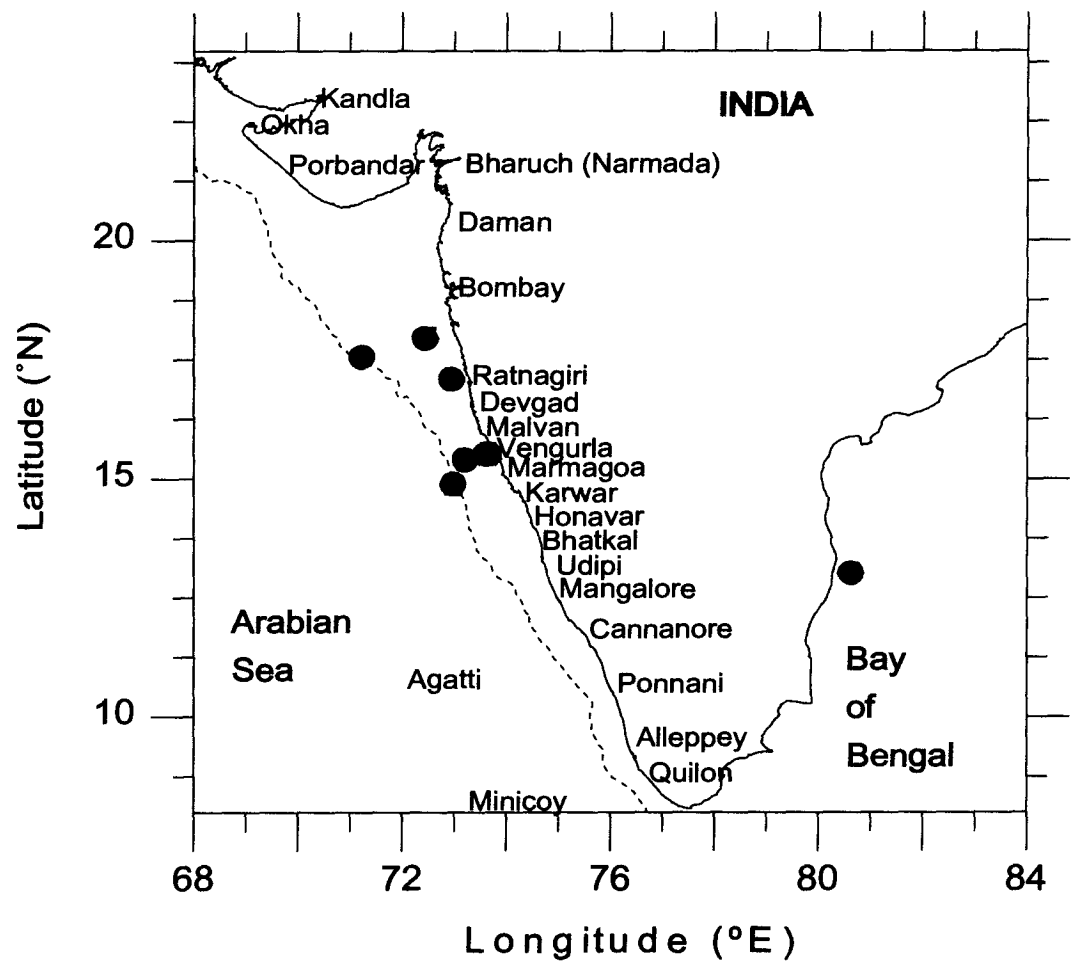
Fig. 2.3. Sampling locations of sediment cores during SK 148 (red circles)
and SK 149d (blue circles).

2.4 Methodology

2.4.1 *Experimental*

2.4.1.1 Sampling and Analysis

In deep sea cruises water samples were collected from selected (mostly standard) depths covering the entire water column (down to bottom) using either Go-flo or Niskin samplers (5/10 - litre capacity) mounted on rosette fitted to Sea-bird CTD (conductivity-temperature-depth, No. SBE 9/11). Temperature and conductivity sensors in the CTD units allowed continuous profiling of these properties. In some cases fluorescence sensor was also used for recording chlorophyll profiles. The salinity and chlorophyll data derived from the in-situ sensors were calibrated through analyses of discrete samples in the laboratory. Temperature recorded by probes was occasionally verified by using reversible thermometers.

Eventhough a portable CTD was generally used during expeditions to coastal and estuarine regions the sharp vertical gradients necessitated (for a check) measurements of temperature with reversible thermometer and analysis of salinity with an Autosal salinometer (model 8400).

The salinity samples were collected in glass bottles after a thorough rinsing (three times) and filled up to the shoulder. The neck of the bottle was dried with a tissue paper so as to avoid salt deposition. The bottles were then capped tightly and kept in a temperature-controlled room until anlaysis.

The samples collected for chemical analyses were first sampled for dissolved gases (O_2, H_2S, N_2O) and then for nutrients. While sampling for dissolved gases, utmost care was taken to avoid any atmospheric

contamination. Chemical analyses of discretely-collected water samples for O_2, hydrogen sulphide (H_2S), and nutrients (NO_3^-, NO_2^-, NH_4^+ and PO_4^{3-}) were performed on board ships whereas those samples collected during the coastal field trips were done in the shore laboratory. N_2O samples were preserved with $HgCl_2$ and analyzed either on board ship or in the shore laboratory.

The primary production was measured at two stations (cruise of CRV Sagar Sukti PI-1) through in-situ incubation of water samples spiked with ^{14}C-labelled bicarbonate. The samples were filtered on the shipboard and analyzed in the shore laboratory. Samples for chlorophyll-a were collected at several stations both during research cruises and field trips, filtered (on board research vessels) and analyzed in the shore laboratory.

2.4.1.2 Dissolved Oxygen

Dissolved oxygen was estimated by the titrimetric Winkler method as modified by Carpenter (1965). The principle of the method is as follows.

The dissolved oxygen in seawater was made to oxidize Mn (II), under strongly alkaline medium, to Mn (III). In the presence of excess iodide Mn (III) liberates iodine on acidification. The iodine released was titrated against sodium thiosulphate. The amount of O_2 was calculated from the thiosulphate consumed.

The dissolved oxygen samples collected during the benthic chamber experiment were estimated colorimetrically. Colorimetric estimation of dissolved oxygen was made according to the method given by Pai et al. (1993). In case of Winkler method the liberated iodine was titrated against

thiosulphate whereas in colorimetric method the iodine was estimated through its absorption at 456 nm. The colorimetric method is more precise particularly for samples containing low O_2 concentrations.

2.4.1.3 Nutrients

All nutrients analyses were done using an automated SKALAR segmented flow analyzer (Model 5100-1) and following the principles discussed in Grasshoff et al. (1983). The primary standards for analysis were prepared in bulk and stored aseptically in ampoules to maintain uniformity.

2.4.1.3.1 Nitrite and Nitrate

The estimation of nitrite in seawater was based on its reaction with an aromatic amine that led to the formation of a diazonium compound, which on coupling with a secondary aromatic amine forms an azo dye (Bendschneider and Robinson, 1952). The absorbance of the pink colored azo dye is measured at 540 nm. The nitrate in seawater was determined based on the reduction of nitrate to nitrite in a reductor column filled with copper-amalgamated cadmium granules following which nitrite was determined via the formation of an azo dye (Grasshoff, 1969). The reduction conditions were maintained using ammonium chloride buffer in such a way that nitrate was almost quantitatively converted to nitrite but not further. The principal reaction that takes place is

$$NO_3^- + Me_{(S)} + 2H^+ \rightarrow NO_2^- + Me^{2+} + H_2O$$
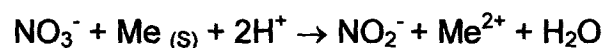
2.4.1.3.2 *Ammonia (NH_4^+ + NH_3)*

Ammonia estimation was based on the improved method given by Koroleff (1970). Ammonia dissolved in seawater reacts with hypochlorite under moderately alkaline conditions forming monochloramine, which in the presence of nitroprusside (as catalyst), phenol and excess hypochlorite forms indophenol blue. The ratio of phenol:active chlorine must be constant and should be close to 25 w/w which otherwise will affect (bleach) the color intensity. The blue colour of the indophenol was then measured at a wavelength of 630 nm.

2.4.1.3.3 *Phosphate*

Inorganic phosphate was estimated by the method given by Koroleff (1963). Phosphate ions in seawater were made to react with acidified molybdate to yield a phosphomolybdate complex, which was then reduced to highly coloured blue compound by ascorbic acid. The absorbance of formed phosphomolybdenum blue was measured at 880 nm. To avoid the interferences from silicate, the pH of the final reaction was less than 1 and the ratio of sulphuric acid to molybdate was maintained between 2 and 3.

2.4.1.4 Hydrogen Sulphide

Hydrogen sulphide was estimated spectrophotometrically by methylene blue method by Fonselius (1962). The method is based on dimethyl-*p*-phenylene diamine reaction in acidic medium with ferric chloride to form an indammonium salt (Bindshedler's green), an intermediate. The product then combines with hydrogen sulphide yielding a thiazine dye (methylene blue). This compound's maximal absorbance occurs at 670 nm.

2.4.1.5 Nitrous Oxide

The estimation of N_2O was carried out by multiple phase analysis as given in McAuliff (1971). An aliquot of 25 ml of seawater sample was taken in 100 ml air-tight syringe that was previously flushed with helium gas to avoid atmospheric contamination. An amount of 25 ml of helium gas was injected into the syringe. During the transfer of both the water sample and helium gas utmost care was taken to avoid contact with atmosphere. The sample was equilibrated for 5 min by vigorous shaking on a mechanical shaker. The N_2O released from water into the headspace was dried by passing over a moisture trap (10cm long, 1cm wide). The sampled gas was then introduced in to the HP 5890 Series II Gas Chromatograph (via a 6-port valve) containing a stainless steel column packed with Chromosorb (80/100 mesh) and maintained at 80°C. The separated N_2O gas then was detected using, Electron Capture Detector (ECD; 10mCi ^{63}Ni foil conditioned at 300°C) (See Fig. 2.4). The extraction was repeated twice more on the same aliquot. The detector output was read in terms of peak area, by a data station. The precision of the method was ~ 4%. Standards were run at the beginning and end of each set of samples to check the drift in the instrumental conditions and response. Air was used as a working standard. Standardization was against a standard mixture of 510 ppb N_2O in nitrogen (Gas standards, Alltech Associated Inc, IL. USA). The calibration curve obtained for the N_2O standard is shown in Fig. 2.5.
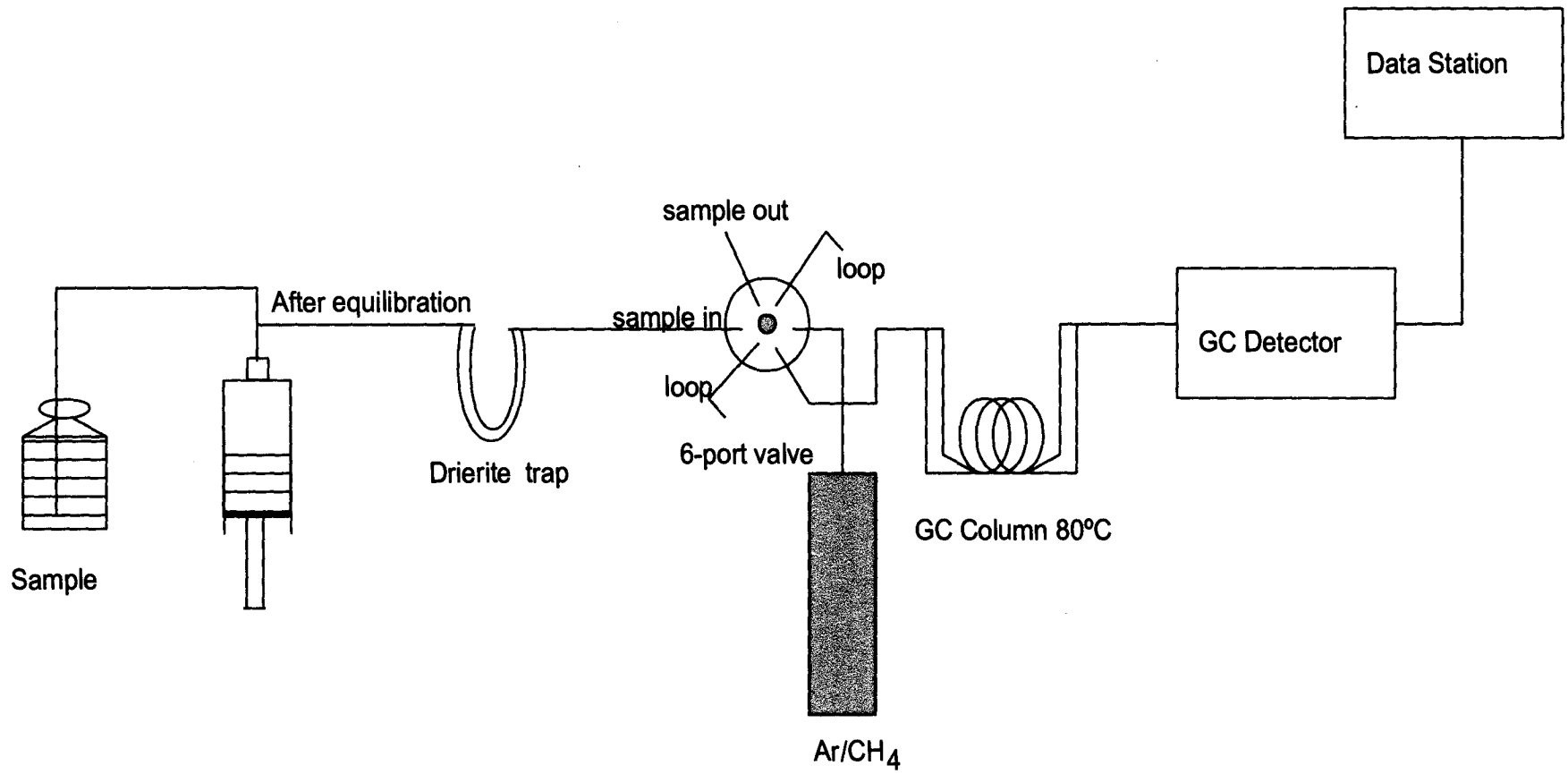
Fig. 2.4. Flow chart for N_2O analysis.

1000

800

600

N$_2$O concentration (nmol)

400

200

0

Least square fit:
N$_2$O = 0.0004850219362
    * Peak area
R^2 = 0.99

0   800000   1600000

Peak area
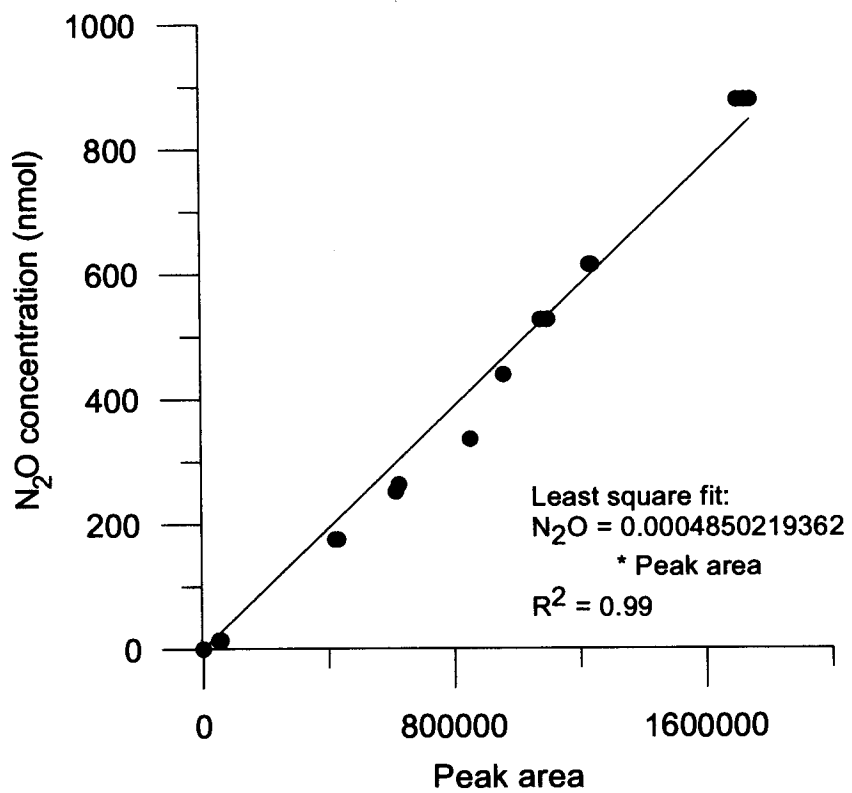
Fig. 2.5. Calibration curve for nitrous oxide analysis.

2.4.1.6 Primary Production

Primary production was measured by ^{14}C technique. Water samples were collected from various depths down to a depth where 1% light intensity (compared to that at surface) reaches. 125 ml of this was then transferred to Nalgene polycarbonate bottles (triplicates). These bottles were spiked with $H^{14}CO_3^-$ solution and conditioned as light and dark bottles as required. The bottled samples were incubated at almost same depths as they originally were, using a polypropylene line and attached to a buoy. Incubation was done for 12 hrs (dawn to dusk). The samples after retrieval were filtered through GF/F (47 mm diameter) filters and stored for processing and counting in the laboratory by using scintillation counter.

2.4.1.7 Chlorophyll a

About 500 ml of each of seawater samples were filtered through Whatman GF/F (47mm diameter) under low vacuum. The chlorophyll a pigments were extracted for 24 hrs in 10 ml of 90% acetone in the dark in refrigerator. Samples were measured by fluorometer, after attaining the room temperature, at the wavelength of 655 nm.

2.4.1.8 Isotopic Analysis

Measurements of nitrogen isotope ratio in NO_3^-, expressed as $\delta^{15}N$ relative to air ($\delta^{15}N$-NO_3^-), were made on two occasions – on cruise SS158 (in August 1997) off Mangalore and on field trip Candolim 22 (in September 2000) off Goa. Samples were taken in 1-litre collapsible bottles and were stored after poisoning with saturated $HgCl_2$ solution. The two sets of samples were analyzed at different places – the former at the University of

Washington, Seattle (USA) and the latter at the Institute for Hydrospheric-Atmospheric Science (IHAS), Nagoya University (Japan) – following slightly different procedures as described below.

The procedure followed at the University of Washington has been described by Brandes and Devol (1997). Briefly, it involved reduction of NO_3^- to NH_4^+ using Devarda's alloy. NH_4^+ was distilled and sorbed into ion sieve. The sorbed material was then filtered onto quartz QM-A filters and sealed into evacuated quartz combustion tubes containing Cu and CuO. Ampoule contents were converted into N_2 with a micro-Dumas combustion method, extracted into liquid N_2-cooled cold fingers containing molecular sieve and analysed for $^{15}N/^{14}N$ using a Finnigan MAT 251 mass spectrometer. The results, reproducible to ±0.2‰ were corrected for an isotopic shift –0.9‰ to account for the reagent blank.

Tanaka and Saino (2002) described the analytical method followed at IHAS for the determination of natural isotope abundance in NO_3^-. Briefly, the 1 liter seawater sample plus 1 liter of deionized water were taken in a round bottom flask containing a few boiling chips and 37.5 g of NaOH. The alkalinized sample was boiled to expel ammonia (NH_3) using a heating mantle and then distilled until its volume was reduced to 1 liter. Dissolved NO_3^- in the residue was converted to NH_3 with aluminum reagent under alkaline condition and the NH_3 so produced was distilled and absorbed into a flask containing an initial amount of 8 ml 0.072N H_2SO_4 solution. The distillate was concentrated in a rotary evaporator. The concentrated sample was made to react with potassium hypobromite to produce N_2 in a vacuum line provided with a gas purification system. The quantity of the produced gas was volumetrically

measured with a pressure transducer. The sample gas was cryogenically collected and sealed in a quartz tube containing molecular sieve. The isotopic measurements were made using a Finnigan MAT 252 mass spectrometer with dual inlet system.

A summary of methodologies used and the associated precision were given in Table 2.4.

2.4.2 Computations

2.4.2.1. Potential Temperature (θ) and Density (σ_θ)

Potential temperature and density were calculated based on algorithms of Fofonoff, 1983, the International Equation of State of sea water of Millero et al. (1980) and Bryden's (1973) formulation of adiabatic temperature gradients (Fofonoff and Millard, 1983).

2.4.2.2. Nitrous Oxide Data Processing

The log of peak area of each extraction is plotted against the extraction number and slope (z) and intercept (I) of each sample is computed. The initial concentration (C_{N2O}) is then obtained from the following equation,

$$C_{N2O} = I/(z-1)$$

2.4.2.3. Air-Sea Fluxes of N_2O

The flux of dissolved N_2O across ocean-atmosphere interface is calculated based on the equation

$$F = k\,(C_w - \alpha C_a)$$

Where k is the gas transfer velocity,

C_w is the gas concentration in seawater near the interface,

Table 2.4. Physical and chemical parameters measured, methods used and associated precisions.

Sr. No.	Parameter	Method	Precision
1	Temperature	Temperature probe	$0.01^{\circ}C$
2	Salinity	Conductivity probe	0.001
3	Dissolved oxygen	Winkler titration method or spectrophotometry	$0.03\mu M$
4	Nitrite	Azo-dye method	$0.01\mu M$
5	Nitrate	Reduction of NO_3 followed by Azo-dye method	$0.01\ \mu M$
6	Ammonia	Indo-phenol blue method	$0.05\mu M$
7	Phosphate	Phospho-molybdenum blue method	$0.03\mu M$
8	Hydrogen sulphide	Methylene blue method	$0.05\mu M$
9.	Nitrous oxide	GC-ECD	4%

$\propto$ is the Ostwald's solubility coefficient,

C_a is the concentration of gas in air.

The gas transfer velocity was obtained from the models of Wanninkhof (1992) and Liss and Merlivat (1986). Solubility was computed with the coefficients of Weiss and Price (1980).

2.4.2.4 Sedimentary Denitrification Rates

Concentration of N_2O in 1 cm section of a core was calculated based on procedures given in sections 2.3, 2.4.2.2 and in Chapter 6. The concentrations were corrected for the total volume of the headspace in the bottle and dilution factor. The rate of N_2O production was calculated for area occupied by each of 1cm section. The rate of N thus calculated was integrated over a core and these rates were extrapolated to the Arabian Sea continental shelf area $(0.5 \times 10^{12} \text{ m}^2)$ to estimate the sedimentary denitrification rate for the continental shelf region.

CHAPTER 3

Salient Features of Hydrography

Chapter 3

Salient features of Hydrography

3.1 Upper-Ocean Circulation

Along with the reversal of winds the near-surface water circulation also reverses completely every six months. Aside from directly affecting the surface flow changes in monsoon winds also give rise to coastal and equatorial Kelvin waves and equatorial Rossby waves that have both annual and sub-annual periods (McCreary et al., 1993). Due to the tropical location of the entire North Indian basin and its relatively small size (as compared to the North Pacific and the North Atlantic) these waves propagate rapidly through the region strongly influencing circulation in areas far away from their origin. This complicates the dynamics of surface waters as the circulation at any site is forced by local as well as remote (large, basin-scale) processes, and therefore it cannot be studied in isolation.

Major surface currents in the Arabian Sea during the two monsoon seasons are schematically depicted in Fig. 3.1. All major currents north of the 10°S undergo seasonal reversal. During the SWM, surface circulation in the Arabian Sea is generally clockwise. The most energetic flow during this season occurs off the East African coast where the East Africa Coastal Current (EACC) feed the Somali Current, which is one of the strongest western boundary currents in the world having a volume transport of 60 Sv (1 Sv=10^6 m^3 s^{-1}), which is of the same magnitude as the Gulf Stream. This flow is distinguished by the existence of several quasi-stationary anticyclonic
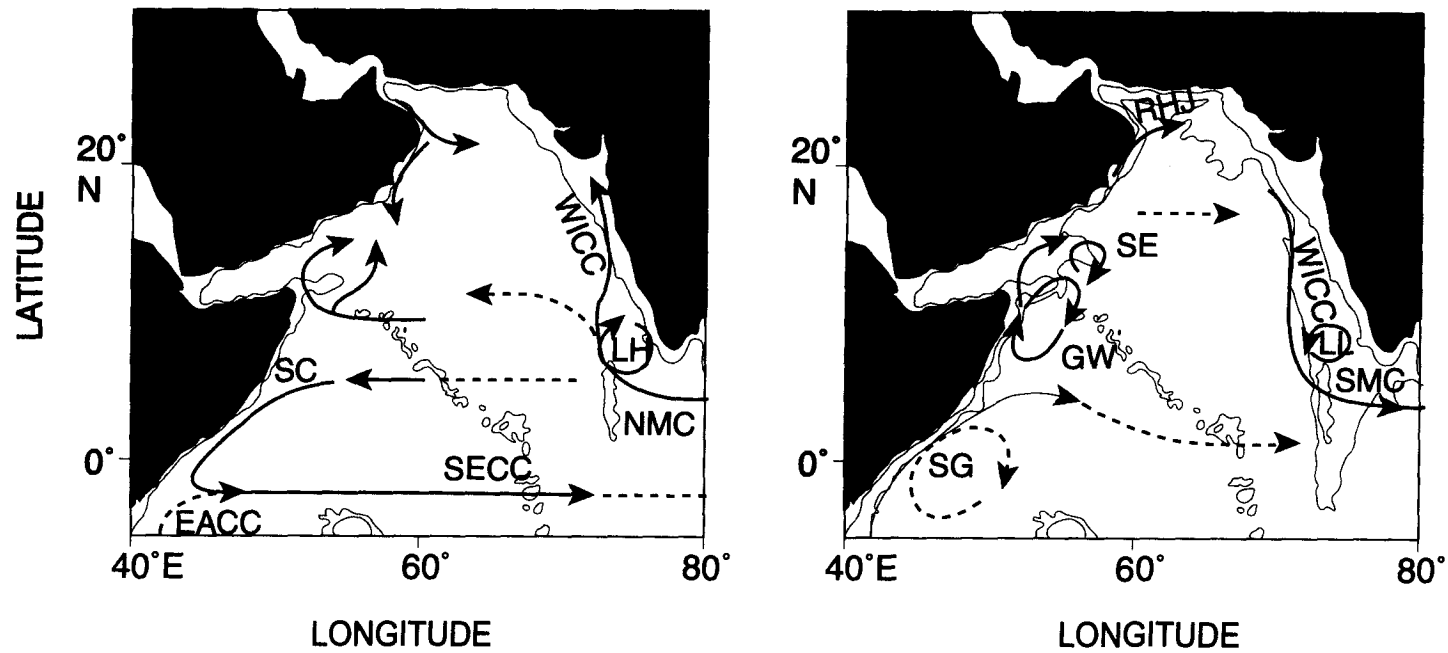
Fig. 3.1. Schematic diagram of surface currents in the Arabian Sea during the two monsoons
(a) NE Monsoon and (b) SW Monsoon.

(EACC - East African Coast Current; SECC - South Equatorial Counter current;
SC - Somali Current; WICC - West Indian Coast Current; NMC - Northeast Monsoon Current;
LH - Lakshadweep High; SG - Southern Gyre; GW - Great Whirl; SE - Socotra Eddy;
RHJ - Ras-al-Hadd Jet; LL - Laccadive Low; SMC - Southwest Monsoon Current).
(Adopted from Schott and McCreary, 2001)

eddies of which the Southern Gyre (SG) and the Great Whirl (GW) are most notable. These eddies cause offshore deflection of most of the water flowing northward around 4° and 10°N, inducing upwelling at these latitudes (Schott and McCreary, 2001). As compared to 4°N, upwelling at 10°N is more pronounced and longer lasting. The water upwelling here spreads far and wide, to the south by the GW and along the axis of the Somali Jet. Further north, strong SWM winds also force intense upwelling along the coasts of Yemen and Oman, but surprisingly the near-surface currents here do not exhibit an organized pattern and seasonality expected from the wind stress except near the coast. Instead, the flow is dominated by meso-scale eddies which also facilitate rapid offshore advection of the cold upwelled water as filaments and plumes that extend up to 1,000 kilometers from the coast (Flagg and Kim, 1998). The resultant coastal upwelling is demonstrated here by the presence of wedge-shaped features [discernible in satellite imageries of sea surface temperature (SST)] along the left (shoreward) shoulders of the SG and GW (Fig 3.2).

In addition to coastal upwelling caused by the strong southwesterly winds, upwelling is also expected to occur offshore during the SWM. This is because strong gradients in wind speed across the Findlater jet leads to Ekman pumping to the left of this jet (Bauer et al., 1991). Although the turbulence caused by strong winds should tend to deepen the mixed layer, the net effect is of entrainment of nutrients into the euphotic zone supplementing the nutrient supply through the offshore advection of upwelled water from the coastal upwelling zones (Smith, 2001).
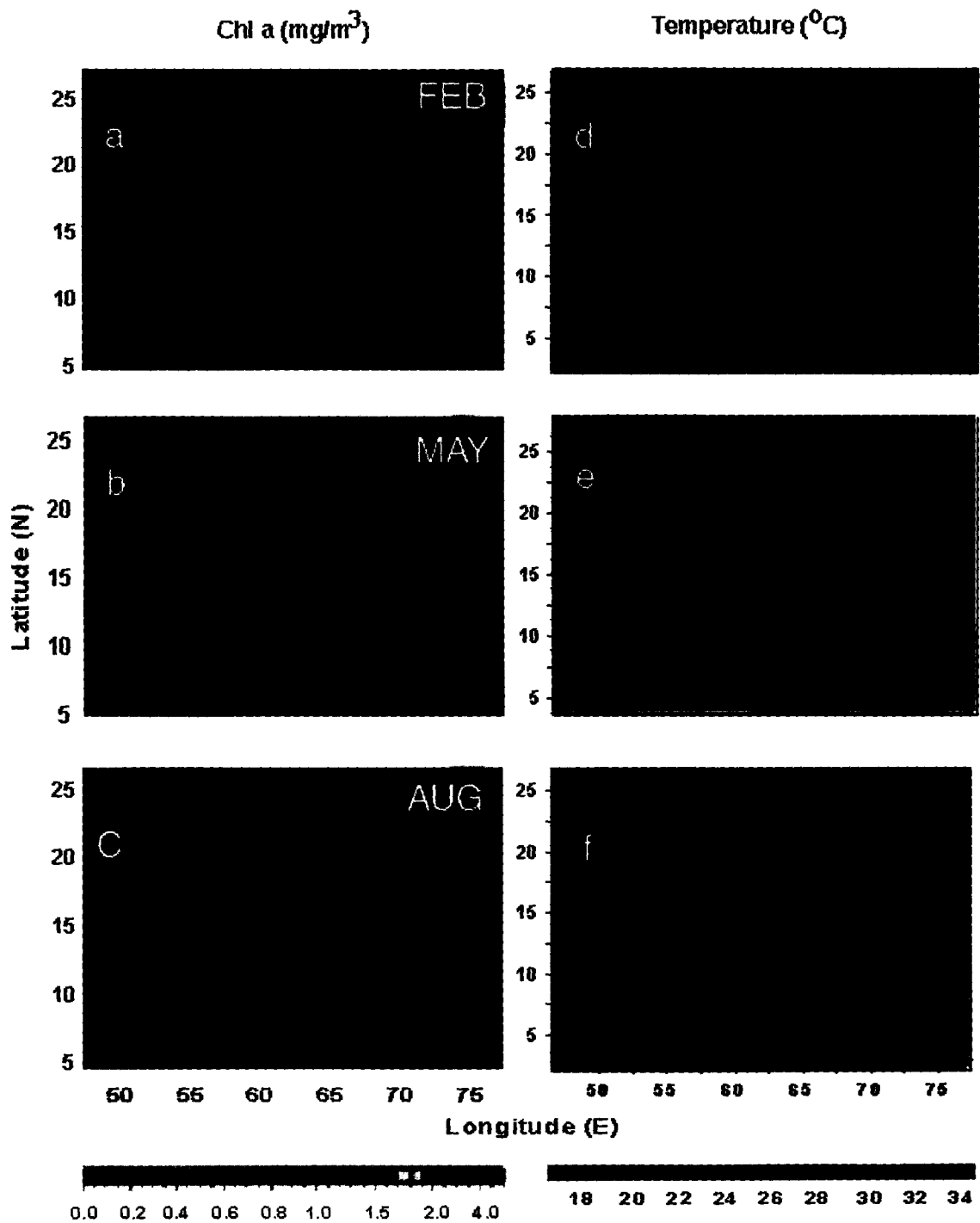
Chl a (mg/m^3) Temperature (^{0}C)

Fig. 3.2. Monthly climatologies of remotely-sensed surface chlorophyll a (a-c) and SST (d-f) for February (a,d), May (b,e) and August (c,f). Source (Jerry Wiggert, University of Maryland and Bob Evans, RSMAS, University of Miami)

Along the west coast of India, the region of the present study, circulation is much less energetic and relatively poorly organized during the SWM. The West India Coastal Current (WICC) flows toward the equator. The southward flow begins in March, becomes strongest by July, and collapses by October (Cutler and Swallow, 1984; Shetye and Shenoi, 1988). It is ~150 km wide and transports 4 Sv in the south and 0.5 Sv in the north (Shetye, 1998).

The southward flowing WICC is expected to bring the thermocline up along the Indian coast. The region does, in fact, experience upwelling, but with characteristics and effects quite different from the western Arabian Sea. The process begins in May along the Malabar Coast (southwestern India) and the west coast of Sri Lanka, and gradually propagates northward. Local winds along these coasts are upwelling-favourable, and so the process is not only more intense here as evident by lower sea surface temperatures (Wyrtki, 1971), it also has a farther offshore reach (beyond the continental shelf) (Shetye et al., 1990). The latter is also due to the existence of the Laccadive Low, a cyclonic eddy, which is an integral part of the SWM circulation (Fig. 3.1). Elsewhere (along the central west coast of India) thermocline shoals up to the coast.

At very shallow depths (often within 10 m of the surface), the upwelled water is generally prevented from reaching the surface by a warmer, fresher-water lens formed from intense precipitation in the coastal zone. Thus, both temperature and salinity effects combine to result in a very pronounced near-surface density gradient that impedes vertical mixing.

Hydrographic conditions described above are clearly seen in vertical sections of properties off Goa presented in Figs. 3.3a-e. This section was

repeated on a number of occasions, in different months and years however, data for only five sets of sampling (SS 141, SK 103, SS 136, SK 140 and SS 128) are used here. Upsloping of isotherms close to the coast was observed on all cruises conducted from June to October-November, providing evidence for upwelling, and the temperature structure just off the continental shelf/slope was indicative of the existence of the undercurrent (upward sloping at the top of this feature and downward tilt close to its bottom; Shetye et al., 1990). The undercurrent is more conspicuous in salinity and oxygen sections (salinity < 35.4; O_2 > 10 μM; e.g., Figs. 3.3b and 3.3c). Although believed to be associated with the SWM circulation, its signatures were often still discernible during other seasons. In fact, as inferred from the tracer distributions, the most intense undercurrent was observed to occur on a cruise undertaken in December 1998 (salinity at its core being < 35.1 – Fig. 3.3d). However, the shallow thermocline near the coast implied that the flow on this occasion was still directed toward the equator; and so, while these conditions were atypical, they provide a measure of the interannual variability. The undercurrent becomes progressively less distinct from the south to the north (Shetye et al., 1990), but still observable at least as far as off Mumbai.

As stated above upwelling along the west coast of India gradually shifts northward. That is, it begins and also ends earlier in the south than in the north. Along the northwest coast of India shallow mixed layers last well into the NEM (up to November-December; Banse, 1968). This implies that upwelling along the Indian west coast cannot be forced by local winds alone. An upwelling of Kelvin wave can explain the northward propagation of low sea levels. Consistent with the observations model simulations suggest that
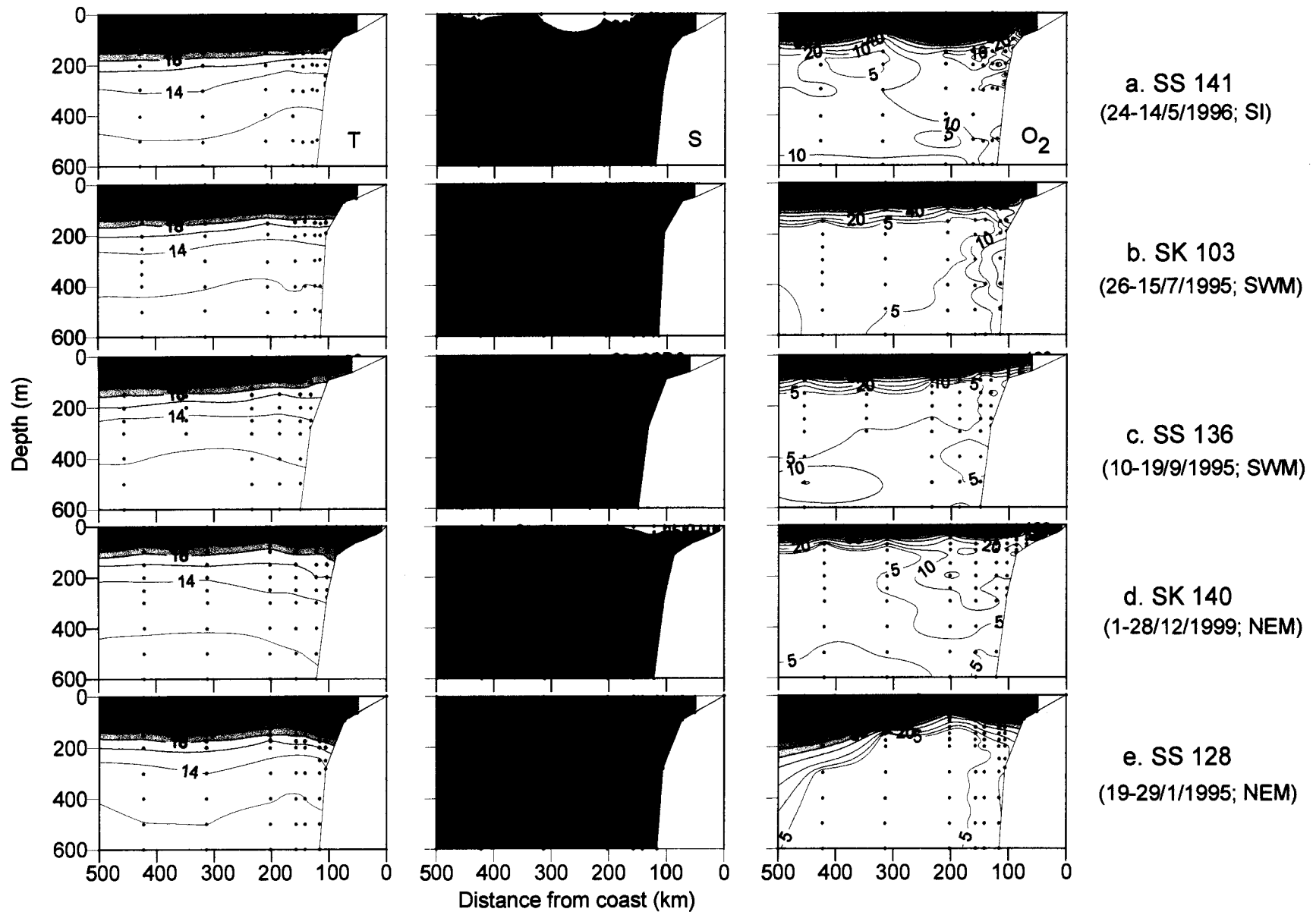
Fig. 3.3. Distribution of temperature (°C), salinity and oxygen (µM) along the cross shelf section off Goa.

remote forcing from the Bay of Bengal plays a major role in driving the WICC and associated upwelling (McCreary et al., 1993).

During the NEM surface circulation in the Arabian Sea is generally counterclockwise (Fig. 3.1). In the western Arabian Sea surface flow (directed southward) is much less vigorous as compared to the SWM, and the upwelling ceases to occur by October. Along the west coast of India, on the other hand, the circulation is best developed during this season in spite of weak winds. In fact, the WICC, which now flows northward, is the most prominent surface current in the entire Arabian Sea during this period. Flowing anomalously into the wind this current is estimated to carry almost twice as much water (~10 Sv) as its southward flowing variant during the SWM (Shetye et al., 1991). As it moves northward it gradually narrows from 400 km at 10°N to 100 km at around 22°N, forming a narrow jet with a transport of 7 Sv (Shetye et al., 1991). The broadening of the WICC off the southwest coast of India is in part due to the presence of an anticyclonic eddy – the Laccadive High – located just north of the islands it is named after Laccadive islands (Bruce et al., 1994), and in part due to the dissipation of energy from this current as it moves northward through the westward radiating Rossby waves. It is obvious that the WICC during the NEM cannot be but remotely forced. It originates as a result of bifurcation of the basin-scale westward-flowing NEM Current in the region southwest of the island of Sri Lanka (Schott and McCreary, 2001). The warm, low-salinity waters of the WICC exert a major control on biogeochemical cycling in the eastern Arabian Sea during the NEM. Outside the region affected by the WICC, the surface waters are cooled to 24-26°C by the northeasterly continental winds leading to

deep mixed layers (MLDs) (Figs. 3.3d and 3.3e) and entrainment of water from the thermocline, a process prevented by strong thermohaline stratification in the WICC.

3.2 Water Masses

For any given region, characteristics of a water mass are expressed with the help of the potential temperature-salinity (θ - S) diagram (Sverdrup et al., 1942). The major water masses in the Arabian Sea along with their respective density (σ_θ) levels have been identified by Wytrki (1971) based on physico-chemical properties.

The Arabian Sea is a region of negative water balance where evaporation exceeds precipitation by as much as 150 cm yr^{-1} off the Arabian coast (this difference decreases to ~-20 along the southwest Indian coast (Venkateswaran, 1956). This results in high surface-salinities. Winter cooling of surface waters in the north leads to the formation of a shallow high-salinity water – the Arabian Sea High Salinity Water (ASHSW) – identified by a salinity maximum at σ_θ = 25 surface (Rochford, 1964). This maximum can be readily identified in the θ-S diagrams shown in Figs. 3.4 – 3.6.

The subsurface (mesopelagic) water-mass structure in the Arabian Sea is affected to a very large extent by outflows from the two marginal seas – the Persian Gulf and the Red Sea – that are connected to the Arabian Sea through the Gulf of Oman and the Gulf of Aden, respectively. The Red Sea is a deep (>2000 m) silled basin (sill depth at the Strait of Bab-el-Mandeb ~100 m); the Persian Gulf is a shallow embayment without a sill at its entrance (the Hormuz Strait) having a maximum depth of 67 m. Both water bodies are

located in very arid regions resulting in surface salinities in excess of 40. The extremely high surface salinities together with cooling in the northern parts of these land-enclosed basins give rise to high-density water masses that spill over their entrances into the gulfs linking them with the Arabian Sea, sink to appropriate depths corresponding to the density achieved after some at their entrance points, and spread horizontally over considerable areas (Rochford, 1964; Wyrtki, 1971; Dietrich, 1973). The outflows are compensated by near-surface flows of lower salinity water into the marginal seas (Grasshoff, 1969, 1975; Morcos, 1970; Hartman et al, 1971). The core layers in the Arabian Sea are characterized by salinity maxima that have been assigned nominal σ_θ values of 26.6 for the Persian Gulf Water (PGW) and 27.1 for the Red Sea Water (RSW) by Wyrtki (1971). The approximate depths of these density surfaces in the Arabian Sea are 250 m and 500 m, respectively.

The composition of water masses in the area of present study can be deduced from the potential temperature – salinity (θ-S) plots. Selected stations along three sections were chosen for this purpose just off the continental margins – the first is off Ponnani in the south (Fig. 3.4), the second is off Goa in the centre (Fig. 3.5), and the third is off Mumbai in the north (Fig. 3.6). θ-S diagrams in the first region exhibit relatively small variations at σ_θ > 25, but large changes at shallow depths (Fig. 3.4). A single broad salinity maximum in the deeper layer evidently corresponds to RSW below which the θ-S relationship is almost linear indicating binary mixing between the Arabian Sea High-Salinity Intermediate Water (cf. Wyrtki, 1973) and the North Indian Ocean Deep Water. Another salinity maximum is found just below the surface mixed layer generally within the σ_θ range of 23-24. Salinity values at this

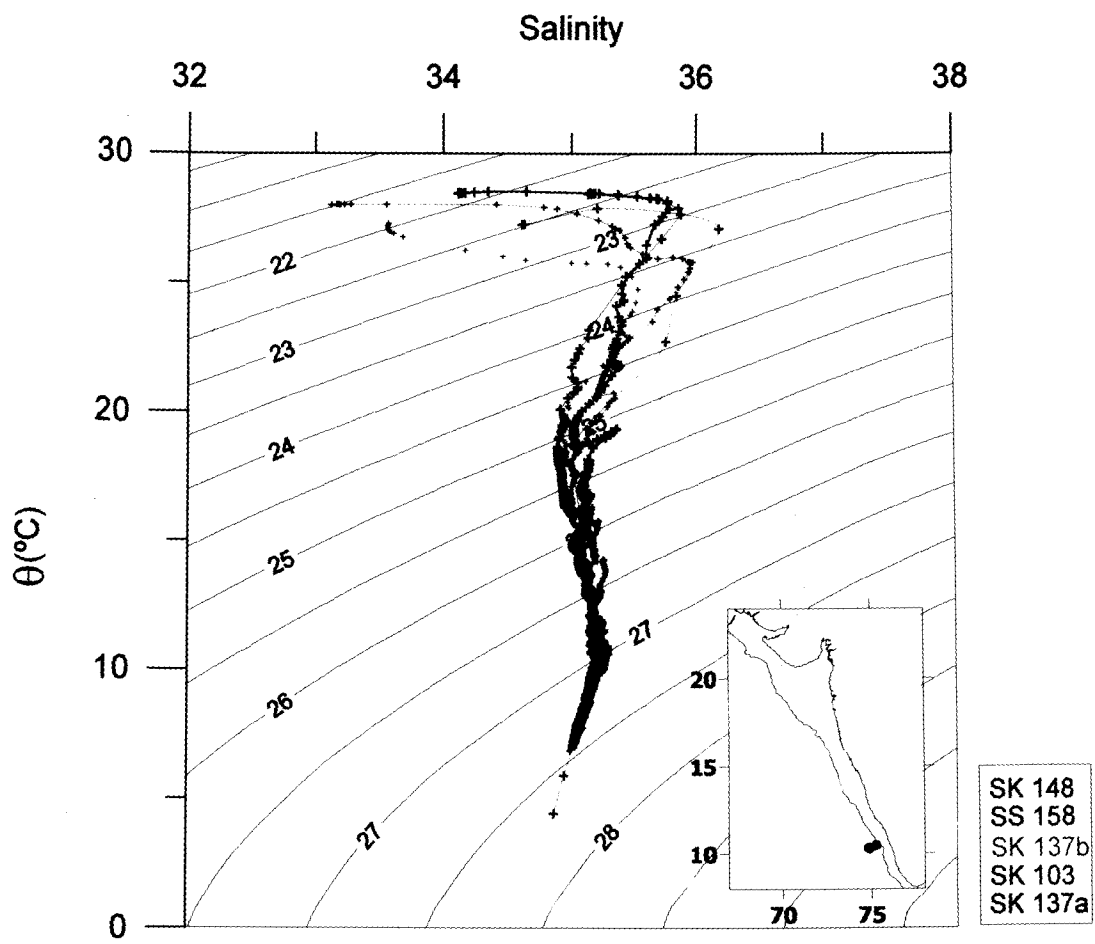Fig. 3.4. Potential temperature (θ) - salinity (S) diagrams for stations off Ponnani.

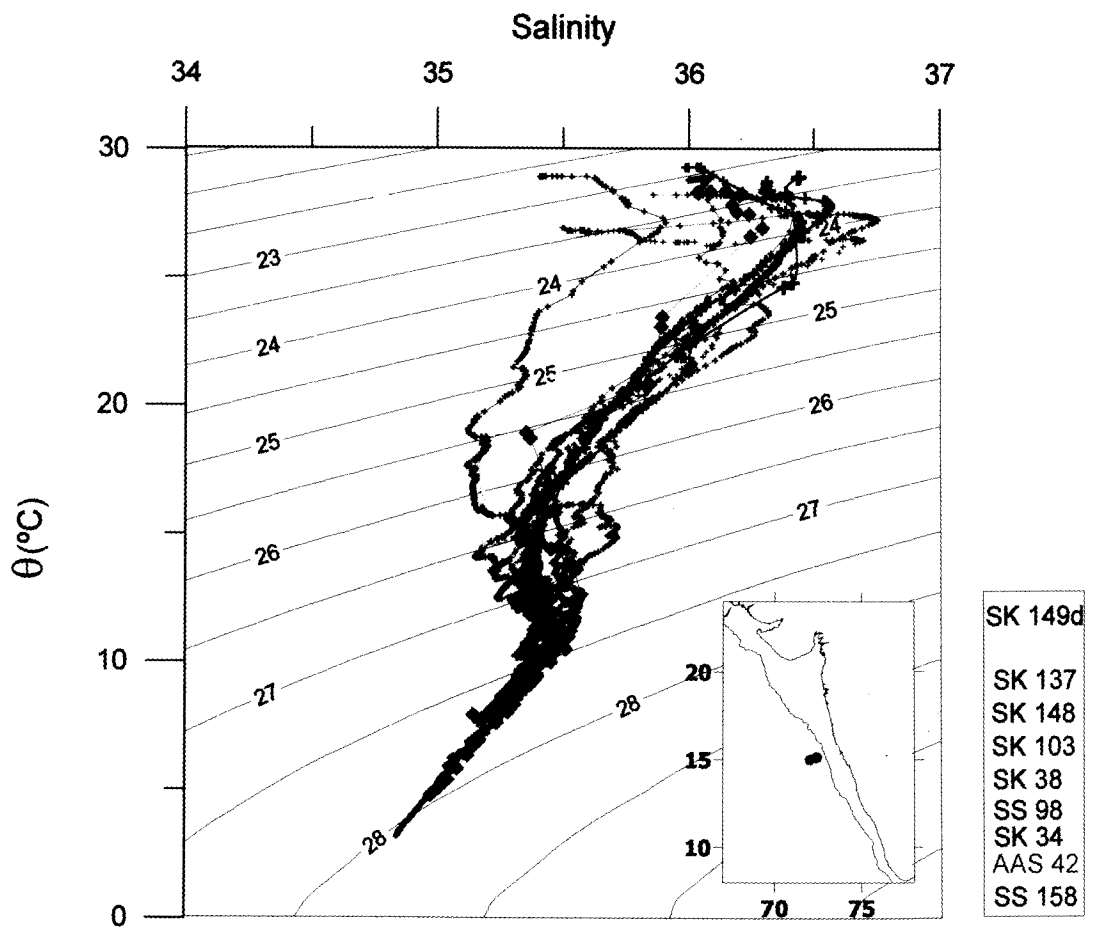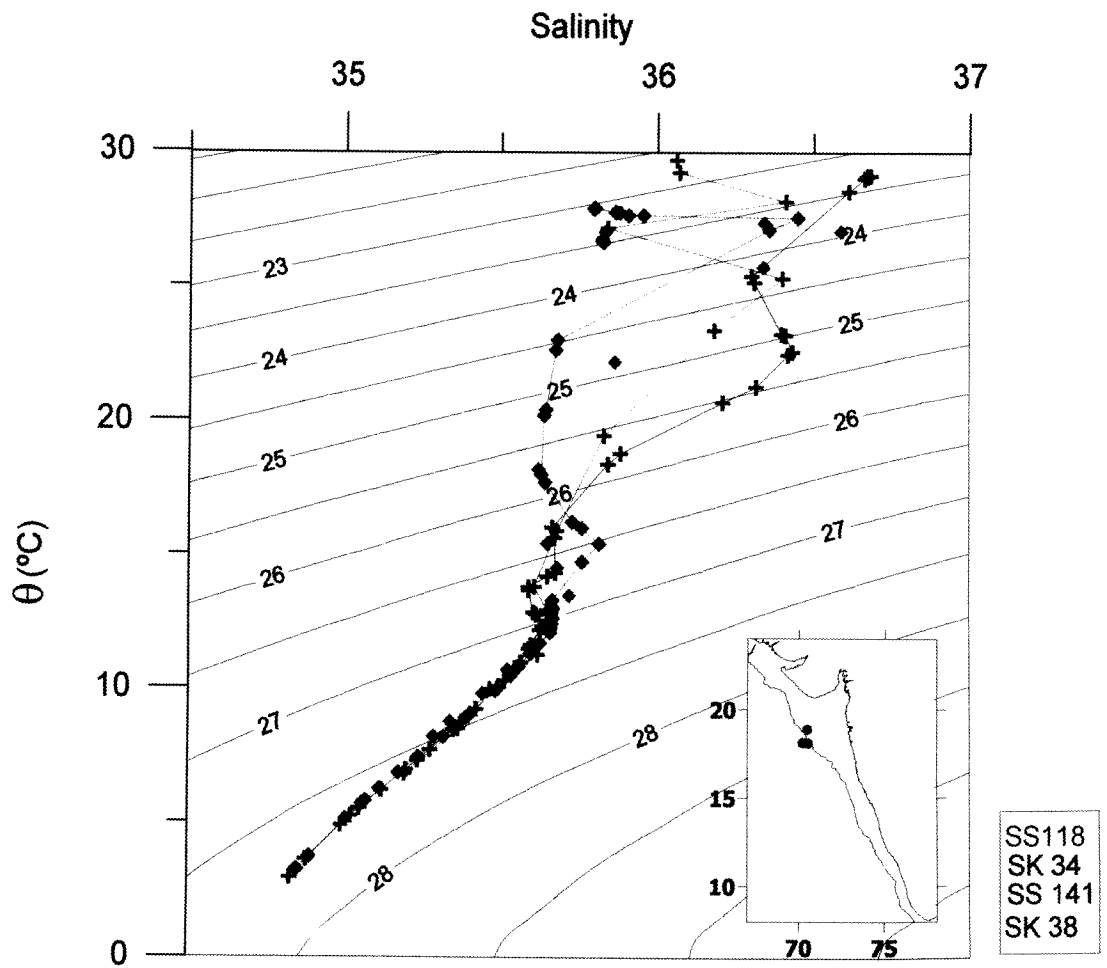Fig. 3.5. Potential temperature (θ) - salinity (S) diagrams for stations off Goa.

Fig. 3.6. Potential temperature (θ) - salinity (S) diagrams for stations off Mumba

maximum approached or exceeded 36 indicating that the water at this depth was of the northern origin. Above this feature salinities decreased rapidly due to the freshening of surface layer. As most of the observations were made during the SWM, this decrease in salinity was apparently brought about by monsoonal precipitation and land runoff. However, a similar freshening of surface layer should be expected to occur during the NEM as well because of the northward advection of low-salinity waters of the WICC. The salinity maximum corresponding to PGW is not seen at this location. Instead the two maxima mentioned above are separated by a broad salinity minimum. This implies northward flow, presumably in the undercurrent.

The RSW is more prominently seen in the θ-S diagrams off Goa (Fig. 3.5). Above this maximum, the θ-S characteristics are a lot more variable than in the south. At about 26.5 σ_θ surface, for example, one usually observes a salinity minimum that can at times be replaced by the salinity maximum of the PGW. When this happens, the salinity minimum is shifted to shallower depths, but it is always present, and as discussed above it probably corresponds to the poleward undercurrent, arguably the major source of low salinity waters in the eastern Arabian Sea. It may be pointed out that temporal changes in circulation at the depth of the undercurrent can make the low-salinity water move up and down the coast; during this process sometimes entraining other water masses, especially PGW, leading to complex thermohaline structure. It may also be noted that the lowest salinities at the minimum were recorded on two cruises (SK140 and 149d) undertaken in early December. As stated earlier, the SK140 observations are probably atypical. However, if the poleward undercurrent is active only during the SWM it is expected to have

maximum impact on tracer distribution in late summer/autumn and these effects should persist for some time even after the surface flow has reversed. The shallow salinity maximum corresponding to ASHSW shows even wider changes, with the maximal and minimal salinity values differing by as much as 1. In general the water is saltier and denser than in the south.

The influence of the RSW is negligible in the north (Fig. 3.6). This is consistent with previous observations. Ramesh Babu et al. (1980), for example, found this watermass to be absent north of about 17°N latitude. On the other hand the PGW acquires greater importance in the north as one gets closer to its source. Sometimes the maximum is broken into several maxima because of entrainment of lower-salinity waters (e.g., from the undercurrent). Consequently, the salinity values at a σ_θ value of 26 vary from 35.2 to 36. The shallow salinity maximum corresponding to ASHSW occurs at higher density surface here than in the south.

CHAPTER 4

Evolution and Effects of Oxygen-Deficiency Over the West Indian shelf

Chapter 4

Evolution and Effects of Oxygen-Deficiency Over

the West Indian Shelf

4.1 Introduction

As discussed in Chapter 3, coastal zone off western India experiences upwelling during June-November (Banse, 1959, 1968). However, the physical forcing and intensity of the process are quite different from those in the upwelling zones of the western Arabian Sea. Forced by strong winds, upwelling is far more energetic in the latter region with the water coming up and getting transported away from the coast rapidly. Along the central west coast of India, the upwelling velocities are probably much lower and the water does not usually surface, let alone advecting hundreds of kilometers offshore, as happens in the west. Instead it reaches within a few meters of the surface and its further ascent is impeded by the presence of a warm, lower-salinity layer formed as a result of intense runoff into the coastal zone (Naqvi et al., 2000; Jayakumar et al., 2001). The presence of nutrient replete water so close to the surface stimulates the growth of phytoplankton, further increasing the oxygen demand in a water that had not been very oxygen-rich, although not suboxic (denitrifying), to begin with.

The near-bottom O_2 depletion over the western Indian shelf develops primarily as a result of natural processes (upwelling, high biological productivity and stratification). Although it has been known to exist since the earliest observations made in the 1950s (Banse, 1959; Carruthers et al.,

1959), it had never been known to support pelagic SO_4^{2-} reduction, a very rare process indeed for open coastal waters. Naqvi et al. (2000) suggested that the coastal O_2-deficiency has intensified in recent years probably in response to increased anthropogenic nutrient loading in coastal waters. This study examines the issue in detail, expanding the previously published data, and provides for the first time a monthly climatology of parameters at a quasi-time series site off Goa. The results provide an insight into the evolution and decay of anoxic conditions in this region, and a measure of the inter-annual changes.

4.2 Significance

Occurrence of O_2-deficient conditions over the shelf has important implications for biogeochemical cycling, especially of nitrogen that has potential to provide feedbacks to global warming through the N_2O link. Coastal anoxia is also known to immensely affect the abundance and composition of marine organisms (Diaz and Rosenberg, 1995). Since these conditions are too harsh for most organisms to survive, the majority of mobile organisms migrate from the O_2-deficient zone, because of which such zones are popularly known as "dead zones" (Malakoff, 1998). There are over 40 "dead zones" that have developed along various coasts globally as a result of human activities (coastal eutrophication; Malakoff, 1998). The closest analogues of the shallow O_2-deficient environment over the western Indian shelf are found off Namibia (Calvert and Price, 1971) and off Peru (Codispoti et al., 1986, 1992). The importance of the O_2-deficient zone over the Indian shelf owes to its large area (~200,000 km^2 with bottom water $O_2 < 0.5$ ml l^{-1};

<22 μM). This is an order of magnitude greater than the area of the largest human-induced hypoxic zone in the Gulf of Mexico (http://state_ofcoast.noaa.gov/bulletins/html/hyp_09/hyp.html).

4.3 Observations

The data used here were collected during the period 1997 to 2002 on a number of cruises (Table 2.1) undertaken along the west coast of India (Fig. 2.1). A series of cross-shelf sections were occupied to make measurements of physical (temperature and salinity) and chemical (nutrients and dissolved gases) parameters. As the focus of this study is on O_2-deficient conditions, most of the observations were made during the period of upwelling with which these conditions are associated. However, the section off Goa was repeated many a time during different seasons including the non-upwelling periods because of logistic reasons (easy accessibility from the National Institute of Oceanography). Thus, the number of samplings varied from just 2 off Ratnagiri to 17 off Goa.

4.4 Property Distributions along Cross-Shelf Sections

Property distributions along seven transects (off Quilon, Cannanore, Mangalore, Karwar, Goa, Ratnagiri and Mumbai) are presented and described in this section to understand the patterns of evolution of O_2-deficient conditions in space and time as well as to evaluate the extent of inter-annual variability.

4.4.1 Off Quilon

This section was covered five times, but only during the SWM (from July to September). All observations show the existence of a well-developed upwelling regime (Fig. 4.1a-e). Shetye et al. (1990) also observed active upwelling in this region during June 1987. The process probably begins even earlier, sometime in March (Dr. S.R. Shetye, unpublished data). Along this section the upwelled water reaches the sea-surface and the SST is lower (minimum 22.8°C, generally < 25°C over the inner shelf) than elsewhere along the Indian west coast (with one exception off Karwar, to be discussed later). Moreover, the upwelled waters, interspersed by pockets of low salinity water, appear to be transported offshore, although not to the extent seen off Somalia and Oman, and shallow mixed layer are observed even offshore, presumably due to shoaling of thermocline due to the presence of the Laccadive low (LL). The poleward undercurrent can be identified from the salinity sections of SK137b (Fig. 4.1c) and SS158 (Fig. 4.1d). Consistent with the previous report (Shetye et al., 1990) this feature occurs at shallower depths along this section as compared to those in the north.

NO_3^- was almost always present in fairly high concentrations (maximum 16 μM; SK 137a - Fig. 4.1b) at the sea surface over the shelf along this transect except on Cruise SS158 (Fig. 4.1c). NO_2^- was also detectable in near surface waters (often as a subsurface maximum); however, since O_2 levels were always higher than those required for denitrification, the most likely process of NO_2^- production should be assimilatory NO_3^- reduction. Low (but not suboxic) O_2 concentrations led to accumulation of N_2O (maximur concentration 85 nM) below the pycnocline, and upwelling of this water rais(
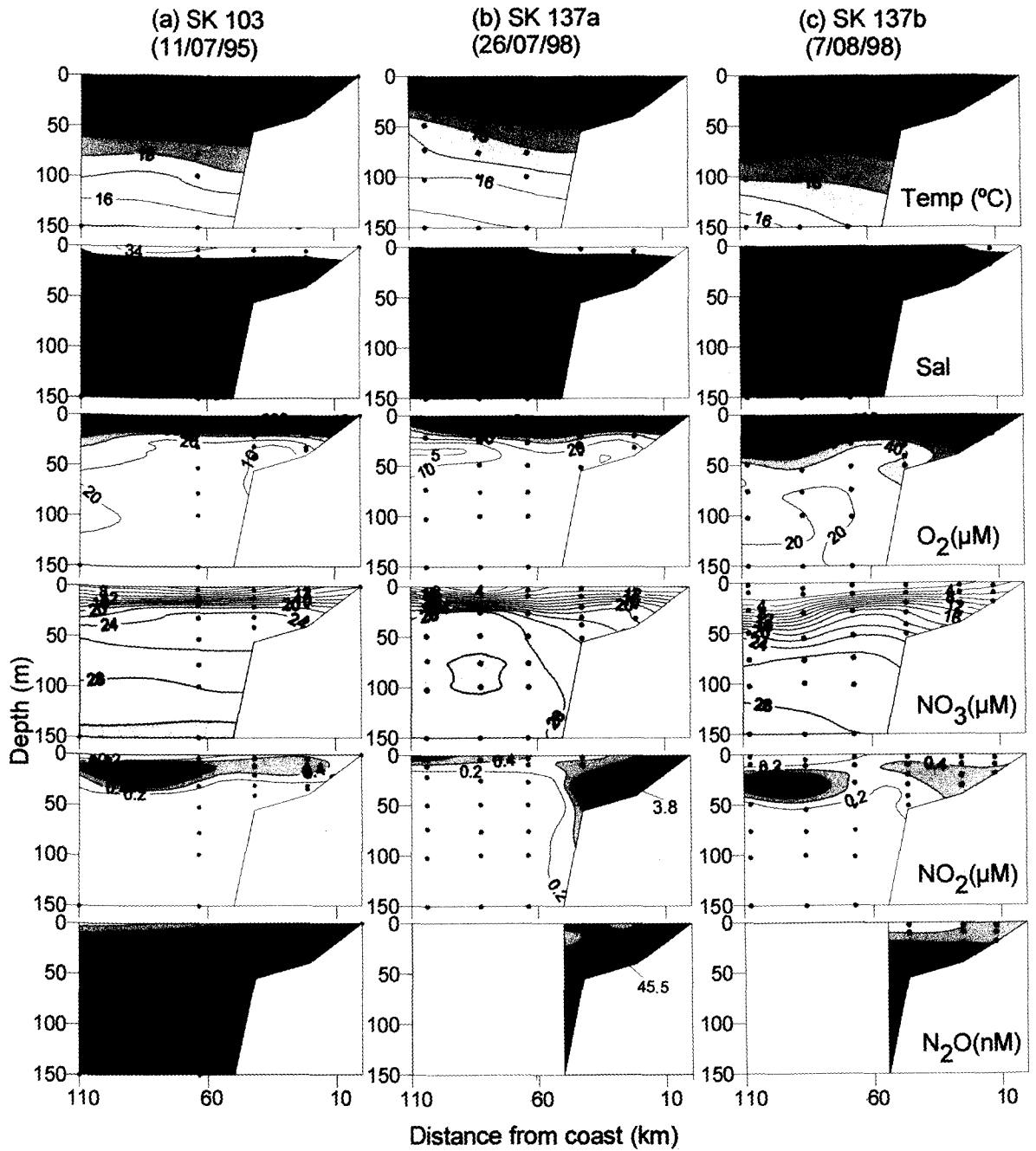
Fig. 4.1. Distribution of water column properties along the cross-shelf transect off Quilon during the months of July and August.
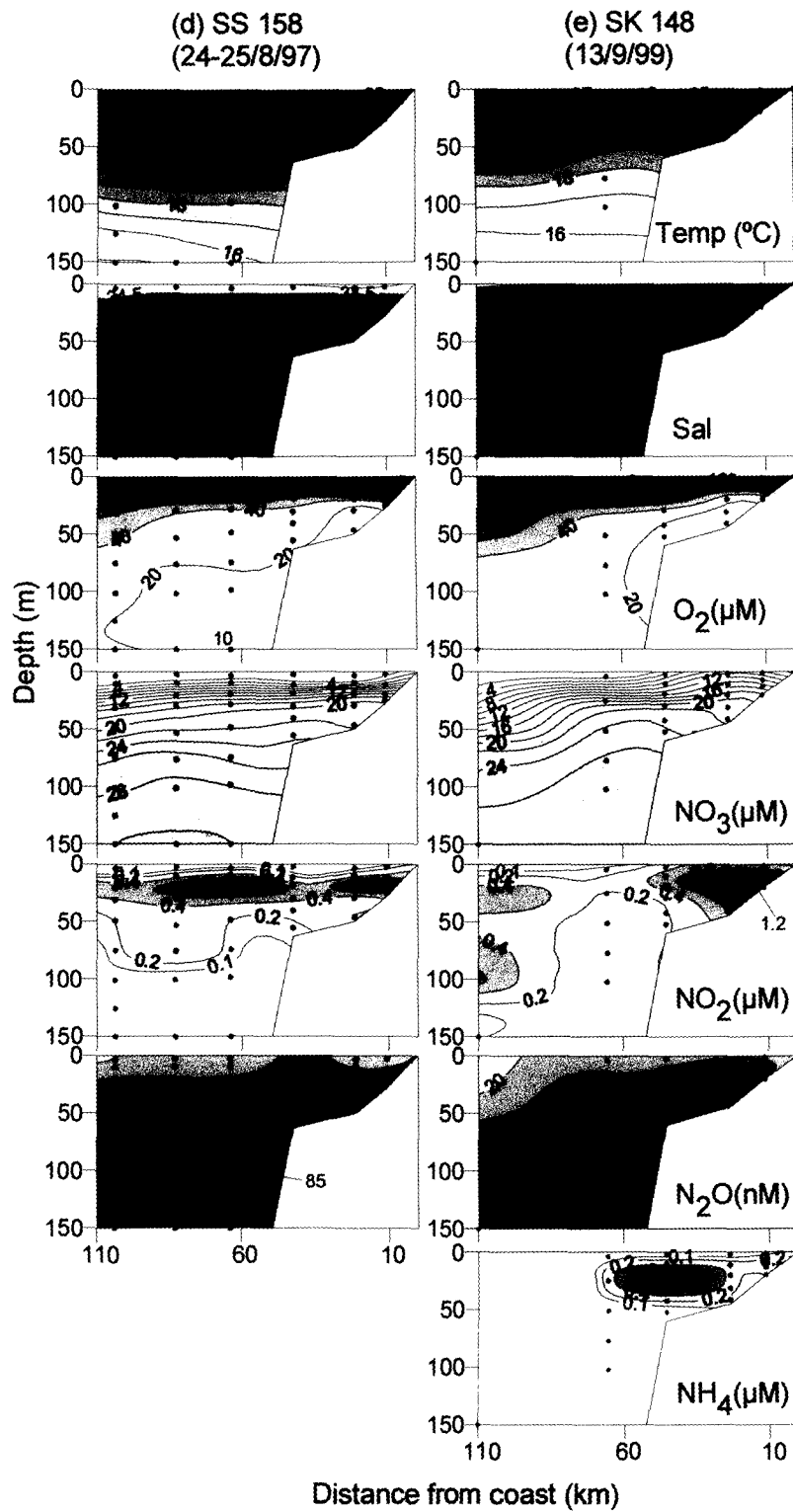
Fig. 4.1. Distribution of properties along the cross-shelf transect off Quilon during the months of August and September.

the surface concentration to a maximum of 45.5 nM. Thus, the N_2O levels were elevated throughout the water column, but not anomalously so as happens along other sections experiencing suboxic conditions (see below).

4.4.2 Off Cannanore

Observations along this section (Fig. 4.2a-d) were made on four occasions on the same cruises (except SK137a) as in case of the Quilon transect, and the property distributions were also very similar to those described above. Upwelling was slightly less pronounced as compared to the Quilon section. The minimum SST (24.9°C) and the maximum surface NO_3^- (9 µM) were recorded at the most inshore station on cruise SS158 (Fig. 4.2c). Instances of complete NO_3^- depletion at the sea surface were more frequent especially on SK148 (September 1999). Sub-pycnocline O_2 levels were lower than off Quilon, but the water was still not suboxic. Consequently, denitrification was not noticeable and, as off Quilon, NO_3^- levels remained high (>20 µM) in near bottom waters over most of the shelf. Similarly, the primary NO_2^- maximum occurred all over the section coinciding with the very shallow pycnocline. However, N_2O concentrations were significantly higher both below the pycnocline (maximum 133 nM) and the sea surface (maximum 70 nM; SK 137-Fig. 4.2b). This is consistent with the lower O_2 concentrations, which probably favoured N_2O production through nitrification and/or nitrification/denitrification coupling (Naqvi et al., 1998).

4.4.3 Off Mangalore

The annual rainfall along the west coast of India is at its maximum near Mangalore, and so the effect of land runoff should be most prominently

Fig. 4.2. Distribution of water column properties along the cross-shelf transect off Cannanore during the months of July and August.

(d) SK 148
(15/9/99)

Temp (°C)

Sal

$O_2(\mu M)$

$NO_3(\mu M)$

$NO_2(\mu M)$

$N_2O(nM)$

Depth (m)

Distant from coast (km)

Fig. 4.2. Distribution of water column properties along the cross-shelf transect
off Cannanore during the month of September.

seen along this section. In accordance with the expectation, surface salinity values were < 32 in the inner shelf on several occasions, fortifying near surface stratification.

Property distributions along this section varied greatly from one set of observations to another, and also from those along the two southern sections described above even though, as in case of Quilon and Cannanore, observations off Mangalore were also confined to the period from July to September. In general, the mixed layer deepened offshore to a greater extent than observed further south. Samplings on the two legs of Cruise SK137 (Fig. 4.3a and b) were undertaken 3 weeks apart. Property distributions during the first survey did, in fact, conform to the patterns observed in the south except that, as expected, the near bottom O_2 concentrations had fallen further and were on verge of turning suboxic. NO_3^- concentrations in upwelled water at the two shallowest stations appeared to be somewhat lower than expected, but this could well be due to uptake by phytoplankton, which (assimilatory reduction) could also account for the mid-depth (primary) NO_2^- maximum (concentration > 2 μM) as it was not associated with suboxic O_2 concentrations. N_2O levels were very similar to those observed off Cannanore with high concentrations (up to 88 nM) below the pycnocline as well as at the sea surface (up to 57.5 nM).

On the return leg of the cruise (SK137b), near-bottom waters over the inner shelf were found to have undergone remarkable transformation (Fig. 4.3b). Upwelling had intensified, as the water was generally cooler. A recently-upwelled parcel of water (characterized by O_2 > 40 μM) was found to spread over mid-shelf. Sandwiched between this parcel and the thin surface
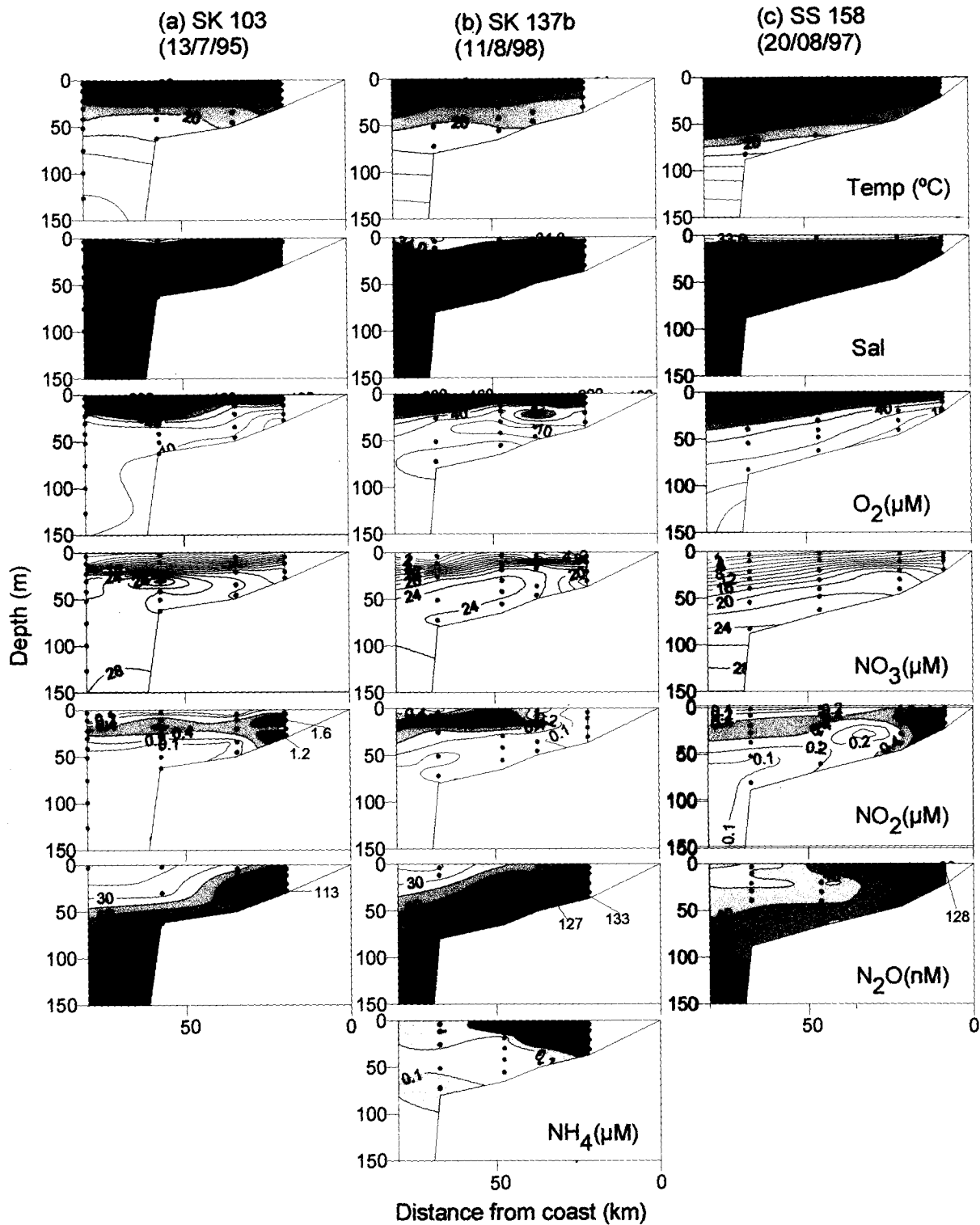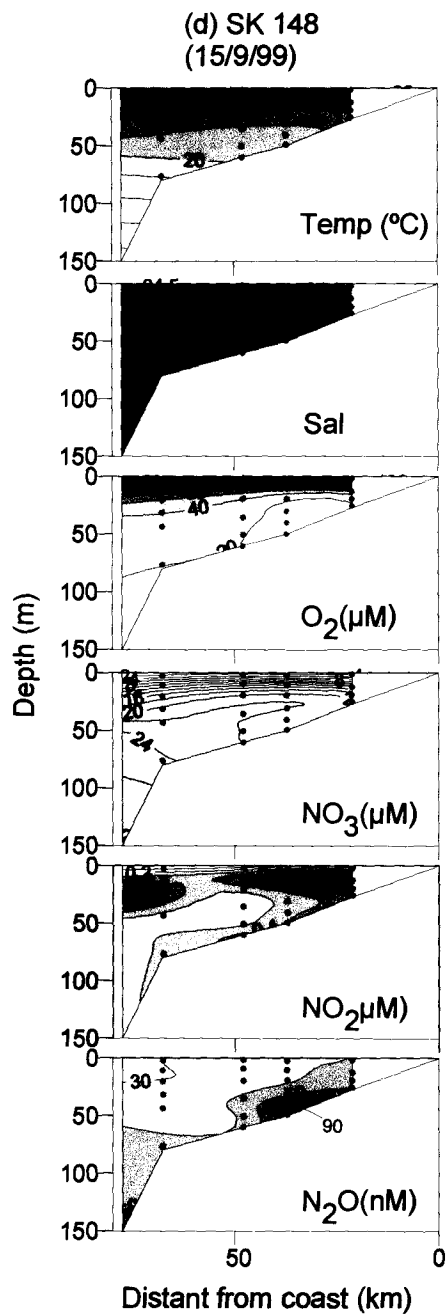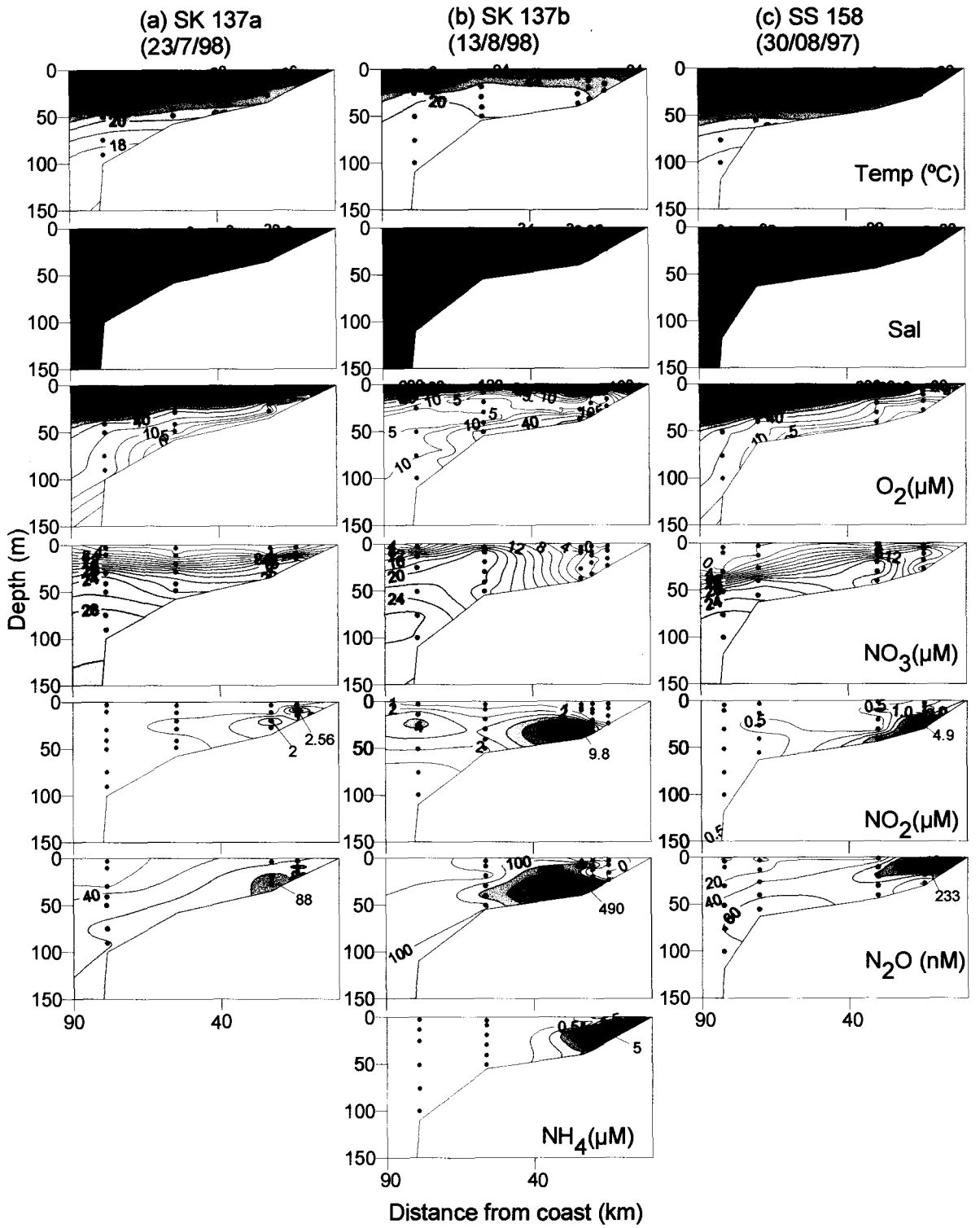
Fig. 4.3. Distribution of water column properties along the cross-shelf transect off Mangalore during the months of July and August.
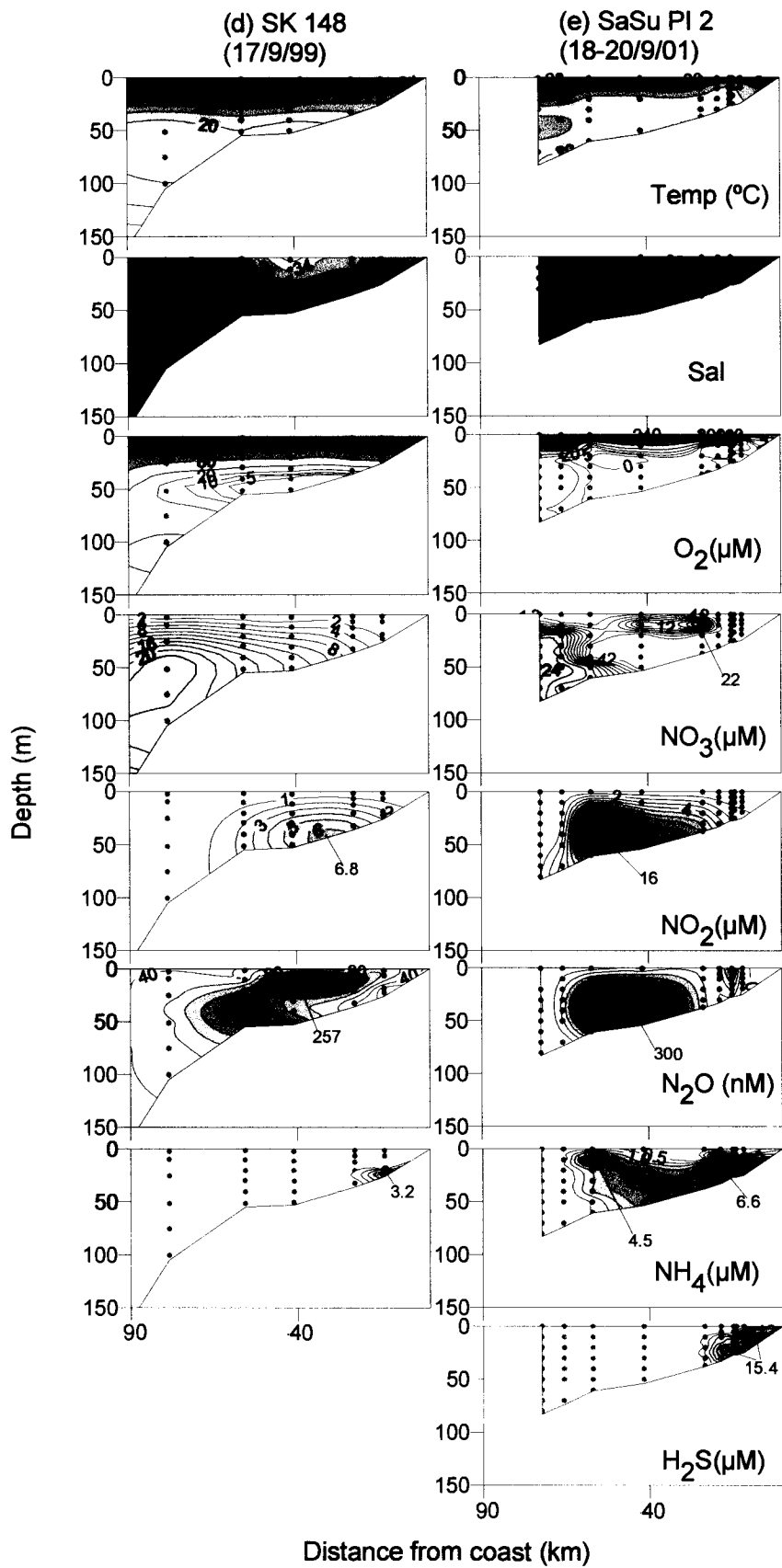
Fig. 4.3. Distribution of water column properties along the cross-shelf transect off Mangalore during the month of September.

layer and extending offshore from the inner shelf was a layer that was anoxic in the inner shelf (i.e. it had lost all its NO_3^-, and was now experiencing sulphate reduction), and suboxic (denitrifying) over mid- and outer-self. High NO_2^- concentrations (up to 9.8 μM) occurred within the latter layer, apparently as a consequence of denitrification. Near bottom waters at the two shallowest stations smelled strongly of H_2S, but its concentration was not measured. It was, in fact, the first occasion when H_2S was noticed in open coastal waters of the Arabian Sea. Occurrence of sulphate reduction was also supported by the accumulation of NH_4^+ (Fig. 4.3b)

Distribution of N_2O bore the greatest impact of altered redox environmental conditions. Concentrations varied greatly over a wide range - from 0.8 to 489.7 nM – the lowest and the highest values coming from the near-bottom waters of the first and second stations from the coast. This is consistent with the observations of Naqvi et al. (2000) who found that reducing conditions in shallow waters could lead to both vigorous production and consumption of N_2O.

The data for August (Fig. 4.3c) were taken a year earlier from the same area. The apparent relaxation of reducing conditions with reference to above observations most likely reflects inter-annual variability. On the other hand, measurements made in September (Figs. 4.3d and e) provide evidence for the prevalence of more intense conditions in 1999 (SK148) and even more so in 2001 (SaSuPl2). On SK148, large parts of the shelf were covered by NO_2^--bearing waters (maximum concentration 6.8 μM). The most inshore station had lost all NO_3^- and traces of H_2S were smelled in waters where accumulation of ammonia was also observed. A few abnormally high

48

(maximum 257 nM) values of N_2O were measured. At the surface the highest concentration came from the most inshore anoxic station where a reversal of the normal depth profile was observed: concentration decreased from 79 nM at the surface to 3 nM at 22 m. The SaSuPI2 cruise was undertaken at very nearly the same time two years later. Reducing conditions on this occasion were the most severe. Near-bottom NO_2^- reached up to 16 μM, the record high for the Arabian Sea and next only to the concentration reported by Codispoti et al. (1986) from the Peruvian upwelling zone. Within the zone of high NO_2^-, N_2O reached maximum values of 300 nM. The peak surface concentration was 124 nM. With the exception of two isolated pockets at mid-depths, NO_3^- was completely reduced within 50 km of the coast and the three shallowest stations experienced anoxia, accumulating both NH_4^+ (maximum 6.6 μM) and H_2S (maximum 15.4 μM) in near-bottom waters. In fact, at another station located close to Mangalore harbour H_2S was present even at 5 m water depth (concentration 8.2 μM) underscoring the severity of O_2 depletion during that cruise.

4.4.4 Off Karwar

Observations off Karwar could be made only in the late SWM; these were made on five cruises of which only two (SS158 and SK 148) provided full cross-shelf sections (Fig. 4.4b and c). Sampling on SK137b was limited to water depths < 40 m, but the fewer data taken on this cruise are extremely interesting. The most inshore station was well mixed down to the maximum depth of sampling (20 m). Temperature and salinity ranged from 21.59 to 21.91°C, and from 34.829 to 34.949, respectively. However, chemical

49

Fig. 4.4. Distribution of water column properties along the cross-shelf transect off Karwar during the months of August and September.

(d) SaSu24
(19/9/02)

(e) SaSu Pl 2
(21/9/01)

Temp (°C)

$O_2(\mu M)$

$NO_3(\mu M)$

$NO_2(\mu M)$

$N_2O(nM)$

$NH_4(\mu M)$

$H_2S(\mu M)$

Depth (m)

Distance from coast (km)
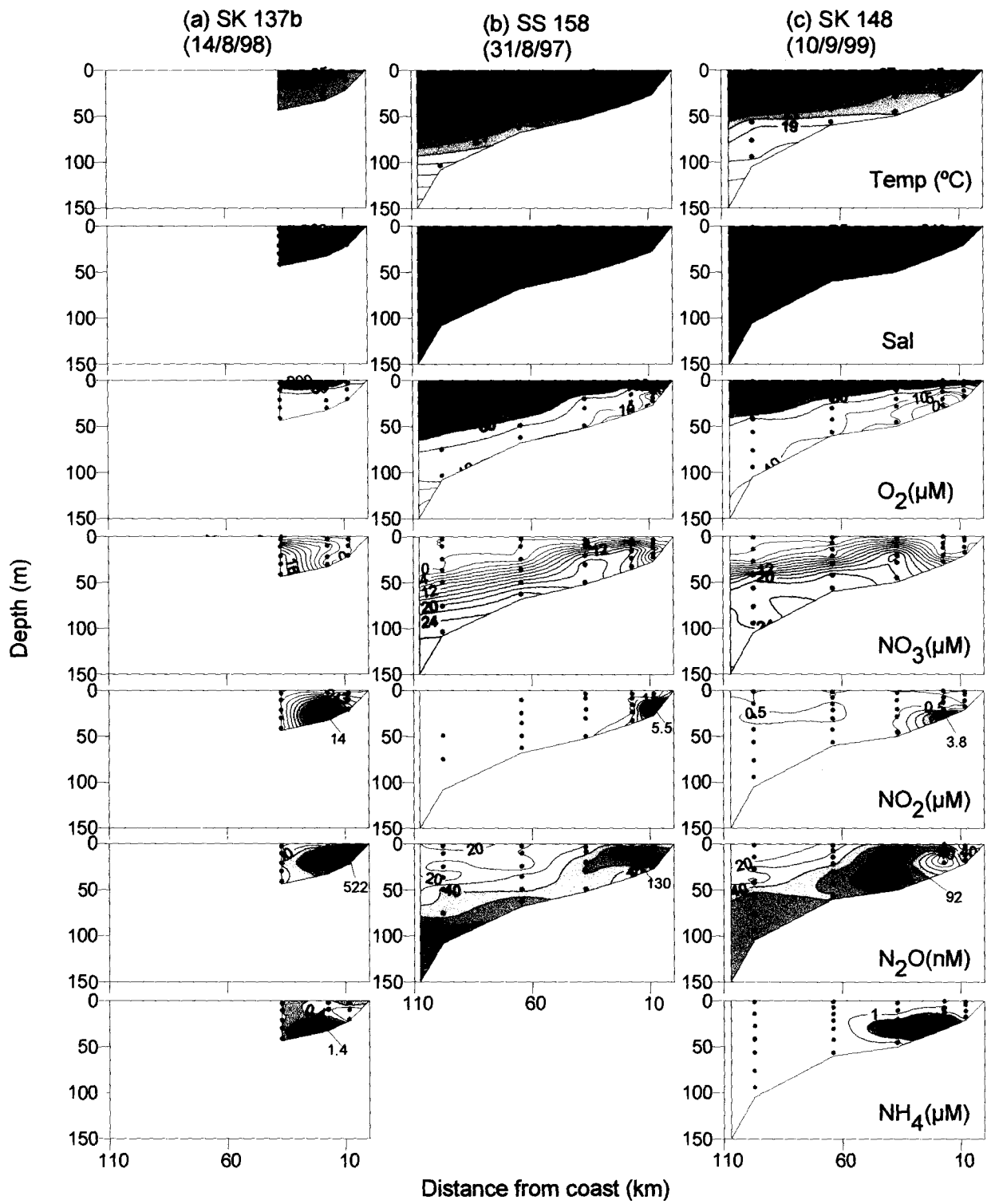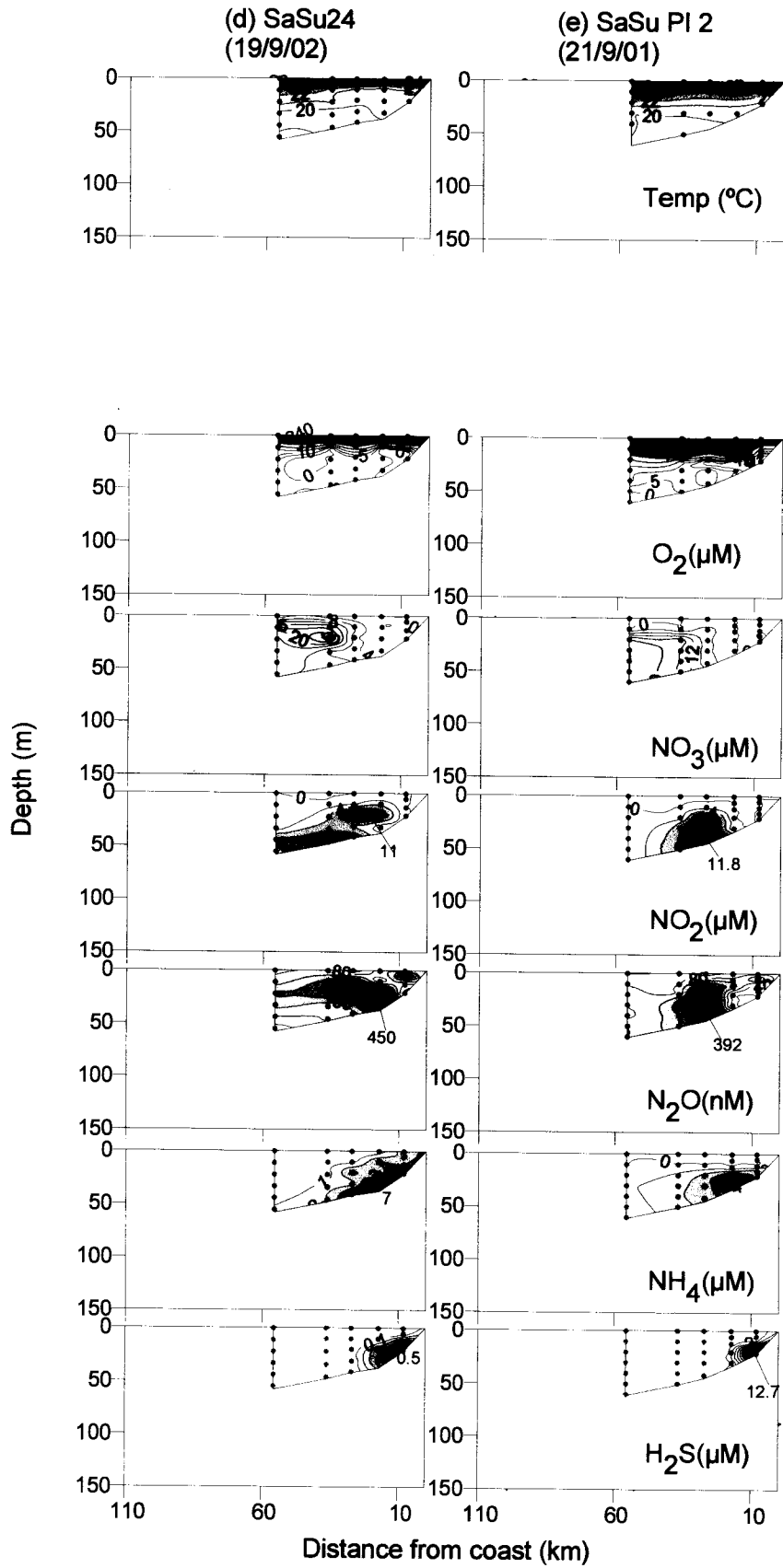
Fig. 4.4. Distribution of water column properties along the cross-shelf transect off Karwar during the month of September.

variables still showed vertical gradients. The O_2 concentration was only 56 μM at the surface decreasing to 7 μM close to bottom; NO_3^- was absent at all depths, but NO_2^- was present with its concentration increasing from 1.18 μM at the surface to 4.4 μM in the deepest sample; PO_4^{3-} concentration also increased similarly from 1.43 to 2.23 μM. However, what was most intriguing was the N_2O profile: 435.9 nM at the surface, 462 nM at 10 m and 522.4 nM at 20 m, higher than any value recorded in seawater at that time. Evidently, the system must have been denitrifying shortly before sampling (as evident by high NO_2^-) before the water column had been mixed vertically and the copious N_2O was probably formed through denitrification. The next station located just 9 km offshore exhibited strong stratification with the temperature and salinity changing rapidly from 26.80 to 21.66°C and from 28.542 to 35.020 from 2 to 9 m, respectively. Thereafter the water was essentially isothermal and isohaline to the maximum depth of sampling (30 m). Here the surface water was supersaturated with O_2, but devoid of nitrogenous nutrients. It contained 56.1 nM N_2O. In the deeper, suboxic layer NO_3^- decreased from 5.66 μM to near-zero level, while NO_2^- increased from 5.74 μM to 14.19 μM. This apparently denitrifying water column had N_2O in the concentration range 230-489 nM. The third and the last station of the section did not experience reducing conditions. Overall, the average N_2O concentration for the three stations was 257.4 nM with the average for the surface being 179.5 nM.

The two sections that covered the entire shelf were sampled during August 1997 (SS158) and September 1999 (SK148); these provide classic

examples of coastal upwelling with the isolines of most physico-chemical parameters sloping upward all the way from the shelf-break to the inner shelf (Figs. 4.4b and c). Most of the interesting features in these sections occurred over the inner shelf. On SS158 (Fig. 4.4b), the first two inshore stations experienced denitrification. NO_2^- concentrations were moderate (maximum 5.47 μM); total NO_3^- loss did not occur; and N_2O did not show any major anomaly: the highest concentrations measured were 50.6 nM at the surface (at the most inshore station) and 130.4 nM at a mid-depth (at the second station from the coastal end of the transect). On SK148 (Fig. 4.4c), NO_3^- was lost completely at the two most inshore stations (except in the near bottom sample of the deeper station). These samples smelled mildly of H_2S, and anoxia was also supported by the accumulation of NH_4^+. The next two stations were affected by mild denitrification. On this cruise, N_2O concentrations were quite modest: the highest concentrations in the surface and subsurface waters were 44 and 92 nM, respectively.

The remaining two sections are based on SaSu cruises 24 and PI2 undertaken very nearly one year apart during the closing stages of the SWM. Both sets of observations (Figs. 4.4d and e) indicated the prevalence of strongly reducing conditions all along the sections extending over 50 kilometers from the shore. The property distributions were quite comparable. In particular the highest values of NO_2^- were quite similar. On SaSu24, complete anoxia occurred only at the first coastal station and the H_2S concentrations were low (0.5 μM). Anomalous N_2O concentrations recurred on this cruise, with the maximum at the surface and at depth being 104 nM and 449 nM at the second station from the shallow end of the track where

again NO_3^- was close to depletion but NO_2^- was moderately high. On SaSuPl2, H_2S was detected at two most inshore stations with a maximum concentration of 12.7 μM. Again anomalously high N_2O concentrations (323-393 nM) were seen below the pycnocline at the station (third from the coast) having high NO_2^- (>11 μM) and low NO_3^- (<6 μM), whereas the highest surface concentration of N_2O (49 .1 nM) was measured at the most inshore station. For reasons not clear, NH_4^+ concentrations measured on the cruise were modest in spite of the prevalence of sulphate reduction.

4.4.5 Off Goa

This section was repeated the most number of times (17), and although the majority of cruises (11) were conducted during June-October, the crucial period in the context of suboxia and elevated N_2O levels, the remainder observations seem to be adequate to provide a reasonable understanding of changes in the biogeochemical environment over the continental shelf off central-western India.

In January, surface waters were found to be well homogenized with SST exceeding 28°C over the entire shelf (Fig. 4.5a). Presence of northward flow of low salinity waters was indicated by salinities < 35 and the depression of the thermocline. Accordingly, the water column was well-oxygenated to a depth of at least 50 m. Nitrogenous nutrient concentrations in the surface layer were close to detection limit even though PO_4^{3-} was present in significant concentrations (not shown). A weak maximum in NO_2^- seems to emanate from the coast, extending offshore; it was, most likely, the primary maximum referred to above. Distribution of N_2O was typical of an open ocean

system, i.e., increase across the thermocline but the concentrations were modest by the Arabian Sea standard.

The NEM circulation was the best developed in February (Fig. 4.5b) as inferred from the low salinities (< 34.5) prevailing within the bulk of the surface layer, and pronounced downwelling occurring over the shelf. The oxycline and nitracline were relatively deeper than in January. Clear signs of substantial near-bottom respiration could be seen in NO_3^-, O_2 and NO_2^- data.

As noted in Chapter 3, observations during the SI season (April, 1996; Fig. 3.3a) did not show upwelling over the Goa shelf. Data collected along an additional, shorter transect occupied during May 2002, are presented in Fig. 4.5c. The observed warm SSTs (>29°C) rule out upwelling at this time. However, the O_2 isolines tend to follow bottom topography (with lower O_2 in near-bottom waters) indicating substantial respiratory activity in the sediments or bottom boundary layer. Importantly the sea was quite rough during this survey that could have led to the dispersal of nutrients regenerated in the benthic layer.

Upwelling signatures were clearly discernible in June even though the inner shelf could not be covered on Cruise SK103 (Fig. 4.5d). The influence of runoff could also be seen in the form of lower near-surface salinities at the shoreward end of the section. The onset of upwelling had brought low-O_2, high-NO_3^-, and high N_2O water close to the surface, with the latter showing no anomaly.

Observations made on the two legs of the SK137 cruise provided representative data for July and August facilitating an understanding of the evolution of early stages of suboxic conditions. The first occupation of the

53

section (Fig. 4.5e) revealed that the upwelled water had just reached the bottom of the most inshore station, but was not suboxic. The well-developed primary NO_2^- maximum that extended across the shelf followed the nitracline, and was evidently formed through assimilatory reduction. A sub-surface chlorophyll maximum was found to accompany this feature. N_2O concentrations were found to increase moderately in the thermocline, as usual. On the return leg (137b), conditions were found to have changed substantially. Denitrification was intense over the inner shelf (depth < 30 m) with NO_2^- reaching peak concentration of 6 μM and NO_3^- not exceeding 10 μM. Elevated N_2O concentrations were observed in this region, the highest being 79.5 nM at the surface and 282 nM at depth.

On SK180 conducted in August 2002, only three stations could be occupied due to technical reasons; these were located within 10 km of the coast. These observations (Fig. 4.5g) showed weaker stratification with the SST ranging from 24.04 to 25.77°C and the surface O_2 concentration as low as 76 μM at the shallowest station. NO_3^- was close to detection limit and NO_2^- concentration also did not exceed 1.3 μM. Apparently near-complete denitrification had occurred in the upwelled water before the water column was vertically mixed due to turbulence. This is similar to the situation encountered off Karwar on SK137b (Fig. 4.4a) except that the NO_2^- concentrations were much lower:

The Goa transect was extended inshore by using a small boat on 1 September 1997 just after sampling on SS158. The conditions encountered

(a) SS 161 (6-7/1/98)

(b) AAS 42 (16/2/02)

Temp (°C)

Sal

O$_2$(μM)

NO$_3$(μM)

NO$_2$(μM)

N$_2$O(nM)

Depth (m)

Distance from coast (km)

Fig. 4.5. Distribution of water column properties along the cross-shelf transect off Goa during the months of January and February.

Fig. 4.5. Distribution of water column properties along the cross-shelf transect off Goa during the months of May, June and July.

Fig. 4.5. Distribution of water column properties along the cross-shelf transect off Goa during the months of August and September.

Fig. 4.5. Distribution of water column properties along the cross-shelf transect off Goa during the month of September.

(l) SaSu Pl 2
(22-23/9/01)

(m) SK 138
(3-4/10/98)

(n) SaSu 1
(5-10/10/01)

Depth (m)

Temp (°C)

Sal

$O_2 (\mu M)$

$NO_3 (\mu M)$

$NO_2 (\mu M)$

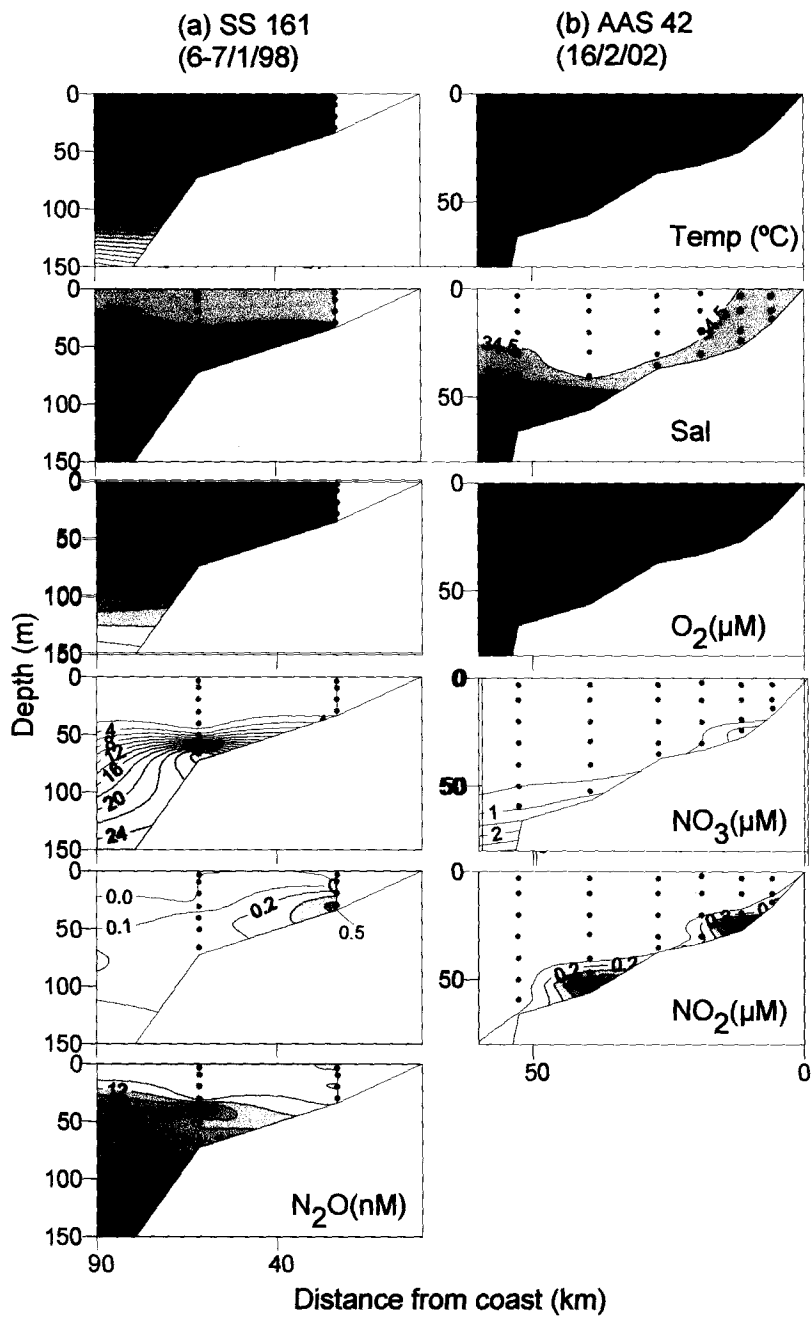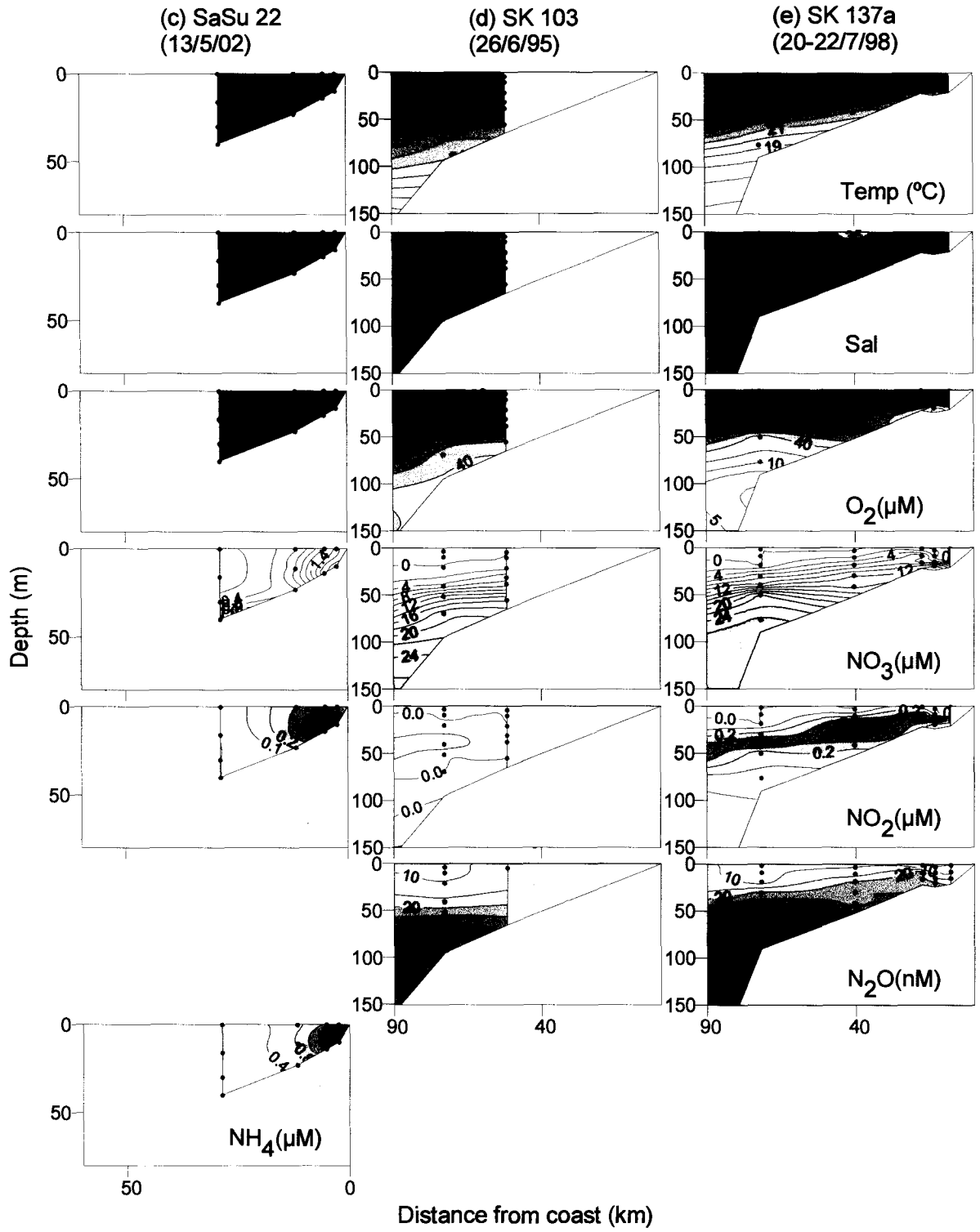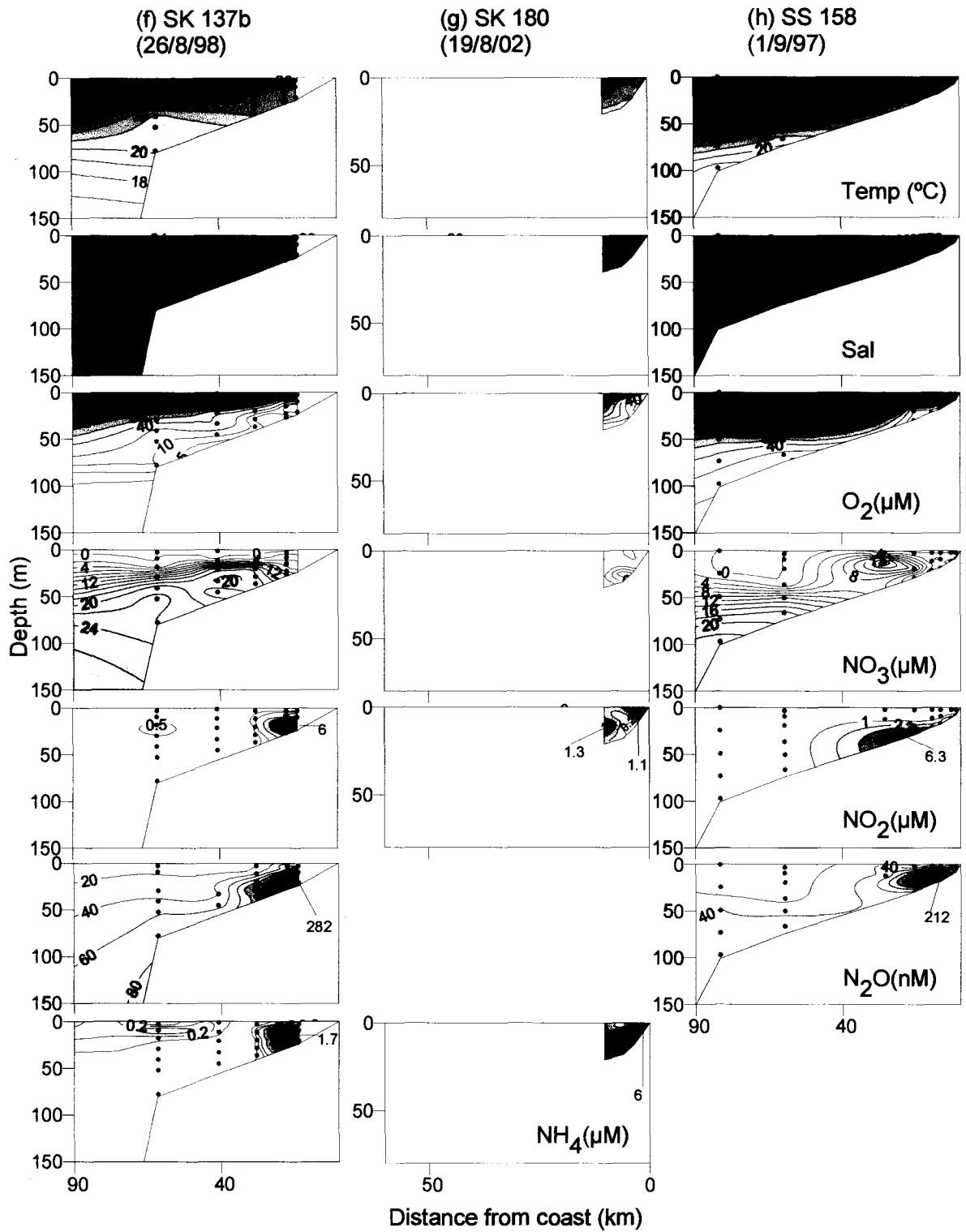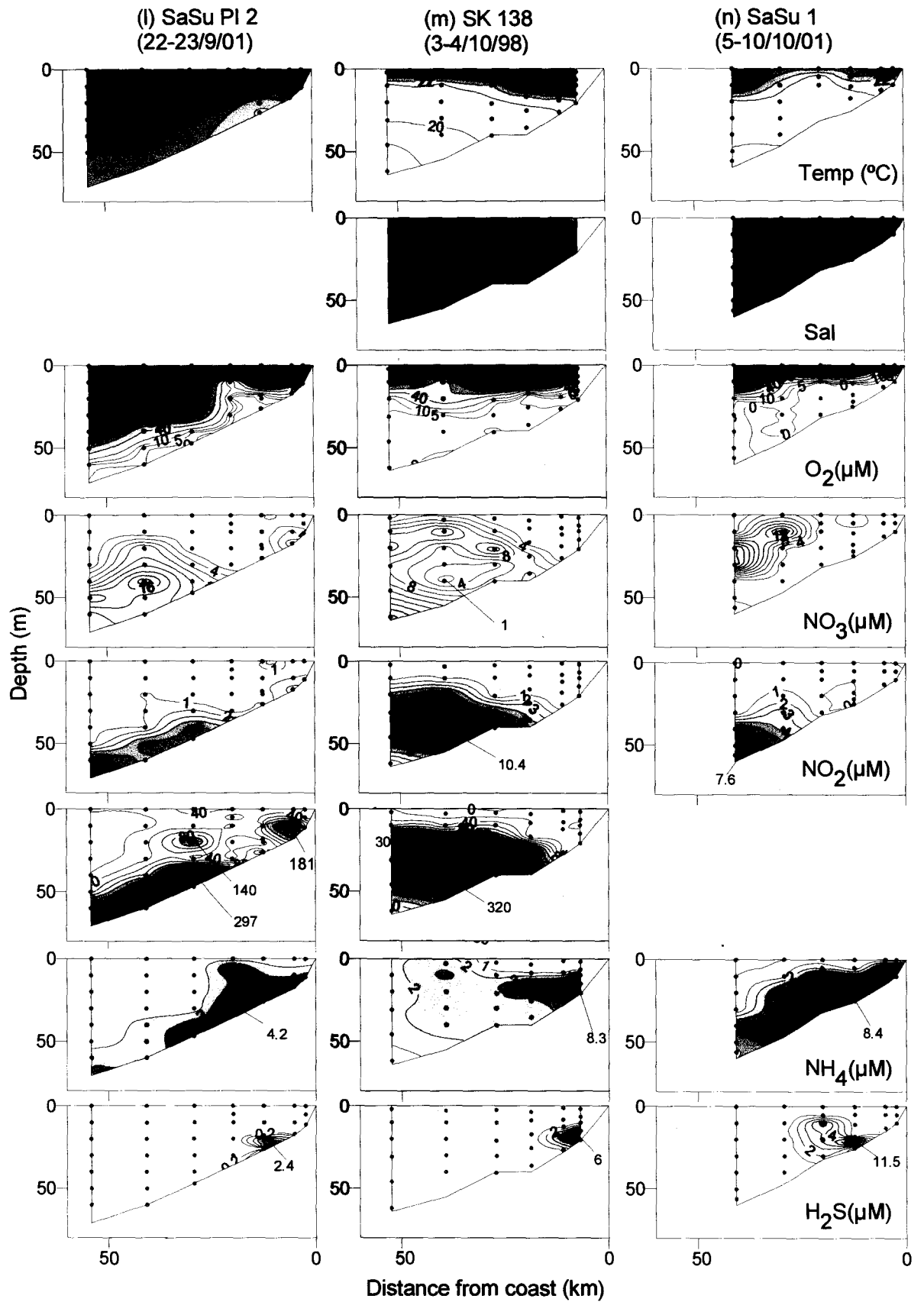$NH_4 (\mu M)$

$H_2S (\mu M)$

Distance from coast (km)

Fig. 4.5. Distribution of water column properties along the cross-shelf transect
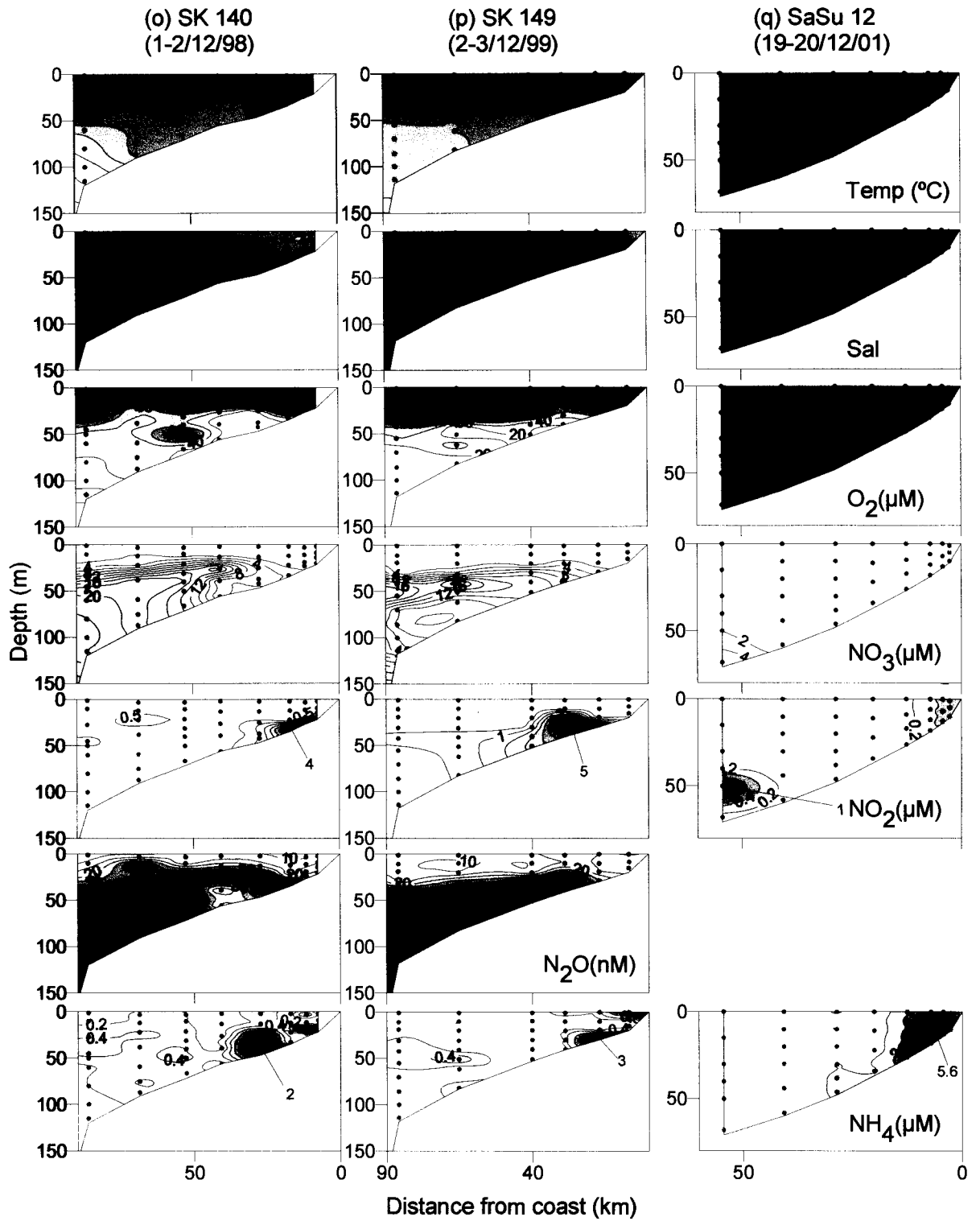off Goa during the months of September and October

Fig. 4.5. Distribution of water column properties along the cross-shelf transect off Goa during the month of December.

(Fig. 4.5h) were quite similar to those on 137b (Fig. 4.5f) discussed above. Suboxic conditions occurred over the inner shelf leading to the buildup of NO_2^- and N_2O to maximal values of 6.3 μM and 212 nM, respectively.

The commissioning of CRV *Sagar Sukti* (SaSu) in 2001 facilitated more frequent sampling off Goa, and while the sections did not cover the entire shelf, the station spacing was closer. These observations revealed that suboxic/anoxic conditions vary considerably over short periods as well as from one year to another. For example, on the SaSuPI1 cruise (Fig. 4.5i), deep water was found ascending the shelf along the bottom as ~20 m thick band from 60 m upward i.e., isolines of O_2, NO_3^- NO_2^- and N_2O ran parallel to the seafloor. The three most inshore stations of the section were oxygenated having low concentrations of NO_3^- and NO_2^-, while denitrification occurred close to bottom in the rest of the section. However, the highest N_2O concentrations (up to 142 nM at the surface, 191 nM at depth) were observed at the shallow end of the section; elsewhere except for the deepest (near bottom) sample the values were generally < 100 nM. Occurrence of NH_4^+ in high concentrations (~6 μM) over mid-shelf was a conspicuous and unexpected feature since these values did not come from the deepest sample, which is usually the case, often caused by NH_4^+ diffusion from the sediments.

In comparison, data from the SaSu24 cruise taken a year later showed more intense O_2 deficiency and over a larger volume of water (Fig. 4.5j). In spite of the fact that upwelled water reached the surface only at the most inshore station, both NO_3^- and NO_2^- were nearly absent and sulphate reduction (maximum H_2S 5.5 μM) occurred close to bottom within 30 km of

the coast. NH_4^+ accumulated to a maximum of 9.7 μM close to bottom in the anoxic zone. The rest of the section experienced intense denitrification within an approximately 30 m thick bottom layer, with NO_2^- reaching a maximum concentration of 13.2 μM. Distribution of N_2O was highly variable. Unlike the trend seen on SaSuPl1, near-bottom waters contained the least quantities of N_2O; instead maximal values were invariably found at mid-depth. The highest concentrations observed were 129 nM at the surface and 765 nM at depth. The latter value is the highest known so far from the oceans. It came from an isolated parcel of water that contained some NO_3^- and NO_2^- (1.4 μM each) in the otherwise anoxic zone.

The SK148 Goa section (Fig. 4.5k) extended further offshore than the SaSu sections (Fig. 4.5i,j). The three shallowest stations on the transect contained NO_3^- and NO_2^- in low concentrations, but traces of H_2S were detected in bottom waters indicating transient conditions. Further seaward the zone of denitrification existed as in the case of SaSu24 data. Distributions of NO_3^-, NO_2^- and NH_4^+ suggest that while the fresh upwelled water moved up close to the seafloor, the older suboxic/anoxic water flowed at mid-depth in the opposite direction. N_2O concentrations were maximal at mid-depth here as well, with the peak values at the surface and at depth being 162 and 291 nM, respectively.

The SaSuPl2 section (Fig. 4.5l) was a repeat of that of SaSuPl1 (Fig. 4.5i). The O_2 deficiency had become more pronounced during the 8 days intervening the two sets of observations, with H_2S being present close to bottom at the third station from the coast. Denitrification occurred further offshore in a larger volume of water. N_2O concentrations were more variable

56

with the highest values recorded in the middle part of the section both at the surface (54 nM) and at depth (297 nM).

On the next cruise (SaSu01) undertaken 12 days after SaSuPl2, conditions had changed even more dramatically. Upwelling had greatly intensified as evident from low SSTs (23.5-26.8°C), and the subsurface waters had turned suboxic/anoxic all along the section (Fig. 4.5n). The oxidized nitrogen species had mostly been consumed within 20 km of the coast with consequent onset of sulphate reduction close to bottom. The highest H_2S concentration measured was 11.5 μM. NH_4^+ was also found to accumulate close to bottom all over the section to a maximum of 8.4 μM. Even at the deepest station NO_3^- concentration did not exceed 7.5 μM reflecting the intensity of denitrification. Due to technical difficulties N_2O was not measured on the cruise, except at two shallowest stations.

One interesting feature observed on SaSu01 (also noticeable to a smaller extent in the SaSuPl2 section) was the occurrence of strongest upwelling in the mid-shelf region. This feature was also observed on SK138c undertaken at about the same time (the first week of October) three years earlier (Fig. 4.5m). NO_3^- and NO_2^- concentrations were comparatively higher and those of H_2S lower in 1998 than in 2001 (Fig. 4.5l). Interestingly peak N_2O concentrations at the surface (25.4 nM) and at depth (320 nM) were found at the deepest station on SK138c.

Of the three sections available for the month of December, two were taken in the first three days of the month, albeit in different years (1998 and 1999). On both occasions (Figs. 4.5o and p) mixed layers were still quite shallow, and the sub-pycnocline O_2 still low, occasionally suboxic. The low

NO_3^- concentrations associated with significant amounts of nitrite in the inner-to mid-shelf regions indicate that denitrification should have taken place in the samples recently, if not continuing at the time of observations. Evidently, the isotherms were leveling as the upwelled waters were retreating offshore. During this period of transition the isotherms are expected to sweep the seafloor and carry the signatures of coastal benthic processes offshore. Abnormally high N_2O concentrations were not observed on any of these cruises.

The third section off Goa for December (Fig. 4.5q) was clearly sampled after the transition to the NEM circulation had been completed. Deep mixed layers with high temperature and high O_2 contrast sharply with the two sections discussed above. NO_3^- was usually below the detection limit except close to bottom at the deepest station; NO_2^- occurred in traces at the shallowest and deepest stations. N_2O was not measured on the cruise (SaSu12), but its concentration is expected to be low in view of the high ambient O_2 levels.

4.4.6 Off Ratnagiri

The Ratnagiri section was first occupied in October 1999 on SK148 and repeated a year later on SaSu01. The SaSu01 (Fig. 4.6a) observations were made up to 65 m water depth whereas sampling on SK148 (Fig. 4.6b) was done all across the shelf. Although the periods of observations differed by only one day of the year, conditions encountered on the two cruises were significantly different. On both occasions upwelled water reached within 10 m of the surface at the most inshore station and its O_2 content was low enough
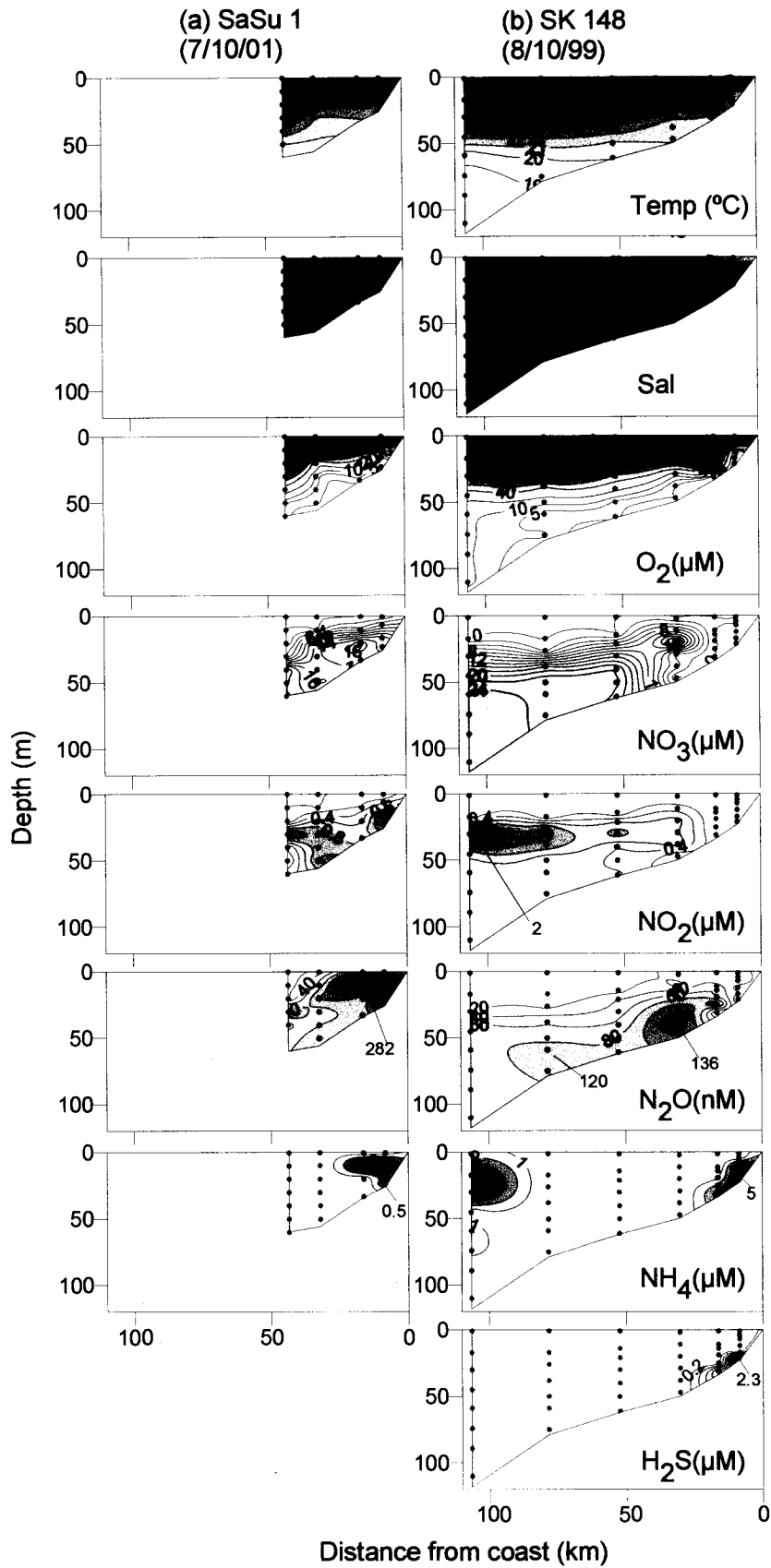
Fig. 4.6. Distribution of properties along the cross-shelf transect off Ratnagiri during the month of October.

to make the environment reducing. Indeed, such conditions did exist during both the cruises, but with differing intensity. On SK148 all NO_3^- and NO_2^- had been consumed and H_2S accumulated in near-bottom waters at the two most inshore stations whereas intense denitrification occurred within the lower ~20 m of water at the third station [even though NO_2^- concentrations were modest; note that the NO_2^- maximum (2 μM) at the most offshore station is probably of the primary category]. On SaSu01, no H_2S was detected because of the presence of NO_3^- in high concentrations (~15 μM) even at the shallowest station. However, NO_2^- was present in low but detectable levels (maximum 1.2 μM) in the subsurface layer throughout the section indicating that the system had perhaps just turned denitrifying. However, despite less severe reducing conditions observed on the SaSu cruise, N_2O concentrations were higher (maximum values being 73 and 34 nM at the surface and 282 and 136 nM at mid-depths on SaSu01 and SK148, respectively).

4.4.7 Off Mumbai

Off Mumbai, the earliest observations in terms of the day of the year were made towards the end of August on SK180 (Fig. 4.7a). These revealed that the upwelled water had just reached the shallowest end of the section even though the bottom water temperature was >25°C. Relatively deep mixed layers and associated well-oxygenated conditions were observed throughout the section; only at the most offshore station O_2 concentration approached suboxia in the near-bottom water. Barring the shallow end of the section NO_3^- concentrations were quite low all over the shelf and traces of NO_2^- observed at mid-depths probably belonged to the primary maximum. These
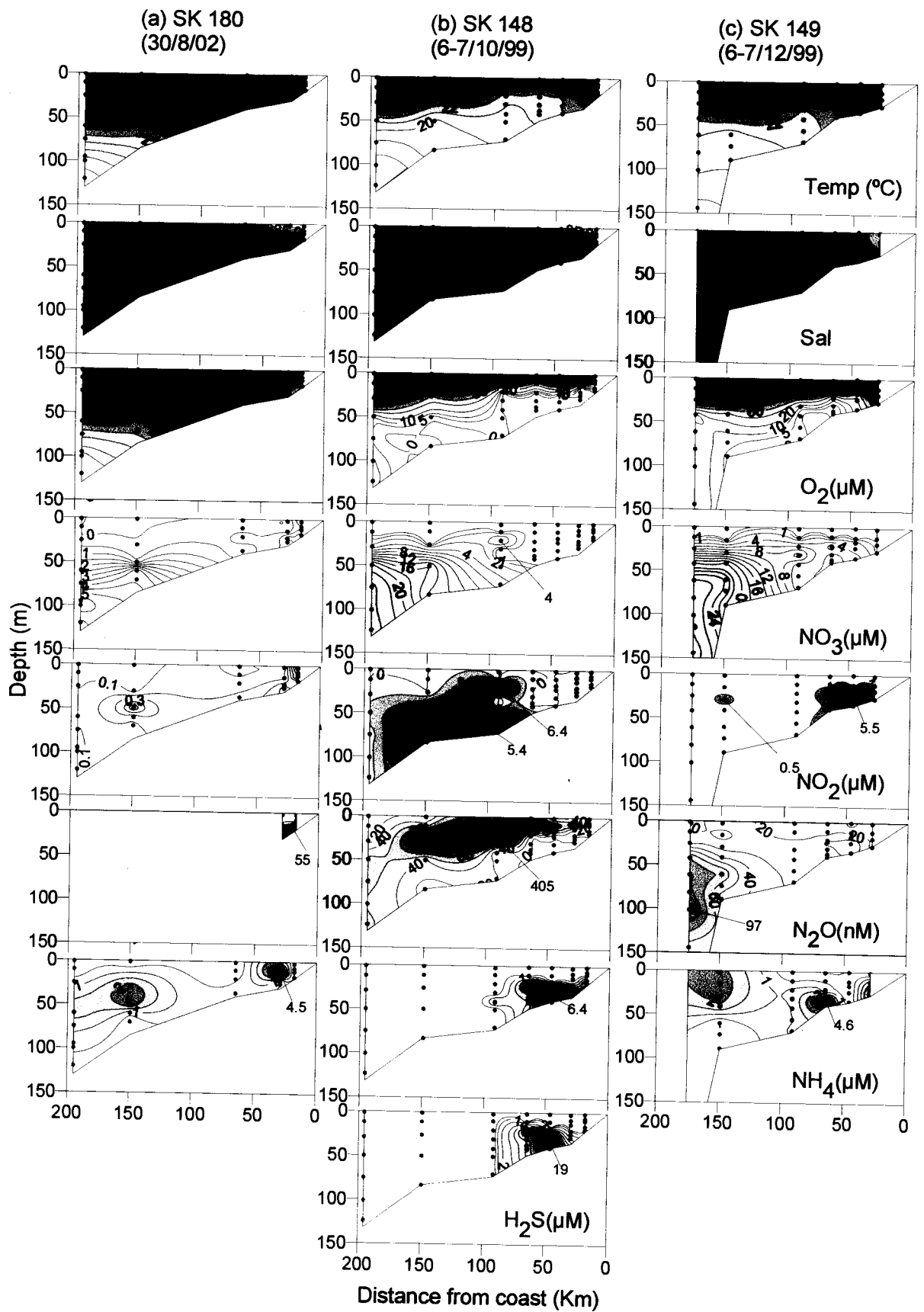
Fig. 4.7. Distribution of water column properties along the cross-shelf transect off Mumbai during the months of August, October and December.

observations support the view that the development of reducing conditions over the shelf of Mumbai lags behind that in the south because of the late arrival of the upwelled water over the shelf in the former region.

The SK148 section demonstrates clearly the sequential transition from hypoxic to suboxic conditions and then to complete anoxia as the upwelled water moved up the shelf (Fig. 4.7b). The inner shelf was quite strongly anoxic where H_2S and NH_4^+ were found to accumulate in near bottom water to 19 and 6.4 μM, respectively. Vigorous denitrification occurred further offshore to the shelf break as indicated by the build-up of NO_2^-. As described previously for several other sections, N_2O distribution was marked with large variability with maxima located at mid depth. In this case, the highest surface concentration was 95 nM while it was 405 nM at depth. Interestingly, as in the previously-noted instance for the SaSu24 section off Goa where the record high N_2O (765 nM) was measured, the highest value for the SK148 section also corresponded to an isolated parcel of water having some NO_3^- (4 μM) and NO_2^- (6 μM) that was surrounded by anoxic water.

Repeat observations exactly two months later showed that the reducing conditions were on the wane (Fig. 4.7c). Upwelling was perceptibly less vigorous (i.e. isotherms deepened) and the upper water column became more oxygenated. Although near complete O_2-depletion still occurred close to bottom, sulphate reduction had ceased to occur, and the distribution of NO_2^- suggested shrunken volume of denitrifying waters. N_2O concentrations were quite moderate, the highest being 29 nM at the surface and 97 nM at depth.

4.4.8 Cross-Shelf Sections: Summary

Upwelling along the west coast of India begins earlier in the south (probably in March) than in the north. Data collected during the present study revealed lowering of SST and fertilization of surface waters due to this process over the shelf off Quilon in July, but off Mumbai such effects were barely noticeable even by the end of August. However, in the north the effect of upwelling was felt at least until early December. Thus, overall upwelling along the west coast of India may occur from March to December; this period far exceeds the duration of the SWM.

Intense rainfall in the coastal zone and the associated land runoff, especially in the region around Mangalore, leads to the formation of a thin ($\leq$ 10 m) lower-salinity layer that normally floats over the upwelled water, preventing it from surfacing. However, along the southwest coast of India, where winds are upwelling favourable, upwelled water does make it to the surface as evident from the low SST and high surface NO_3^- content. The effect of upwelling also extends further offshore here both because of offshore advection of upwelled water and uplift of pycnocline associated with the Laccadive Low. The process becomes gradually confined closer to the coast toward the north. However, there are times when upwelling is more intense at some distance away from the coast. Two instances of this phenomenon were noticed off Goa in early October.

At the shelf break (depth 100-150 m), O_2 concentrations in near bottom waters were never found to be suboxic (i.e. supporting denitrification as inferred from the accumulation of NO_2^-). However, as the upwelled water

moves up the shelf it gradually loses O_2, ostensibly due to respiration of organic matter sinking to the seafloor. Along the two southern sections studied here (off Quilon and Cannanore), O_2 does not reduce to suboxic levels (i.e. low enough to necessitate denitrification). But further north (off Mangalore, Karwar, Goa, Ratnagiri and Mumbai) suboxic stage is reached with the advent of the season. The exact time when the threshold is crossed varies from north to south – it seems to occur gradually later from the south to the north – and also from one year to another for the same region. It may occur the earliest (in July) off Mangalore and the latest (early September) off Mumbai. Further intensification of the suboxic system leads to anoxia (i.e., sulphate reduction). The month during which such transition was recorded in our data set was as follows: off Mangalore – August; Off Karwar –September; off Goa – September; off Ratnagiri – October; and off Mumbai – October. Repeat sections at about the same time, but in different years showed substantial inter-annual changes in the state of redox environment. It must be noted that the shallow, seasonal suboxic zone develops independently and is geographically separated from the deeper and perennial suboxic zone occurring beyond the continental shelf.

A number of repeat sections off Goa are available for different seasons to gain insights into changes that occur over a full annual cycle. Downwelling associated with the northward flow of the WICC during the NEM results in deep mixed layers and well-oxygenated conditions over the shelf. However, where sampling was achieved close to the seafloor significant decrease in bottom-water O_2 could be noticed as a result of intense benthic respiration. With the onset of the SWM in June, upwelling brings in deeper water over the

shelf that is already depleted in O_2. As stated, suboxic conditions develop in August and following the complete loss of NO_3^- through denitrification sulphate reduction begins in September. The termination of anoxic conditions begins in November with the retrieval of upwelled water and by late December the water column becomes well oxygenated all over the shelf. In September-early October, when the anoxia peaks, the oxic, suboxic and anoxic systems are found sequentially from the outer shelf to inner shelf. However, the intensity and spatial extent of various zones vary considerably over short periods of time and from year to year. For example, the conditions were more severe and lasted longer in 2001 as compared to 2002.

Extremely large variability in N_2O distribution seems to occur, both in space and time, in reducing environments especially when waters become completely anoxic. Many instances of anomalously high N_2O concentrations – the highest recorded anywhere in the oceans – were found in the region between Mangalore and Mumbai. In most cases the N_2O accumulation seems to occur in waters experiencing intense denitrification with maxima located mostly at mid-depths.

4.5 Quasi-Time-Series Measurements

Sustained observations have been made since 1997 at five fixed stations located off Candolim-Goa (Fig. 2.2). The frequency of these observations has not been fixed for logistic or technical reasons. For example, it is not possible to access the area during the peak of the SWM (June-August) except with large ships because of inclement weather. Also, during the NEM large variability is not expected because oxic conditions
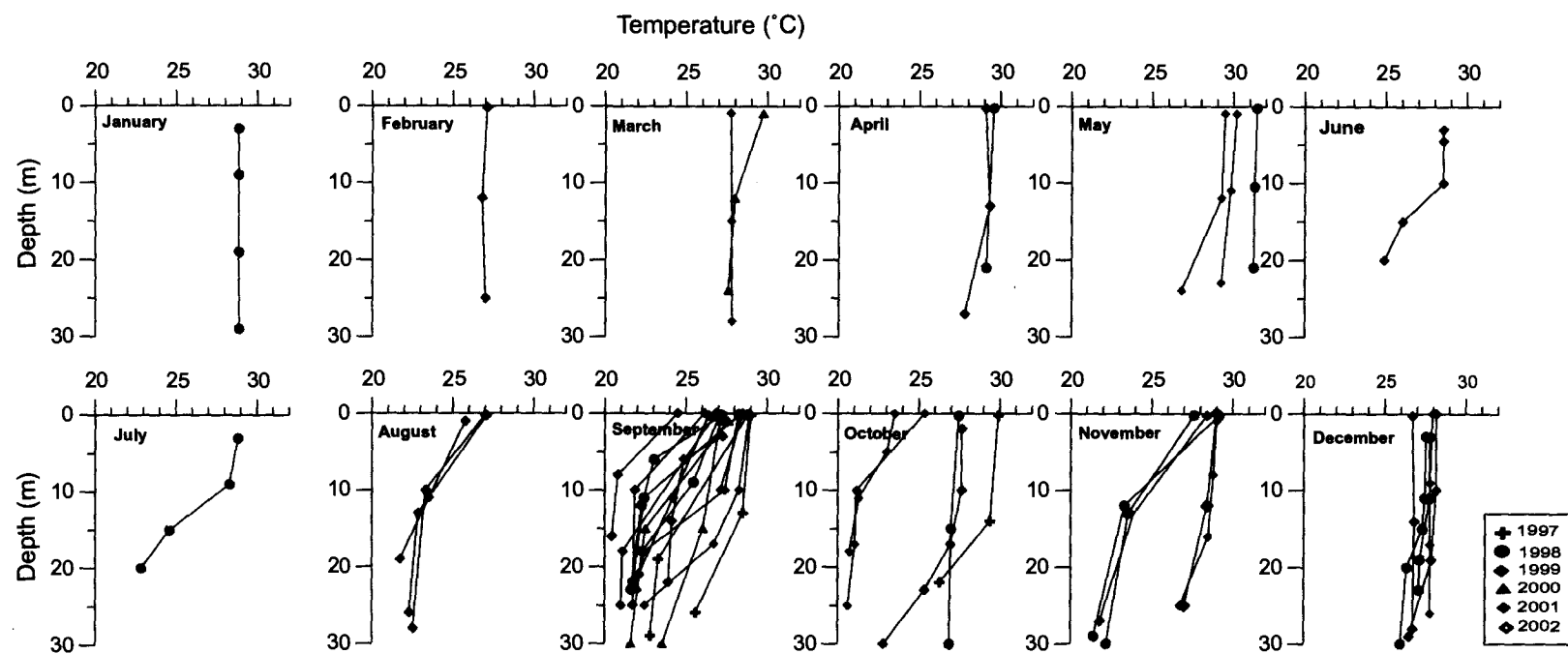
Temperature (°C)

Fig. 4.8. Vertical profiles of temperature (°C) at the CAndolim Time Series (CATS) site (15°31'N, 73°39'E).

prevail in the water column. As a result most of the observations were concentrated during September-December. The last station of this shallow transect, located at Lat. 15°31'N and Long. 73°39'E at a water depth of ~28 m, was also occupied on almost all the cruises undertaken during the present study. Data from this station [hereafter referred to as the CAndolim Time Series (CATS)] have been processed to evaluate the temporal changes in the biogeochemical environment in coastal waters of Goa. Individual vertical profiles of physical and chemical properties at CATS are presented in Figs. 4.8-4.12.

4.5.1 Temperature (Fig. 4.8)

Vertical profile for the months of January and February showed well-mixed water column. Of the profiles – two each – for March and April, one in each case indicated isothermal conditions with the other showing some decrease (by 1-2°C) in temperature in the near bottom water as compared to the surface. Three profiles are available for May, of which two showed vertically homogenous water column with the third (for 2001) showing a decrease in temperature close to bottom, possibly indicating the initiation of upwelling. The single profiles for June and July provide clear evidence of upwelling as do the three profiles for August. The numerous temperature profiles for September showed extremely large variability. At mid-depth, for example, the observed temperature span was over 8°C. Part of this variability should be due to mixing caused by tides and waves, but it may also reflect inter-annual changes in upwelling pattern and intensity. A close examination of the data indicates that the lowest temperatures correspond to 2002

whereas the highest came from 1997 and 2001. However, the October data did not exhibit exactly the same pattern in that the temperatures were much lower throughout the water column in 2001 as compared to the three other profiles. Only one profile (in 1999) exhibited vertically-mixed water column. But this was probably due to turbulence since two profiles in the next month (November) showed the presence of upwelled water, very similar to the profile for 1999. The fourth profile (corresponding to 2001) showed generally warmer temperatures with slightly cooler water present close to bottom. All profiles for December indicated isothermal conditions in the month of December.

4.5.2 Salinity (Fig. 4.9)

Salinity profiles closely followed those of temperature. Distribution in the water column from January to May was vertically homogenous. High salinities during the pre-SWM period were the result of increased evaporation due to high air temperatures and higher incoming solar radiation. During the SWM surface salinity decreased as a result of fresh water inputs from land and monsoonal rains. The rainy season begins in June and lasts till September, but the effect of the dilution continues for some time (up to November) after the cessation of rains. The absence of this effect in the lone July profile (for 1998) must have been due to an event of vertical mixing just prior to sampling. As in case of temperature, salinity values for September also varied over a wide range, but most of this variability was confined to the surface layer. The lowest salinity of 22 was recorded during one of the observations made in 1998. This year was exceptional in that the rainy
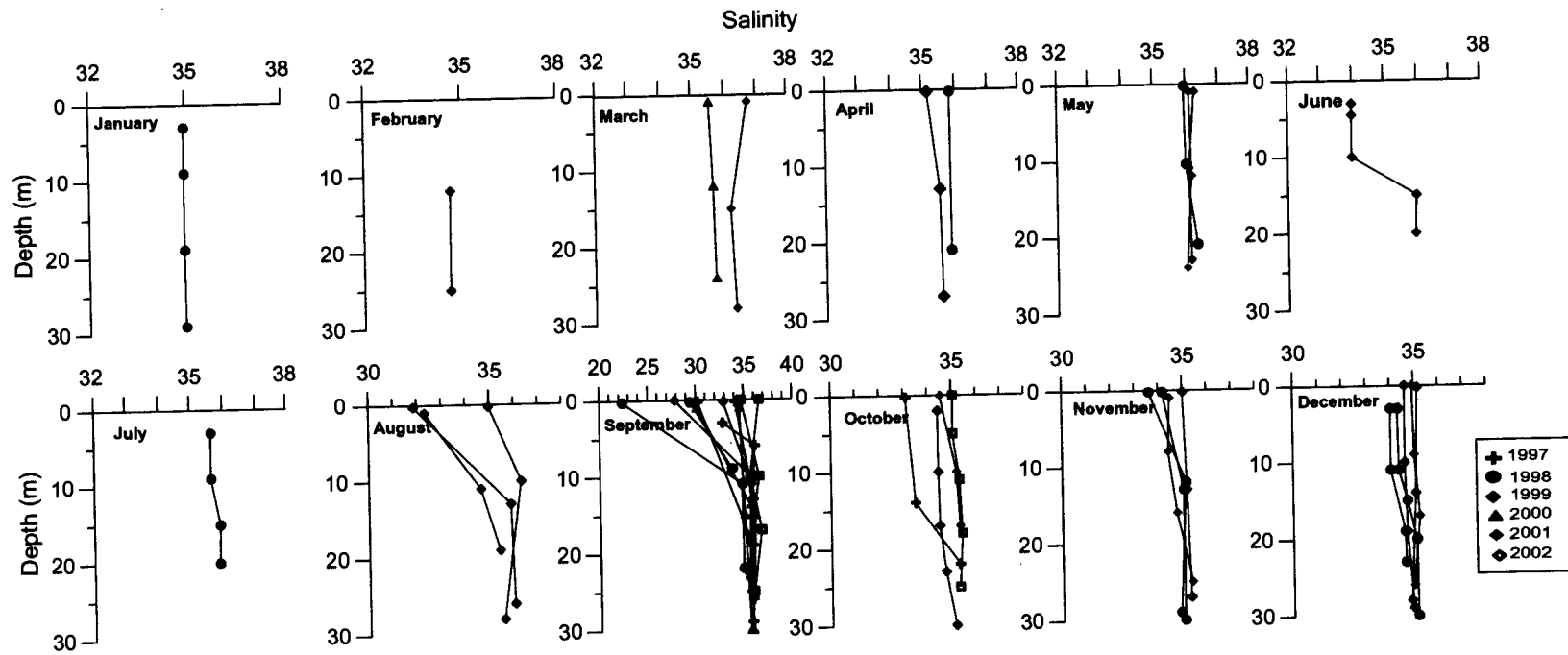
Fig. 4.9. Vertical profiles of salinity at the CAndolim Time Series (CATS) site (15°31'N, 73°39'E).

season continued till November. Because of this lower salinities persisted to some extent even in December, when during a normal year salinity profiles do not usually exhibit significant vertical gradients.

4.5.3 Oxygen (Fig. 4.10)

Vertical distribution of O_2 was also similar to that of temperature and salinity, but the gradients were more pronounced. From January to March the water column was well oxygenated even though some decrease in O_2 concentration was observed in the March 2000 profile. In April the near-bottom values fell close to zero both in 1998 and 1999 indicating high respiration at depth. Surprisingly the gradients were less steep and bottom O_2 depletion in April could have been due to stagnation caused by calm weather conditions. The near-bottom O_2 was low but not suboxic in June and July, but in August suboxia begins to show up in the deeper layer. The profile for August 1999, however, showed relatively higher O_2 (~50 μM). As in case of temperature, and perhaps for the same reasons discussed in Section 4.5.1, O_2 distribution was also extremely variable in the month of September. Higher values of O_2 were recorded in 1997, 1998, 2001 and 2002 during this month. By contrast the October data showed very low values for 2001. It would thus appear that in 2001 upwelling and associated O_2 deficiency peaked in October whereas in the case of 2002 they peaked in September. The year 1997, an El Nino year, appears to have been characterized by somewhat suppressed upwelling and higher O_2 levels. O_2 depletion in the subsurface layer can be seen in all four profiles for November, but is not evident in any of
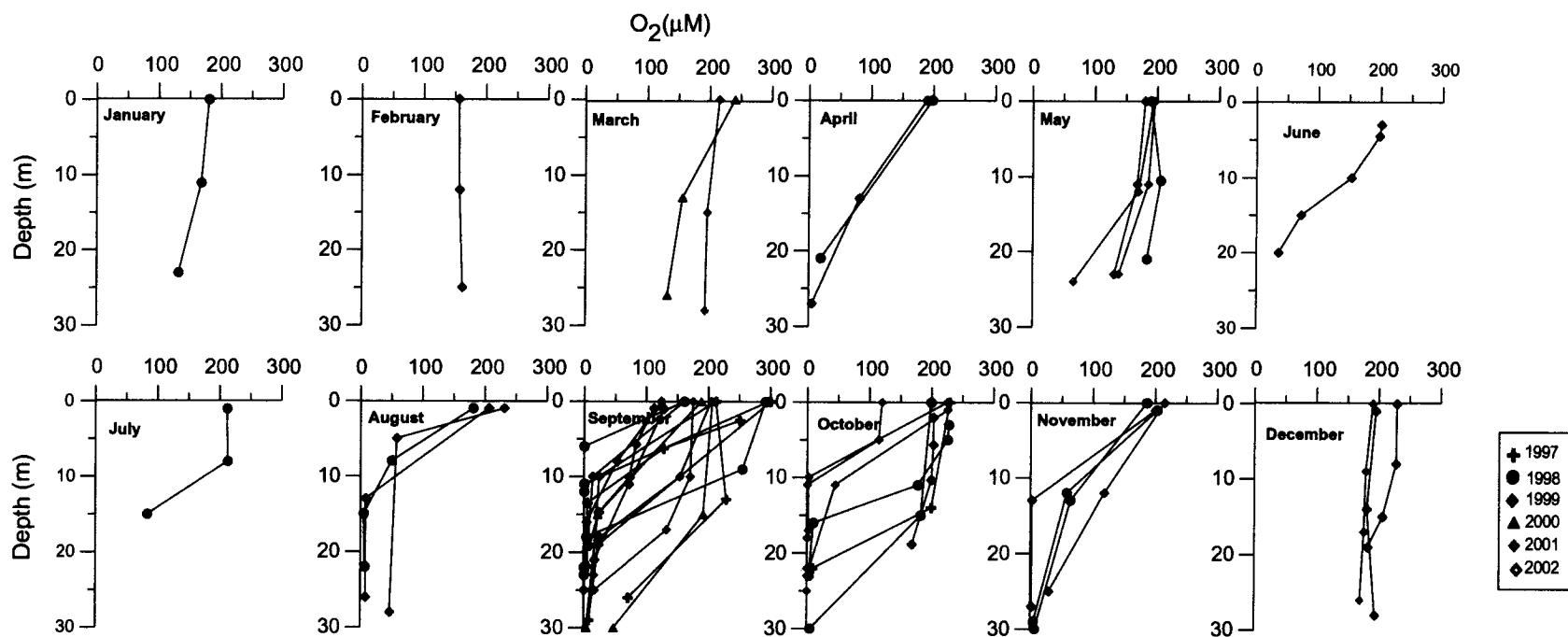
Fig. 4.10. Vertical profiles of dissolved oxygen (µM) at the CAndolim Time Series (CATS) site (15°31'N, 73°39'E).

the profiles for December clearly pointing to a change in hydrographical conditions.

4.5.4 Hydrogen Sulphide (Fig. 4.11)

H_2S was only found at mid-depth and/or close to bottom during September to November, and that too not at all times in these months. H_2S distribution exhibited considerable short-term variations. In one case two sets of observations conducted within one week in September 2001 showed contrasting results. It must be borne in mind that due to the shallow depth of the CATS site, any meteorological event that produces turbulence can potentially lead to removal of H_2S through oxidation. Hence individual profiles sometimes may not be representative of the entire month. Nevertheless, the results suggest considerable inter-annual variability. Consistent with temperature and O_2 distributions discussed above, H_2S data also indicate that while anoxic conditions peaked in October 2001, they peaked a month earlier in 2002. Such inter-annual changes have important implications for coastal fisheries. H_2S was detected only on one occasion (in 1999).

4.5.5 Chlorophyll (Fig. 4.12)

Sufficient measurements of chlorophyll a are available only for September to draw generalized inferences. These reveal generally high concentrations (in one case exceeding 6 mg m^{-3}) in the near-bottom water perhaps reflecting enhanced preservation of chlorophyll under reducing conditions. However, elevated chlorophyll a concentrations should be expected during the period May-November, with lower values during the rest of the year. The lone set of observations for December indicated uniformly
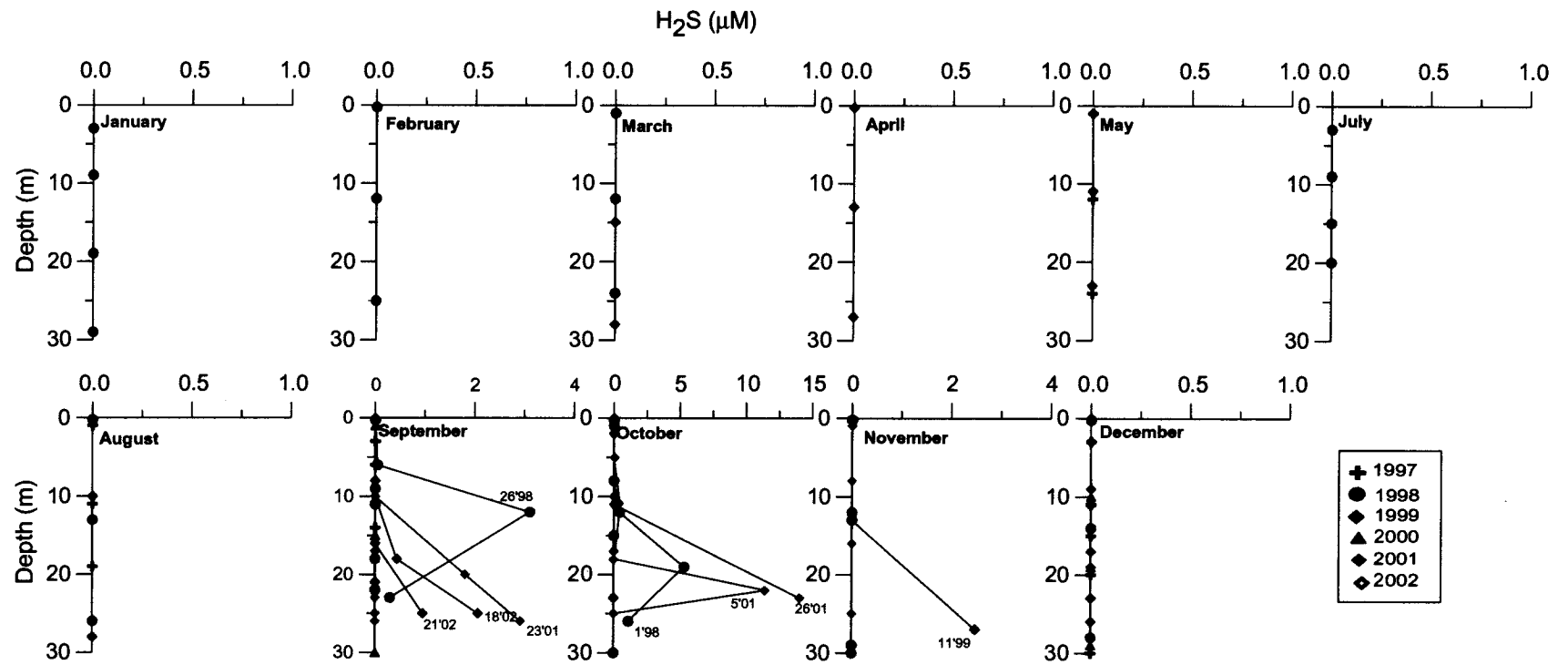
Fig. 4.11. Vertical profiles of hydrogen sulphide (μM) at CAndolim Time Series (CATS) site (15°31'N, 73°39'E). Numbers within the graphs indicate sampling dates.
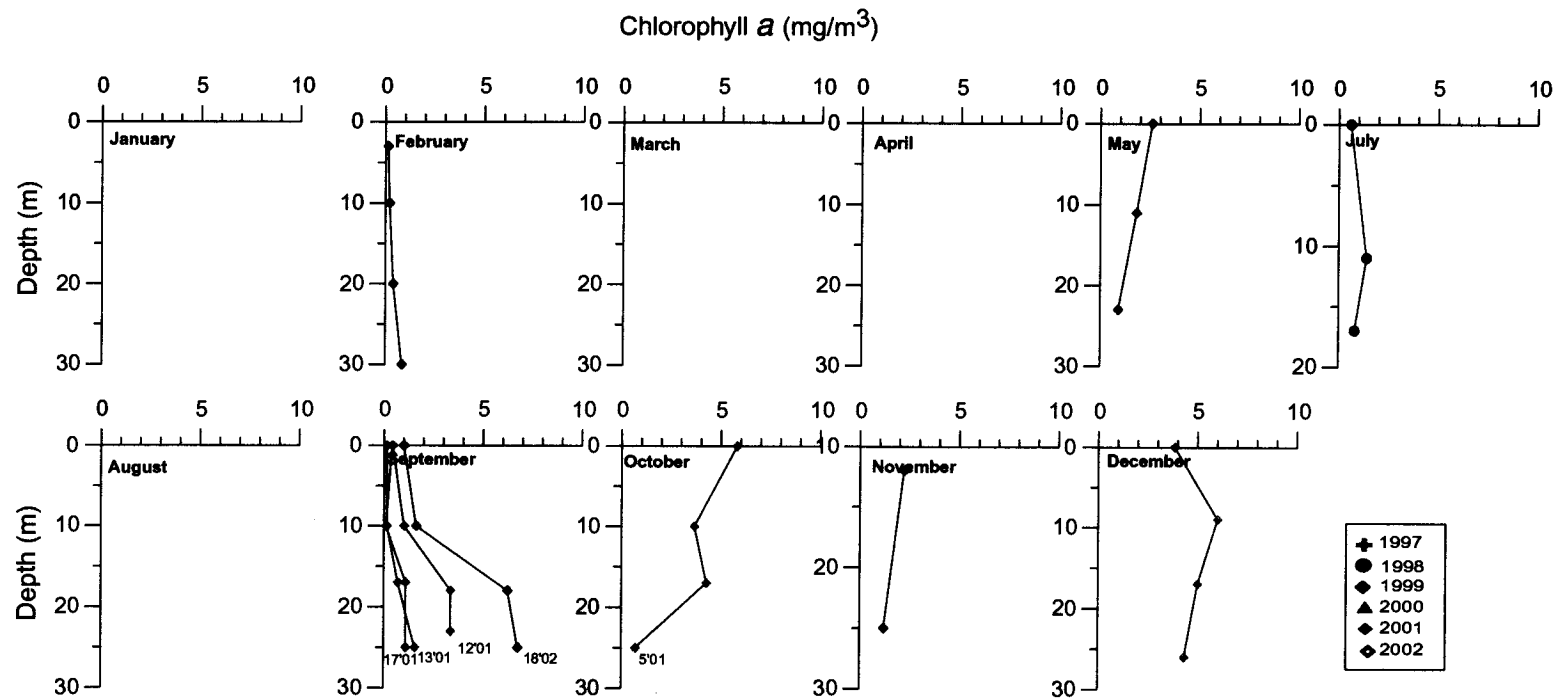
Chlorophyll a (mg/m^3)

Fig. 4.12. Vertical profiles of chlorophyll a (mg m^{-3}) at CAndolim Time Series (CATS) site (15°31'N, 73°39'E). Numbers within the graphs indicate sampling dates

high concentrations throughout the water column. This might either be due to human-induced eutrophication or caused by a short term meteorological event that could have churned up the water column bringing up nutrients from the sediments. Still another possibility is the occurrence of *Trichodesmium* blooms that are known to occur during the NEM and SI seasons (Sreekumaran et al., 1992).

4.6 Climatology of Oceanographic Variables

The data presented in Figs. 4.8-4.12 have been combined to construct monthly climatologies of nine physical and chemical variables. For this purpose all data collected during 1997-2002 at the CATS site were pooled and been averaged for every 2 metres for each month. The results, shown in Figs. 4.13a-i, provide for the first time records of changes in these parameters over one complete annual cycle including the evolution of O_2-deficiency in shallow waters in response to the monsoonal forcing.

Major features of the mean conditions depicted in Fig. 4.13 are, of course, in accordance with the individual profiles discussed in the preceding section. Temperature exhibits a bimodal distribution pattern with maximal values occurring during the SI and late FI seasons. A minor minimum in temperature occurs during winter, but the main minimum is found during the SWM extending into the early FI. This is because of upwelling, which at its peak in September lowers the near-bottom temperature below $21^\circ C$. The lowest recorded temperature was $20.43^\circ C$ at 16 m on 18th September 2001, whereas the lowest SST was $23.5^\circ C$ on 5th October 2001.

(d) Nitrate (µM)

(e) Nitrite (µM)

(f) Nitrous Oxide (nM)

(g) Ammonia (µM)
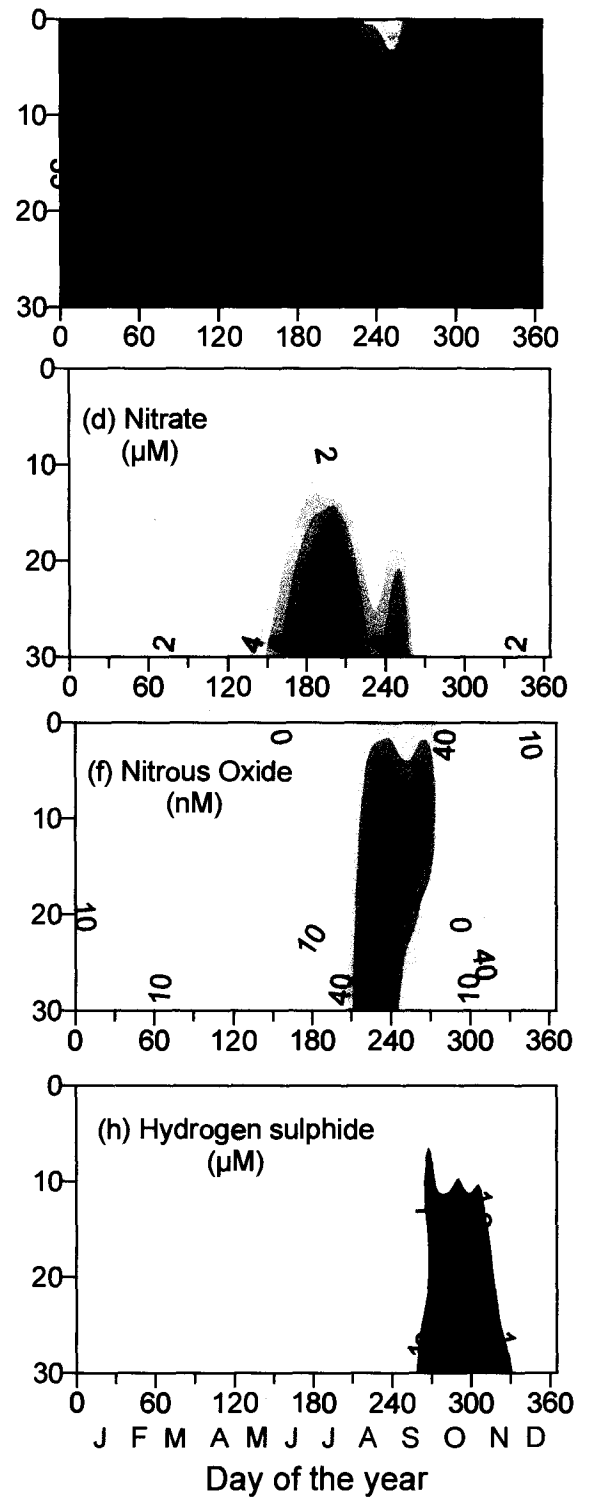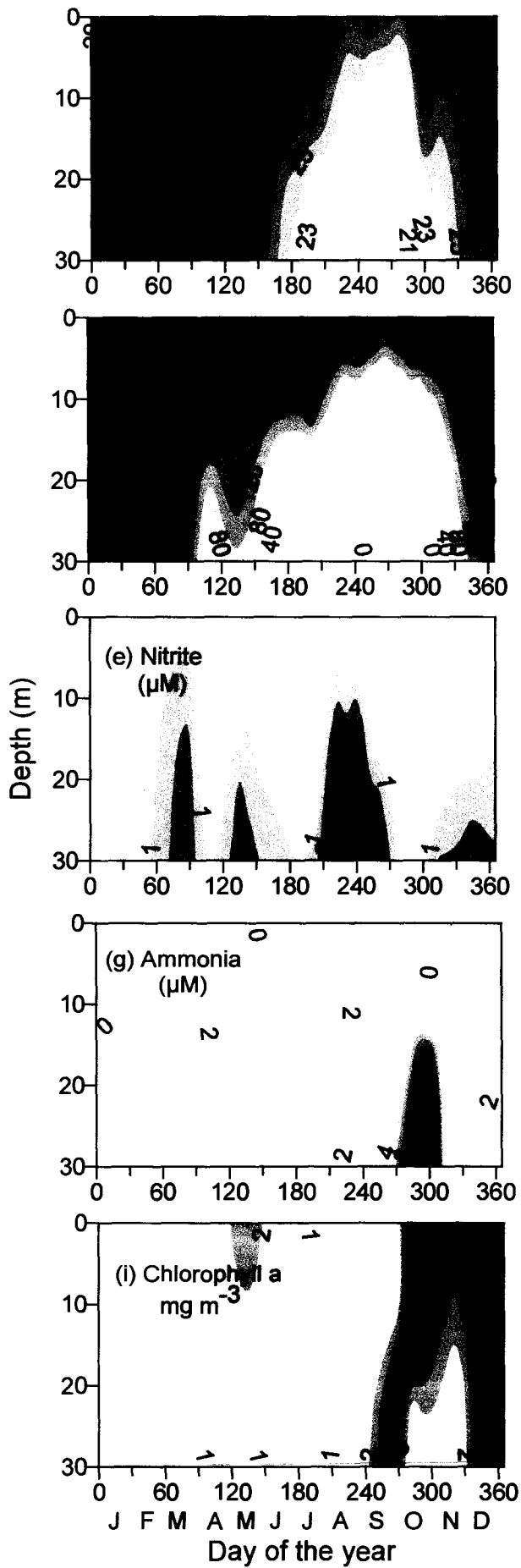
(h) Hydrogen sulphide (µM)

(i) Chlorophyll a mg m⁻³

Fig. 4.13. Annual cycle of physico-chemical characteristics at CAndolim Time Series (CATS) station.

The water column is well mixed from January to April. However, the salinity changes considerably. During winter the WICC brings fresher waters from the south, and this is reflected by lower salinities prevailing in the first two months of the year. The highest salinity values ($\geq$ 36) occur during the following SI season before the monsoonal rainfall produces a fresher-water lens that is clearly seen in Fig. 4.13b during June-September. Following the reversal of currents and the cessation of upwelling water column gets vertically mixed again in November/December.

The duration of low-O_2 conditions in subsurface waters is little longer than expected from the temperature structure (Fig. 4.13c). The lowest O_2 concentrations (<10 μM) are, however, confined only to the period of upwelling (July-November). The decrease in O_2 in subsurface waters is mirrored by an increase in NO_3^- (Fig. 4.13d). However in August NO_3^- concentration begins to decrease as denitrification is initiated. Within a period of about 1 month, all NO_3^- is used up by this process.

Traces of NO_2^- occur in subsurface waters even when the environment is not reducing (Fig. 4.13e). These are most likely produced through the assimilatory nitrate reduction pathway by phytoplankton. However, when the water becomes denitrifying, NO_2^- accumulates in high concentrations with the highest averaged value of ~ 5 μM occurring close to bottom. This happens during August-September. However, the ensuing anoxic conditions in September-October lead to the disappearance of NO_2^-.

One of the most interesting aspects of the coastal suboxic environment, to be discussed in more detail later, that distinguishes it from the perennial suboxic system of the open ocean, is the co-existence of NO_2^- and

N_2O in high concentrations. The averaged concentrations of N_2O (Fig. 4.13f) reached a maximum of 190 nM during the suboxic period, indicating that denitrification was the major process responsible for N_2O production. However, towards the end of the suboxic period, N_2O concentrations fell rapidly, reaching near-zero levels as sulphate reduction set in. Another increase in N_2O concentration, albeit to a much smaller extent, is observed to occur in November after sulphate reduction ceases to take place.

The near-complete disappearance of N_2O coincides with the accumulation of both NH_4^+ and H_2S (Fig. 4.13g and h). NH_4^+ has been known to accumulate in anoxic waters because its oxidation by sulphate is not thermodynamically feasible. The anoxic events are generally restricted to late September and October. However in rare cases these may extend to November.

As stated earlier, the data on chlorophyll a (Fig. 4.13i) are rather limited except from the month of September. These data indicate that the productivity at the CATS site is high, but not excessively so. Chl a concentrations exceeding 5 mg m^{-3} are rarely observed. An interesting observation is the accumulation of chlorophyll in near bottom waters during the suboxic period indicating greater preservation in the near absence of O_2. The subsequent increase in surface chl a during the late Fl-early NEM should be viewed with caution in view of paucity of data.

4.7 Primary Production

Measurements of primary production (PP) were made at three stations over the shelf during the SWM. The first station was located at the inner shelf off Quilon (Lat. 9.027°N, Long. 76.403°E; water depth 28 m; date of sampling
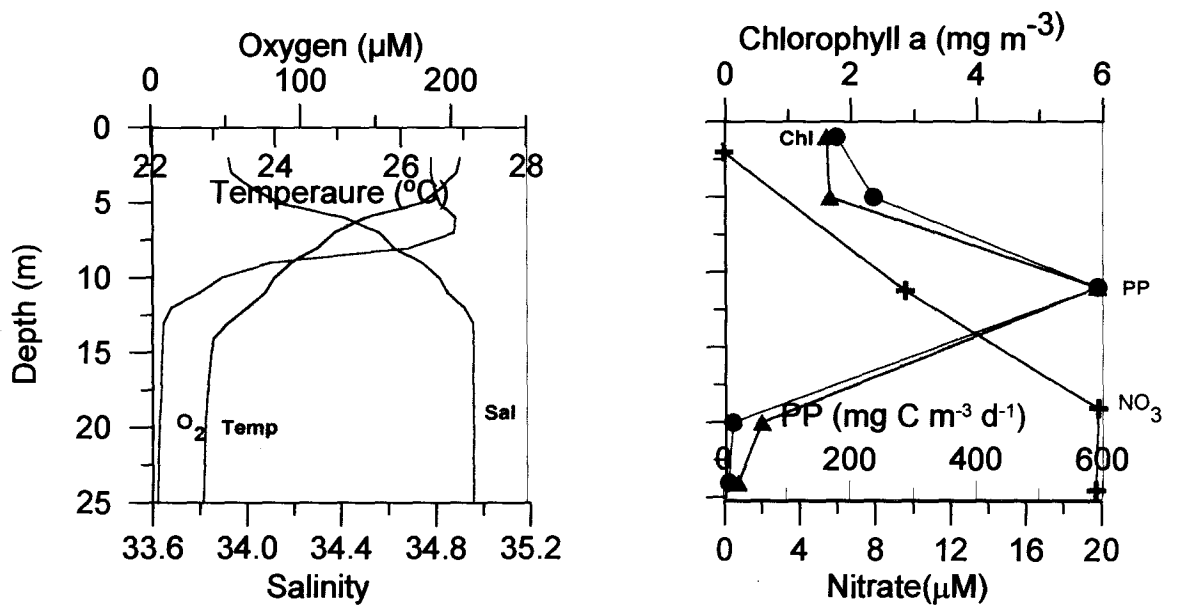
Fig. 4.14. Vertical profiles of physical, chemical and biological properties
at Sta. SS 3915 (Lat: 9.027°N, Long: 76.403°E; water depth:
28m; sampled on 25/8/97)

25/08/1997). At this station, samples spiked with ^{14}C-labeled $NaHCO_3$ were incubated on deck under simulated light conditions rather than in-situ as was the case with the other two stations. The results are presented in Fig. 4.14 along with profiles of temperature, salinity and O_2 generated with sensors mounted on the CTD-frame. The O_2 profile was calibrated with titrimetric analysis of discrete samples. Vertical distributions of NO_3^- and chl a at the station are also shown.

The surface mixed layer, if at all present, was <5 m thick at this station. In fact, the thermocline and halocline began at the shallowest depth of observations. However, O_2 concentrations remained high down to ~6 m (where a maximum was observed presumably due to production through photosynthesis) and then decreased abruptly to near-zero level at ~12 m. NO_3^- concentration was below detection limit at 2 m, but increased rapidly to ~10 μM at ~10 m. Thus, the nutrients-rich waters were located well within the euphotic zone. This stimulated phytoplankton growth with both chl a and PP maxima located below the surface. Both parameters decreased rapidly with depth thereafter. These decreases were most likely caused by the absence of O_2, which, it is speculated, might not allow the phytoplankton cells to perform their respiratory functions. In spite of the low PP in the lower part of the euphotic zone, the column-integrated value at this site (6.2 g C m^{-2} d^{-1}) is the highest recorded anywhere in the Arabian Sea.

The second station where PP measurements were made was positioned close to the shelf edge off Mangalore (Lat. 12.907°N, Long. 74.176°E; water depth 83 m; date of sampling 20/09/2001). The conditions

here (Fig. 4.15) were more or less similar to those at the first station (Fig. 4.14) except that the mixed layer was little thicker (~10 m). PP and Chl a distributions were qualitatively similar to those just described above, but the maximal values of PP and Chl a were lower by factors of about 3 and 2, respectively. Accordingly column production was lower as well (2.15 g C m^{-2} d^{-1}).

Note that the second PP station formed the most offshore part of the SaSuPl2 section for which data have been previously presented (Fig. 4.3e) and discussed (4.4.3). The nearshore portion of the section was characterized by anoxic conditions below ~10 m. It was within this zone where the third PP station was located (Lat. 13.129°N, Long. 74.634°E; water depth 27 m; date of sampling 19/09/2001). As in case of the first PP station, this station was also distinguished by strong thermohaline stratification in the near-surface layer (Fig. 4.16). NO_3^- concentrations were very close to zero at all depths, but as the waters were sulphate reducing at and below 10 m, NH_4^+ accumulated to a maximum of 4 μM in the deepest sample. Despite the absence of NO_3^- in the euphotic zone, PP values were quite high with the maximal production occurring at 5 m depth. Apparently, the production was fuelled by NH_4^+ being supplied to the thin surface layer through eddy diffusion. This represents an extraordinary situation where the new production is supported by NH_4^+ rather than NO_3^-, which is usually the case. Low PP in the anoxic zone could again be attributed to the inability of normal phytoplankton to tolerate near-zero O_2 concentrations. Such an inhibitory effect of anoxia on PP is expected, but has not been reported from the oceans simply because there are not many analogues elsewhere in the ocean to the system presently being studied (i.e.
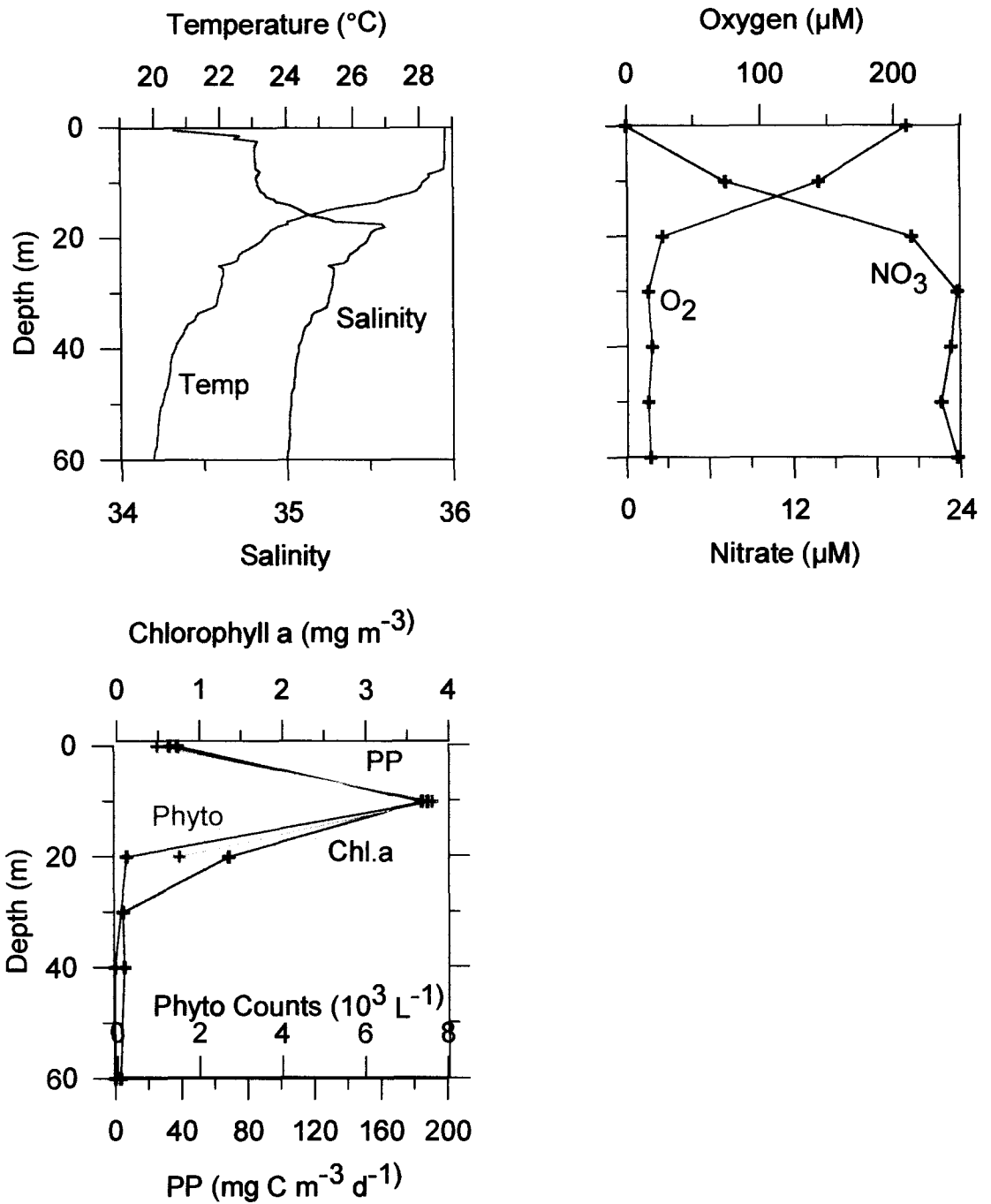
Fig. 4.15. Vertical profiles of physical, chemicaland biological properties at Sta. SaSuPl2 M8 (Lat: 12.907°N, Long: 74.176°E; water depth: 83m; sampled on 20/9/01)
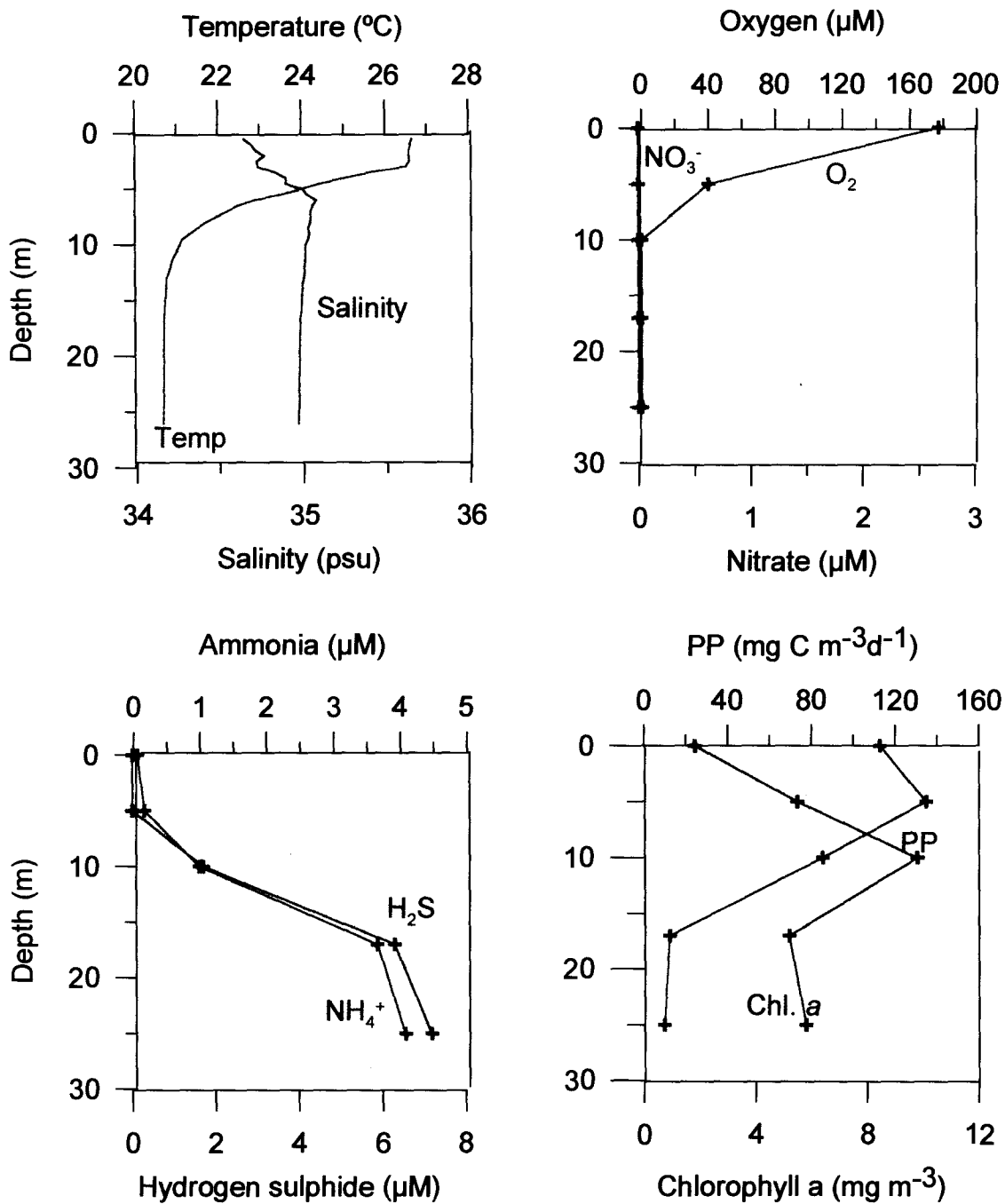
Fig. 4.16. Vertical profiles of physical, chemical and biological properties at Sta. SaSuPl2 M1A (Lat: 13.129°N, Long: 74.176°E; water depth: 27m; sampled on 19/9/01)

the O_2 minimum layer normally does not reach up to the euphotic zone). However, while the PP declined with depth, chl *a* concentrations first increased to a maximum value of ~ 10 mg m^{-3} at 10 m and then declined to concentrations comparable to that at 5 m. These observations are consistent with those described previously for the CATS site during the anoxic period supporting the notion of suppressed chlorophyll degradation under anoxic conditions. Although the PP data obtained in this study are limited, these nevertheless clearly demonstrate that PP over the western Indian continental shelf during the SWM is probably higher than anywhere else in the Indian Ocean. Although PP was not measured on the few cruises that were undertaken during the NEM period, the oligotrophic conditions suggested by our data would imply much lower values during this season.

4.8 Pelagic Denitrification Rate over the Shelf

Direct measurements of the rate of water column denitrification over the shelf were not made in the present study. However, an order-of-magnitude estimate of the rate can be obtained from changes in $NO_3^-+NO_2^-$ concentration observed when repeat sampling was performed at the same location over reasonably short times. The data used for this purpose are presented in Table 4.1. As a caveat it must be stated that the approach suffers from considerable uncertainty stemming largely from the assumption that the same water was sampled on the repeat collection. In an area distinguished by extremely large changes in both space and time this assumption is almost certainly not valid. However, it is reasonable to assume that given a large sample size the approach can still yield a value that should

Table 4.1. Water column denitrification rates derieved from repeat samplings at fixed sites.

Cruise / Field trip.	Depth (m)	Long (°E)	Lat (°N)	Dates of sampling	(NO$_3$ + NO$_2$) (µM)	Denitrification Rates (µ mole d^{-1})
Candolim 1	11	73.742	15.522	4.9.1997	7.42	0.328
Candolim 2	12	73.742	15.522	18.9.1997	2.83	
Candolim 1	19	73.700	15.517	4.9.1997	13.81	0.794
Candolim 2	20	73.700	15.517	18.9.1997	2.69	
Candolim 1	29	73.650	15.510	4.9.1997	7.42	0.291
Candolim 2	26	73.650	15.510	18.9.1997	3.35	
Candolim 16	12	73.729	15.522	17.8.1999	8.11	0.877
Candolim 17	12	73.732	15.520	26.8.1999	0.22	
Candolim 16	26	73.650	15.512	17.8.1999	13.22	0.983
Candolim 17	28	73.650	15.520	26.8.1999	4.37	
Candolim 22	17	73.700	15.517	12.9.2000	9.71	0.556
Candolim 23	17	73.700	15.518	29.9.2000	0.26	
Candolim 22	30	73.517	15.478	12.9.2000	18.94	1.096
Candolim 23	30	73.649	15.539	29.9.2000	0.3	
Candolim 8	18	73.717	15.531	17.9.1998	2.33	0.443
Candolim 9	15	73.701	15.524	21.9.1998	0.56	
SaSu PI 1 (Goa)	18	73.700	15.517	12.9.2001	7.08	0.459
SasSu PI2 (Goa)	17	73.700	15.517	17.9.2001	4.86	
SasSu PI2 (Goa)	25	73.650	15.510	17.9.2001	16.36	2.974
SasSu PI2 (Goa)	26	73.650	15.510	22.9.2001	1.25	
SK 137 (Mangalore)	19	74.559	13.101	23.7.1998	19.3	0.891
	20	74.592	13.100	13.8.1998	0.45	
SK 137 (Mangalore)	27	74.559	13.101	23.7.1998	19.1	0.675
	32`	74.592	13.100	13.8.1998	4.823	
SK 137 (Goa)	20	73.629	15.529	20.7.1998	13.7	0.511
	20	73.626	15.529	16.8.1998	0	
					Average	0.837 ± 0.664

be good to a first approximation. The rate was computed by dividing the decrease in $NO_3^- + NO_2^-$ concentration with the time interval between the pair of observations. The average rate so obtained was 0.83 ± 0.66 μmole NO_3^- l^{-1} d^{-1}. There is one other way to compute the rate: It was seen that after the onset of reducing conditions (i.e. denitrification) it takes about a month before the system becomes completely anoxic (i.e. it loses all NO_3^- and NO_2^-). If we assume the initial NO_3^- concentration to be 24 μM (just before denitrification) the average rate would be (24/30=) 0.8 μmole NO_3^- l^{-1} d^{-1}, remarkably close to the value derived from the pairs of repeat observations. It must be pointed out that this estimate is strictly for nitrate reduction, which is expected to be smaller than the extent of denitrification (Codispoti and Christensen, 1985). The other uncertainties concern with the volume of denitrifying waters and the duration of the process. The total shelf area affected by hypoxia has been estimated to be about 180,000 km^2 by Naqvi et al. (2000). However, as the entire shelf does not experience water column denitrification this can only be taken as an upper limit. To arrive at a lower limit it is assumed that a third of the shelf gets affected by reducing conditions every year in which case the area would be at least 60,000 km^2. If the thickness of the denitrifying layer is taken as 20 m, the total volume of water affected by reducing conditions would range between 1.2 and 3.6 x 10^{12} m^3. As for the duration of the reducing conditions, it is assumed to be 90 days. With these values the pelagic denitrification rate works out to be 1.3-3.8 Tg N y^{-1}. This corresponds to 4-12% of the denitrification rate for the perennial suboxic zone of the open Arabian Sea (Naqvi, 1987).

4.9 N₂O Emission to the Atmosphere

As described in Section 4.4 anomalously high N_2O concentrations occur in near-surface waters during the SWM all along the west coast of India especially when the subsurface waters become reducing. The average of all (241) surface measurements made during the upwelling period was found to be 37.3 nM (range 5-435.9 nM). Using the individual data and employing two different models of sea to air fluxes, i.e. of Liss and Merlivat (1986) and Wanninkhof (1992), the flux of N_2O to the atmosphere was computed to range from −1.2 μmole m^{-2} d^{-1} (the only negative value indicating the flux directed from atmosphere to ocean) to 3243.2 μmole m^{-2} d^{-1} (Table 4.2) at wind speeds ranging from 5 to 10 m s^{-1}. The average flux ranges from 39.1 to 263.8 μmole m^{-2} d^{-1}. Since high surface N_2O levels prevail even during the early phase of upwelling (Naqvi et al., 1998), this flux was extrapolated over a period of six months and an area of 180,000 km^2 to arrive at a total N_2O efflux of 0.05-0.38 Tg N_2O from the study region. This is roughly of the same magnitude as the most recent estimate of N_2O efflux (0.39 Tg N_2O y^{-1}) from the entire Arabian Sea (Bange et al., 2000). It may be pointed out that this estimate should be regarded as a minimum value because a significant fraction of N_2O would be transported out of the shelf and perhaps be ventilated to the atmosphere elsewhere.

Table 4.2. Ranges and averages of sea-to-air N$_2$O fluxes over the Indian Shelf during the upwelling period.

	N$_2$O conc. (nM)	Wind speed (m/s)	N$_2$O flux (Wanninkoff) (μmole m^{-2} d^{-1})	N$_2$O flux (Liss and Merlivat) (μmole m^{-2} d^{-1})
Min	5	5	-2.1	-1.2
Max	435.9	5	810.8	481.3
Avg	37.31	5	65.9	39.1
Min	5	10	-8.4	-5.1
Max	435.9	10	3243.4	1972.2
Avg	37.31	10	263.8	160.4

4.10 Discussion

4.10.1 *Shallow-Suboxic Zone – Natural Versus Anthropogenic Origin*

It has been mentioned earlier that the O_2-deficiency in coastal waters of western India is primarily of natural origin. It is in that sense different from the O_2 deficiency being experienced by numerous other coastal areas in response to human-induced eutrophication (Malakoff, 1998). The largest and the best known of such zones lies in the inner Gulf of Mexico over the Louisiana continental shelf adjacent to the deltas of the Mississippi and Atchafalaya rivers (Rabalais and Harper, 1991). The seasonally recurring "dead zone" here has been expanding rapidly in recent years (http://www.nos.noaa.gov/products/pubs_hypox.html).

The shallow O_2-deficient zone along the west coast of India has been known to exist since the earliest observations made in the 1950s (Banse, 1959, 1968; Carruthers et al., 1959). But chemical measurements made in this zone have been restricted largely to O_2. The present study provides the first comprehensive data set including a large number of chemical parameters covering the entire shelf. It revealed intense denitrification followed by sulphate reduction on many occasions during late SWM - early Fall Intermonsoon in the region north of about 12°N. The highest H_2S concentration of 21 μM was measured at station off Goa in October, 2001. It must be pointed out that sulphate reduction is a very rare phenomenon in open coastal waters and the few instances of its occurrence have been recorded only off Peru (often without H_2S analysis; Codispoti and Packard, 1980; Codispoti et al, 1986). It may be argued that anoxic conditions might

have occurred all along the Indian coast as well, but these were missed earlier due to the lack of measurements of the right type and during the right time. This is unlikely. Under the UNDP/FAO-supported Pelagic Fishery Project implemented between 1971 and 1975, O_2 data were collected round the year along a number of cross-shelf transects located between 7 and 17°N (UNDP/FAO report, 1973). On the SWM cruises the observed O_2 distribution was very similar to that observed in the present study, but with the minimal O_2 levels slightly higher (by up to 10 μM) than observed presently. Nutrients and H_2S were not measured during the UNDP/FAO project. However, it is unlikely that H_2S was present in the water column at that time because, firstly, "zero" O_2 concentrations characteristic of anoxic environments were not reported, and secondly, it is hard to miss H_2S because of its strong odour and any instance of its occurrence should have attracted attention. Limited observations made subsequently (unpublished data available at the Indian National Oceanographic Data Centre, Goa), which also covered nutrients, again did not yield any "zero" O_2 values, but frequent presence of NO_2^- in conjunction with low NO_3^- in sub-pycnocline waters indicated the seasonal occurrence of denitrification. Inquiries with the colleagues who collected these data confirmed the absence of detectable H_2S in these samples.

In view of the above, it is difficult to escape the conclusion that even though the coastal eastern Arabian Sea did always experience O_2 deficiency due to natural processes, it was not anoxic (i.e., sulphate reducing) and that an intensification of O_2 deficit over the western Indian shelf has occurred in recent years. At this point it cannot be established whether this change has been brought about by an increased nutrient loading or a modified physical

forcing. As in other areas, consumption of nitrogen-based fertilizers in the coastal belt has increased by an order of magnitude over the past four decades. Surface $NO_3^- + NO_2^-$ concentrations in the Mandovi and Zuari estuaries (Goa) were as high as 10 μM during a period of heavy runoff in July 2000 whereas rainwater collected on our Institute's campus contained on an average ~10.36 ± 8.31 μM ($NO_3 + NO_2$), n = 5. However, while significant nitrogen loading occurs through both runoff and precipitation, elevated surface NO_3^- concentrations were not noticed on any of the cruises except when the pycnocline was eroded by turbulence. This indicates that the nitrogen added with freshwater was quickly removed by algae.

4.10.2 Cause of Anomalous N_2O Accumulation

One of the most important results obtained in the present study was the accumulation of N_2O during the late SWM and early FI over the inner- and mid-shelf regions north of about 12°N. The magnitude of this accumulation is unprecedented for any part of the oceans: the highest N_2O concentration recorded in this study (765 nM) is more than 4 times the highest concentration reported from elsewhere in the oceans (173 nM from the coastal waters off Peru; Codispoti et al., 1992). Surprisingly, barring a few surface values, all concentrations in excess of ~150 nM were generally associated with reducing (denitrifying) waters having high NO_2^- content (Fig. 4.17). This pattern is diagonally opposite to that noticed in the perennial suboxic zones where, as indicated earlier, N_2O invariably exhibits a broad mid-depth minimum that coincides with the SNM (Cohen and Gordon, 1978; Codispoti and Christensen, 1985; Naqvi and Noronha, 1991; Bange et al., 2001).
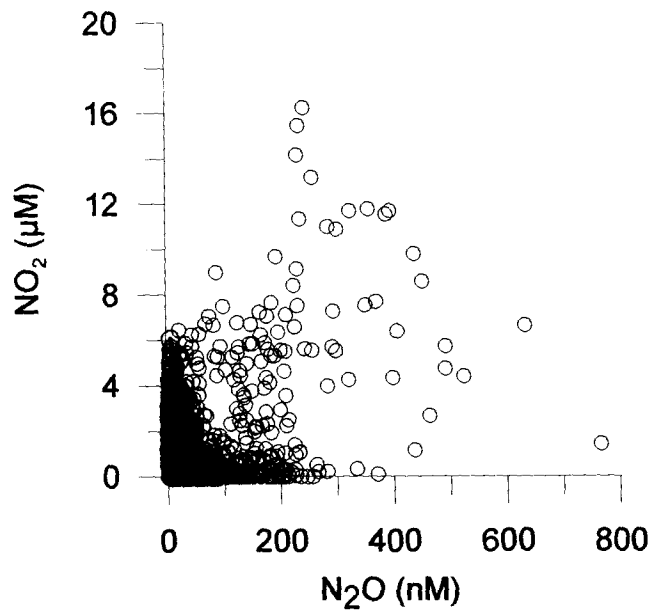
Fig. 4.17. Plot of NO_2^- versus N_2O in the shallow (pink circles) and deep (blue circles) suboxic zones.

N$_2$O distribution exhibits extremely high variability in both space and time in the reducing zone with both high and low concentrations occurring in waters experiencing seemingly similar conditions at different times and places. Nevertheless, near bottom waters in the reducing zone were generally (but not always) characterized by N$_2$O depletion (invariably so when these were affected by sulphate reduction) because of which maxima in N$_2$O were generally located at mid depth. Moreover, the abnormally high concentrations (including the world-record value of 765 nM) occurred in isolated water parcels that were apparently strongly denitrifying as indicated by the NO$_3^-$ and NO$_2^-$ concentrations; these parcels were surrounded by anoxic waters that were N$_2$O-depleted presumably due to its consumption. These observations strongly point to the formation of N$_2$O from NO$_3^-$ through the reductive pathway. It may be pointed out that in addition to classical denitrification pathway, it is also possible that NO$_3^-$ is reduced through its reaction with H$_2$S. The occurrence of high N$_2$O in the proximity of the sulphide bearing waters implies that this reaction may potentially produce N$_2$O, but the significance of such a process needs to be evaluated.

In order to investigate the role of denitrification in the production of N$_2$O, an experiment was conducted in which a sample of water collected from a depth of 40 m (Lat. 12.915°N, Long. 74.216°E; water depth 63 m; date of sampling 30/08/1997) was incubated in an air-tight aluminum bag with an inert lining. The initial concentrations of O$_2$, NO$_3^-$ and NO$_2^-$ in the sample were 15, 21.8 and 0.06 μM, respectively (i.e., the sample was not suboxic). Changes in the chemical composition were monitored during the course of incubation. The results (Fig. 4.18) revealed that NO$_3^-$ was largely converted to NO$_2^-$ in the
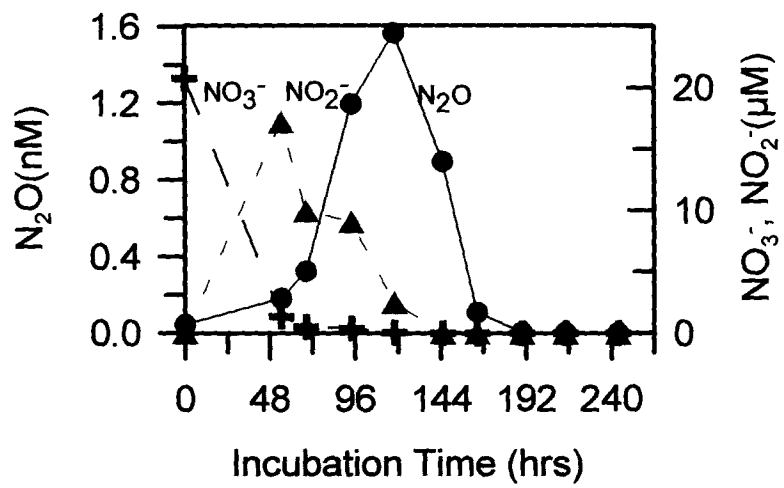
Fig. 4.18. Changes in concentration of nitrogen species
with time in an incubation experiment.

first two days, and the combined $NO_3^- + NO_2^-$ concentration rapidly fell close to zero in six days. Interestingly, the N_2O concentration rose from an initial value of 48.5 nM to a maximum of 1,568 nM before declining sharply after five days. All oxidized forms were completely consumed in eight days. The transient accumulation of N_2O during this experiment demonstrates that under some circumstances denitrification may be the major mechanism of N_2O production.

The open-system field data differ somewhat from the pattern seen in the closed-system incubation set up. Specifically, the mid-depth build-up of N_2O is usually associated with significant NO_3^- and NO_2^- concentrations, whereas in the incubation experiment N_2O accumulation occurred only after NO_3^- had been largely depleted. However, the low O_2 conditions are also known to enhance the yield of N_2O during nitrification (Goreau et al., 1980), and so the possibility of some contribution coming through this pathway cannot be ruled out.

A very similar pattern of N_2O accumulation has been reported from some freshwater lakes and attributed to a high yield of N_2O during denitrification in the presence of small amounts (~5 μM) of O_2 (Yoh et al., 1983). It is proposed that such an accumulation may be a common feature of all aquatic bodies where suboxia occurs close to the surface. The O_2 concentration can affect N_2O production by regulating (1) nitrification activity and the yield of N_2O during this process; (2) rate of NO_3^- production and hence its availability for denitrification (the low N_2O concentration in near-bottom waters may in part be due to this effect); and (3) N_2O reductase activity. It has been reported that in a young denitrifying system the consumption of N_2O by denitrifiers occurs only after *de novo* synthesis of N_2O

reductase (Firestone and Tiedje, 1979). Thus, frequent aeration through turbulence can rejuvenate suboxic waters (affecting the activity of this enzyme) when denitrification occurs at shallow depths thereby sustaining a very high N_2O yield. Moreover, N_2O so produced can easily escape to the atmosphere. The sites such as the coastal suboxic zone of the eastern Arabian Sea are, therefore, expected to make a disproportionately large contribution to the emission of N_2O to the atmosphere.

CHAPTER 5

Stoichiometric Relationships and Nitrogen Isotopic Abundance

Chapter 5

Stoichiometric Relationships and Nitrogen Isotopic

Abundance

5.1 Introduction

Phytoplankton photosynthesize organic matter by taking up dissolved inorganic carbon (DIC) and nutrients in the euphotic zone. A part of this organic matter sinks from the euphotic zone to subsurface waters where it is mineralized releasing DIC and nutrients back to seawater. Thus, the biological activity leads to sequestration of carbon from the surface to subsurface waters. This process is known as the "biological pump".

The organic matter produced by phytoplankton contains the principal elements carbon (C), nitrogen (N) and phosphorus (P) in approximately fixed ratios of 106:16:1, by atoms. A.C. Redfield was the first to point it out and recognize the importance of the near-constancy of C:N:P ratios (appropriately called the Redfield ratios) in ocean biogeochemistry (Anderson and Sarmiento, 1994). These ratios have since been used widely by oceanographers for the conversion of the concentration/flux of one nutrient to that of another. For example, an evaluation of new production in the euphotic zone can be made based on the fluxes of fixed nitrogen from outside.

Organic matter in the ocean is generally decomposed by bacteria using O_2 as the oxidant, and this process causes O_2 concentration to fall below the saturation in aphotic layers of the ocean. The degree to which such O_2

depletion takes place depends upon the balance between the rates of its consumption and supply through circulation. In most parts of the ocean, physical processes facilitate enough O_2 replenishment to make up for its consumption. However, there are a few areas where this balance is not achieved and the O_2 concentrations fall to near-zero levels. When this happens, the bacteria switch over to NO_3^-, the next preferred oxidant, resulting in its reductive removal from seawater.

After NO_3^- has also been removed completely, sulphate, one of the major constituents of seawater, begins to act as an electron acceptor thereby producing H_2S. Sulphides are highly toxic and are hazardous to marine organisms (Richards, 1965).

Each of the above pathways of respiration (oxic, suboxic and anoxic metabolisms which respectively make use of O_2, NO_3^- and sulphate as the terminal electron acceptors) has its own stoichiometry i.e. the ratios in which the oxidant is consumed and metabolic products are regenerated (Richards, 1965). However, departures from these expected ratios have been known to occur and such departures provide important insights into biogeochemical cycling in a particular environment. One of the principal objectives of the present study is to investigate the ratios of concomitant changes in order to gain such insights for the region under investigation that experiences diverse redox conditions. Limited data on natural nitrogen isotope abundance in NO_3^- will also be examined and discussed.

5.2 Pathways of Oxidation of Organic Matter

For expressing the composition of organic matter in the oceans the oxidation states of carbon, nitrogen and phosphorus are assumed to be as in carbohydrates, ammonia, and orthophosphoric acid, respectively, and the organic matter is empirically formulated as $(CH_2O)_{106}$ $(NH_3)_{16}$ H_3PO_4; degradation of this hypothetical organic matter through different pathways can then be expressed as follows (Richards, 1965):

5.2.1 Aerobic Respiration

$(CH_2O)_{106}(NH_3)_{16} H_3PO_4 = 106 CH_2O + 16 NH_3 + H_3PO_4$

$106 CH_2O + 106 O_2 = 106 CO_2 + 106 H_2O$

$16 NH_3 + 32 O_2 = 16 HNO_3 + 16H_2O$
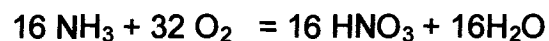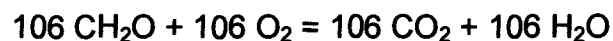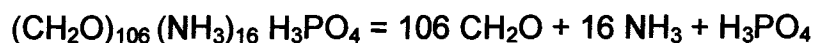
Addition of above equations yields,

$(CH_2O)_{106}(NH_3)_{16} H_3PO_4 + 138 O_2 = 106 CO_2 + 16 HNO_3 + H_3PO_4 + 122 H_2O$

---- (i)
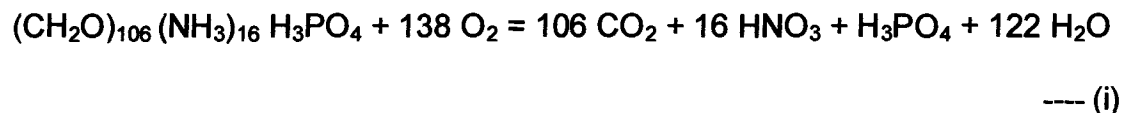
This reaction implies that for the complete oxidation of organic matter 276 atoms of oxygen are consumed that leads to the regeneration of 106 atoms of carbon as CO_2, 16 atoms of nitrogen as NO_3^- and 1 atom of phosphorus as H_3PO_4.

5.2.2 Denitrification

The uncertainty in expressing this process arises from the unknown fate of ammonia released from the organic matter. That is, while in the aerobic degradation it is known to get oxidized to NO_3^- (nitrification), it is not still clear

whether it is oxidized by NO_3^- in denitrification. Without such oxidation the reaction can be expressed as:

$$(CH_2O)_{106} (NH_3)_{16} H_3PO_4 + 84.8HNO_3 =$$

$$106\ CO_2 + 42.4\ N_2 + 16\ NH_3 + H_3PO_4 + 148.4\ H_2O \qquad \text{---- (ii)}$$
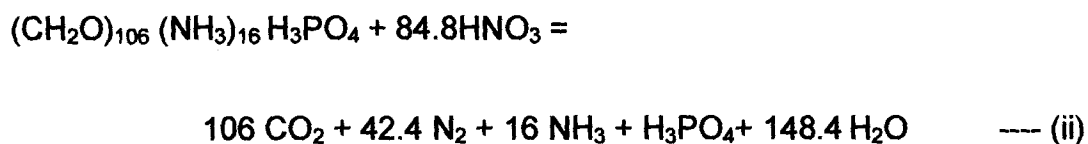
and if the oxidation of NH_3 proceeds as follows:

$$5NH_3 + 3HNO_3 = 4N_2 + 9H_2O$$
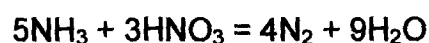
then the overall reaction becomes:

$$(CH_2O)_{106} (NH_3)_{16} H_3PO_4 + 94.4\ HNO_3 =$$

$$106\ CO_2 + 55.2\ N_2 + H_3PO_4 + 177.2\ H_2O \text{---- (iii)}$$
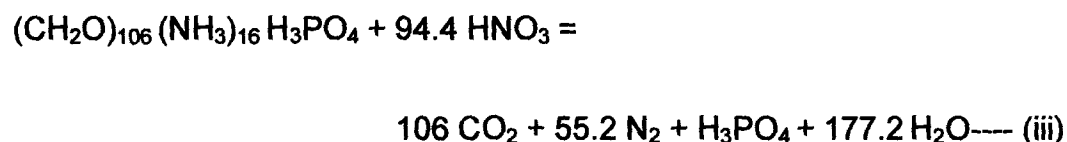
Reaction (iii) predicts that in the degradation of organic matter by NO_3^-, for each 94.4 atoms of nitrogen used as NO_3^-, 106 atoms of carbon are regenerated as CO_2 and 1 atom of phosphorus is released as H_3PO_4.

5.2.3 Sulphate Reduction

There is lesser uncertainty in expressing the degradation of organic matter with sulphate as an electron acceptor because NH_3 regenerated from organic matter cannot be oxidized by sulphate. The reaction can be expressed as follows:

$$(CH_2O)_{106} (NH_3)_{16} H_3PO_4 + 53SO_4^{2-} =$$

$$106\ CO_2 + 53\ S^{2-} + 16\ NH_3 + H_3PO_4 + 106\ H_2O \text{-----(iv)}$$
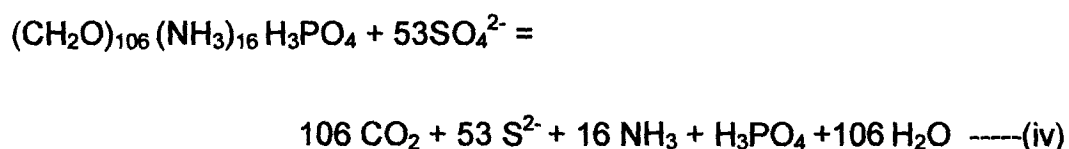
It indicates that for 53 atoms of sulphur used as sulphate are converted to sulphide, 106 atoms of carbon are regenerated as CO_2, 16 atoms of nitrogen are regenerated as NH_3 and 1 atom of phosphorus is regenerated as H_3PO_4.

Organic matter degradation also occurs using other electron acceptors the most important of which are $Mn(IV)$, Fe (III), $I(V)$ (iodate) and CO_2. For the first three oxidants the free energy change is comparable to that of denitrification, so they are expected to proceed at the same time as denitrification (Farrenkopf et al., 1997). In the case of CO_2 the free energy change is least favourable (it occurs after sulphate reduction). In any case, the concentrations of these species are much smaller than that NO_3^-, and so their contribution to respiration in water column can be assumed to be insignificant.

5.3 Significance of the Study

The Arabian Sea is one of very few areas of the world oceans where all the three major respiratory pathways are found to occur in the open coastal waters. It therefore provides an excellent opportunity for testing the predicted stoichiometric relationships associated with the organic matter decomposition and how these might be modified by local processes. The present study provides the first ever detailed data from one single environment outside the land locked seas where both oxic and suboxic/anoxic metabolisms occur in close spatial and temporal proximity to each other. These data are expected to improve our understanding of biogeochemical transformations in the O_2-depleted oceanic environments.

5.4 Methodology

The large amount of data presented here originated from various cruises of ORV *Sagar Kanya*, FORV *Sagar Sampada*, AA *Sidorenko*, and CRV *Sagar Sukti* during the period 1997-2002 (Table 2.1). Data from 294 stations covering the western continental shelf of India (depth ≤ 200 m) have been utilized. These data includes dissolved O_2, dissolved inorganic nitrogen (DIN = NO_3^- + NO_2^- + NH_4^+), dissolved inorganic phosphorus (DIP = $H_2PO_4^-$ + HPO_4^{2-} + PO_4^{3-}, often expressed simply as PO_4^{3-}, the analytically-determined "phosphate" concentration) and hydrogen sulphide (H_2S). Inter-relationships between various parameters were examined through least squares regression analyses for selected pairs of variables *viz.* DIN versus DIP, DIP versus H_2S; and NH_4^+ versus H_2S.

5.5 Results

The DIP versus DIN plot for the pooled data shows three interesting trends (Fig 5.1a). The trend of oxic degradation can be easily discerned from the cluster of points around the expected Redfield relationship (16:1). The second trend is that of denitrification. The reason for the third trend (rapid increase in DIP at low DIN levels) is less apparent. All the three trends exhibited a great deal of scatter. In order to better resolve the effects resulting from various metabolic pathways, the data were further processed as follows:

For the first trend DIP and DIN data were selected for the samples containing NO_2^- < 1μM, DIP < 2.5μM and NO_3^- > 0. The purpose of this filtering procedure was to isolate the samples affected only by aerobic respiration. The reason for selecting NO_2^- < 1μM is that NO_2^- is an immediate
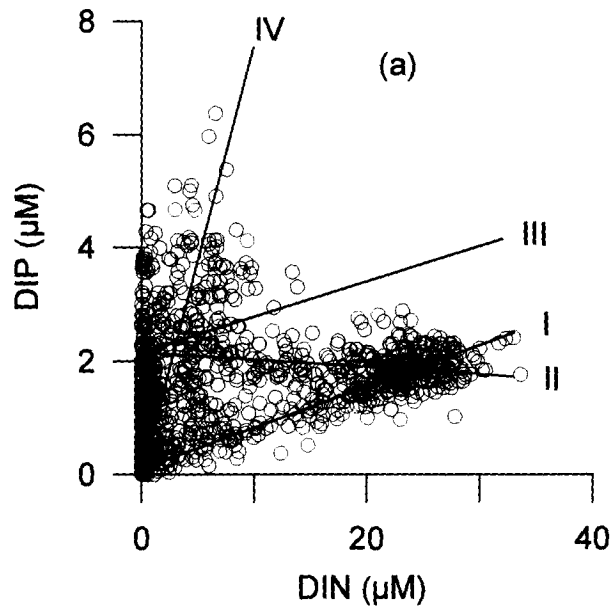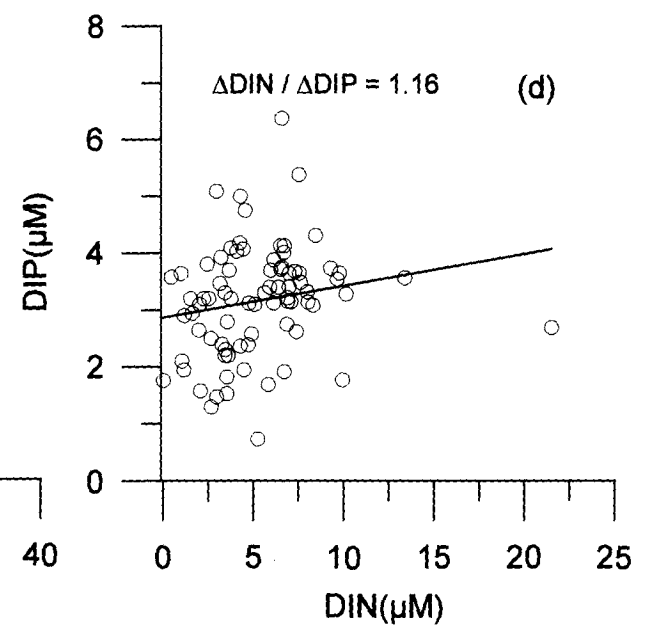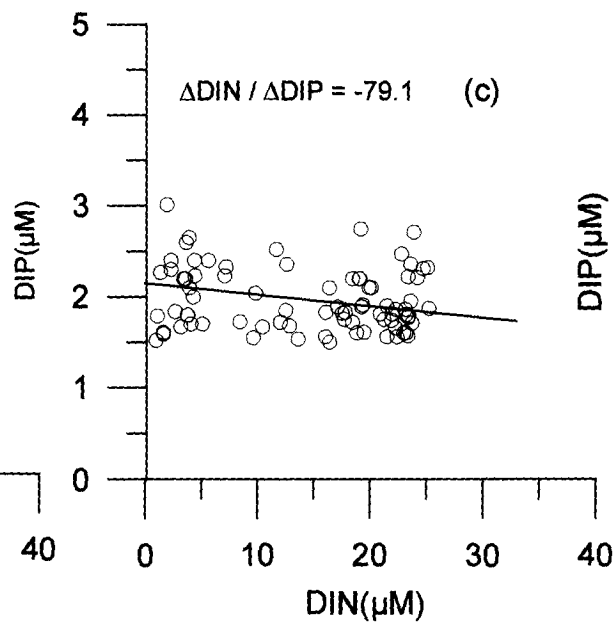
Fig. 5.1. Plots of DIN vs DIP for
    (a) all samples taken for depths < 200m.
    (b) samples not experiencing reducing conditions
    (c) samples experiencing denitrification
    (d) samples experiencing sulphate reduction
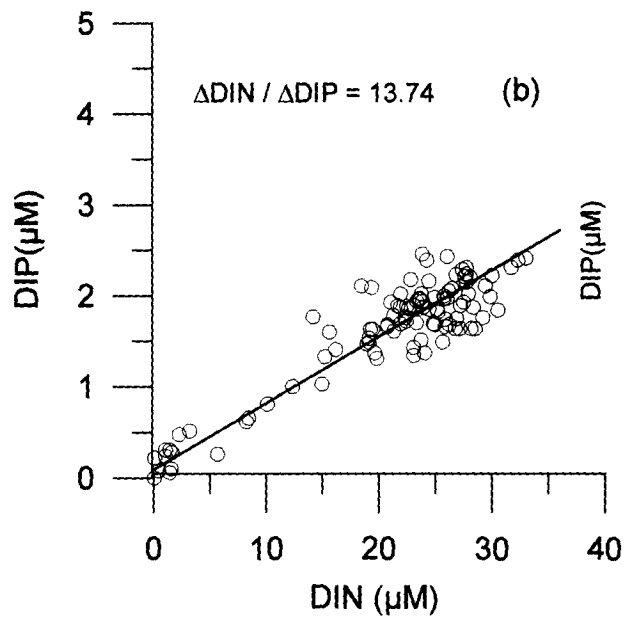
5.6 Discussion

The slope of the DIN/DIP regression line in oxic waters (13.74) is close to the Redfield value (16). It is quite likely that in spite of the efforts to filter out data affected by denitrification, the relationship might still have been influenced by this process (i.e. waters not experiencing denitrification might still show NO_3^- deficits due to mixing with waters affected by denitrification; Codispoti et al., 2001).

The slope of the DIN/DIP ratio for denitrifying water (-79.1) is higher than Richards' (1965) value (-94.4) for the case when NH_3 is oxidized by NO_3^- but close to the value (-84.8) for the case when such an oxidation does not take place. While it may be argued that, given the large scatter in the data, the observed difference could well be within the margin of error of computations, it should be pointed out that there is some evidence in the literature indicating that a substantial part of NH_3 released from organic matter may, in fact, be assimilated by organisms instead of getting oxidized to N_2 (Lipschultz et al., 1990). There are no previous estimates in the literature based on field measurements of DIN/DIP ratio for denitrification with which to compare the present results. It may be pointed out that the DIN/DIP ratio may be even higher (i.e. less negative) in case of a nitrification denitrification coupling (e.g. -81.6; Codispoti and Christensen, 1985). However, results of the present study cannot differentiate between these possibilities.

The results presented in Fig. 5.1 may be visualised in terms of spatio-temporal evolution of anoxia in a parcel of initially oxygenated water parcel as it moves up over the continental shelf during upwelling and undergoes sequential changes in redox conditions. First, the decay of organic matter in

the presence of O_2 increases the concentrations of both DIN and DIP in conformity with the Redfield stoichiometry (represented by line I in Fig. 5.1a) until the O_2 falls below the threshold for denitrification to set in (<0.02 ml I^{-1}; Morrison et al., 1999; Naqvi et al., 2003). Once this threshold is crossed (at this point DIN concentration is on an average ~24 μM), NO_3^- is used by the bacteria, and the concentration of DIN decreases rapidly, but that of DIP increases slowly. As discussed above, the relative changes in DIN and DIP during this transition (represented by Line II in Fig. 5.1a) conform to theoretical considerations [reaction (ii)].

When the system turns anoxic (after complete loss of NO_3^- that seems to take place when DIP concentration reaches on an average 2.15 μM), the relative changes in DIN and DIP exhibit complete departure from the theoretical value. That is, as NH_3 released from organic matter cannot be oxidized by sulphate, one would expect the DIN and DIP values to fall along the hypothetical Line III in Fig. 5.1a. Such is not the case. Instead, all data points are located to the left and above this line. Moreover, while there is considerable scatter in data, there seems to be a suggestion of a nearly linear trend (Line IV in Fig. 5.1a) extending toward the origin of the graph. It is obvious that processes other than simple degradation of organic matter by sulphate should be responsible for this trend.

Under oxidizing conditions (Eh>~200 mV), PO_4^{3-} is known to get adsorbed onto iron hydroxide thereby forming complex iron-oxyhydroxo-phosphates (FeOP), which settles to seafloor; PO_4^{3-} is released back from sediments to the overlying water when FeOP complex dissolves under reducing conditions (Shaffer 1986). The complex is formed when $Fe^{2+}/(HPO_4^{2-}$

+$H_2PO_4^-$) ratio exceeds 2 (Gunnars et al, 2002). It would appear that once the overlying waters turn anoxic over the Indian shelf PO_4^{3-} is mobilized in large quantities from the sediments. The Fe^{2+} released into solution in reducing waters may be removed as its insoluble sulphide but PO_4^{3-} is expected to accumulate (Gächter and Müller, 2003). This appears to be the most probable cause of the observed departure of the DIN/DIP variations from the theoretical trend in anoxic waters.

The extension of the anoxic trend to waters with low DIN and DIP values can be explained as follows: During the later part of the SWM and early Fall Intermonsoon, the anoxic subsurface layer is directly overlain by the oxic layer without a transient suboxic layer separating the two (see, for example, Fig. 4.16). The upper layer is nutrient-depleted, while the lower one has high DIP and moderate amounts of DIN (present almost entirely as NH_4^+). Mixing between these two end-members is expected to lead to DIP and DIN concentrations that should cluster around Line IV in Fig. 5.1a.

The relation between H_2S and DIP is linear with a slope of 7.62. This value is much lower than the theoretical value (53) given by Redfield et al. (1963) and Richards (1965). As in the case of the DIN/DIP relationship, this departure can also be ascribed to the mobilization of PO_4^{3-} from the sediments. Additionally, oxidative loss of H_2S is also expected to result in lower H_2S /DIP ratio.

Relationship between H_2S and NH_4 exhibited a slope value of 4.79, which is unexpectedly higher than the theoretical value of 3.3. However, the scatter in data is large with significant intercept on the NH_4^+ axis (Fig. 5.3). This means that NH_4^+ found in water at very low H_2S concentrations is

probably not produced during sulphate reduction and could have diffused out of sediments. Normally one would expect H_2S to be oxidized quickly in near surface waters, where the oxidation of NH_4^+ may be inhibited by light. Moreover, anoxic conditions have been observed to inhibit (oxygenic) photosynthesis (Fig. 4.16), and while there is a possibility that anoxygenic photosynthesis and chemosynthesis could occur in the anoxic waters, the NH_4^+ uptake rates should not be very high (much lower than the sulphide oxidation rate). The generally low concentrations of H_2S do strongly point to its loss through oxidation. Such a loss is, in fact, suggested by data from individual stations – for example, at Sta. M1a occupied on SaSuPl2, that experienced well-developed anoxic conditions, H_2S and NH_4^+ showed excellent linear relationship with a slope of 1.74 (Fig. 5.4). Thus, the higher slope value obtained from the pooled data is not easy to explain.

5.7 Implications for Biogeochemical Cycles

Fixation of molecular nitrogen is an important source of biologically useful nitrogen in oceanic surface waters that increases the productivity of phytoplankton, thus influencing the global carbon cycle (Falkowski, 1997). Most of the marine nitrogen fixation is carried out by the cyanobacterium *Trichodesmium* (Capone et al., 1997) and in some areas of the ocean as much as half of the new nitrogen could come through this pathway (Karl et al., 1997). The enzyme nitrogenase responsible for N-fixation has a high requirement for iron and this may lead to Fe limitation of N-fixation in remote parts of the sea (Falkowski, 1997; Codispoti et al., 2001). One other
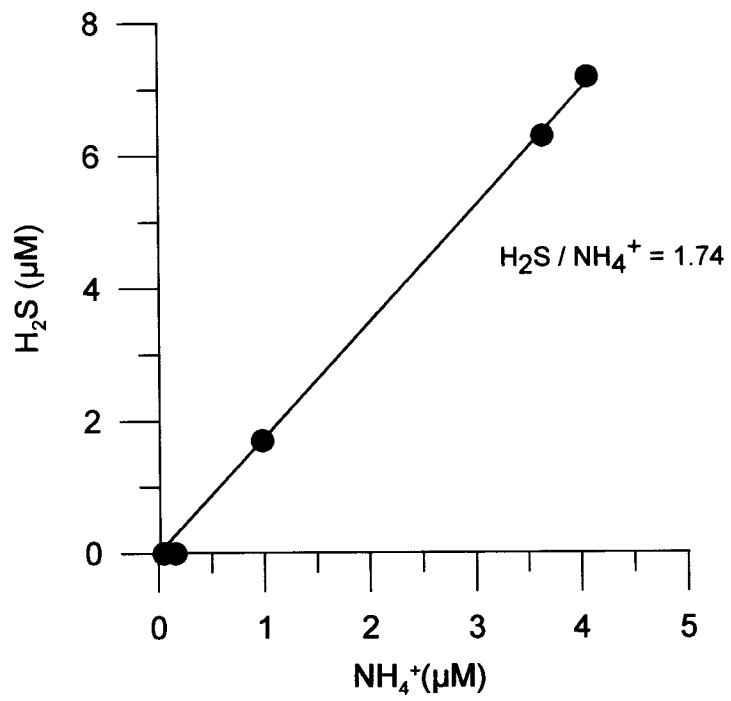
Fig. 5.4. Relationship between H_2S and NH_4^+ at the Sta
SaSu M1A (see Fig. 4.16 for vertical profiles)

necessary condition for N-fixation to take place is that PO_4^{3-} must be present in sufficient quantities.

The results of the present study clearly demonstrate that anoxic conditions lead to a large excess of PO_4^{3-} in coastal waters, which in conjunction with adequate supply of Fe (both from land and through mobilization in anoxic waters) should prime the system for N-fixation. This implies that N-fixation could be tightly coupled with denitrification in waters over the western Indian continental shelf and also probably on a global scale. It is therefore not surprising that extensive blooms of Trichodesmium occur on a regular basis in the eastern Arabian Sea following the cessation of upwelling (during the NEM and SI periods). Such blooms add new nitrogen to the system, partially compensating for the loss through denitrification and contributing significantly to biogeochemical cycles (Devassy et al., 1978).

5.8 Isotopic Composition of Nitrate

Limited measurements of nitrogen isotope ratio in NO_3^-, expressed as $\delta^{15}N$ relative to air* ($\delta^{15}N\text{-}NO_3^-$), were made on two occasions – on cruise SS158 (in August 1997) off Mangalore and on field trip Candolim 22 (in September 2000) off Goa. On both occasions the waters sampled were affected by denitrification.

Hydrographic and chemical data at station SS 3939 along with the $\delta^{15}N\text{-}NO_3^-$ values are plotted against depth in Fig. 5.5. Temperatures and salinity profiles were typical of this region for the survey period, showing strong near-surface thermohaline stratification and isothermal and isohaline

---

* $\delta^{15}N = [(^{15}N/^{14}N)_{sample}/(^{15}N/^{14}N)_{atm-N2} - 1] \times 1000$
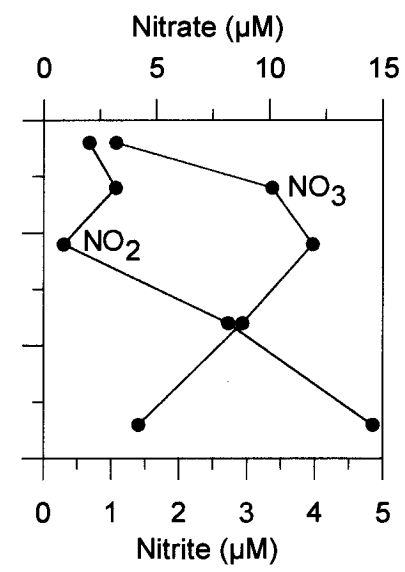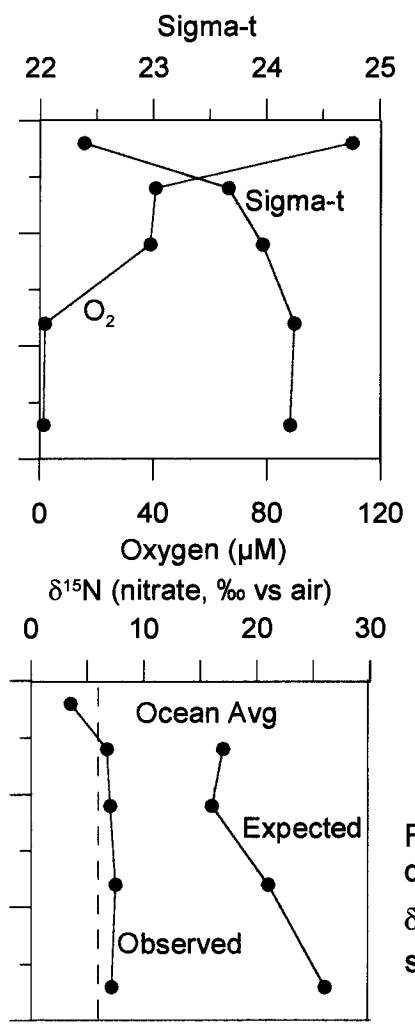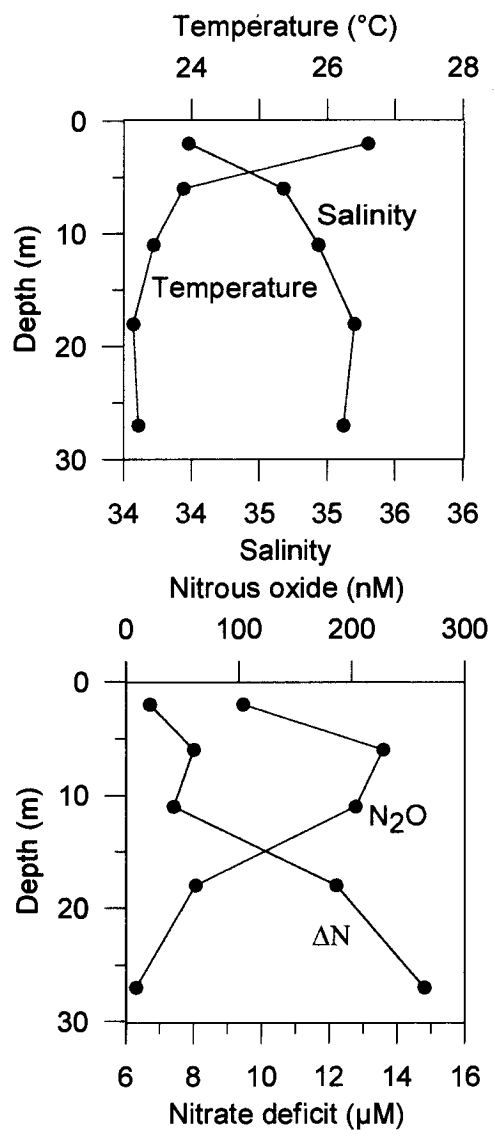
Fig. 5.5. Vertical profiles of temperature, salinity, density, inorganic nitrogen species and $\delta^{15}N$ of NO_3^- at Sta 3939 (13.126°N; 74.631°E sampled on 30/8/1997)

conditions below the shallow pycnocline. Similarly, the two deepest samples also experienced near-complete O_2 depletion that is characteristic of the sampling period. NO_3^- profile exhibited a mid-depth maximum below which concentrations decreased due to loss through denitrification while the NO_2^- concentrations showed a concomitant increase with depth. NO_3^- deficit was calculated as the difference between the expected and observed NO_3^- concentrations [the former was approximately quantified by dividing the apparent oxygen utilization (AOU) with 8.65, the ratio between O_2 consumption and NO_3^- regeneration for aerobic respiration; Richards, 1965]. This deficit increased with depth reaching the peak value of just under 15 μM in the deepest sample. While all the above parameters exhibited expected depthwise changes, the profile of $\delta^{15}N$-NO_3^- deviated greatly from that expected. That is, given the high NO_3^- deficit in subsurface waters the $\delta^{15}N$-NO_3^- values should have ranged between 17 and $26^{o}/oo$ in subsurface waters if the isotopic fractionation factor reported by Brandes et al. (1998) for the open ocean suboxic zone (25 ‰) was also applicable to the shallow suboxic zone. The values measured were consistently lower. In fact, all the four samples taken from within or below the pycnocline yielded $\delta^{15}N$-NO_3^- values (6.65-7.41 ‰) that were quite close to the oceanic average (5.7 ‰; Altabet et al., 1995; marked by the dashed vertical line in the figure) with no depthwise variability. NO_3^- in the only sample taken from the surface layer was distinctly lighter (3.43).

Three possible explanations may be offered for the above anomaly: (1) The value of the isotopic fractionation factor for the deeper perennial suboxic

zone may not be valid for the seasonal suboxic zone over the shelf. In support of this view there is some experimental evidence which suggests that the factor may vary with denitrification rate (Dr. K.K. Liu, personal communication); (2) Denitrification within the sediment might account for the bulk of NO_3^- deficit observed in the water column. Relative to pelagic denitrification, the process in sediments results in little isotopic fractionation (~3 ‰; Codispoti et al., 2001); (3) Low $\delta^{15}N$-NO_3^- could be produced as a result of complete denitrification followed by mixing with freshly upwelled water. In order to further illustrate this possibility the following hypothetical scenario may be considered: Suppose a parcel of water is subjected to complete denitrification, it will lose both $^{15}NO_3^-$ and $^{14}NO_3$. Now if it is quickly diluted with equal volumes of freshly-upwelled water having a NO_3^- content and $\delta^{15}N$ of, say, 24 μM and 7 ‰, respectively, the resultant mixture will possess the isotopic characteristics of the upwelled water (7 ‰), but it will show a NO_3^- deficit of 12 μM. The relative importance of the above possible factors in lowering the $\delta^{15}N$-NO_3^- cannot be evaluated with the help of available data.

However, the other set of isotopic measurements did reveal enrichment of the heavier isotope in residual NO_3^- (Table 5.1). In order to compare the magnitude of this enrichment with that observed in the offshore suboxic zone, an attempt was made to compute the fractionation factor, ε_{denit} [$=10^3(1-\alpha)$, where α is the ratio between the rates of utilization of $^{15}NO_3^-$ and $^{14}NO_3^-$], using a simple advection-reaction model. This model ignores diffusion and the water mass is assumed to advect into the suboxic zone without undergoing

Table 5.1. Hydrographic, chemical and isotopic data at selected depths and locations along the Candolim transect sampled on 12/9/2000.

Stn. No.	Depth (m)	Temperature (°C)	Salinity	O_2 (µM)	NO_3 (µM)	δ^{15} N-NO_3 (‰ relative to air)
3	15	22.20	36.03	4	2.45	22.5
4	17	22.10	35.70	4	9.63	15.4
5	15	22.50	36.11	22	2.24	14.4
	30	21.60	35.74	4	15.37	6.5

any mixing in the vertical and horizontal directions. As the stations were located very close to each other, this assumption seems justifiable. The isotopic distribution could thus be modelled with a simple Rayleigh equation (Bender, 1990):

$$\delta^{15}N\text{-}NO_3 = 10^3(\alpha\text{-}1)\ \ln f_{NO3} + (\delta^{15}N\text{-}NO_3)_{init}$$

where f_{NO3} is the ratio between the observed and expected $NO_3^- + NO_2^-$ concentrations and $(\delta^{15}N\text{-}NO_3)_{init}$ gives the isotopic composition of the initial (unaltered) material.

The plot of $\delta^{15}N\text{-}NO_3$ versus $\ln f_{NO3}$ for the five samples (Fig. 5.6) from the Candolim transect indicates a good linear correlation ($r^2 = 0.91$) with the slope of the regression ($-\varepsilon_{denit}$) line being -7.70. Inclusion of data from Sta. SS3939 leads to a little change in the slope (-7.21), but the correlation is deteriorated ($r^2 = 0.44$). At the first glance these results appear to support the notion of lower fractionation factor in the coastal suboxic zone. However, as discussed above, the possibility of other factors being also responsible for pulling down the $\delta^{15}N$ value of NO_3^- of coastal waters experiencing denitrification cannot be ruled out.
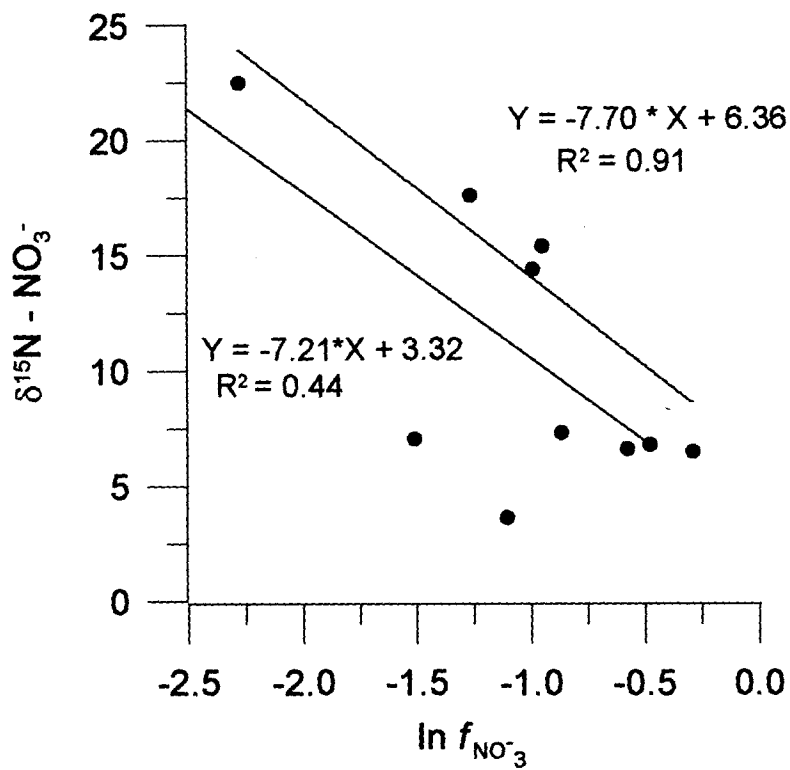
Fig. 5.6. The $\delta^{15}N$ - NO_3^- (‰ relative to air) vs. the natural log of f.
(red circles indicate data at Sta. SS3939; Blue circles indicate
data from Candolim transect).

CHAPTER 6

Sedimentary Nitrogen Cycling over the Western Continental Shelf of India

Chapter 6

Sedimentary Nitrogen Cycling over the Western Continental

Shelf of India

6.1 Introduction

The ultimate fate of nitrogen that is released from organic matter decomposition in water column and sediments is of great significance because of the ongoing overloading of nitrogen into the coastal marine environment as a result of human activities (e.g. discharge of sewage and unused fertilizers from the agricultural fields). Sedimentary denitrification is the most important process that can counter coastal eutrophication. It has been estimated that 80% of the nitrogen load reaching coastal areas is removed by benthic denitrification (Seitzinger, 1990). However, the rate of sedimentary denitrification is regulated to a large extent by the ambient O_2 levels in bottom waters. This is because the bottom water O_2 levels critically affect the activity of burrowing organisms thereby regulating the exchanges of O_2 and NO_3^- across the sediment-water interface. Diminished supply of O_2 limits nitrification and facilitates denitrification in bottom waters (e.g. Devol and Christensen, 1993). As stated in the previous chapter, there are several sites scattered in the world where eutrophication has led to the development of O_2-deficient conditions in near-bottom waters over the past four decades. Moreover, there is a strong possibility that some sites that experienced O_2-

deficiency due to natural processes have become further O_2-depleted. The eastern Arabian Sea is perhaps the largest such site in the world. Yet, virtually nothing is known about sedimentary nitrogen cycling in this region and how it has been affected by human activities. Results of the maiden attempt to gain insight into this important aspect of nitrogen cycling over the western continental shelf of India are presented here based on three approaches: (1) incubation of sediment cores; (2) deployment of an indigenously-fabricated benthic chamber; and (3) porewater profiling of a number of dissolved inorganic nitrogen species. Besides evaluating the potential of sediments in removing nitrogen of anthropogenic origin, the other important issue is the quantitative importance of sediments in the cycling of N_2O in coastal waters. The latter issue assumes higher significance in view of the results presented in the previous chapter that established the coastal zone off western India as a globally significant source of this important greenhouse gas.

6.2 Quantification of Denitrification in Marine Sediments

The available data on the extent of denitrification in sediments are largely based on measurements of the N_2:Ar ratio or NO_3^- in the interstitial waters. For example, Barnes et al., 1975 found that denitrification in the sediments of the Santa Barbara Basin resulted in elevated N_2 levels in interstitial waters. He proposed a model that envisaged coupling between nitrification and denitrification i.e. oxidation of NH_4^+ by nitrifiers followed by reduction of the oxidized species to N_2 by denitrifiers as sufficient O_2 diffused into the upper few centimeters of the sediments to support nitrification. However, this model did not specify whether nitrification and denitrification in

98

the upper few centimeters took place simultaneously or they were spatially separated.

Vanderborght and Billen (1975) used porewater profiles of NO_3^- in coastal sediments in a one-dimensional model involving nitrification near the sediment surface and denitrification at greater depths. Similar models have since been used by several other workers (Jahnke et al., 1982; Goloway and Bender, 1982; Grundamanis and Murray, 1977; Christensen and Rowe, 1984). However, estimates of dentrification derived from the diffusion-reaction models suffer from a number of uncertainties. For example, it is very difficult to model vertical distribution of NO_3^- in most of the coastal sediments because of extremely steep gradients and disturbance caused by faunal activity (bioturbation), which greatly influences the interstitial water chemistry (Goldhaber et al., 1977; Koike and Sorensen, 1988). Grundamanis and Murray (1977) reported vertical zonation of nitrification and denitirification processes in sediments of the Puget Sound. Irrigation by burrowing benthic organisms led to mixing of interstitial waters with nitrification in an intermediate sedimentary zone, oxygenated by intruding bottom waters, sandwiched between zones of denitrification.

The first attempt to directly determine the rate of denitrification in marine sediments was made by Kaplan et al. (1979) who covered a portion of sediment with a bell jar and measured the concentration of N_2 gas in the enclosed overlying water. Developing this approach further, Seitzinger et al. (1980) incubated undisturbed sediment in Narragansett Bay in gas-tight glass chambers under lowered N_2 phase content. The major disadvantage of this technique is that it requires long incubation times, and since N_2 is the

dominant constituent of the atmosphere, utmost care is needed for avoiding contamination from air.

An isotopic method for estimating the sedimentary denitrification rate was introduced by Goering and Pamatmat (1970). This technique involves incubation of sediment samples to which ^{15}N-labeled NO_3^- is added in excess followed by the extraction of dissolved gases to determine ^{15}N enrichment. This method has been improved upon by several workers (Koike and Hattori , 1978; Oren and Blackburn, 1979; Nishio et al, 1982). One of the several advantages of this technique, when applied to the undisturbed sediment cores, is that the microenvironments are not damaged. Moreover, it provides rate of denitrification together with those of O_2 and NO_3^- consumption. It also enables identification of the source of NO_3^- undergoing reduction. However, the procedure requires long incubation times (a few days) and a mass spectrometer for precision isotopic analysis.

The C_2H_2 reduction technique is by far the most popular method for determining the rate of denitrification in sediments. It had been found that the reduction of N_2O to N_2 by denitrifying bacteria is blocked by C_2H_2 such that the NO_3^- undergoing reduction is converted to N_2O (Balderston et al, 1976; Yoshinari and Knowles, 1976). Based on this phenomenon, Sorensen (1978) developed a very simple, sensitive and inexpensive method wherein N_2O accumulation is measured in sediment cores incubated after the injection of sufficient quantities of C_2H_2-saturated water. The concentration of inhibitor required for the blockage has been proposed to be 5-10% v/v (Anderson et al., 1984; Jorgensen and Sorensen, 1985). The advantages of this method include the ease and low cost of measurements so that the method can be

used for rapid and routine analysis. The physical disturbance is minimal and near-in situ profiles can be obtained in short time incubation. However, the major drawback of this technique is that at low NO_3^- concentration inhibition of N_2O reduction by C_2H_2 is sometimes incomplete (Kaspar, 1982; Oremland et al., 1984; Jorgensen and Sorensen, 1985). Besides, C_2H_2 may also affect other pathways of the nitrogen cycle, such as the rate of NO_3^- reduction (Walter et al., 1979).

In spite of the varying uncertainties associated with different techniques, comparative studies have shown surprisingly similar results. For example, for the Bering Sea sediments the rates obtained by the ^{15}N technique and by diffusion-reaction models have been found to be quite close (Koike and Hattori, 1979) and are also comparable to those derived from the C_2H_2 inhibition method (Haines et al., 1981). Similar agreement has been found between the estimates based on the C_2H_2 block method and the ^{15}N method of Nishio et al. (1983). Therefore, C_2H_2 block technique appears to be reliable and well suited for measurements of sedimentary denitrification rates and hence this technique was adopted in the present study.

6.3. Significance of the study

It has been demonstrated in Chapter 4 that O_2-deficient conditions prevail in subsurface waters along the west coast of India for several months every year with the hypoxic waters covering almost the entire shelf region during the late SWM – FI seasons. This is related to high rates of biological productivity fuelled primarily by the nutrients supplied by the natural process of upwelling and possibly also, to a lesser extent, by the enhanced fertilizer

inputs from land. The resultant high organic loading into the sediments is expected to cause substantial denitrification. It has been suggested that the magnitude of sedimentary denitrification may match that of the water column denitrification in the perennial suboxic zone of the central Arabian Sea (Bange et al., 2000). However, the sedimentary denitrification rate has not been directly measured previously, and the present study provides the first set of data on this aspect. The results are expected to be useful not only for evaluating the nitrogen budget in this unusual environment, but also for predicting trends for other areas experiencing somewhat similar conditions (e.g. off Peru/Chile and Namibia).

6.4 Incubation Experiments

6.4.1 *Methodology*

Sedimentary denitrification rates were measured through deck incubations aboard O.R.V. *Sagar Kanya* during Cruises SK148 and SK149 undertaken during 4 September - 10 October and 2-9 December, 1999, respectively. These periods correspond to late SWM and the FI. Sediment sampling was done at eight locations on the continental shelf - seven along the west coast and one on the east coast of India (Fig. 2.3; Table 2.4). A spade (box) corer (30 x 30 cm) was used to collect undisturbed cores of up to 30 cm length. Sub-cores were taken in three acrylic core liners (internal diameter of 5 cm) immediately after the arrival of the corer on deck. The overlying water was removed and the headspace was flushed with N_2 gas. In one of the tubes that possessed two rows of ports fitted with silicon rubber septa at 1-cm intervals, C_2H_2-saturated water was injected through the ports

in four different directions to give an approximately 10% C_2H_2 saturation in the porewater. This sub-core was incubated for 1-1.5 hr in a cold, dark room along with another un-amended sub-core to serve as the control. The third sub-core was used for nutrient analysis.

At the end of the incubation period, N_2O concentrations in the overhead gas phase were measured in both the blank (control) as well as the C_2H_2-amended core-tubes. The cores were then sectioned into 1-cm thick slices and the material of each slice was quantitatively transferred to a 60-ml wide-mouth bottle containing 10 ml of surface seawater free of N_2O. The overhead space in the bottle had been previously flushed with N_2 and the entire operation beginning with the sectioning of core was carried out in a glove compartment under N_2 atmosphere. The bottle was capped with a rubber stopper and shaken vigorously for 3 minutes. Sample of the overhead gas was extracted with a syringe and injected through a 1-ml sampling loop into a gas chromatograph for N_2O analysis.

For the analysis of nutrients in porewaters the 1-cm slices of the core were placed in centrifuge tubes and centrifuged at 1000 rpm for 30 minutes. The supernatant was frozen immediately and later analysed for nutrients (NO_3^-, NO_2^-, NH_4^+ and PO_4^{3-}).

6.4.2 *Results*

6.4.2.1 Composition of Near-bottom Waters

Concentrations of dissolved O_2 and nitrogen species in near-bottom samples, taken within 5 m of seafloor, at the experimental sites are presented in Table 6.1. Most of the observations were made over the inner and mid-shelf

Table 6.1. Composition of bottom waters at the coring sites.

Core No.	DO (μM)	NO$_2$ (μM)	NO$_3$ (μM)	NH$_4$ (μM)	N$_2$O (nM)
1b	8	0.00	35.80	-	-
15b	9	0.25	28.01	-	43
19b	14	0.23	23.04	0.21	61
20b	12	0.82	1.45	0.00	112
2	75	3.67	2.84	2.97	26
16	4	0.00	27.53	Nd	57
19	3	1.00	3.31	2.50	22
22	45	3.63	7.35	0.13	41

regions (depths 23-76 m) during the Fall Intermonsoon and early NEM, and may not therefore be truly representative of all seasons and depth ranges. Although the Bay of Bengal site is O_2-depleted, it does not experience suboxic conditions in the water column as evident from the absence of NO_2^- in conjunction with high NO_3^- concentration (35.8 µM) in the near-bottom water (Table 6.1). By contrast, the site of the deepest (300 m) core (SK148-15b) along the western Indian continental margin is affected by mesopelagic suboxia characteristic of the northern Arabian Sea. The presence of the poleward undercurrent brings about substantial seasonal changes in redox conditions just off this margin (Naqvi et al., 1990). At the time of this study NO_2^- was present in detectable amount while the NO_3^- concentration was moderately low (~8 µM lower than the value for SK148-1b – Table 6.1) suggesting loss through denitrification. Denitrification also appeared to be active (e.g. SK149d-19) or occurred in the recent past (e.g. SK149d-22) in near-bottom waters at all the sampling sites located over the continental shelf with the exception of SK149d-16, as indicated by detectable NO_2^- (0.23-3.67 µM), and low NO_3^- (1.45-28.0 µM) and O_2 (3-75 µM). Cruise SK149d was undertaken during early December by which time the upwelling and related suboxia are expected to have waned. Their late persistence in 1999 was probably unusual. However, at two of the four sites sampled during this cruise (SK149d-02 and SK149d-22) bottom water O_2 had increased substantially (75 and 45 µM, respectively) in spite of high NO_2^- (3.67 and 3.63 µM, respectively) and low NO_3^- (2.84 and 7.35µM, respectively). This indicates that the sampling period was of transition from suboxic to oxic conditions. Bottom water composition is expected to undergo rapid changes during such a

transition, which may account for the modest correlations between the concentrations of O_2 and those of nitrogen species. (Table 6.1; Fig. 6.1).

6.4.2.2 Downcore Property Distributions

Nitrate concentrations (10.33 µM) in the interstitial water in the top 1 cm of the Core 148-1b was lower by ~25 µM than the value for the near bottom water sample at the same site. Moreover, NO_2^- was also present in high concentration (4.26 µM) in the core top sample. Concentrations of both NO_3^- and NO_2^- decreased rapidly with depth, reaching near-zero values in the 3-4 cm segment (Fig. 6.2). The interstitial waters were devoid of the oxidized nitrogen forms below this level. These results strongly point to the occurrence of denitrification, with a flux of NO_3^- directed into the sediments from the overlying seawater. The NH_4^+ concentration increased very rapidly with depth near the core top, and was relatively invariant (56.7-88 µM) below 2 cm. N_2O in the interstitial water was higher at the core top but, as in case of both NO_3^- and NO_2^-, it also decreased rapidly to near-zero values below 3 cm. While the high N_2O concentration (161 nM) at the core top suggested net production, presumably through a reductive pathway, the depletion at depth could only be due to net consumption through conversion to N_2.

As in case of Core 148-1b, the core-top porewater NO_3^- content (4.66 µM) in Core 148-15b (Fig. 6.3) was also substantially lower (by ~23 µM) than the bottom-water NO_3^- concentration (Table 6.1) which should drive a flux of NO_3^- into the sediments. However, while the NO_3^- concentration decreased to near-zero values at 2-4 cm, it increased slightly in the deeper segments with mid-depths maxima in both NO_3^- and NO_2^- found between 12 and 15 cm (Fig.
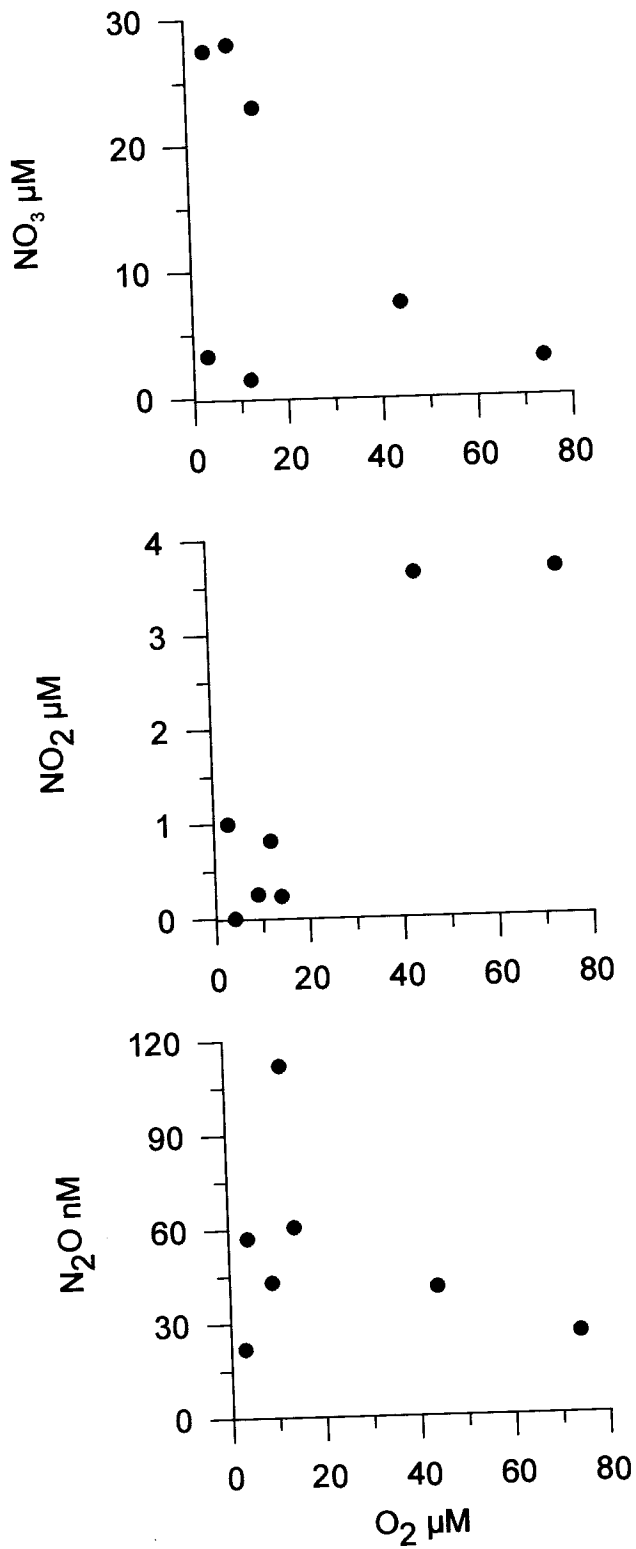
Fig. 6.1 Correlations between oxygen and nitrogen species
in near bottom waters.

NO₃(μM)

Fig. 6.2. Upper Panels:Vertical profiles of nitrate, nitrite and ammonia in interstitial waters of core SK 148 - 1b.

Lower panels: Vertical profiles of nitrous oxide in interstitial waters.

Fig. 6.3. Upper Panels:Vertical profiles of nitrate, nitrite and ammonia in interstitial waters of the core SK 148 - 15b.

Lower panels: Vertical profiles of nitrous oxide in interstitial waters.

6.3). NH_4^+ concentration increased with depth to 10 cm and decreased thereafter with the subsurface minimum centered around 14-17 cm. The presence of subsurface NO_3^- and NO_2^- peaks with relatively lower NH_4^+ suggests substantial bioturbation in spite of low ambient O_2 levels (9 µM). The prevalence of reducing conditions is reflected by the low N_2O concentrations (generally <10 nM, undetectable below 8 cm); these imply that unlike Core 148-1b sediments act as net sink for N_2O at Core 148-15b.

Core 148-19b was taken from the mid-shelf (depth 76m) off Goa where the near-bottom water was O_2-depleted and weakly denitrifying (low NO_2^- but high NO_3^-). Both NO_3^- and NO_2^- occurred in low but detectable (<2 µM) concentrations in the upper ~10 cm of the core, whereas NH_4^+ generally increased with depth. NO_3^- and N_2O were consumed in the upper sedimentary column through active denitrification (Fig. 6.4).

Core 148-20b, also located off Goa over the inner shelf (depth 23 m), was exposed to strongly reducing conditions in the overlying water as indicated by the low NO_3^- concentration (1.45 µM; Table 6.1). The concentration of NO_3^- was $\leq$ 1 µM throughout the core while that of NO_2^- was below detection limit (Fig. 6.5). NH_4^+ level was high (>100 µM) even at the core top increasing further with depth. The core top N_2O concentration was much lower (by >60 nM) than in the overlying bottom water (Table 6.1) but decreased with depth. Apparently denitrification resulted in the consumption of NO_3^- as well as N_2O in the sediments.

Core 149d-2 exhibited somewhat similar conditions to those for 148-20b located in the same area. However, as the 149d-2 was sampled towards the end of the upwelling period, the bottom water O_2 content had increased to
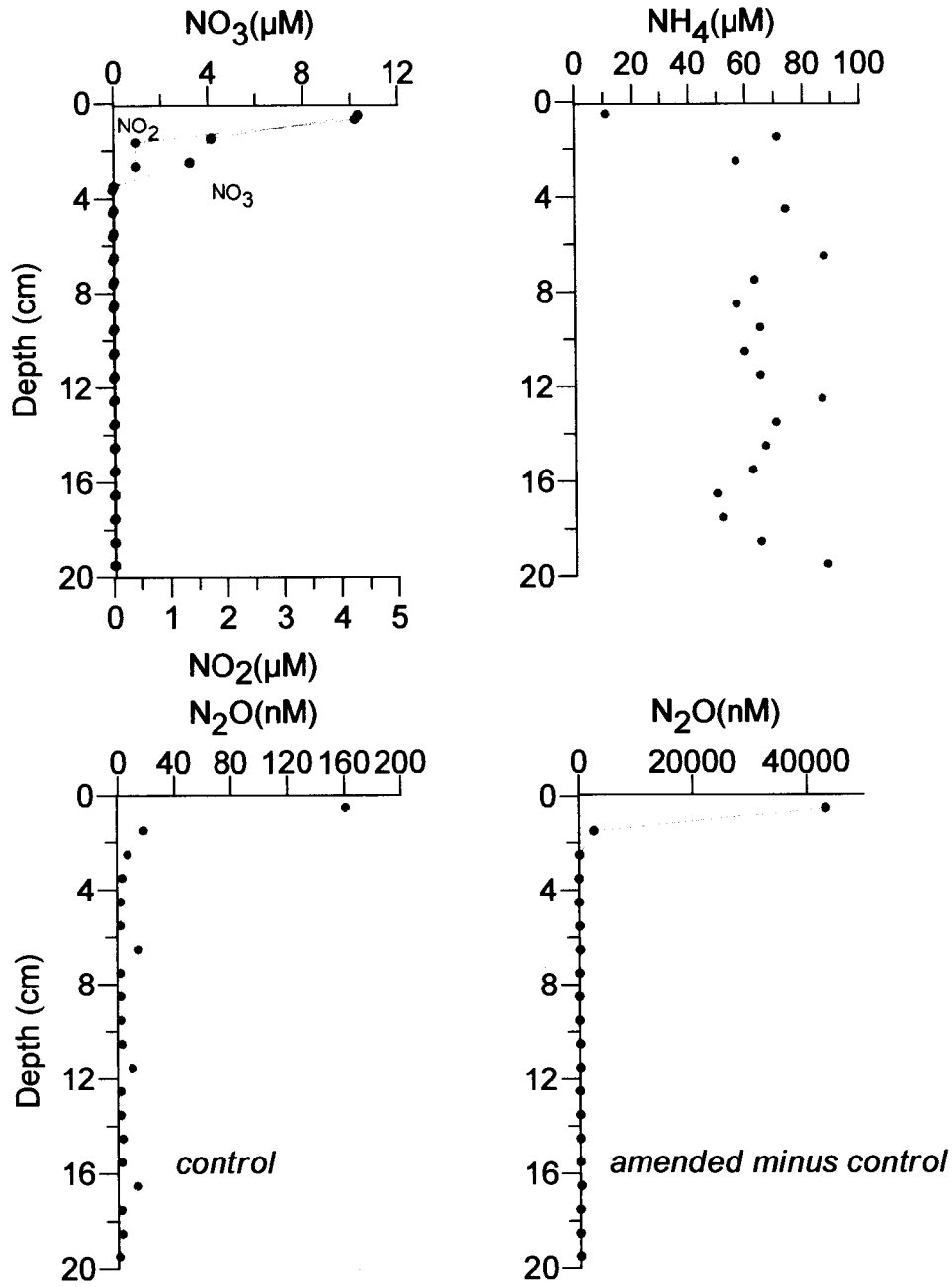
Fig. 6.4. Upper Panels:Vertical profiles of nitrate, nitrite and ammonia in interstitial waters of core SK 148 - 19b.

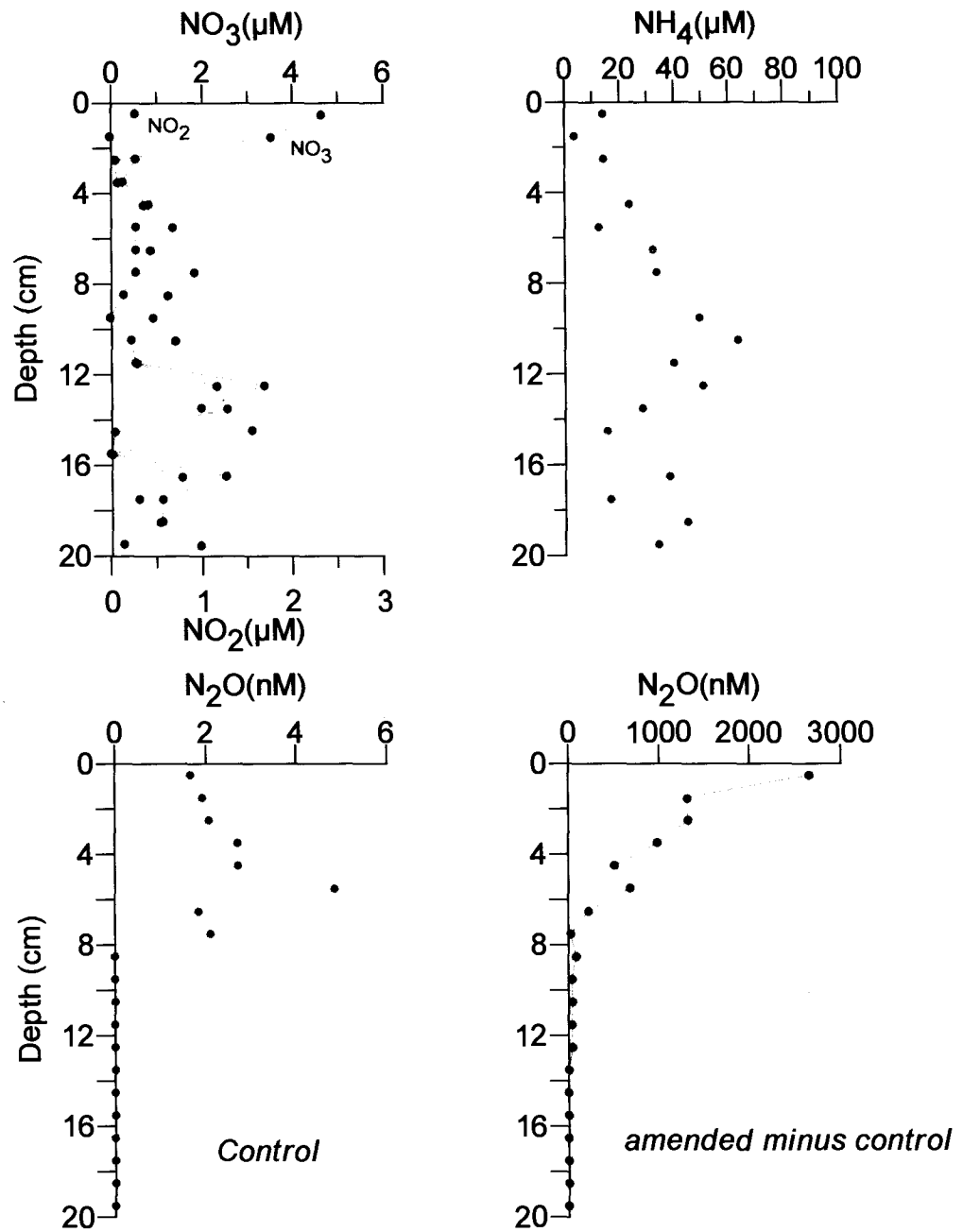Lower panels: Vertical profiles of nitrous oxide in interstitial waters.

Fig. 6.5. Upper Panels:Vertical profiles of nitrate, nitrite and ammonia in
interstitial waters of core SK 148 - 20b.

Lower panels: Vertical profiles of nitrous oxide in interstitial waters.

Fig. 6.6. Upper Panels:Vertical profiles of nitrate, nitrite and ammonia in interstitial waters of core SK 149d - 2.

Lower panels: Vertical profiles of nitrous oxide in interstitial waters.

75 μM, even though the low NO_3^- and high NO_2^- levels suggest that denitrification had occurred in bottom waters in very recent past. The combined NO_3^- and NO_2^- concentration was only slightly lower in the shallowest interstitial water sample than that in the overlying bottom water. Both NO_3^- and NO_2^- were depleted below detection limits at depth > 5 cm (Fig. 6.6). Concentration of NH_4^+ varied within a narrow range (~200-235 μM). Surprisingly the highest concentration was recorded near the core top with the minimum occurring at ~5 cm below which it increased slowly with depth. Diffusion of NH_4^+ from the sediments to overlying waters raised its concentration in the bottom water as well. N_2O was measured in moderate concentrations (~20 nM, marginally lower than that in the bottom water) in the upper few centimeters, but was undetectable below ~7 cm.

Core 149d-16 was collected from a depth (27 m) comparable to the two shallow cores described above, but from a more northerly location. Although the bottom water O_2 was very low, the absence of NO_2^- and high NO_3^- in bottom waters reflected low denitrification activity in the bottom waters. While nutrients could not be measured in this core, very low (< 2 nM) N_2O concentrations throughout this core (Fig. 6.7) suggested reducing environment that should have resulted in rapid consumption of both NO_3^- and N_2O diffusing downward from the overlying waters.

Core 149d-19 collected from a depth of 39m (mid shelf) south of Mumbai exhibited somewhat unusual features in the sedimentary column. Overlying waters were clearly suboxic (O_2 ~ 3μM), supporting denitrification. Concentrations of NO_3^- in near-surface interstitial waters were comparable with those in overlying waters, but substantially higher between 2 and 5 cm

N2O(nM)

0   1   2   3

N2O(nM)

0   1000 2000 3000

Depth (cm)

0

4

8

12

16

20

control

0

4

8

12

16

20

amended minus control
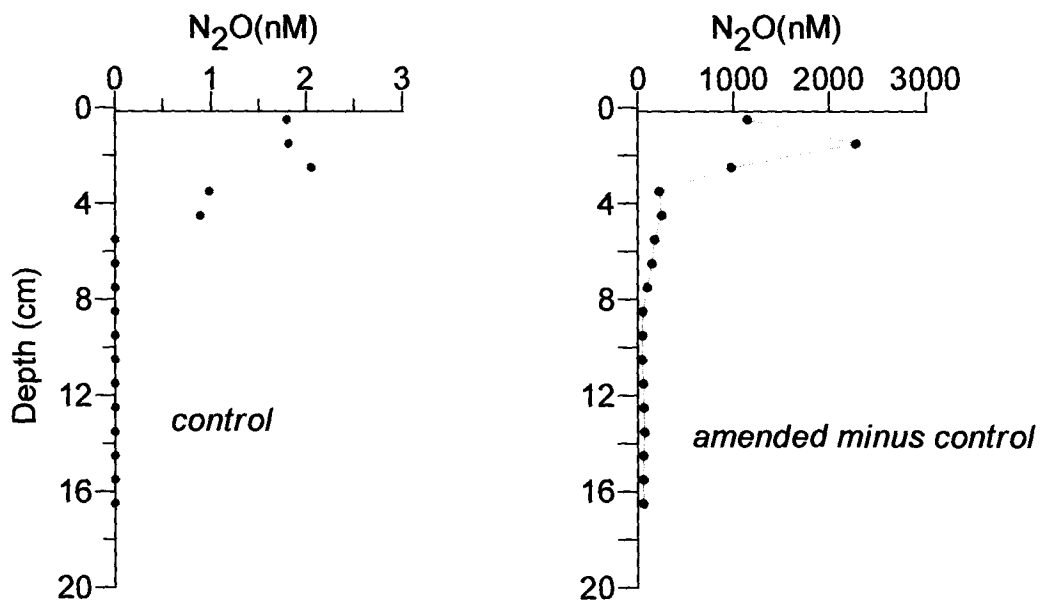
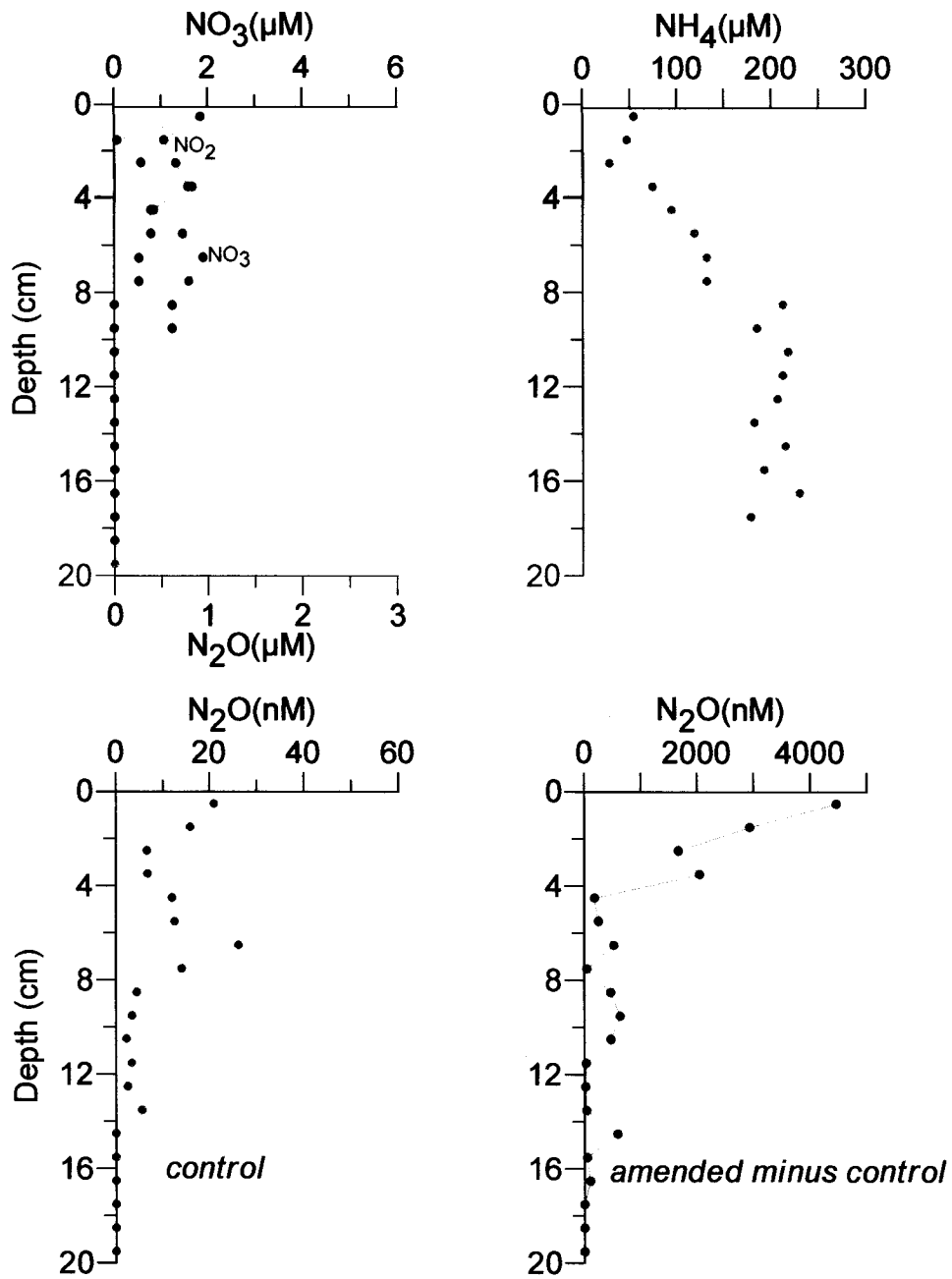Fig. 6.7. Vertical profiles of nitrous oxide in interstitial waters
core SK 149d - 16.
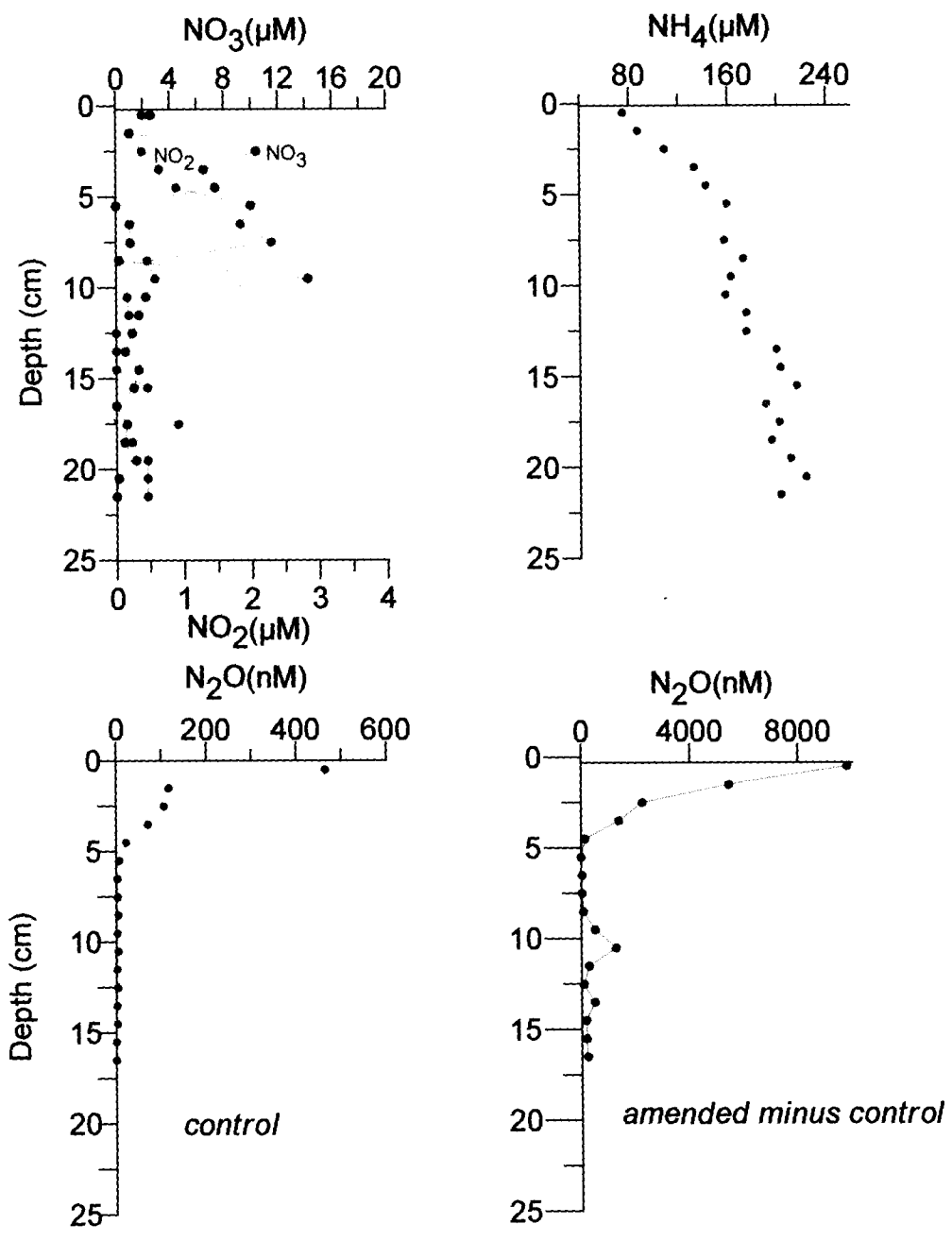
Fig. 6.8. Upper Panels:Vertical profiles of nitrate, nitrite and ammonia in interstitial waters of core SK 149d - 19.

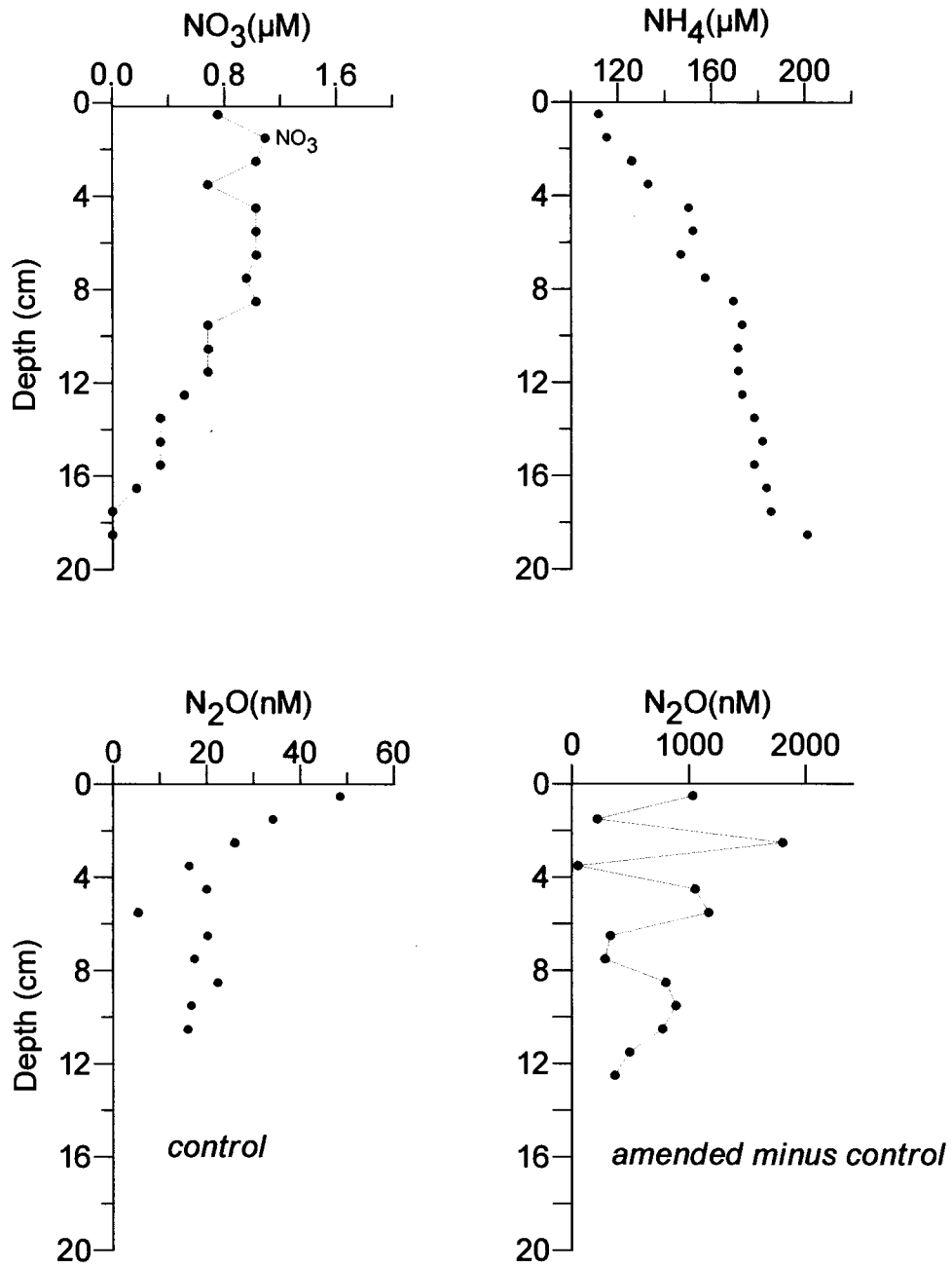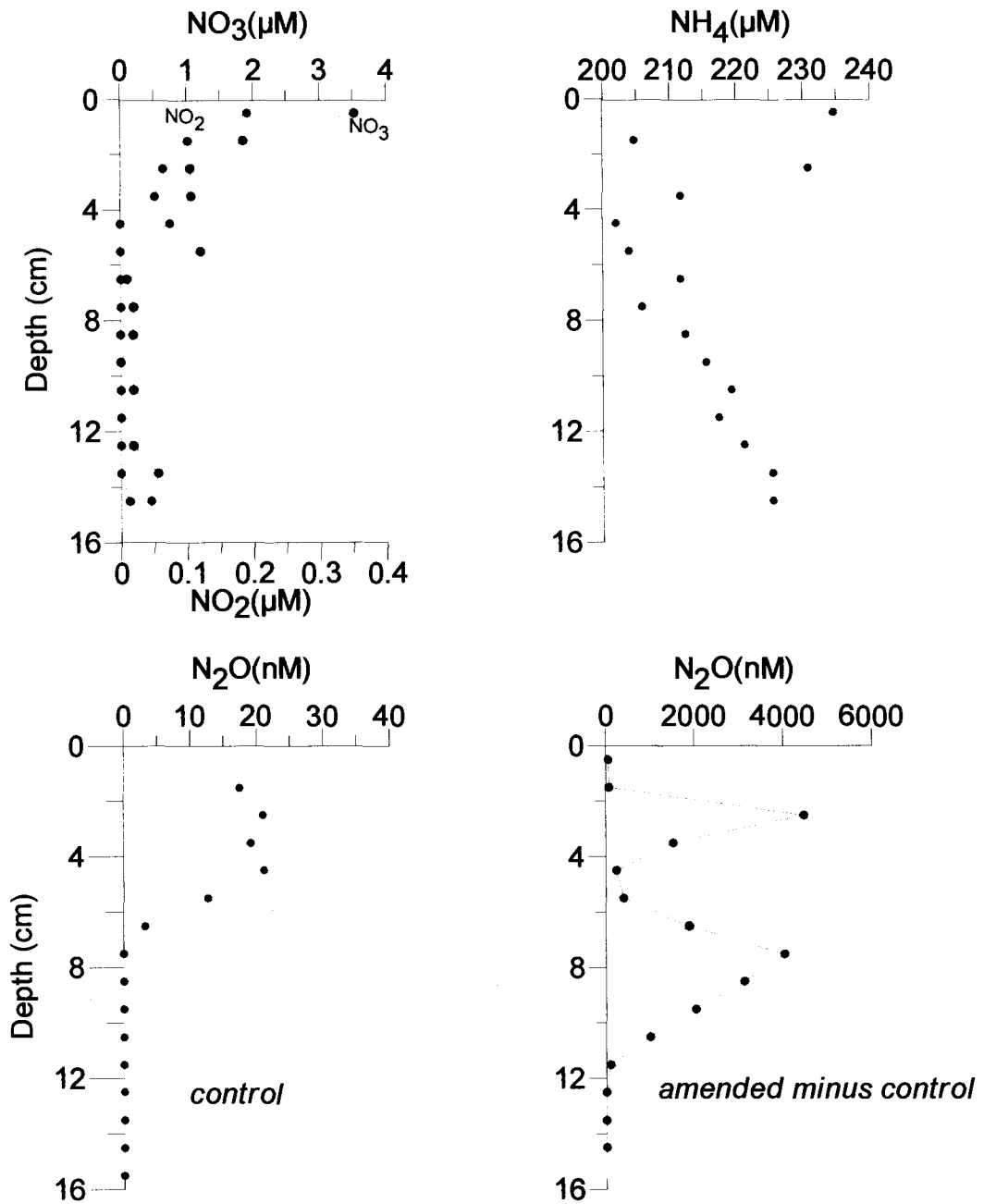Lower panels: Vertical profiles of nitrous oxide in interstitial waters.
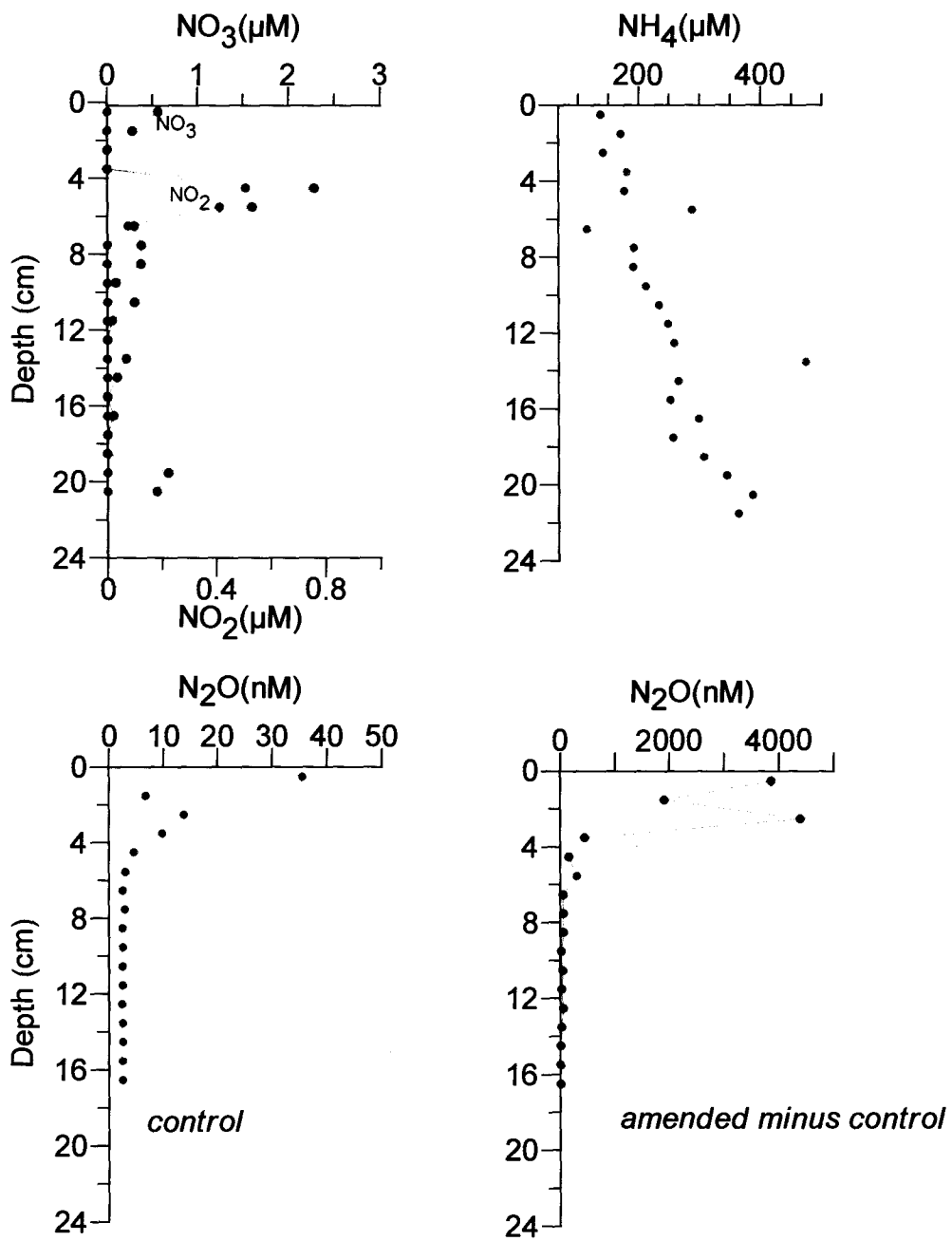
Fig. 6.9. Upper Panels:Vertical profiles of nitrate, nitrite and ammonia in interstitial waters of core SK 149d - 22.

Lower panels: Vertical profiles of nitrous oxide in interstitial waters.

(Fig. 6.8). Below 5 cm, low NO_3^- concentrations prevailed throughout the core. The NO_2^- profile also contained a subsurface maximum, but at a slightly deeper level (5-8 cm). Core top N_2O concentration was exceedingly high (466 nM), decreasing rapidly with depth to near-zero levels below 5 cm, the sediment obviously serving as a source of N_2O for the overlying waters. The same was the case with NH_4^+ that occurred in high concentration even at the core top (accounting for the substantial NH_4^+ present in the bottom water), increasing further with depth.

Core149d-22, from the mid-shelf (depth 43m) slightly to the south of 149d-19, had been affected by denitrification in the overlying waters in the period just preceding the observations even though at the time of sampling O_2 concentration in the bottom water (45 μM) was not conducive for the nitrate reduction to occur. Concentrations of NO_3^- and NO_2^- were low in this core (Fig. 6.9) except for slightly elevated levels between 4 and 6 cm. N_2O levels were also low, while NH_4^+ concentration was high (137-474μM). These results indicate the general prevalence of strongly reducing conditions throughout the core.

6.4.2.3 N_2O Accumulation in C_2H_2-amended Cores

Accumulation of N_2O occurred in the upper portions of all cores after incubation with C_2H_2. The greatest accumulation (43,355 nM) was found to occur in the Bay of Bengal core (148-1b; Fig. 6.2). Of the cores collected along the Indian west coast, the greatest accumulation (9,790 nM) was seen in 149d-19 (Fig. 6.8) while the lowest (1,034 nM) was found for 148-20b (Fig. 6.5). In most cases, peak accumulation occurred right at the core top,

decreasing rapidly with depth being significant down to 2-5 cm. One notable exception was the pattern observed in 149d-2 (Fig. 6.6) where negligible accumulation occurred in the upper 2 cm and two subsurface maxima in N_2O accumulation were found around 2-3 and 7-8 cm. Thus significant accumulation of N_2O extended much deeper in this core (~10 cm) than in other cases (except 148-20b, where the downcore variations were quite irregular).

The sedimentary denitrification rate (SDR) computed by integrating the values to the depth where significant N_2O accumulation occurred are presented in Table 6.2. The highest SDR (1.45 pmol NO_3 cm^{-2} s^{-1}) was estimated for 149d-19. This value is higher than that for the Bay of Bengal core 148-1b (1.18 pmol NO_3 cm^{-2} s^{-1}) where the peak value was much higher but decreased to negligible value below 2 cm. The lowest rate (0.166 pmol NO_3 cm^{-2} s^{-1}) was obtained for 148-15b. The average rate ($\pm$ standard deviation) for all the Arabian Sea cores was 0.491 $\pm$ 0.45 pmol NO_3 cm^{-2} s^{-1}.

In order to get insights into the various controlling factors the SDRs were plotted against depth and bottom water characteristics such as O_2, NO_3^- and N_2O (Fig. 6.10). Surprisingly, the correlations between the SDR and these variables were quite poor and not very significant.

Table 6.2. Integrated Sedimentary denitrification rates in the cores studied.

Core No.	Depth (m)	SDR (pmol NO_3 cm^{-2} s^{-1})
1b	150	1.180
15b	300	0.166
19b	76	0.374
20b	23	0.200
2	29	0.268
16	27	0.301
19	39	1.445
22	43	0.687
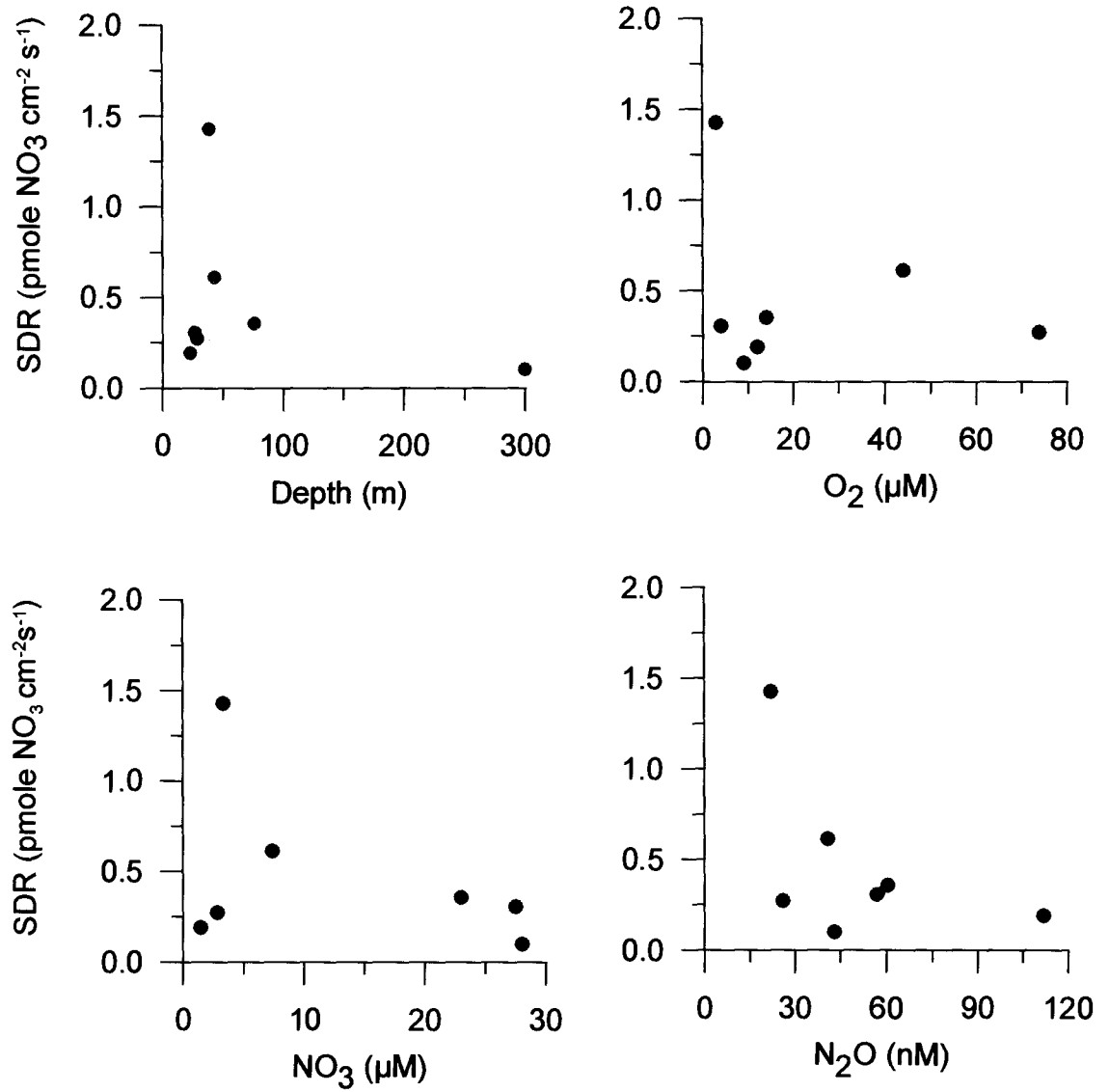
Fig. 6.10. Correlations of SDR with depth and bottom water properties
[Oxygen, Nitrate, and Nitrous Oxide].

6.4.3 Discussion

The chemical composition of bottom waters displayed large variability; O_2-depleted (3 – 75 µM) and reducing conditions contributed to highly variable NO_3^-, NO_2^- and N_2O concentrations (Table 6.1). The apparent decoupling between the sedimentary respiration and chemical composition of bottom waters, indicated by weak correlations between the SDR and bottom water characteristics (Fig. 6.10), probably resulted from large temporal variability of the latter such that the sedimentary processes probably responded to conditions averaged over a time period of several days/weeks rather than those prevailing at the instant of sampling.

Chemical characteristics of bottom waters (generally low O_2 and NO_3^- and high NO_2^-) and interstitial waters [low oxidized N species concentrations (NO_3^-, NO_2^- and N_2O), especially below the top few cm] and high NH_4^+ concentrations (that increased steadily with depth) provide a clear evidence that at all the locations studied, the sediments were fairly intensely reducing. Still, the measured SDRs were not very high as compared to other areas (see below; Table 6.3). This could be due to several reasons. (1) The prevalence of generally low NO_3^- concentrations in the overlying waters implies that the diffusion of NO_3^- in to sediments would not be very large. (2) The low O_2 levels at the sediment-water interface would ensure that copious amounts of NH_4^+ in the interstitial waters remain largely unutilized unlike in sediments that are exposed to well-oxygenated bottom waters where the production through nitrification is a major source of NO_3^- undergoing denitrification (Koike and Hattori, 1979; Seitzinger et al., 1984; Devol, 1991; Brandes and Devol, 1995).

Table 6.3. Comparison of SDR estimated in the present study with literature values.

Location	SDR (pmole NO_3 cm^{-2} s^{-1})
North Sea (Billen, 1978)	0.79
Narragansett Bay (Seitzinger et al, 1984)	4.8
Washington Shelf (Christensen et al, 1987)	0.57
Washington Shelf (Devol 1991)	0.9 - 6.13
Eastern North Pacific (Devol and Christensen, 1993)	0.96 - 6.13
Gulf of Maine (Christensen et al, 1996)	0.8 - 1.2
Present estimates in Arabian Sea	0.1 - 1.45 (0.49)

(3) It is possible that during the non-upwelling periods SDRs over the western Indian continental shelf are higher and (4) The estimates of SDR presented here must be treated as conservative. This is because of a disadvantage that the C_2H_2-block technique suffers from. When the ambient O_2 concentrations are low (<10 μM) the inhibition of N_2O reductase by C_2H_2 is incomplete (Seitzinger, 1988; Knowles, 1990; Chistensen et al., 1989). Moreover, the co-inhibition of nitrification by acetylene may lead to an exhaustion of the pore water NO_3^- pool (Lohse et al, 1996). As a consequence, the denitrification rates may be underestimated by as much as 30-50% (Lohse et al., 1993; Seitzinger et al., 1993).

In many of the cores studied, concentrations of N_2O in the shallowest interstitial water sample substantially exceeded that in the near-bottom water, even when the latter was apparently denitrifying, suggesting that N_2O was a significant product of denitrification at the core top and that it would sustain a positive flux of N_2O from the sediments to the water column. However, deeper down in the sedimentary column, the N_2O concentration decreased rapidly to undetectable levels indicating its reductive loss. In most probability N_2 is the dominant end-product of denitrification. Although it has been reported previously that the dissimilatory nitrate reduction to ammonium (DNRA) could be significant in surficial sediments (Macfarlane and Herbert, 1984; Dunn et al., 1980), the low NO_3^- and high NH_4^+ levels in all cores examined in the present study suggest that the accumulation of the latter was predominantly due to anaerobic decomposition of organic matter. With the exception of 149d-2, the lowest NH_4^+ concentrations were always observed at the core top (where the rate of NO_3^- reduction was the highest) and increased steadily with

depth. This implies that the NH_4^+ distribution was determined by its upward diffusion from deeper layers of the core where denitrification is insignificant and sulphate (SO_4^{2-}) reduction the major respiratory pathway. Indeed, accumulation of NH_4^+ is a common feature of all SO_4^{2-} reducing environments as the NH_3 produced from the organic matter cannot be oxidized by SO_4^{2-}. The diffusion of NH_4^+ to the overlying waters is significant, as evident from the substantial presence of NH_4^+ observed in several instances, and this should be an important source of nitrogen for primary production in shallow waters.

In most cases the combined concentration of NO_3^- and NO_2^- was higher in bottom waters than in the corresponding core top interstitial water value, which points to a flux of oxidized forms of nitrogen into the sediments. Some of the pore water profiles (148-15b; Fig. 6.3, 148-19b; Fig. 6.4, 149d-19; Fig. 6.8 and 149d-22; Fig. 6.9) contained local maxima and minima in NO_3^- and NO_2^-. Similar features have been reported previously from other areas (e.g., Grundmanis and Murray, 1977) and have been attributed to deep macrofaunal irrigation. Mixing of interstitial and oxygenated bottom water via irrigation by burrowing benthic organisms results in nitrification in the intermediate sedimentary zone, above and below which denitrification predominates. However, corresponding features in the SDR (N_2O profiles after incubation with C_2H_2) were not noticed in any of these cores. Core 149-2 (Fig. 6.6) exhibited two well-defined peaks in the SDR at 2-3 and 7-8 cm with low values in the upper 2 cm and at 4-6 depth intervals with some indication of deep irrigation that could have increased NO_3^- concentration slightly at 5-6 cm. A more complex vertical profile of SDR was obtained for 148-20b (Fig. 6.5). These inconsistencies in the NO_3^-/NO_2^- and SDR profiles probably

indicate considerable time lapse since the bioturbation events; while the effect was still discernible in porewater profiles it was generally not reflected in the SDR profiles. Alternately, it is possible though unlikely that the spatial variability was so high that even the sub-cores taken from the same box-core were not exactly identical. Significant NH_4^+ concentrations in bottom waters at the 149d-2 and 149d-19 core sites also suggest that significant bio-irrigation occurred at these sites.

The SDR estimates obtained in this study are compared to those from other areas in Table 6.3. It is clear that while the SDR values from the Indian shelf agree with those reported from other continental margin sediments, they are close to the lower end of the range of published values. Conditions most favourable for sedimentary denitrification include high sedimentary organic carbon content, moderate bottom water O_2 concentration and adequate NO_3^- supply. As described in Chapter 4, the western Indian coastal zone experiences seasonal O_2 deficiency in near-bottom waters as a consequence of which even when the organic carbon supply to sediments is high the low near-bottom concentrations of both O_2 and NO_3^- constrain denitrification in sediments.

One region which is almost similar to the coastal eastern Arabian Sea in terms of the subsurface O_2 deficiency is the inner Gulf of Mexico although the O_2 depletion in the Gulf of Mexico is primarily due to coastal eutrophication. Recent measurements of denitrification rates using the C_2H_2 block technique in surface sediments of the northern Gulf of Mexico have yielded values ranging from 1.11 to 3.0 pmol cm^{-2} s^{-1} (Childs et al., 2002). The highest rates were recorded when the O_2 concentrations were between ~30

and 90 µM and the denitrification activity was significantly lower when O_2 concentrations were outside this range. However, the estimates of Childs et al. (2002) were lower than those of Gardner et al. (1993) based on deployment of benthic chambers over the Louisiana continental shelf. This could have been due to the aforementioned underestimation of SDR by the C_2H_2 block method.

Apart from influencing the SDR by limiting the supply/production of NO_3^-, low bottom water O_2 concentration also modulates the material exchange across the sediment-water interface through controls on bioturbation by benthic organisms. The activity of macrobenthos is higher at O_2 concentrations in excess of 40 µM (Devol and Christensen, 1993). Lower O_2 concentrations will exclude large population of macrobenthos responsible for sediment mixing (Jahnke et al., 1990). Under such conditions the dominant process responsible for transport is molecular diffusion in the sediments (Murray et al, 1978; Grundmanis and Murray, 1982). Conditions observed during the present study (Table 6.1) appear to conform to such a scenario.

Shelf sediments overlain by oxygenated bottom waters are generally characterized by higher denitrification rates than those observed in the present study. For example, direct measurements of denitrification through analysis of N_2 in the overlying waters within benthic chambers deployed over the continental margin in the eastern North Pacific yielded values ranging from 0.9 to 6.1 (average 3.7) pmol N cm^{-2} s^{-1} (Devol, 1991). The flux of NO_3^- from overlying waters to sediments was only 1.5 pmol N cm^{-2} s^{-1} indicating that a larger fraction of N_2 gas was produced through the nitrification-denitrification coupling within the sediments. Similar results were obtained in

another study conducted in the same region – in this case N_2 flux from sediments to overlying water varied from 1.2 to 5.5 pmole N cm^{-2} s^{-1} (Devol and Christensen, 1993). These values are higher than most values listed in Table 6.3 (e.g. Christensen et al, 1987) for the other continental shelf areas. However, SDR of comparable magnitude (2.6 pmol N cm^{-2} s^{-1}) has also been recorded for the Baltic Sea.

Denitrification rates in the sediments have been found to exhibit considerable seasonal variations. For example, observations in the Patuxent Estuary showed that there was a strong coupling between nitrification and denitrification and > 99% of nitrate produced by nitrification was denitrified during the spring (Jenkins and Kemp, 1984). On the other hand, low O_2 concentrations during the summer greatly suppressed this coupling leading to lower denitrification rates. Data from a shallow Danish estuary collected with the C_2H_2 inhibition technique showed a similar decline in denitrification rate from 5.9 pmol N cm^{-2} s^{-1} in the early spring to 0.35 pmol cm^{-2} s^{-1} in the early summer (Jenkins and Kemp, 1984). Changes in bottom water O_2 concentration in the area of the present study are expected to bring about variations in the SDR, but the available data are inadequate to evaluate seasonal trends.

In order to compute the total sedimentary denitrification rate for the continental shelves of the Arabian Sea, the measured SDR was extrapolated to the total shelf area of 0.51 x 10^{12} m^2 (Bange et al., 2000). This gave estimates ranging from 0.38 to 3.5 Tg N y^{-1} with an average of 1.33 Tg N y^{-1}. For the reasons mentioned earlier this estimate should be regarded as conservative. In comparison, Bange et al. (2000) arrived at a value of 6.8 Tg

N y^{-1} from an empirical model that relates the SDR to primary productivity. Given the uncertainties in the present measurements and model predictions our results are in reasonable agreement with those of Bange et al. (2000). The above range (0.4 and 7 Tg N y^{-1}) is roughly of the same magnitude as the previously estimated rate of water column denitrification within the seasonal shallow suboxic zone of the eastern Arabian Sea.

Sources of N$_2$O in sediments: Since the oxic-anoxic environments are located in close proximity to each other and transient sites are common in surficial sediments, N$_2$O can be produced either through denitrification or nitrification. For denitrification to occur O$_2$ concentration must fall below a threshold value (Payne, 1973; Morrison et al., 1999; Naqvi and Jayakumar, 2000), but accumulation of N$_2$O during this process is transient; very often, N$_2$O is reduced to N$_2$ by the denitrifying bacteria (Delwiche, 1959; Bryan, 1981). On the other hand, N$_2$O formation through nitrification requires O$_2$ supply, although the N$_2$O yield during this process is greatly enhanced under semi-aerobic conditions (Goreau et al., 1980; Jorgensen et al., 1984). Thus production of N$_2$O through both mechanisms is highly sensitive to the environmental conditions, especially the ambient O$_2$ levels. For example, Jensen et al. (1984) recorded diurnal variations in N$_2$O exchange at the sediment-water interface in coastal environments of Denmark with higher fluxes occurring at night (0.4-4 µmol N$_2$O-N m^{-2} h^{-1}) than during the day (-0.4-0.4 µmol N$_2$O-N m^{-2} h^{-1}) (the negative flux indicates that the sediment sometimes acts as a sink for N$_2$O). The production of N$_2$O in these sediments was largely through denitrification. Due to the lack of O$_2$ production at night denitrification occurred close to the sediment-water interface thereby

increasing N_2O flux to the overlying water. The production of N_2O has also been found to be dependent on the availability of NO_3^- (Seitzinger and Nixon, 1985; Middleburg et al., 1995), which also points to denitrification as the dominant pathway of N_2O production in the sediments. As pointed out earlier, the core top interstitial values were generally higher than those in the bottom water in the majority of cores investigated by us. And since the bottom waters were mostly suboxic, it would imply that the denitrification was the major process responsible for N_2O accumulation in this region as well and that the surface sediments served as a net source of N_2O to overlying waters. On the other hand, low N_2O concentrations in the deeper sedimentary column are indicative of its reductive loss to N_2.

In conclusion, the present study implies that benthic denitrification does have the potential to remove substantial quantities of nitrogen added to coastal areas. However, since a large fraction of nitrogen reduced ends up as N_2O it is of little benefit to the environment.

6.5 Benthic Chamber Experiments

6.5.1 *Methodology*

An indigenously-fabricated benthic chamber was deployed by SCUBA divers on two occasions (26/6/2001 and 10/1/2002) off *Sagar Sukti* docked at the Old Goa Jetty in the Mandovi Estuary. The area of the seafloor covered was 0.15 m^2, while the volume of the water enclosed was ~0.031 m^3. The water depth at the experimental site is ~ 4 m and the water column is well oxygenated throughout the year.

The chamber was made of transparent acrylic material. It had a motor mounted on top for gently stirring the water inside; power supply to the motor was provided from the vessel. An outlet tubing allowed the sampling of water from within the chamber at regular intervals, and this water was replaced by that stored in a collapsible bag filled with the same sample as enclosed by the chamber at the start of the experiment. Air-tight gas syringes were used for drawing the sample through the Teflon tube. Due care was taken to flush thoroughly the sampling tube as well syringes avoiding any air bubbles. Dissolved O_2 was fixed within the syringe and after acidification the absorbance was determined at 456 nm (Pai et al., 1993). pH was measured colorimetrically. Nutrients were analysed using a Skalar analyser. N_2O was analysed using a gas chromatograph and TCO_2 by coulometer. Dissolved O_2 measurements were made aboard *Sagar Sukti* whereas samples for the remaining parameters were brought immediately to the shore laboratory for analysis.

6.5.2 *Results and Discussion*

O_2 concentrations within the chamber decreased with time in both experiments (Figs. 6.11 and 6.12). In the first experiment (Fig. 6.11) the concentration dropped from 213 to 150 µM over the 19-hr experimental duration; NO_3^- increased concurrently from 5.8 to 10.2 µM. NO_2^- concentration increased from 0.34 to 0.5 µM initially and then decreased to 0.37 µM, but NH_4^+ accumulated monotonously (from 1 to 3.8 µM) within the chamber. As expected, the change in pH was similar to that of O_2 – it decreased from 7.8 to 7.3, while that of pCO_2 was in the opposite sense – it rose from 620 to 1500 µ

Fig. 6.11. Changes in chemical composition of water within the benthic chamber deployed at Old Goa jetty in Mandovi estuary on 26/6/2001.

atm. An interesting aspect of the data in the context of the present study was that the N_2O concentration in the enclosed water nearly doubled during the incubation period.

The second experiment was of 18 hr duration and covered fewer variables (Fig. 6.12), but their trends of variability were generally consistent with those observed in the first instance with the initial and final values being 243 and 161 μM for O_2, 0.92 and 1.35 μM for NO_3^-, 0.37 and 0.51 μM for NO_2^-, and 6.31 and 12.63 μM for NH_4^+.

The decrease in O_2 is apparently the consequence of its uptake by the sediments for respiration by the biota while the increases in nutrients reflect their diffusion from the sediments where they are regenerated as a result of degradation of organic matter. The large increase in pCO_2 is presumably due to the decrease in pH during respiration. The increases in DIN ($NO_3^- + NO_2^- + NH_4^+$) concentration are quite significant and correspond to average fluxes of 26.2 and 26.6 mg-at N m^{-2} d^{-1} for the two observational periods. These results imply that the sediments of the Mandovi Estuary probably serve as an important source of nutrients for the overlying waters.

The observed increase in pCO_2 indicates that exchanges across the sediment-water interface could contribute significantly to the previously reported enhancement of pCO_2 in the estuaries of Goa (Sarma et al., 2001). The same appears to be true for N_2O as well. Unfortunately, for technical difficulties the experiment could not be repeated. However, the observed trend is consistent with the previously discussed porewater profiles from the open coastal sediments that often indicated higher concentrations of N_2O in the surficial sediments than in the overlying waters. Obviously, more data are
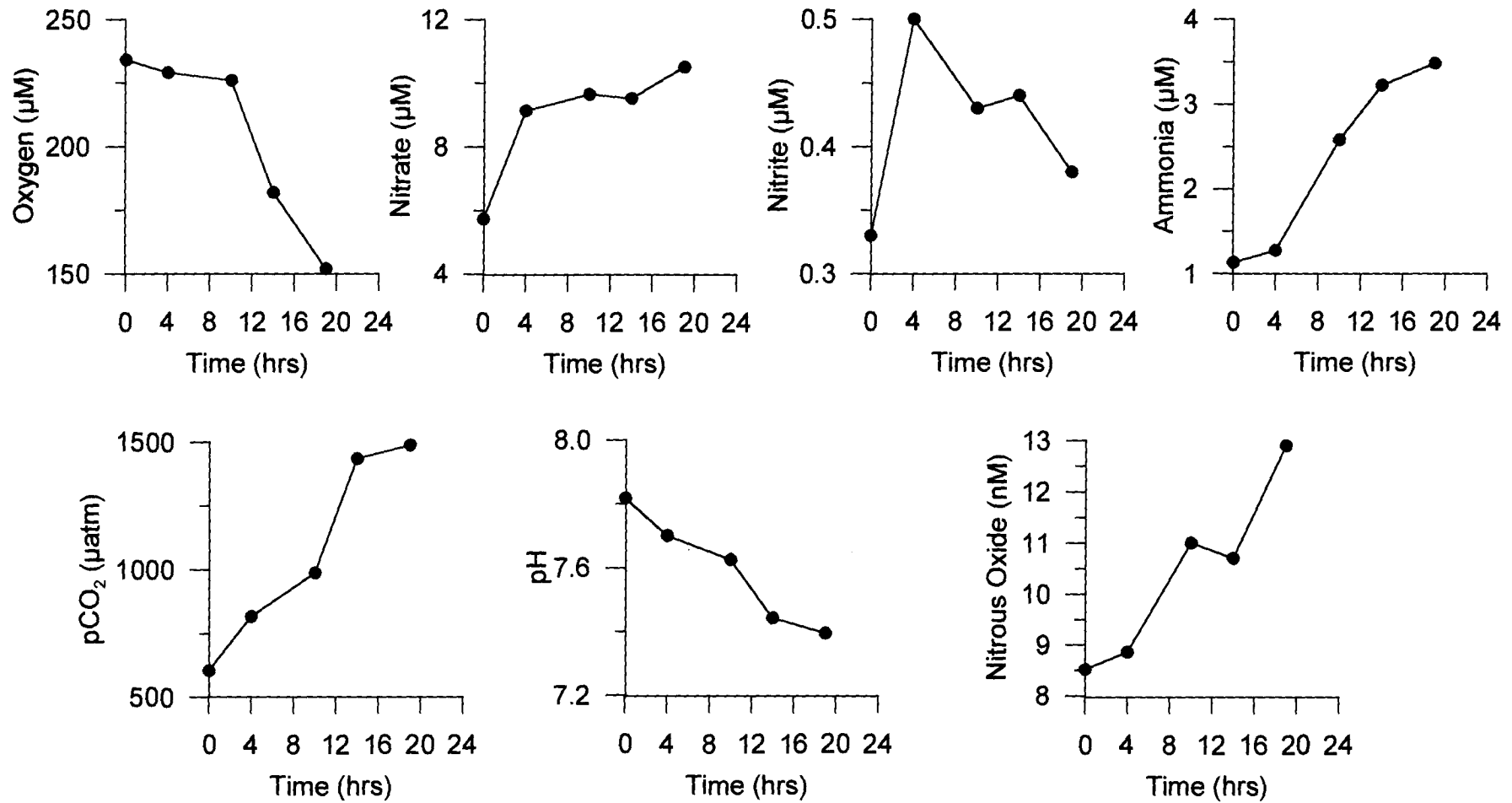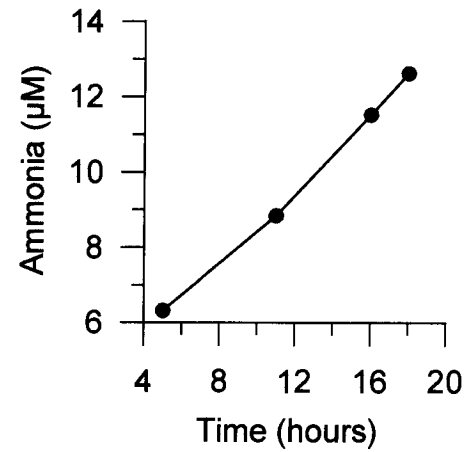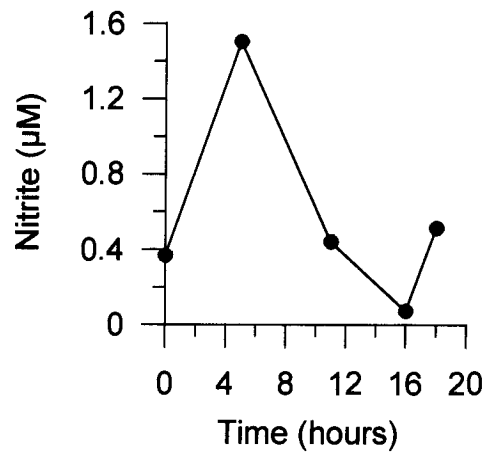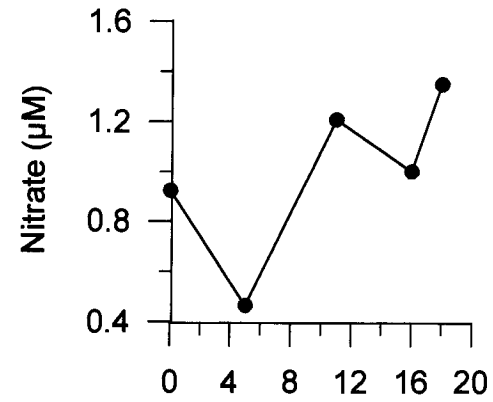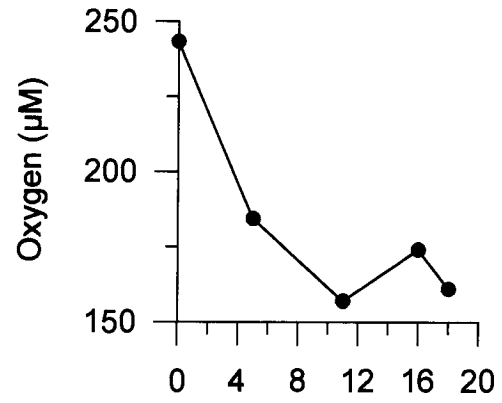
Fig. 6.12. Changes in chemical composition of water within the benthic chamber deployed at Old Goa jetty in Mandovi estuary on 10/1/2002.

required to confirm this feature and to quantify N_2O emission from the sediment to overlying water column.

6.6 Modelling of Porewater Profiles

6.6.1 *The Model*

Interstitial NO_3^- data from three sediment cores were fitted into a simple one-dimensional reaction-diffusion model to derive the set of constants that best simulated the observed distributions. This model, developed by Vanderborght and Billen (1975), is briefly described below:

The diagenetic equation for NO_3^- in porewaters can be formulated as

$$\partial C/\partial t = D(\partial^2 C/\partial z^2) - \omega(\partial C/\partial z) - k_d C \qquad (1)$$

where D is the diffusivity of NO_3^- in the porewater ($cm^2\ s^{-1}$), k_d is the first order rate constant of denitrification (s^{-1}), C is NO_3^- concentration (μM), ω is the sedimentation rate ($cm\ yr^{-1}$) and z is the depth in sediments (cm).

If we assume a steady state, C would not change with time and equation (1) becomes

$$0 = D\ (\partial^2 C/\partial z^2) - \omega(\partial C/\partial z) - k_d C \qquad (2)$$

Applying the following boundary conditions,

$$C = C_0 \quad \text{for } z = 0$$

and

$$C = 0 \quad \text{for } z = \infty,$$

the solution of the equation (2) is

$$C = C_0.\exp\{[\omega/2D-(\omega^2/4D^2+k_d/D)^{1/2}].\ z\} \qquad (3)$$

As $\omega/2D$ is insignificant equation (3) can be simplified to

$$C = C_0 e^{-(k_d/D)^{1/2}.z} \qquad (4)$$

In order to get the best fit of observations to the profiles predicted by Equation (4), the following procedure was adopted. The value of C_o was obtained by extrapolation of each profile to z=0 (the observations yielded an average value for the upper cm nominally taken to represent the 0.5 cm level). k_d was considered to be constant for any given profile and its magnitude was determined from the measured denitrification rate (r_d) and NO_3^- concentration (C) assuming a first order reaction (i.e. $r_d = k_d$ C). The values were averaged using the upper data points where the rate was significant. The value of D, initially fixed arbitrarily at 1×10^{-5}, was raised in increments of 1×10^{-6} computing every time the sum of squares of the difference between the observed and predicted values of C for all depths until this sum was at its minimum.

6.6.2 Results and Discussion

The values of C_o and depth-averaged k_d, and the best fit value of D for each core are listed in Table 6.4. The best-fit profiles along with the measured NO_3^- concentrations are shown in Fig. 6.13. k_d varied from 1.4×10^{-5} to 2.54×10^{-5} s^{-1} while D was within the range from 3.2×10^{-5} to 10.1×10^{-5} cm^2 s^{-1} (Table 6.4). These values are quite comparable with those available in the literature (e.g., Vanderborght and Billen, 1975; Aller, 1983). This, in turn, indicates that the sedimentary denitrification rates measured in the present study are of right magnitude. The observed order of magnitude (10^{-5} cm^{-2} s^{-1}) of NO_3^- diffusivity is the same as given by Berner (1971). However, in the upper few centimeters of sediments the diffusivity could be of higher order

Table 6.4. Surface NO_3^- concentrations (C_o), first-order denitrification rate constant (k_d) and nitrate diffusivity (D) at the three pore water modeling sites.

Core no.	Depth (m)	C_0 (μM)	K_d x 10^{-5} (s^{-1})	D x 10^{-5} (cm^2s^{-1})
148-1b	150	13.5	1.6	3.2
148-15b	300	5.25	1.4	4.8
149-2	29	4.4	2.54	10.1
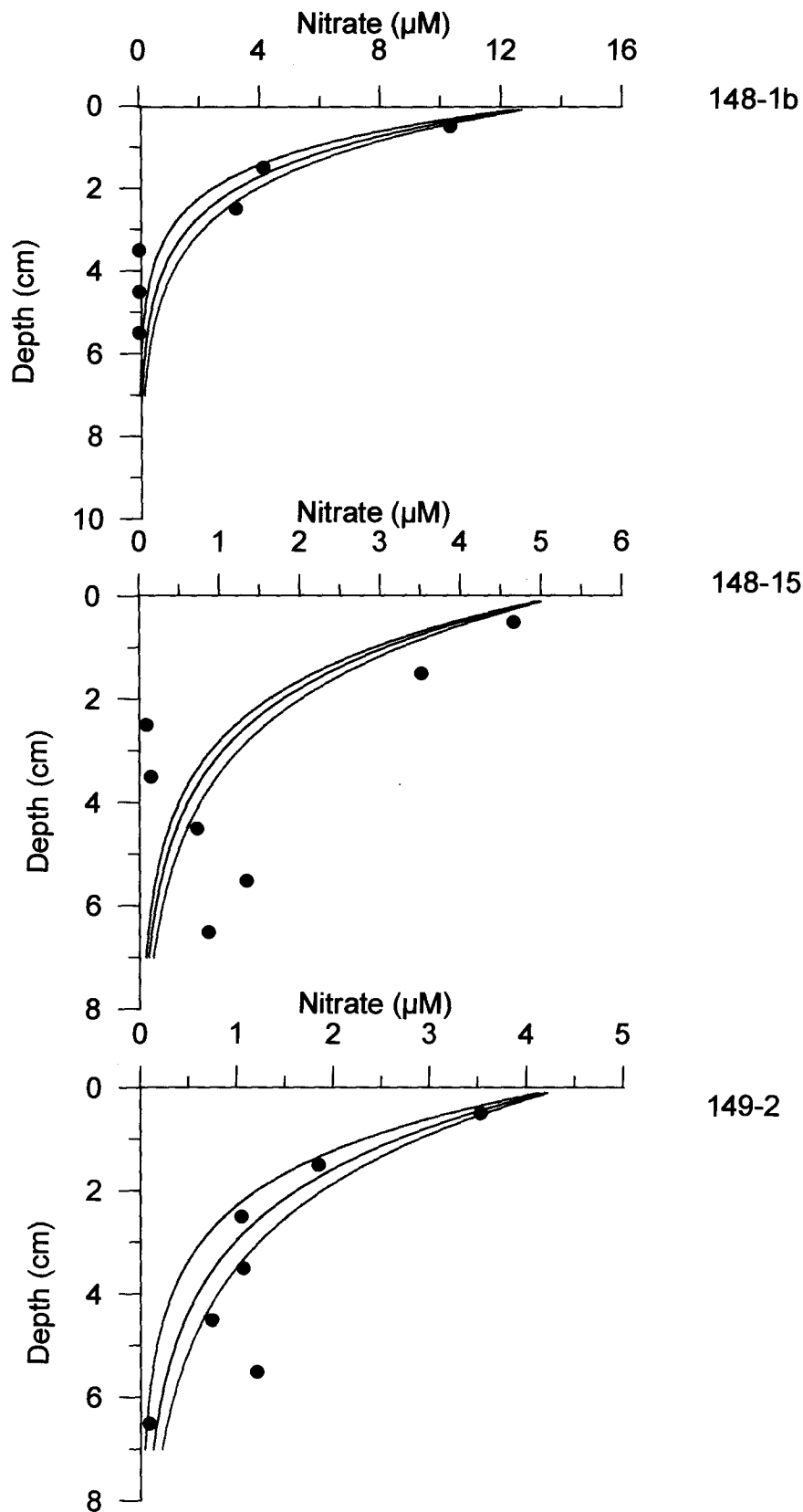
Fig. 6.13. Vertical profiles of observed(circles) and theoretical nitrate concentrations (lines) in pore water using one-dimensional model. The curve in black gives the stastically best fit to observations.

(10^{-4} cm^{-2} s^{-1}) due to bioturbation by benthic organisms (Vanderborght and Billen, 1975).

The three cores selected for simulation represented different environments and came from depths ranging from 29 to 300 m (Table 6.4). Still the k_d values do not show much variability. Values of D are relatively more variable. The computed diffusivity was the highest for the core 149-2. The bottom water at this site contained sufficient O_2 (~75μM) that would favour macrobenthic activity and this seems to account for the higher value of D for this core.

CHAPTER 7

Summary and Recommendations

Chapter 7

Summary and Recommendations

The western continental margin of India offers intriguing conditions for oceanographers to explore. Located in the monsoon region, surface currents along the Indian west coast, like elsewhere in the North Indian Ocean, are reversed completely every six months: the West India Coastal Current (WICC) flows equatorward during the Southwest Monsoon (SWM) and poleward during the Northeast Monsoon (NEM). However, these currents are not forced by local winds alone. Instead, circulation in the region, forms a component of the large-scale circulation in the entire North Indian Ocean, and is, to a large extent, remotely forced.

Seasonal changes in hydrography and circulation along the west coast of India bring about large variations in biogeochemical cycling. However, biogeochemical processes over this shelf had not been studied systematically and in detail so far. The present study provides the first comprehensive set of data on several physical, chemical and biological variables based on observations made on more than twenty cruises covering the entire shelf. Most of these cruises were undertaken after 1995 and included observations along fixed cross-shelf sections. In addition, a short (~10 km), shallow (depth < 30 m) section consisting of five stations off Candolim (Goa) has been occupied frequently since 1997 to investigate temporal changes in the coastal biogeochemical environment. Major results of the investigation are given below.

7.1 Major Findings

7.1.1 *Pelagic Processes over the Western Indian Continental Shelf*

- In conformity with previous reports, upwelling has been found to occur along the entire coast with a gradual progression from the south to the north. While the data generated in the present study show that upwelling goes on from June to December, earlier reports indicated that the process begins in the south in February/March (observations were not made in the present study during February-June in the southern region). This implies that the length of the upwelling period far exceeds that of the SWM, underscoring the role of remote processes in forcing upwelling along this coast. There are two aspects of upwelling in this region that distinguish it from the same process off the Somali and Arabian coasts: (1) Upwelling velocities are probably much lower off India; and (2) The cold upwelled water is generally prevented from reaching the surface by a thin (~10 m) warm, low-salinity layer that is formed due to intense precipitation and land runoff, and maintains strong near-surface thermohaline stratification. These peculiarities entail a more effective utilization of upwelled nutrients locally and a more severe O_2 depletion in subsurface waters over the Indian shelf.

- Beneath the equatorward surface flow there exists a poleward undercurrent that brings fresher and relatively oxygenated water from the south to the eastern Arabian Sea just off the continental slope. Although this undercurrent is a component of the SWM circulation, its signatures have been noticed on occasions during the NEM as well, implying

considerable interannual variability. The water upwelling along the Indian coast, derived from the region affected by the undercurrent, is initially O_2-poor but not suboxic ($O_2 > 25$ μM). However, over the continental shelf it loses the small quantities of dissolved O_2 due to respiration both with time and distance inshore such that at its peak the hypoxic ($O_2 < 22$ μM) zone includes the entire shelf. The area of this natural hypoxic zone (~180,000 km^2) is an order of magnitude greater than the area of the largest human-induced hypoxic zone in the Gulf of Mexico.

- The upwelled water is initially rich in nutrients ($NO_3^- > 20$ μM), and once it gets close to the euphotic zone it stimulates rich plankton growth. Due to the strong near-surface stratification, maximal primary productiion often occurs a few metres below the surface. Column production in the region (up to 6 g C m^{-2} d^{-1}) has been found to be among the highest observed anywhere in the Arabian Sea. The eventual decay of organic matter completely strips the sub-pycnocline waters of dissolved O_2 over large parts of the inner- and mid-shelf, triggering extensive denitrification. This process begins in July off Mangalore, in August off Goa and in September off Mumbai. South of about 12°N latitude, O_2 concentrations over the shelf do not generally fall to suboxic levels (<1 μM). Within about a month of the onset of denitrification, all oxidized nitrogen forms are lost over the inner- and sometimes the mid-shelf regions resulting in sulphate reduction in near-bottom waters. Anoxic conditions may last up to November/December in the north (off Mumbai), but are probably terminated earlier (September/October) in the south (off Mangalore). This

follows the reversal of surface current and the establishment of the NE Monsooon circulation: the poleward WICC causes downwelling over the Indian shelf and the water column becomes well oxygenated. Relatively oligotrophic conditions prevail during the NE Monsoon and Spring Intermonsoon seasons.

- Quasi-time-series observations along the shallow Candolim section have facilitated the construction of monthly climatologies of various physical and chemical variables. The results provide for the first time records of changes in these parameters over one complete annual cycle including the evolution of O_2-deficiency in shallow waters, in response to the monsoonal forcing. The seasonal changes displayed by the climatology are similar to those observed during numerous repeat samplings along longer cross-shelf Goa transect, but appreciable interannual changes in the timing and spatial patterns of suboxic and anoxic conditions have been recorded.

- Repeat observations at same sites have been used to arrive at an order-of-magnitude estimate of pelagic denitrification rate - 0.8 µmole NO_3^- l^{-1} d^{-1}, on an average. The total rate over the shelf has been estimated to be 1.3-3.8 Tg N y^{-1}. This corresponds to 4-12% of the denitrification rate for the perennial suboxic zone of the open Arabian Sea.

- H_2S was detected in concentrations reaching up to 21 µM off Goa, 15 µM off Mangalore and 20 µM off Mumbai. Such high levels of H_2S, seldom seem in open coastal waters, were never reported previously from the Arabian Sea and probably reflect an intensification of the shallow O_2-

deficient system through enhanced anthropogenic nitrogen loading in recent years.

- As expected NH_4^+ is found to accumulate in high concentrations (up to 21 μM) in the sulphide bearing waters. Its upward diffusion seems to sustain moderate primary production in the thin oxygenated layer overlying anoxic waters. In contrast, primary productivity rate in the O_2-depleted waters is very low even when these waters are found well within the euphotic zone.

- An unexpected feature of the nitrogen cycling was an unprecedented accumulation of N_2O – the highest concentration observed (765 nM) being over 4 times the highest value previously reported from the ocean. Association of the high N_2O concentrations with very high NO_2^- (up to 16 μM) suggests production through denitrification; this is supported by laboratory experiments involving incubation of water samples. Transient build up of N_2O probably occurs due to the low N_2O reductase activity in shallow, rapidly denitrifying waters that are subjected to frequent aeration through turbulence. This sustains a high rate of emission of N_2O to the atmosphere (up to 0.38 Tg N_2O y^{-1}). These observations imply that a very substantial fraction of NO_3^- undergoing denitrification may end up as N_2O.

- Inter-relationships between the dissolved inorganic nitrogen (DIN = NO_3^- + NO_2^- + NH_4^+), dissolved inorganic phosphorus (DIP) and H_2S reveal that while the atomic DIN/DIP ratios maintained during decay of organic matter using O_2 and NO_3^- as the oxidants are only slightly lower than the theoretical (Redfield) values, the expected ratio is not maintained during sulphate reduction. That is, there exists much more DIP in the sulphide bearing waters than the amount expected from the DIN concentration. This

is attributed to the mobilization of phosphate from sediments under anoxic conditions through dissolution of the iron-oxyhydroxo-phosphates (FeOP) complex. The same process also seems to lower the H_2S/DIP ratio. The observed H_2S/NH_4^+ ratio is slightly higher than the theoretical value, but the scatter is large and the departure might result from the diffusion of NH_4^+ from sediments to the overlying bottom waters.

- Isotopic composition of NO_3^- in shallow suboxic waters shows much smaller enrichment of heavier isotope (^{15}N) associated with denitrification than observed in the open ocean denitrifying zones. The results indicate a lower isotopic fractionation factor in the shallow suboxic zone (7.4°/oo as compared to 25°/oo in the open ocean). Alternatively, denitrification in sediments and mixing between anoxic and oxic waters might also pull down the $\delta^{15}N$ values of NO_3^- in the area of study.

7.1.2 Sedimentary Nitrogen Cycling

- The continental shelf sediments examined are found to serve as a sink for combined nitrogen. With the exception of two cores, N_2O concentrations at the sediment surface were higher (21-466 nM), indicating that the sediments serve as a source of N_2O to the overlying water column. A net consumption of N_2O has been found to occur deeper in the sedimentary column (a few centimeters below the sediment-water interface).

- Sedimentary denitrification rate measured with the acetylene block technique range between 0.17 and 1.45 pmol NO_3^- cm^{-2} s^{-1} with the maximum observed in the mid-shelf region. The rates are on the lower side of the range reported from other continental margin sediments. When

extrapolated to the total area of continental shelves in the Arabian Sea $(0.51 \times 10^{12} \text{ m}^2)$ the total sedimentary denitrification rate works out to be 0.38-3.5 (average 1.33) Tg N y^{-1}, which is of the same order of magnitude as the pelagic denitrification rate over the Indian shelf. Thus, while benthic denitrification over the Arabian Sea continental shelves has the potential to counter inputs of combined nitrogen due to human activities, the fact that a substantial fraction of nitrogen is reduced to N_2O means that this process is of little environmental benefit.

• Significant changes have been observed in the concentrations of nutrients and dissolved gases in bottom waters enclosed by benthic chambers deployed over periods of ~24 hours. While the dissolved O_2 levels decreased with time, those of pCO_2 and N_2O showed the opposite trend. These results imply that the respiratory processes within the sediments result in the supply of significant quantities of nutrients and gases to overlying waters sustaining biological production and emission of radiatively important gases to the atmosphere.

• Porewater NO_3^- profiles have been simulated with a simple one-dimensional reaction-diffusion model. The three cores selected for simulation represented different environments and came from depths ranging from 29 to 300 m. Still values of the first order denitrification rate constant (k_d) do not show much variability $(1.4 \times 10^{-5} \text{ to } 2.54 \times 10^{-5} \text{ s}^{-1})$. Estimates of NO_3^- diffusivity (D) corresponding to best fits of simulated profiles to observations are more variable $(3.2 \times 10^{-5} \text{ to } 10.1 \times 10^{-5} \text{ cm}^2 \text{ s}^{-1})$. The diffusivity was the highest for the core having the highest bottom water O_2 concentration that presumably favoured macrobenthic activity.

The present estimates for D are in good agreement with the literature values suggesting that the measured denitrification are perhaps of the right magnitude.

7.2 Recommendations for Future Research

- The results of the present study suggest that the coastal zone along India is being adversely impacted by anthropogenic activities that have potential not only to affect local living resources but also to provide positive feedback to global warming through enhanced emissions of greenhouse gases, particularly N_2O. A long term programme to monitor the physico-chemical environmental changes and assess their impact on ecosystems must be initiated. Such a multi-disciplinary programme should have both observational and modeling components. Its should aim at reaching an understanding of the budgets and interactive transformations of the major biogenic elements (carbon, nitrogen, phosphorus, silicon and sulphur) over the continental margin of India and their links with open-ocean biogeochemical processes, ultimately leading to system models capable of predicting the impacts of climate shifts on the global scale as well as of local/regional environmental changes on our coastal seas.

- There is very little quantitative information presently on the fluxes of nutrients from the land to coastal seas through atmosphere and rivers from South Asia, a region that accounts for roughly one-fifth of the total global consumption of nitrogenous fertilizers. As the results of the present study clearly show, the coastal oceanic environment in the region is extremely variable and hypersensitive to minor changes in the nutrient supply.

Therefore, the anthropogenic inputs of nutrients to our coastal seas need to be adequately quantified in order to control to the maximum possible extent the overfertilization of coastal waters and to mitigate its adverse effects.

- In order to refine estimates of sedimentary denitrification, more measurements are required covering a wider depth range and with better seasonal coverage. Direct measurements of N_2 flux to the overlying waters should be made through deployments of benthic landers. These should be supplemented with incubation experiments involving isotope-pairing.

- Large departures of the observed relationships between DIN, DIP and H_2S expected from the Redfield-Ketchum-Richards (RKR) model seem to suggest adsorsption/desorption of phosphorus on sediments exposed to different redox conditions. There is also a possibility that redox cycles of nitrogen and trace metals may be to some extent coupled in the investigated area. Detailed investigations on these aspects fell outside the scope of the present study, but should be taken up in future.

- The Arabian Sea has long been recognized as a region of significant N-fixation, mostly through blooms of *Trichodesmium* during the late NEM and SI. However, such blooms, extensively observed previously (Devassy et al., 1978), were not sighted in the coastal zone during any of the cruises/field trips undertaken as a part of this study. It is possible that a decrease in the abundance of *Trichodesmium* has occurred recently in response to elevated combined nitrogen levels in surface waters due to anthropogenic loading. Measurements of N-fixation, although planned initially, were not made due to the absence of *Trichodesmium*, but a

detailed study dealing with the impact of eutrophication on N-fixation is required for a more complete understanding of nitrogen cycling in this part of the ocean that has few analogues elsewhere.

References

References

Aller, R.C. (1983). The importance of diffusive permeability of animal burrow linings in determining marine sediment chemistry. *J. Mar. Res.*, 41, 299-322.

Altabet, M.A., R. Francois, D.W. Murray and W.L. Prell (1995). Climate-related variations in denitrification in the Arabian Sea from sediment $^{15}N/^{14}N$ ratios. *Nature*, 373, 506-509.

Altabet, M.A., M.J. Higginson and D.W. Murray (2002). The effect of millennium scale changes in Arabian Sea denitrification on atmospheric CO_2 *Nature*, 415, 159-162.

Anderson, T.K., M.H. Jensen and J. Sorensen (1984). Diurnal variations of nitrogen cycling in coastal marine sediments. I. Denitrification. *Mar. Biol.*, 83, 171-176.

Anderson, L.A. and J.L. Sariemento (1994). Redfield ratios of remineralization determined by nutrient data analysis. *Global Biogeochem. Cycles*, 8, 65-80.

Andreae, M.O. and P.J. Crutzen (1997). Atmospheric aerosols: Biogeochemical sources and role in atmospheric chemistry. *Science*, 276, 1052-1058.

Balderston, W.I., B. Sherr and W.J. Payne (1976). Blockage by acetylene of nitrous oxide reduction in *Pseudomonous perfectomarinous*. *Appl. Environ. Microbiol.*, 31,501-8.

Bange, H.W., S. Rapsomanikis and M.O. Andreae (1996). Nitrous oxide emissions from the Arabian Sea. *J. Geophys. Res. Lett.*, 23, 3175-3178.

Bange, H.W., T. Rixen, A. M. Johansen, R. L. Siefert, R. Ramesh, V. Ittekkot, M. R. Hoffmann and M. O. Andreae (2000). A revised nitrogen budget for the Arabian Sea. *Global Biogeochem. Cycles*, 14, 1283-1297.

Bange, H.W, M.O. Andreae, S. Lal, C.S. Law, S.W.A. Naqvi, P.K. Patra, T. Rixen and R.C. Upstill-Goddard (2001). Nitrous oxide emissions from Arabian sea: A Synthesis, *Atmos.Chem. Phys*,1, 61-71.

Banse, K. (1959). On upwelling and bottom trawling off the southwest coast of India. *J. Mar. Biol. Ass. India*, 1, 33-49.

Banse, K. (1968). Hydrography of the Arabian Sea Shelf of India and Pakistan and effects on demersal fishes. *Deep-Sea Res. I*, 15, 45-79.

Barber, R.T., J. Marra, R.R. Bidigare, L.A. Codispoti, D. Halpern, Z. Johnson, M. Latasa, R. Goericke and S.L. Smith (2001). Primary productivity and its regulation in the Arabian Sea during 1995. *Deep-Sea Res. II*, 48, 1127-1172.

Barnes, R.O., K.K. Bertine and E.D. Goldberg (1975). N_2:Ar, nitrification and denitrification in southern California borderland basin sediments. *Limnol. Oceanogr.*, 20, 962-970.

Bauer, S. G., L. Hitchcock and D.B. Oslon (1991). Influence of monsoonally forced Ekman dynamics upon surface layer depth and plankton biomass distribution in the Arabian Sea. *Deep-Sea. Res. I*, 38,531-553.

Bender, M.L. (1990). The delta ^{18}O of dissolved O_2 in seawater: A unique tracer of circulation and respiration in the deep sea. *J. Geophys. Res. C-Oceans*, 95, 22243-22252.

Bendschneider, K. and R.G. Robinson (1952). A new spectrophotometric method
for the determination of nitrite in sea water. *J. Mar. Res.*, 11, 87-96.

Berner, R.A. (1971). Principles of chemical sedimentology: New York, McGraw Hill, 240p.

Brandes, J.A. and A.H. Devol (1995). Simultaneous nitrate and oxygen respiration in coastal sediments: Evidence for discrete diagenesis. *J. Mar. Res.*, 53, 771-797.

Brandes, J. A. and A. H. Devol (1997). Isotopic fractionation of oxygen and nitrogen in coastal marine sediments. *Geochim. Cosmochim. Acta*, 61 1793-1802.

Brandes, J. A., A.H. Devol, D.A. Jayakumar, T. Yoshinari and S.W.A. Naqvi (1998). Isotopic composition of nitrate in the central Arabian Sea and eastern tropical North Pacific: a tracer for mixing and nitrogen cycles. *Limnol. Oceanogr.*, 43, 1680-1689.

Broecker, W.S. (1974). 'NO', a conservative water mass tracer. *Earth Planet. Sci. Lett.*, 23, 100-107.

Bruce, J.G., D.R. Johnson and J.C. Kindle (1994). Evidences for formation in the eastern Arabian Sea during the northeast monsoon. *J. Geophy. Res.*, 99, 7651-7664.

Bryan, B.A. (1981). Physiology and biochemistry of denitrification In: C.C.

Delwiche (ed.), *Denitrification, nitrification and atmospheric Nitrous oxide.* Wiley, New York, 67-84pp.

Bryden, H.L. (1973). New polynomials for thermal expansions, adiabatic temperature gradient and potential temperature of sea water. *Deep-Sea Res.I*, 25, 315-322.

Calvert, S.E. and N. B. Price (1971). Upwelling and nutrient regeneration in the Benguela Current. *Deep-Sea Res. I*, 18, 505-523.

Capone, D.G., J.P. Zehr, H.W. Paerl, B. Bergman and E.J. Carpenter (1997). *Trichodesmium*: a globally significant marine cyanobacterium. *Science*, 276, 1221-1229.

Carpenter, J. H. (1965). The Chesapeake Bay Institute technique for the Winkler dissolved oxygen method. *Limnol. Oceanogr.*, 10, 141-143.

Carruthers, J.N, S.S. Gogate, J.R. Naidu, T. Laevastu (1959). Shoreward upslope of the layer of minimum oxygen off Bombay: Its influence on Marine biology, especially fisheries. *Nature*, 183, 1084-1087.

Childs, C.R., N.N. Rabalais, R.E. Turner and L.M. Proctor (2002). Sediment denitrification in the Gulf of Mexico zone of hypoxia. *Mar. Ecol. Prog. Ser.*, 240, 285-290.

Christensen, J.P. and G.T. Rowe (1984). Nitrification and oxygen consumption in northwest Atlantic deep-sea sediments. *J. Mar. Res.*, 42, 1099 -1116.

Christensen, J.P., J.W. Murray, A.H. Devol and L.A. Codispoti (1987). Denitrification in continental shelf sediments has major impact on the oceanic nitrogen budget. *Global Biogeochem. Cycles*, 1, 97-116.

Christensen, P.B., L.P. Nielsen, N.P. Revsbech and J. Sorensen (1989). Microzonation of denitrification activity in stream sediments with a combined oxygen and nitrous oxide micro-sensor. *Appl. Environ. Microbiol.*, 55,1234-1241.

Cline, J. D. and F.A. Richards (1972). Oxygen deficient conditions and nitrate reduction in the eastern tropical North Pacific Ocean. *Limnol. Oceanogr.*, 17, 885-900.

Codispoti, L.A. and F.A. Richards (1976). An analysis of the horizontal regime of denitrification in the eastern tropical North Pacific. *Limnol. Oceanogr.*, 21, 379 - 388.

Codispoti, L.A. and T.T. Packard (1980). Denitrification rates in the eastern tropical South Pacific. *J. Mar. Res.*, 38, 453 - 477.

Codispoti, L.A. and J.P. Christensen (1985). Nitrification, denitrification and nitrous oxide cycling in the eastern tropical South Pacific Ocean. *Mar. Chem.*, 16, 277-300.

Codispoti, L.A., G.E. Friederich, T.T. Packard, H.T. Glover, P.J. Kelly, R.W. Spinrad, R.T. Barber, J.W. Elkins, B.B. Ward, F. Lipschultz and L. Lostanua (1986). High nitrate levels off the coast of Peru: A signal of high instability in the marine denitrification rate. *Science*, 233, 1200 -1202.

Codispoti, L.A., G. E. Friederich, C.M. Sakamoto, J. Elkins, T.T. Packard and T. Yoshinari (1992). Nitrous oxide cycling in upwelling regions underlain by low oxygen waters, In: B.N. Desai (ed.), *Oceanography of the Indian Ocean*. Oxford & IBH, New Delhi, 271-284pp.

Codispoti, L.A, J.A. Brandes, J.P. Christensen, A.H. Devol, S.W.A. Naqvi, H.W. Paerl and T. Yoshinari (2001). The oceanic fixed nitrogen and nitrous oxide budgets: Moving targets as we enter the anthropocene. *Sc. Mar.*, 85-105.

Cohen, Y. and L. Gordon (1978). Nitrous oxide in the oxygen minimum of the eastern tropical North Pacific: evidence for its consumption during denitrification and possible mechanisms for its production. *Deep-Sea Res.I*, 25, 509-524.

Cutler, A.N., and J.C. Swallow (1984). Surface currents of the Indian Ocean (To 25°S, 100°E): compiled from historical data archived by the Meteorological office, (Bracknell, UK: *Institute of Oceanographic Sciences*, Wormley, Report No. 187, 36 Charts), 8p.

Delwiche, C.C. (1959). Production and utilization of nitrous oxide by *Pseudomonas denitrificans. J. Bacteriol.*,77, 55-59.

Deuser, W.G., E.H. Ross, and Z.J. Mlodzinska (1978). Evidence for and rate of denitrification in the Arabian Sea. *Deep-Sea Res.I*, 25, 47-146.

Devassy, V.P., Bhattathiri, P.M.A. and Qasim, S.Z. (1978) *Trichodesmium* phenomenon. *Indian J. Mar. Sci.*, 7, 168-186.

Devol, A. (1991). Direct measurements of nitrogen gas fluxes from continental shelf sediments. *Nature*, 349, 319-321.

Devol, A.H. and J.P. Christensen (1993). Benthic fluxes and nitrogen cycling in Sediments of continental margin of the eastern North Pacific. *J. Mar. Res.*, 51, 345-372.

de Wilde, H.P.J. and W. Helder (1997). Nitrous oxide in the Somali Basin: the role of upwelling. *Deep-Sea Res. II*, 44, 1319-1340.

Diaz, R.J. and R. Rosenberg (1995). Marine benthic hypoxia: A review of its ecological effects and the behaviour responses of benthic macrofauna. *Oceanogr. Mar. Biol. Ann. Rev.* 33, 245-303.

Dietrich, G. (1973). The unique situation in the environment of the Indian Ocean. In: B. Zeitzschel (ed.), *The Biology of the Indian Ocean*, Springer Verlag, 1-6 pp.

Dugdale, R.C. and J.J. Goering (1967). Uptake of new and regenerated forms of nitrogen in primary productivity. *Limnol. Oceanogr.*, 12, 196-206.

Dunn, G.M., J.N. Wardell, R.A. Herbert, and C.M. Brown (1980). Enrichment, enumeration and characterization of nitrate-reducing bacteria present in sediments of the River Tay Estuary. *Proc. R. Soc. Edin.*, 78B, 47-56.

Falkowski, P.G. (1997). Evolution of the nitrogen cycle and its influence on the biological sequestration of CO_2 in the ocean. *Nature*, 387, 272-275.

Farrenkopf, A.M., M.E. Dollhopf, S.N. Chadhain, G.W. Luther III and K.H. Nealson (1997). Reduction of iodate in seawater during Arabian Sea shipboard incubations and in laboratory cultures of the marine bacterium *Shewanella putrefaciens* strain MR-4. *Mar. Chem.*, 57, 347-354.

Findlater, J. (1971). Mean monthly airflow at low levels over the western Indian Ocean. *Geophys. Mem*, London, 115, 55pp.

Firestone, M.K. & J.M. Tiedje (1979). Temporal change in nitrous oxide and dinitrogen from denitrification following onset of anaerobiosis. *Appl. Environ. Microbiol.*, 38, 673-679.

Flagg, C.N., and Kim, H.S. 1998. Upper ocean currents in the northern Arabian Sea from shipboard ADCP measurements collected during the 1994-1996 U.S. JGOFS and ONR programs. *Deep Sea Res.II*, 45, 1917-1959.

Fofonoff, N.P. and R.C. Jr. Millard (1983). Algorithms for computation of fundamental properties of seawater, UNESCO-Tech.-pap. *Mar. Sci.*, Paris, France, Unesco, 44, 53p

Fonselius, S.H. (1962). Determination of hydrogen sulphide, In: K. Grasshoff, M. Ehrhardt and K. Kremling, (ed.), *Methods of seawater analysis*. Verlag chemie. Weinheim. New York, 71p.

Gächter, R. and B. Müller (2003). Why the phosphorus retention of lakes does not necessarily depend on the oxygen supply to their sediments surface. *Limnol. Oceanogr.*, 48, 929-933.

Ganeshram, R.S., T.F. Pederson, S.E. Calvert and W.L. Prell (1995). Large changes in oceanic nutrient inventories from glacial to interglacial periods. *Nature,* 376, 755-758.

Gardener, W.S., E.E. Briones, E.C. Kaegi and G.T. Rowe (1993). Ammonium excretion by benthic invertebrates and sediment-water nitrogen flux in the Gulf of Mexico near the Mississippi River plume. *Estuaries,* 16, 799-808.

Garfield, P.C., T.T. Packard, G.E. Friederich and L.A. Codispoti (1983). A subsurface particle maximum layer and enhanced microbial activity in the secondary nitrite maximum of the northeastern tropical Pacific Ocean. *J. Mar. Res.*, 41, 747-768.

Gilson, H.C. (1937). The nitrogen cycle. In: *Scientific reports. John Murray expeditions.* 1933-1934. 2, 21-81pp.

Goering, G.G. and M .M. Pamatmat (1970). Denitrification in sediments of the sea off Peru. *Invest. Pesq.*, 35, 233-242.

Goldhaber, M.B., R.C. Aller, J.K. Cochran, J.K. Rosenfield, C.S. Martens and R.A. Berner (1977). Sulfate reduction, diffusion and bioturbation in Long Island Sound sediments. Report of the FOAM Group. *Am. J. Sci.* 277, 193-237.

Goloway, F. and M. Bender (1982). Diagenetic models of interstitial nitrate profiles in deep-sea suboxic sediments. *Limnol. Oceanogr,* 27, 624-638.

Goreau, T.J., W.A. Kaplan, S.C. Wofsy, M.B. McElroy, F.W. Valois, and S.W. Watson (1980). Production of NO_2^- and N_2O by nitrifying bacteria at reduced concentrations of oxygen. *Appl. Environ. Microbiol.,* 40, 526-532.

Grasshoff, K. (1969). Zur Chemie des Roten Meeres und des inneren Golf von Aden nach Beobachtungen von F S 'Meteor' wahrender Indischen Ozean Expedition 1964/65. *Meteor Foprschungsergeb,* Reihe A, A6, 76p.

Grasshoff, K. (1975). The hydrochemistry of landlocked basins and fjords. In: J. P. Riley and G. Skirrow (eds.), *Chemical Oceanography,* Vol. 2, Academic Press, New York, 455-597pp.

Grasshoff, K., M. Ehrhardt and K. Kremling (1983). *Methods of Seawater Analysis,* Verlag Chemie, New York, NY, 419pp.

Grundamanis, V.and J.W. Murray (1977). Nitrification and denitrification in marine sediments from Puget Sound. *Limnol. Oceanogr.*, 22, 804-813.

Grundamanis, V. and J.W. Murray (1982). Aerobic respiration of pelagic marine sediments. *Geochim. Cosmochim. Acta*, 46, 1101-1120.

Gunnars, A.S., Blomqvist, P. Johansson and C. Anderson (2002). Formation of Fe(III) oxyhydroxide colloids in freshwater and brackish seawater, with incorporation of phosphate and calcium. *Geochim. Cosmochim. Acta.*, 66, 745-758.

Haines, J.R., R.M. Atlas, R.P. Griffiths and R.Y. Morita (1981). Denitrification and nitrogen fixation in Alaskan continental shelf sediments. *Appl. Environ. Microbiol.*, 41, 412-421.

Hartmann, M., H. Lange, E. Seibold and E. Walger (1971). Oberflaschensedimente im Persischen Golf und Golf von Oman. I. Geologisch-hydrologischer Rahmen und erste sedimentologish Ergebnisse. *Meteor Forschungsergebnisse*, Reihe C, 4, 1-76.

Howell, E.A., S.C. Doney, R.A. Fine and D.B. Oslon (1997). Geochemical estimates of denitrification in the Arabian Sea and Bay of Bengal. *J. Geophys. Res. Lett.*, 24, 2549-2552

Jahnke, R.A., S.R. Emerson and J.W. Murray (1982). A model of oxygen reduction, denitrification, and organic mater mineralization in marine sediments. *Limnol. Oceanogr.*, 27, 610-623.

Jahnke, R. A., C.E. Reimers and D.B. Craven (1990). Organic matter recycling at the seafloor: intensification near ocean margins. *Nature*, 348, 50-54.

Jayakumar, D.A., S.W.A. Naqvi, P.V. Narvekar and M.D. George (2001). Methane in coastal and offshore waters of the Arabian Sea. *Mar. Chem.*, 74, 1-13.

Jenkins, M. C. and W. M. Kemp (1984). The coupling of nitrification and denitrification in two estuarine sediments. *Limnol. Oceanogr.*, 29, 609-619.

Jensen, H.B., K.S. Jorgensen and J. Sorensen (1984). Diurnal variation of nitrogen cycling in coastal marine sediments II. Nitrous oxide emission. *Mar. Biol.*, 83,177-183.

Jorgensen, B.B. and J. Sorensen (1985). Seasonal cycle of O_2, NO_3, and SO_4^{2-} reduction in estuarine sediments: the signification of an NO_3 reduction maximum in spring. *Mar. Ecol. Prog. Ser.*, 24, 65-74.

Jorgensen, K.S., H.B. Jensen, and J. Sorensen. (1984). Nitrous oxide production from nitrification and denitrification in various sediments at low oxygen concentrations. *Can. J. Microbiol.*, 30, 1073-1078.

Kaplan, W., I. Valiela and J.M. Teal (1979). Denitrification in a salt marsh ecosystem. *Limnol. Oceanogr.*, 24, 726-734.

Karl, D.M., R. Latelier, L. Tupas, J. Dore, J. Christian and D. Hebel (1997). The role of nitrogen fixation in Biogeochemical cycling in subtropical North Pacific Ocean. *Nature*, 388, 533-538.

Kaspar, H.F. (1982). Denitrification in marine sediment: measurement of capacity and estimate of *in-situ* rate. *Appl. Environ. Microbiol*, 43, 522-527.

Kasting, J. F. (1990). Bolide impacts and the oxidation state of carbon in the earth's early atmosphere. *Life Evol. Biosphere*, 20, 199-231.

Knowles, R. (1990). Acetylene inhibition technique: development, advantages and potential problems. In: Revsbech, N.P. and Sorensen, J., (eds.), *Denitrification in Soil and Sediment*. Plenum Press, New York, 151-156 pp.

Koike, I. and A. Hattori (1978). Simultaneous determination of nitrification and nitrate reduction in coastal sediments by an N^{15} dilution technique. *Appl. Environ. Microbiol.*, 35, 853-857.

Koike, I., and A. Hattori (1979). Estimate of denitrification in sediments of the Bering Sea shelf. *Deep Sea Res.I*, 26, 409-415.

Koike, I. and J. Sorensen (1988). Nitrate reduction and denitrification in marine sediment, In: T.H. Blackburn and J. Sorensen (eds.), *Nitrogen cycling in Costal Marine Environment*. Wiley, NY, 251-274pp.

Koroleff, F. (1963). Determination of phosphate, In: K. Grasshoff, M. Ehrhardt and K. Kremling, (ed.), *Methods of seawater analysis*. Verlag chemie. Weinheim. New York, 117p.

Koroleff, F. 1970 Determination of ammonia, In: K. Grasshoff, M. Ehrhardt and K. Kremling, (ed.), *Methods of seawater analysis*. Verlag chemie. Weinheim. New York, 126p.

Lal, S. and P.K. Patra (1998). Variabilities in the fluxes and annual emissions of nitrous oxide from the Arabian Sea. *Global Biogeochem. Cycles*, 12: 321-327.

Law, C.S. and N.J.P. Owens (1990). Significant flux of atmospheric nitrous oxide from the northwestern Indian Ocean. *Nature,* 346, 826-828.

Lipschultz, F., S.C. Wofsy, B.B. Ward, L.A. Codispoti, G. Friedrich and J.W. Elkins (1990). Bacterial transformations of inorganic nitrogen in the oxygen-deficient waters of the Eastern Tropical South Pacific Ocean. *Deep Sea Res.I,* 37, 1513-1541.

Liss, P. and L. Merlivat (1986). Air-sea gas exchange rates: Introduction and synthesis, In: P. Buat – Menart (ed.), *The role of air-sea exchange in geochemical cycling,* N. A. M.T.O.A.S.I. Series, 185, 113-128pp.

Lohse, L., J.F.P. Malschaert, C.P. Slomp, W. Helder and W. van Raaphorst (1993). Nitrogen cycling in North Sea sediments: interaction of denitrification and nitrification in offshore and coastal areas. *Mar. Ecol. Prog. Ser.,* 101, 283-296.

Lohse, L., H.T. Kloosterhuis, W.van Raaphorst and W. Helder (1996). Denitrification rates as measured by the isotope pairing method and by the acetylene inhibition technique in continental shelf sediments of the North Sea. *Mar. Ecol. Prog. Ser.,* 132, 169-197.

MacFarlane, G,T. and R.A. Herbert (1984). Nitrate dissimilation by *Vibrio* spp. isolated from esturine sediments. *J. Gen. Microbiol.,* 128, 2463-2468.

Malakoff, D. (1998). Death by suffocation in the gulf of Mexico. *Science,* 281, 190-192.

Mantoura, R.F.C., C.S. Law, N.J.P. Owens, P.H. Burkill, E.M.S. Woodward, R.J.M. Howland and C.A Llewellyn (1993). Nitrogen biogeochemical cycling in the northwestern Indian Ocean. *Deep Sea Res. II,* 40, 651-671.

McAullife, C. (1971). GC determination of solutes by multiple phase equilibration. *Chem. Tech.,* 1, 46-50.

McCreary, J.P., P.K. Jr. Kundu and R.L. Molinari (1993). A numerical investigations of dynamics, thermodynamics and mixed layer processes in the Indian Ocean. *Prog. Oceanogr.,* 31,181-244.

McElroy, M.B. (1983). Marine biological controls of atmospheric CO_2 and climate. *Nature,* 302, 328-329.

Middelberg, J.J., G. Klaver, J. Nieuwenhuize, R. M. Markusse, G. Vlug and F.J.W.A. van der Nat (1995). Nitrous oxide emission from estuarine sediments. *Hydrobiologia,* 311, 43-55.

Millero, F.J., C.T. Chen, A.L. Bradsha and K. Schleiche (1980). A new high pressure equation of State for Sea water. *Deep Sea Res.I,* 27, 255-264.

141

Morcos, S.A. (1970). Physical and Chemical Oceanography of the Red Sea. *Oceanogr. Mar. Biol. Ann. Rev.*, 8, 73-202pp.

Morrison, J.M., L.A. Codispoti , S.L. Smith, K. Wishner, C. Flagg, W.D. Gardner, S. Gaurin, S. Naqvi, V. Manghnani, L. Prosperie and J.S. Gundersen (1999). The oxygen minimum zone in the Arabian Sea during 1995. *Deep-Sea Res. II*, 46, 1903-1931.

Murray, J.W., V. Grundmanis and W.H. Jr. Smethie (1978). Interstitial water chemistry in the sediments of saanich inlet. *Geochim. Cosmochim. Acta*, 42,1011-1026.

Naqvi, S.W.A. (1987). Some aspects of the oxygen-deficient conditions and denitrification in the Arabian Sea. *J. Mar. Res.*, 49, 1049-1072.

Naqvi, S.W.A . (1991). Geographical extent of denitrification in the Arabian Sea in relation to some physical processes. *Oceanol. Acta*, 14, 281-290.

Naqvi, S.W.A. and R. Sen Gupta (1985). 'NO' a useful tool for the estimation of nitrate deficits in the Arabian Sea. *Deep-Sea Res II.*, 35, 665-674.

Naqvi, S.W.A. and R.J. Noronha (1991). Nitrous oxide in the Arabian Sea. *Deep-Sea Res. II*, 38, 871-890.

Naqvi, S.W.A. and M.S. Shailaja (1993). Activity of the respiratory electron transport system and respiration rates within the oxygen minimum layer of the Arabian Sea. *Deep-Sea Res. II*, 40, 687-695.

Naqvi, S.W.A., and D. A. Jayakumar (2000). Ocean biogeochemistry and atmospheric composition: significance of the Arabian Sea. *Curr. Sci.*, 78, 289-299.

Naqvi, S.W.A., R.J. Norhona and C.V.G. Reddy (1982). Denitrification in the Arabian Sea. *Deep-Sea Res. II*, 29, 459-469.

Naqvi, S.W.A., Hema Naik and P.V. Narvekar (2003). The Arabian Sea. In: K. Black and G. Shimmield, (eds.), *Biogeochemistry of Marine Systems.* Sheffield Academic Press (in press).

Naqvi, S.W.A., R.J. Noronha, K. Somasundar and R. Sen Gupta (1990). Seasonal changes in the denitrification regime of the Arabian Sea. *Deep-Sea Res. II*, 37, 693-711.

Naqvi, S.W.A., M.D. Kumar, P.V. Narvekar, S.N. De Sousa, M.D. George, and C. D'Silva (1993). An intermediate Nepheloid layer associated with high

microbial metabolic rates and denitrification in the Northwest Indian Ocean. *J. Geophys. Res.*, 98, 16,469-16,479.

Naqvi, S.W.A., T. Yoshinari, J.A. Brandes, A.H. Devol, D.A. Jayakumar, P.V. Narvekar, M.A. Altabet and L.A. Codispoti (1998). Nitrogen isotopic studies in the suboxic Arabian Sea. *Proc. Indian Acad. Sci. Earth Planet Sci.*, 107, 367-378.

Naqvi, S.W.A., D. A. Jayakumar, P. V. Narvekar, H. Naik, V. Sarma, W. D'Souza, S. Joseph and M. D. George (2000). Increased marine production of N_2O due to intensifying anoxia on the Indian Continental Shelf. *Nature*, 408, 346-349.

Nevison, C.D., R.F. Weiss and D.J. Erickson III (1995). Global oceanic emissions of nitrous oxide. *J. Geophys. Res.*, 100 (C8), 15,809 -15,820.

Nevison, C. and E. Holland (1997). A re-examination of the impact of anthropogenically fixed nitrogen on atmosphere N2O and the stratospheric O_3 layer. *J. Geophysics. Res.- Atmos.*, 102, 25519 -25536.

Nishio, T., I. Koike and A. Hattori (1982). Denitrification, nitrate reduction, and oxygen consumption in coastal and estuarine sediments. *Appl. Environ. Microbiol*, 43, 648-653.

Nishio, T., I. Koike and A. Hattori (1983). Estimates of denitrification in coastal and estuarine sediments. *Appl. Environ. Microbiol*, 45, 444-450.

Oremland, R.S., C. Umberger, C.W. Culbertson and R.L. Smith (1984). Denitrification in San Francisco Bay sediment. *Appl. Environ.Microbial.*, 47, 1106-1112.

Oren, A. and T. H. Blackburn (1979). Estimation of sediment denitrification rates at *in-situ* nitrate concentration. *Applied Environ. Microbial*, 37, 174-176.

Pai, S., G. Gong and K. Liu (1993). Determination of dissolved oxygen in seawater by direct spectrophotometry of total iodine. *Mar. Chem.*, 41, 343-351.

Patra, P.K., S. Lal, S. Venkataramani, S.N. de Sousa, V.V.S.S. Sarma, and S. Sardessai (1999). Seasonal and spatial variability in N_2O distribution in the Arabian Sea. *Deep-Sea Res. I*, 46, 529-543.

Payne, W.J. (1973). Reduction of nitrogenous oxide by microorganisms. *Bacteriol. Rev.*, 37, 409-452.

Rabalais, N.N. and D.E. Jr. Harper (1991). Studies of the benthic oxygen depletion phenomenon off Louisiana. In: H.J. Krock and D.E. Jr. Harper, (eds.) *International Pacifica Scientific Diving Symposium*, 57-63pp. Proceedings-of-the-American Academy of Underwater Sciences Eleventh Annual Scientific Diving Symposium, Honolulu, Hawaii, September-25-30.

Rabalais, N. N. and S. W. Nixon (2002). Preface: Nutrient Over-enrichment of the Coastal Zone. Dedicated Issue Nutrient Over-enrichment in Coastal Waters: Global Patterns of Cause and Effect. *Journal of the Estuarine Research Federation*, vol. 25, 639 p.

Ramesh Babu, V., M.J. Varkey, V. Kesava Das and A.D. Gouveia (1980). Water masses and general hydrography along the west coast of India during early March. *Indian J. Mar. Sci.*, 9, 82-89.

Redfield, A.C., B.H. Ketchum, and F.A. Richards (1963). The influence of organisms on the composition of seawater. In: M.N. Hill, (ed.), *The Sea*, Vol. 2, Interscience, New York, 26-77pp.

Richards, F.A. (1965). Anoxic basins and fjords. In: J.P. Riley and G. Skirrow (eds.), *Chemical Oceanography*, Vol. 1, Academic Press, 611-645.

Rochford, D.J. (1964). Salinity maxima in the upper 1000 meters of the Northern Indian Ocean. *Aust. J. Mar. Freshw. Res.*, 15, 1-24.

Sarma, V.V.S.S., M.D. Kumar and M. Manerikar (2001). Emission of carbon dioxide from a tropical estuarine system, Goa, India. *Geophys. Res. Lett.*, 28, 1239-1242.

Schott, G. (1935). *Geographie des Indischen und Stillen Ozeans, Verlag Boysen*, Hamburg.

Schott, F. and J.P. McCreary (2001). The monsoon circulation of the Indian Ocean. *Prog. Oceanogr.*, 51, 1-123.

Seitzinger, S.P. (1988). Denitrification in freshwater and coastal marine ecosystems: ecological and geochemical significance. *Limnol. Oceanogr.*, 33, 702-724.

Seitzinger, S.P. (1990). Denitrification in aquatic sediments. In: Revsbech NP, Sorensen J. (eds.), *Denitrification in aquatic sediments denitrification in soil and sediments*. FEMS Symposium, plenum press, New York, 301-322pp.

Seitzinger, S.P. and S.W. Nixon. (1985). Eutrophication and the rate of

dinitrification and N₂O production in coastal marine sediments. *Limnol. Oceangr.*, 29, 73-83.

Seitzinger, S.P., S.W. Nixon, and M.E.Q. Pilson (1984). Denitrification and nitrous oxide production in coastal marine ecosystem. *Limnol. Oceanogr.*, 29, 73-83.

Seitzinger, S., S. Nixon, M.E.Q. Pilson and S. Burke (1980). Denitrification and N₂O production in near-shore marine sediments. *Geochim. cosmochim. Acta*, 44, 1853-1860.

Seitzinger, S. P., L. P. Nielsen, J. Caffrey and P.B. Christensen (1993). Denitrification measurements in aquatic sediments: a comparison of three methods. *Biogeochemistry*, 23, 147-167.

Sen Gupta, R., V.N. Sankaranarayanan, S.N. De Sousa and S.P. Fondekar. (1976a). Chemical oceanography of the Arabian Sea: Part III — Studies on nutrient fraction and stoichiometric relationships in the northern and eastern basins. *Indian J. Mar. Sci.*, 5, 58-71.

Sen Gupta, R., M.D. Rajagopal and S.Z. Qasim (1976b). Relationship between dissolved oxygen and nutrients in the north-western Indian ocean. *Indian J. Mar. Sci.*, 5, 201-211.

Shaffer, G. (1986). Phosphate pumps and shuttles in the Black Sea. *Nature*, 321, 515-517.

Shetye, S.R. (1998). West India coastal current and Lakshadweep High/Low. *Sadhana*, 23, 637-651pp.

Shetye, S.R. and S.S.C. Shenoi (1988). The seasonal cycle of surface circulation in the coastal north Indian Ocean. *Proc. Indian Acad. Sci., (Earth Planet Sci.)* 97, 53-62.

Shetye, S.R., A.D. Gouveia, S.S.C. Shenoi, D. Sundar, G.S. Michael, A.M. Almeida and K. Santanam (1990). Hydrography and circulation off the west coast of India during the Southwest Monsoon 1987. *J. Mar. Res.* 48, 359-378

Shetye, S.R., A. D. Gouveia, S.S.C. Shenoi, G.S. Michael, D. Sundar, A.M. Almeida, and K. Santanam (1991). The coastal current off western India during northeast monsoon. *Deep-Sea Res. I*, 38, 1517-1529.

Smith, S.L. (2001). Understanding the Arabian Sea: Reflections on the 1994-1996 Arabian Sea Expedition. *Deep-Sea Res. II*, 48, 1385-1402.

Sorensen, J. (1978). Denitrification rates in a marine sediment as measured by the acetylene inhibition technique. *Appl. Environ. Microbiol.*, 36, 139-143.

Spinrad, R.W., H. Glover, B.B. Ward, L.A. Codispoti and and G. Kullenberg (1989). Suspended particle and bacterial maxima in Peruvian coastal waters during a cold water anomaly. *Deep-Sea Res. I*, 36, 715-733.

Sreekumaran, N.S.R., V.P. Devassy and M. Madhupratap. (1992). Blooms of phytoplankton along the west coast of India associated with nutrient enrichment and the response of zooplankton. In: R.A. Vollenweider, R. Marchetti, R. Viviani (eds.), *Marine Coastal Eutrophication*. Suppl. 819-828pp.

Suntharalingam, P. and J.L. Sarmiento (2000). Factors governing the oceanic nitrous oxide distribution: simulations with an ocean general circulation model. *Global Biogeochem. Cycles*, 14, 429-454.

Sverdrup, H.H., M.W. Johnson and R.H. Fleming (1942). The Oceans: their physics, chemistry and general biology. Prentice Hall, New Jersey, 696pp.

Tanaka, T. and T. Saino (2002). Modified Method for the Analysis of Nitrogen Isotopic Composition of Oceanic Nitrate at Low Concentration. *J. Oceanogr.*, 58, 539-546.

Upstill-Goddard, R.C., J. Barnes and N.J.P. Owens (1999). Nitrous oxide and methane during the 1994 SW monsoon in the Arabian Sea/northwestern Indian Ocean. *J.Geophys. Res.*, 104, 30,067-30,084.

Vanderborght, J.P. and G. Billen (1975). Vertical distribution of nitrate in interstitial water of marine sediments with nitrification and denitrification. *Limnol. Oceanogr.*, 20, 953-961.

Venkateswaran, S. V. (1956). On evaporation from the Indian Ocean. *Indian J. Met. Geophys.*, 7, 265-284.

Wada, E. and A. Hattori (eds.) (1991). In: *Nitrogen in the Sea: Forms, Abundances and Rate Processes*, CRC Press, 208 p.

Walter, H.M., D.R. Keeney and I.R. Fillery (1979). Inhibition of nitrification by acetylene. *Soil Sci. Soc. Am. J.*, 43, 195-196.

Wanninkhof, R. (1992). Relationship between wind speed and gas exchange over the ocean. *J. Geophys. Res.*, 97, 7373-7382.

Warneck, P. (1988). Chemistry of the Natural Atmosphere (Academic, New York).

Warren, B.A. (1994) Context of the suboxic layer in the Arabian Sea. *Proc. Indian Acad. Sci. (Earth Planet. Sci.)*, 103, 301-314.

Weiss, R. F. and B. A. Price (1980). Nitrous oxide solubility in water and Seawater. *Mar. Chem.*, 8, 347-359.

Wong, G.T.F. (1990). The oxidation state diagram-a potential tool for studying redox chemistry in seawater. *Mar. Chem.*, 9, 13-24.

Wyrtki, K. (1971). *Oceanographic Atlas of the International Indian Ocean Expedition*, National Science Foundation, Washington D.C., 531p.

Wyrtki, K. (1973). Physical oceanography of the Indian Ocean. In: B. Zeitzschel, (ed.), *The biology of the Indian Ocean,* Springer-Verlag, Berlin, 18-36pp.

Yoh, M., H. Terai and Y. Saijo (1983). Accumulation of nitrous oxide in the oxygen deficient layer of freshwater lakes. *Nature*, 301, 327-329.

Yoshinari, T. and R. Knowles (1976). Acetylene inhibition of nitrous oxide reduction by denitrifying bacteria. *Biochem. Biophys. Res. Common.*, 69, 705-710.

Yukashev, E.V. and L.N. Neretin (1997). One dimensional modeling of nitrogen and sulfur cycles in the aphotic zones of the Black and Arabian Seas. *Global Biogeochem. Cycles*, 11, 401-414.

147